JGRG23

Proceedings of
the 23rd Workshop on General Relativity
and Gravitation in Japan

5—8 November 2013

50th Anniversary Auditorium, Hirosaki University

Aomori, Japan

Volume 2

Oral Presentations: Second Day

Contents

Oral Presentations: Second Day

Wednesday 6 November

Morning 1 [Chair: Masumi Kasai]

9:00 Ignazio Ciufolini (University of Salento) [Invited]
"Dragging of Inertial Frames, Fundamental Physics and the LARES space experiment"
[JGRG23(2013)110601]

10:00 Kei Yamada (Hirosaki University)
"Quantum interferometry in Chern-Simons gravity"
[JGRG23(2013)110602]

10:20 Ayumu Terukina (Hiroshima University)
"Hydrostatic equilibrium of gas distribution in Coma cluster and a test of chameleon gravity model"
[JGRG23(2013)110603]

10:40-11:00 Break

Morning 2 [Chair: Masahide Yamaguchi]

11:00 Yi-Peng Wu (RESCEU/National Tsing Hua University)
"The temporally enhanced curvature perturbation from the shift-symmetry breaking of a galileon field"
[JGRG23(2013)110604]

11:20 Masa-aki Watanabe (Kyoto University)
"An Inflationary Universe in Weyl Gauge Theory of Gravitation"
[JGRG23(2013)110605]

11:40 Yuki Watanabe (RESCEU, Univ. of Tokyo)
"Gravitational particle production and modulated reheating after inflation"
[JGRG23(2013)110606]

12:00 Naoyuki Takeda (ICRR, University of Tokyo)
"I-ball formation with log potential"
[JGRG23(2013)110607]

12:20 Katsuki Aoki (Waseda University)
"Cosmology in ghost-free bigravity theory with twin matter fluid"
[JGRG23(2013)110608]

12:40-14:20 Photo & Lunch (main hall closed 12:40-13:50)

Afternoon 1 [Chair: Masaru Shibata]

14:20 Kenta Hotokezaka (Kyoto University) [Invited]
"Numerical relativity: Application to gravitational-wave science and astrophysics"
[JGRG23(2013)110609]

15:10 Yuichiro Sekiguchi (Yukawa Institute for Theoretical Physics)
"Binary neutron star merger with a 'soft' equation of state and r-process"
[JGRG23(2013)110610]

15:30 Motoyuki Saijo (Waseda University)
"Nonlinear r-mode instability in rotating stars"
[JGRG23(2013)110611]

15:50-16:10 Break

Afternoon 2 [Chair: Tomohiro Harada]

16:10 Akira Oka (University of Tokyo)
"Cosmological Upper-Bound for f(R) Gravity through Redshift-Space Distortion"
[JGRG23(2013)110612]

16:30 Lingyao Kong (Fudan University)
"Testing the cosmic censorship conjecture with observations"
[JGRG23(2013)110613]

16:50 Takao Kitamura (Hirosaki University)
"Microlensed image centroid motions by an exotic lens object with negative convergence or negative mass"
[JGRG23(2013)110614]

Afternoon 3

17:10-18:20 Poster viewing

“Dragging of Inertial Frames, Fundamental Physics and the LARES space experiment”

by Ignazio Ciufolini (invited)

[JGRG23(2013)110601]

Dragging of Inertial Frames, Fundamental Physics and the LARES space experiment

Towards a One Percent Measurement of Frame-Dragging with the LARES space experiment

Ignazio Ciufolini
University of Salento, Lecce

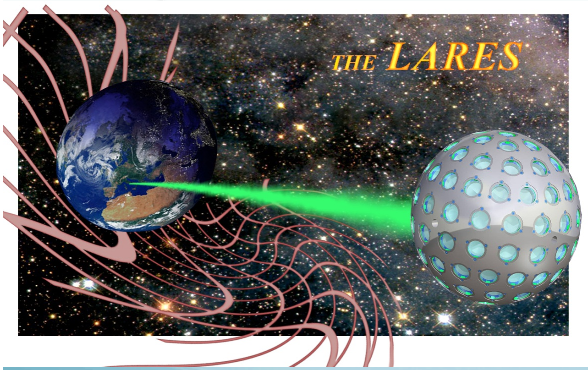

A. Paolozzi*, E. Pavlis*, R. Koenig*, J. Ries*, R. Matzner*, V. Gurzadyan*, R. Penrose*, G. Sindoni*, C. Paris*

*Sapienza Un. Rome,
*Maryland Un.,
*Helmholtz Cent.-GFZ, Potsdam
*Un. Texas Austin
*Alikhanian Nat. Lab., Yerevan
*Oxford Un.

JGRG23, HIROSAKI, JAPAN, 5-8 NOVEMBER 2013

LARES (Laser Relativity Satellite)

* Overview of the LARES Satellite
* Frame-Dragging, Gravitomagnetism and String Theory
*Previous Measurements of Frame-Dragging with LAGEOS, LAGEOS 2 and GRACE, and GP-B
* Error Analyses and Monte Carlo Simulations of the LARES space experiment
* Preliminary Results of the LARES Orbital Analysis

Current orbital analyses of the LARES observations

IC et al., Eur. Phys. J. Plus (2012) 127: 133

- Using the first few months of laser ranging data (since 17th February 2012) of LARES, we measured on its orbit the smallest residual (i.e., mismodelled or un-modelled) mean along-track acceleration than any other artificial satellite.
- We measured a *residual mean* along-track acceleration of LARES of less than 4×10^{-13} m/s^2: LARES is a nearly ideal test-particle for the gravitational field-geodesic motion.

EPJ Plus

EPJ .org

your physics journal

With highlight in EPJ and other international journals

Eur. Phys. J. Plus (2012) **127**: 133 DOI 10.1140/epjp/i2012-12133-8

Testing General Relativity and gravitational physics using the LARES satellite

Ignazio Ciufolini, Antonio Paolozzi, Erricos Pavlis, John Ries, Vahe Gurzadyan, Rolf Koenig, Richard Matzner, Roger Penrose and Giampiero Sindoni

Società Italiana di Fisica Springer

LARES
(LAser RElativity Satellite)

LARES was successfully launched and very accurately injected in the nominal orbit on the 13th of February 2012 with the new launching vehicle of ESA/ASI built by AVIO/ASI/ELV.

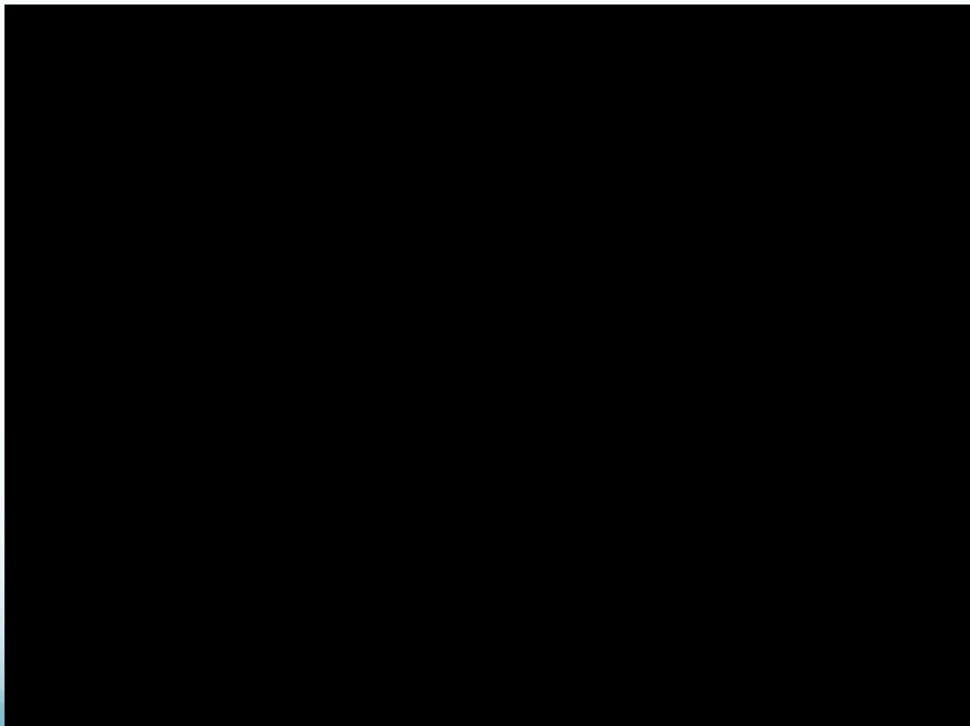


A BALL OF TUNGSTEN, THAT
BECAME THE LARES SATELLITE
AFTER CARVING THE HOUSING
OF THE CCR.
This Tungsten ball was built in China


A BALL OF TUNGSTEN, THAT
BECAME THE LARES SATELLITE
AFTER CARVING THE HOUSING
OF THE CCR

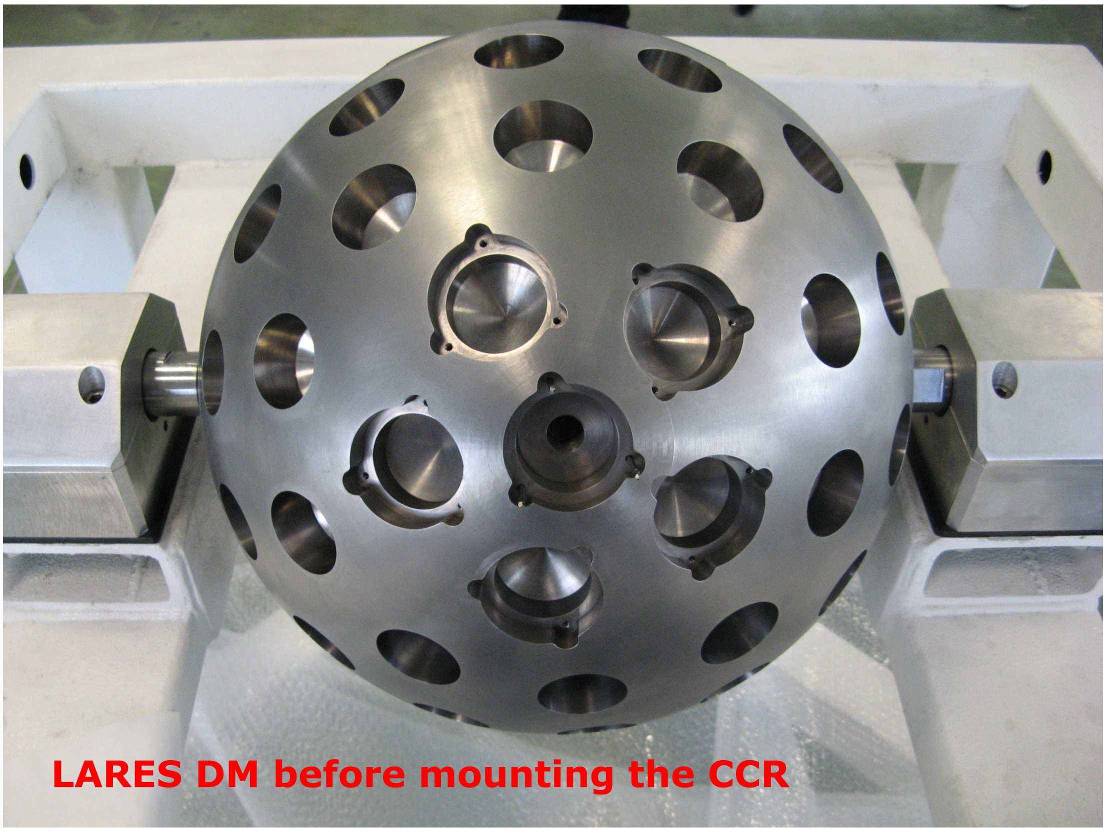
LARES DM before mounting the CCR

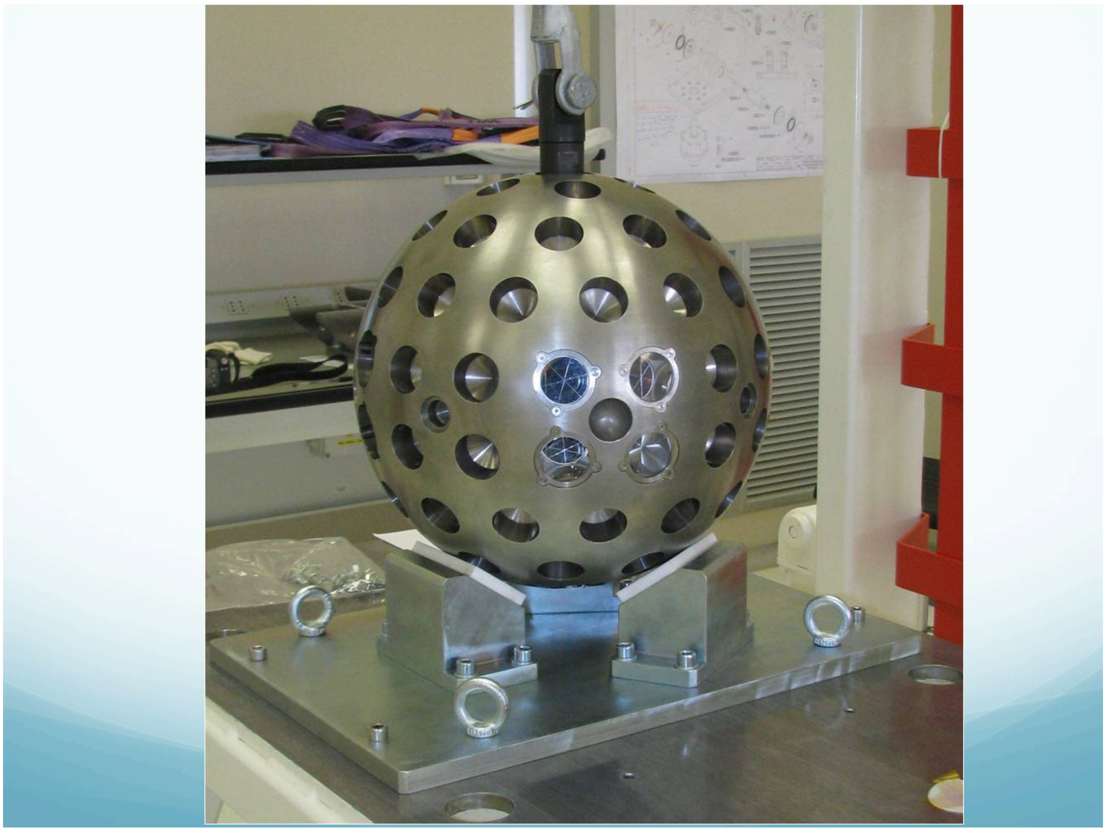

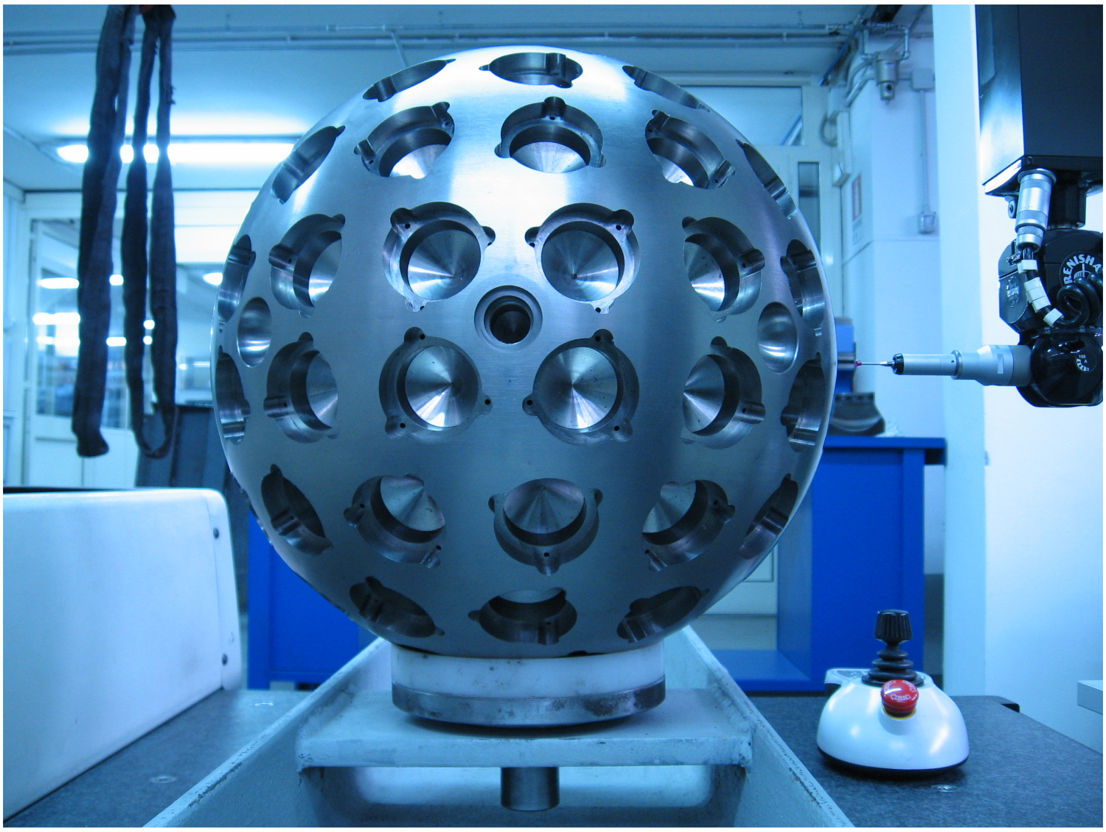

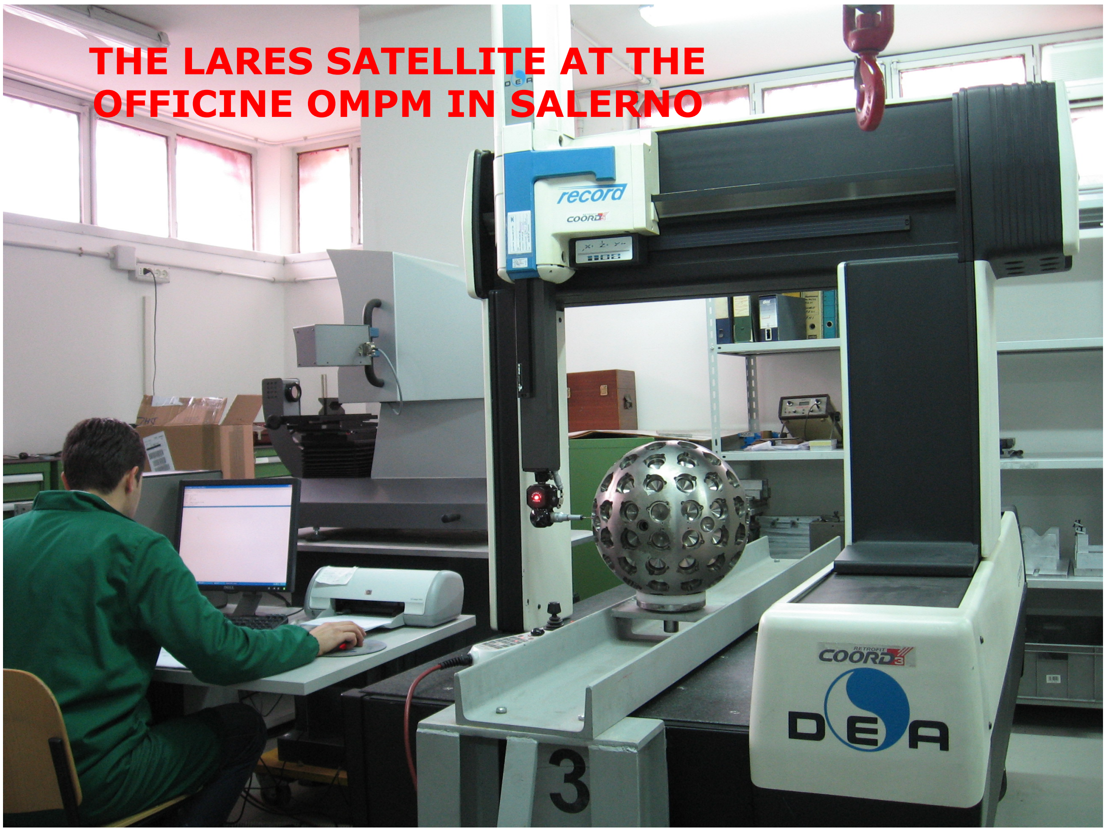
THE LARES SATELLITE AT THE
OFFICINE OMPM IN SALERNO
record
DEA

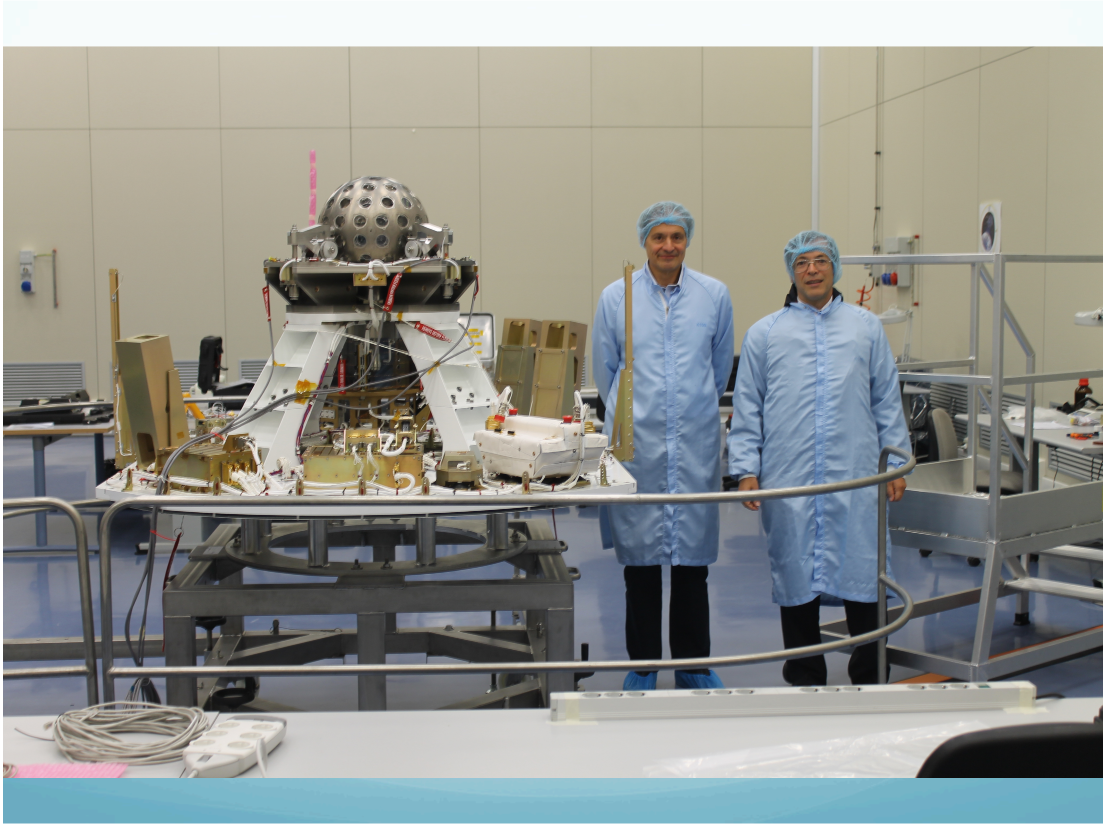

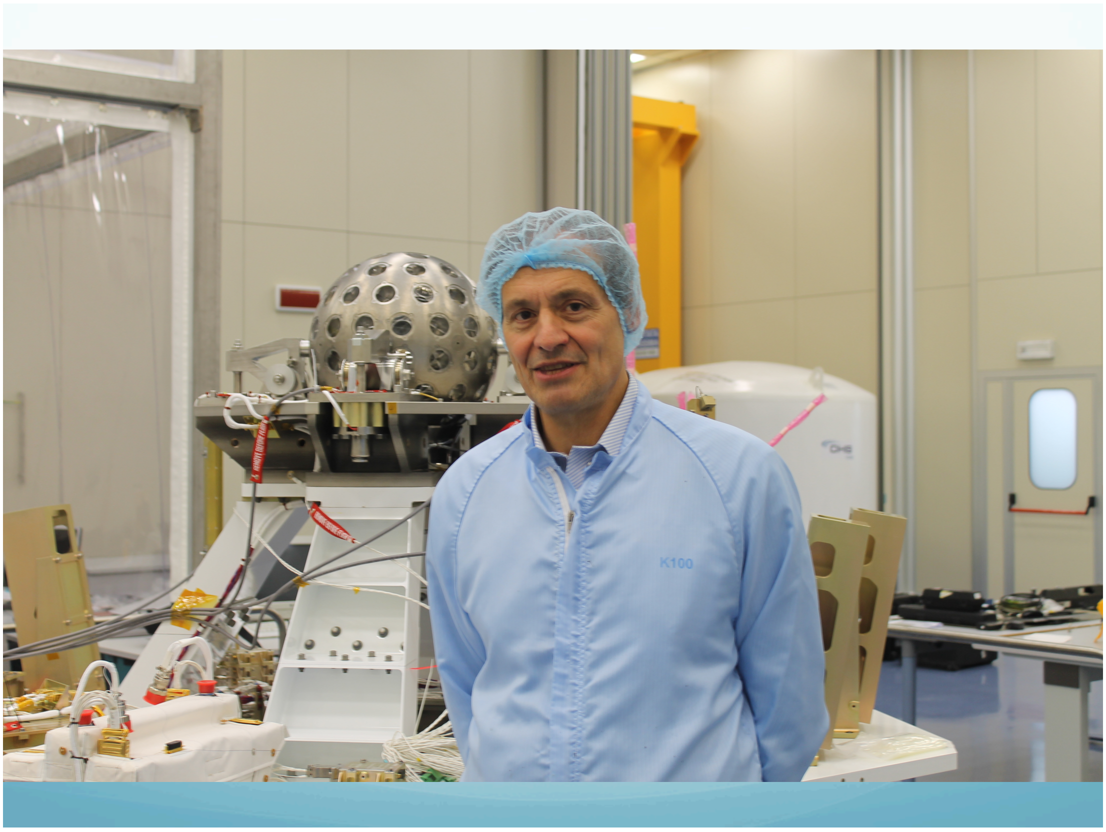
K100

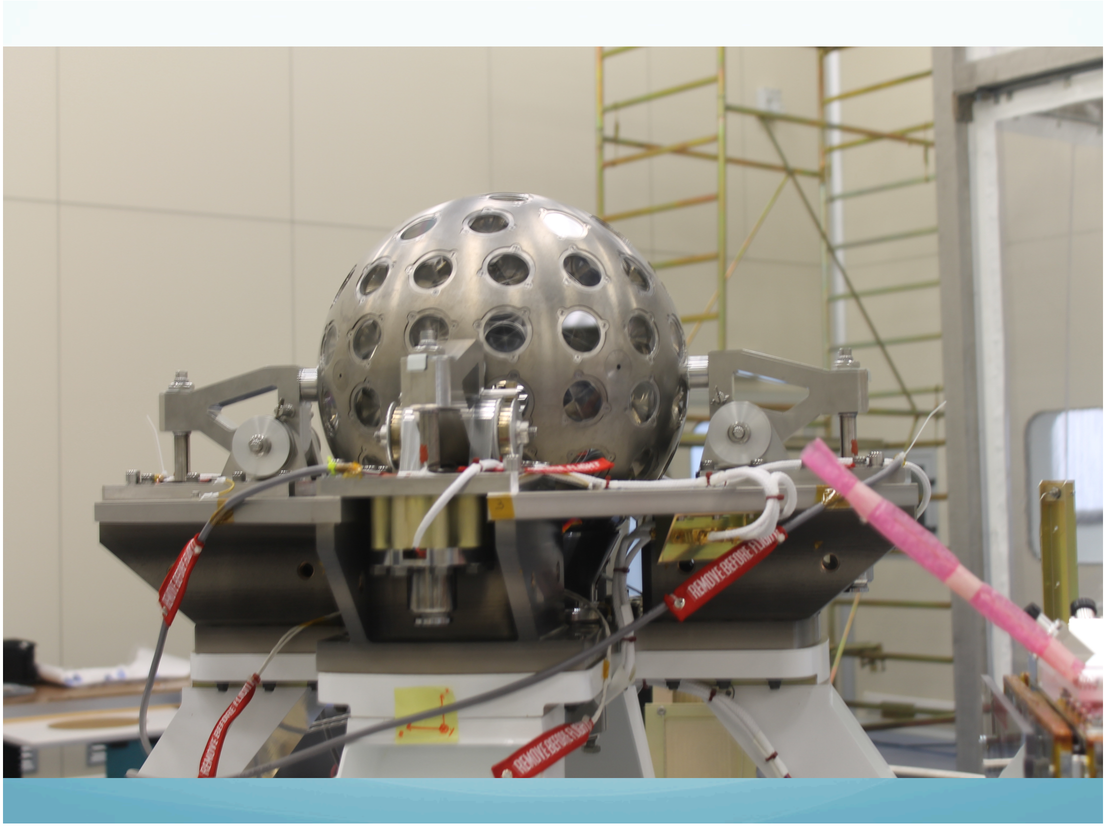
REMOVE BEFORE FLIGHT

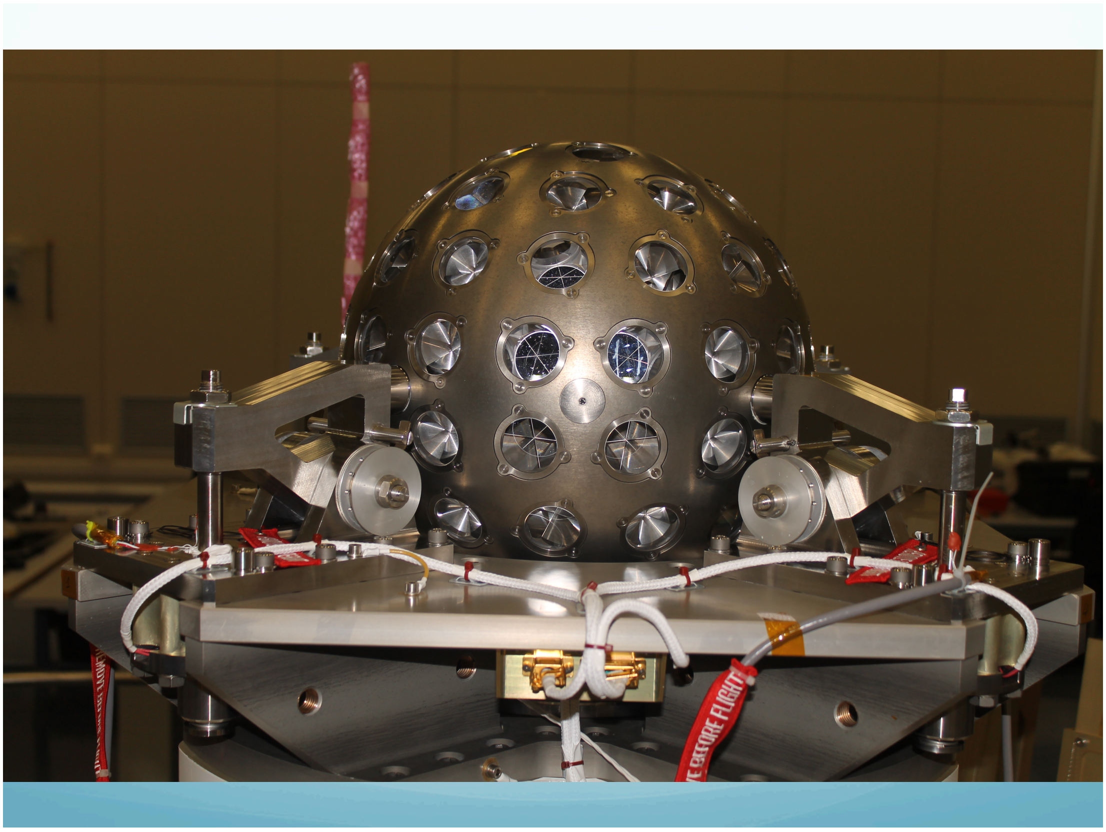

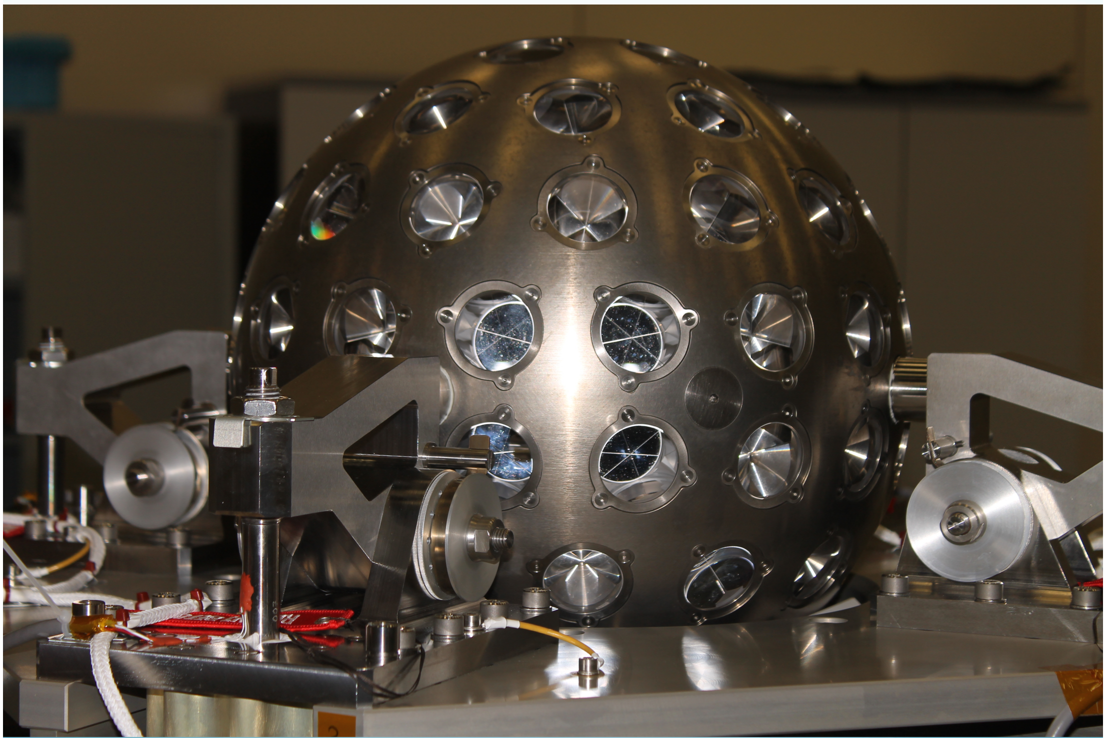

LARES: the first three achievements

1. The satellite has been exactly injected in the nominal orbit thanks to the qualifying flight of the new ESA launch vehicle VEGA (ELV, AVIO-ASI).
2. The laser return signals from LARES measured at the ILRS stations are of outstanding quality: LARES is well observed by the stations of the ILRS.
3. The structure of the satellite minimizes its non-gravitational orbital perturbations, i.e., its orbit is mainly affected by the gravitational field apart from small non-gravitational perturbations that can be accurately modelled, its residual accelerations are smaller than those of any other artificial satellite: after removing the known non-gravitational perturbations it has nearly geodesic motion.

LARES orbital elements

LARES orbital element	Nominal	Actual
Semimajor Axis	7825 km	7820 km
Inclination	69.5 °	69.5 °
Eccentricity	0	0.0007

LARES return signals

(November 2013)

Satellite	Site Name	Station	Start Date	End Date	No. Passes	No. Points
LARES	Altay	1879	2012-04-25 15:18:40	2013-10-20 19:46:02	106	1,287
LARES	Arequipa	7403	2012-04-02 15:18:08	2013-10-30 18:11:31	408	3,614
LARES	Arkhyz	1886	2012-09-13 23:03:51	2013-10-31 15:36:06	139	812
LARES	Badary	1890	2012-04-02 16:23:28	2013-10-21 18:44:48	140	1,458
LARES	Baikonur	1887	2012-05-04 19:31:38	2013-10-14 16:04:51	198	2,031
LARES	Beijing	7249	2012-04-02 16:17:50	2013-10-29 17:58:38	129	1,273
LARES	Changchun	7237	2012-02-24 19:41:48	2013-11-01 08:45:50	1,041	6,821
LARES	Concepcion	7405	2012-03-01 05:13:31	2013-10-26 08:09:51	233	1,177
LARES	Grasse	7845	2012-02-21 13:34:21	2013-10-28 22:45:51	162	2,757
LARES	Graz	7839	2012-02-17 13:53:12	2013-10-29 00:40:24	831	15,040
LARES	Greenbelt	7105	2012-02-17 21:41:37	2013-09-18 13:08:23	653	9,354
LARES	Haleakala	7119	2012-02-24 01:05:06	2013-11-01 23:48:31	376	5,115
LARES	Hartebeesthoek	7501	2012-03-12 22:29:18	2013-11-02 23:44:29	421	5,231
LARES	Herstmonceux	7840	2012-02-25 15:13:58	2013-11-03 01:17:02	584	7,173
LARES	Katzively	1893	2012-02-19 03:55:07	2013-10-21 16:29:27	286	2,646
LARES	Kiev	1824	2012-03-23 21:01:25	2013-10-31 23:31:59	198	1,551
LARES	Koganei	7308	2012-02-20 05:09:27	2013-09-27 10:46:44	43	464
LARES	Komsomolsk-Na-Amure	1868	2012-05-09 16:15:51	2013-10-24 09:29:42	36	252
LARES	Matera	7941	2012-02-18 04:49:34	2013-10-31 15:33:25	806	8,620
LARES	McDonald	7080	2012-02-29 10:38:17	2013-11-02 20:58:55	154	1,181
LARES	Monument Peak	7110	2012-02-18 01:36:49	2013-11-01 23:58:16	419	6,069
LARES	Mount Stromlo	7825	2012-02-17 18:46:03	2013-10-27 03:51:50	736	6,972
LARES	Potsdam	7841	2012-02-20 06:40:10	2013-10-31 21:30:18	584	8,513
LARES	San Fernando	7824	2012-04-22 20:14:12	2013-10-08 05:35:38	134	786
LARES	San Juan	7406	2012-04-03 01:20:25	2013-10-29 08:53:24	343	4,045
LARES	Shanghai	7821	2012-03-13 17:58:21	2013-10-27 18:17:53	188	1,231
LARES	Simeiz	1873	2012-03-08 00:22:18	2013-10-21 16:24:25	250	2,474
LARES	Simosato	7838	2012-02-20 07:06:50	2013-11-01 14:55:29	179	2,687
LARES	Svetloe	1888	2012-04-01 02:16:19	2013-10-14 20:00:43	61	507
LARES	Tahiti	7124	2012-03-07 10:35:53	2013-10-31 12:23:48	92	1,306
LARES	Tanegashima	7358	2012-03-21 15:22:40	2012-04-17 12:02:29	6	51
LARES	Wettzell	8834	2012-02-21 05:33:20	2013-10-19 20:36:55	892	8,010
LARES	Yarragadee	7090	2012-02-17 10:34:54	2013-11-03 06:14:00	1,747	25,060
LARES	Zelenchukskaya	1889	2012-04-05 20:52:44	2013-10-26 15:04:15	29	322
LARES	Zimmerwald	7810	2012-02-20 16:42:49	2013-11-02 17:21:56	983	14,008

Laser Ranged Satellites

The purpose of laser-ranged satellites is to minimize the non-gravitational orbital perturbations, such as atmospheric drag and radiation pressure, in order to get an orbit that is 'only' affected by gravitation.

In that way we can very accurately determine and study the gravitational field of Earth, not only its 'classical' (i.e., non-relativistic) part, but also its General Relativistic corrections.

This has been achieved by the LARES special design and by minimizing its dimensions and maximizing its weight LARES is the single orbiting body in the Solar System with highest mean density.

- LARES has a very high mean density: it has a weight of about 387 kg and a radius of about 18 cm: its cross-sectional-to-mass-ratio A/M is smaller than any other satellite (it is almost 3 times smaller than that of LAGEOS that before LARES had the smallest A/M ratio).
- It has a very special design: it is a *single-piece* very small sphere (made of a Tungsten alloy) covered with retro-reflectors.

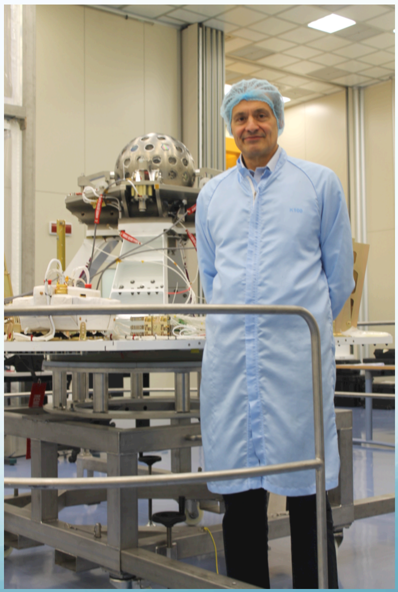

LARES

(LAser RElativity Satellite)

Italian Space Agency

- Combined with the LAGEOS and LAGEOS 2 orbital data and using the GRACE Earth gravity field determinations, LARES would provide a confirmation of Einstein General Relativity, the measurement of frame-dragging, with accuracy of about 1%.

DRAGGING OF INERTIAL FRAMES

(*FRAME-DRAGGING* as Einstein named it in 1913)

- Spacetime curvature is generated by mass-energy currents: $\varepsilon\ u^{\alpha}$

$$G^{\alpha\beta} = \chi\ T^{\alpha\beta} =$$

$$= \chi\ [(\varepsilon + p)\ u^{\alpha} u^{\beta} + p\ g^{\alpha\beta}]$$

- It plays a key role in high energy astrophysics (Kerr metric)

Thirring 1918
Braginsky, Caves and Thorne 1977
Thorne 1986
I.C. 1994-2001

THE WEAK-FIELD AND SLOW MOTION ANALOGY WITH ELECTRODYNAMICS

Gravitomagnetic Field in General Relativity

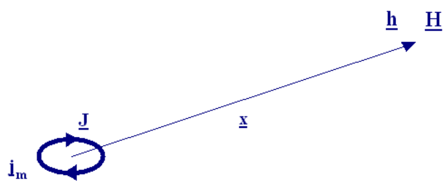

From weak field and slow motion limit of G= χ T:

$$\Delta\, h_{0i} \;\cong\; 16\,\pi\,\rho\, v^i \qquad \text{Lorentz gauge}$$

Electromagnetism

$$\Delta\,\mathbf{A} \;=\; -\frac{4\pi}{c}\,\mathbf{j}$$

where $\mathbf{h} \equiv (h_{01},\ h_{02}\ , h_{03})$ is the gravitomagnetic potential

$$h_{0i}\,(\mathbf{x}) \;\cong\; -\;4\int \frac{\rho(\mathbf{x}')v^i(\mathbf{x}')}{|\mathbf{x}-\mathbf{x}'|}\,d^3x' \qquad \mathbf{A}\,(\mathbf{x}) \;=\; \frac{1}{c}\int \frac{\mathbf{j}(\mathbf{x}')}{|\mathbf{x}-\mathbf{x}'|}\,d^3x'$$

$$\mathbf{h}\,(\mathbf{x}) \;\cong\; -2\,\frac{\mathbf{J}\times\mathbf{x}}{|\mathbf{x}|^3} \qquad \mathbf{A}\,(\mathbf{x}) \;\cong\; \frac{\mathbf{m}\times\mathbf{x}}{|\mathbf{x}|^3}$$

The gravitomagnetic field is:

$$\mathbf{H} \;=\; \nabla\times\mathbf{h} \;\cong\; 2\left[\frac{\mathbf{J}-3(\mathbf{J}\cdot\hat{\mathbf{x}})\,\hat{\mathbf{x}}}{|\mathbf{x}|^3}\right] \qquad \mathbf{B} \;=\; \nabla\times\mathbf{A} \;\cong\; \frac{3\,\hat{\mathbf{x}}\,(\hat{\mathbf{x}}\cdot\mathbf{m})\;-\;\mathbf{m}}{|\mathbf{x}|^3}$$

From weak field and slow motion limit of D u=0:

$$m\,\frac{d^2\mathbf{x}}{dt^2} \;\cong\; m\,\left(\mathbf{G} + \frac{d\mathbf{x}}{dt}\times\mathbf{H}\right) \qquad m\,\frac{d^2\mathbf{x}}{dt^2} \;=\; q\,\left(\mathbf{E} + \frac{d\mathbf{x}}{dt}\times\mathbf{B}\right)$$

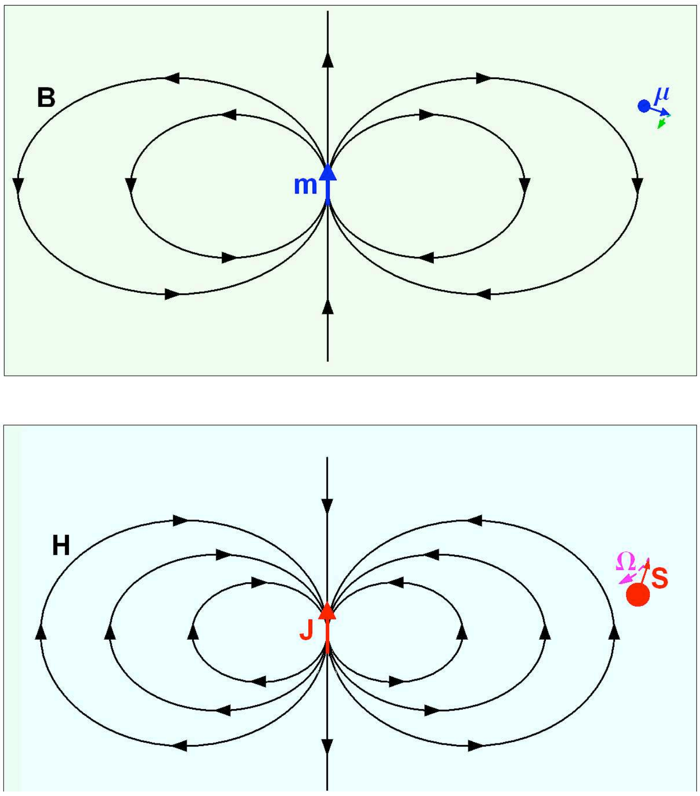

a

b

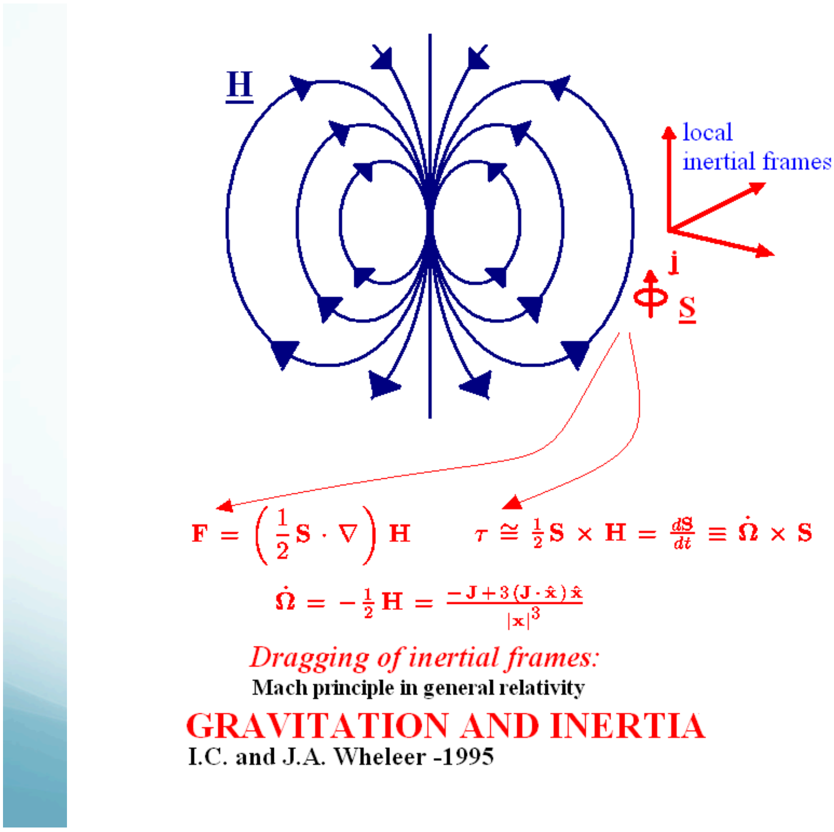
H
local
inertial frames
i
S
$\mathbf{F} = \left(\frac{1}{2}\mathbf{S}\cdot\nabla\right)\mathbf{H}$
$\tau \cong \frac{1}{2}\mathbf{S}\times\mathbf{H} = \frac{d\mathbf{S}}{dt} \equiv \dot{\mathbf{\Omega}}\times\mathbf{S}$
$\dot{\mathbf{\Omega}} = -\frac{1}{2}\mathbf{H} = \frac{-\mathbf{J}+3(\mathbf{J}\cdot\hat{\mathbf{x}})\hat{\mathbf{x}}}{|\mathbf{x}|^3}$
Dragging of inertial frames:
Mach principle in general relativity
GRAVITATION AND INERTIA
I.C. and J.A. Wheleer -1995

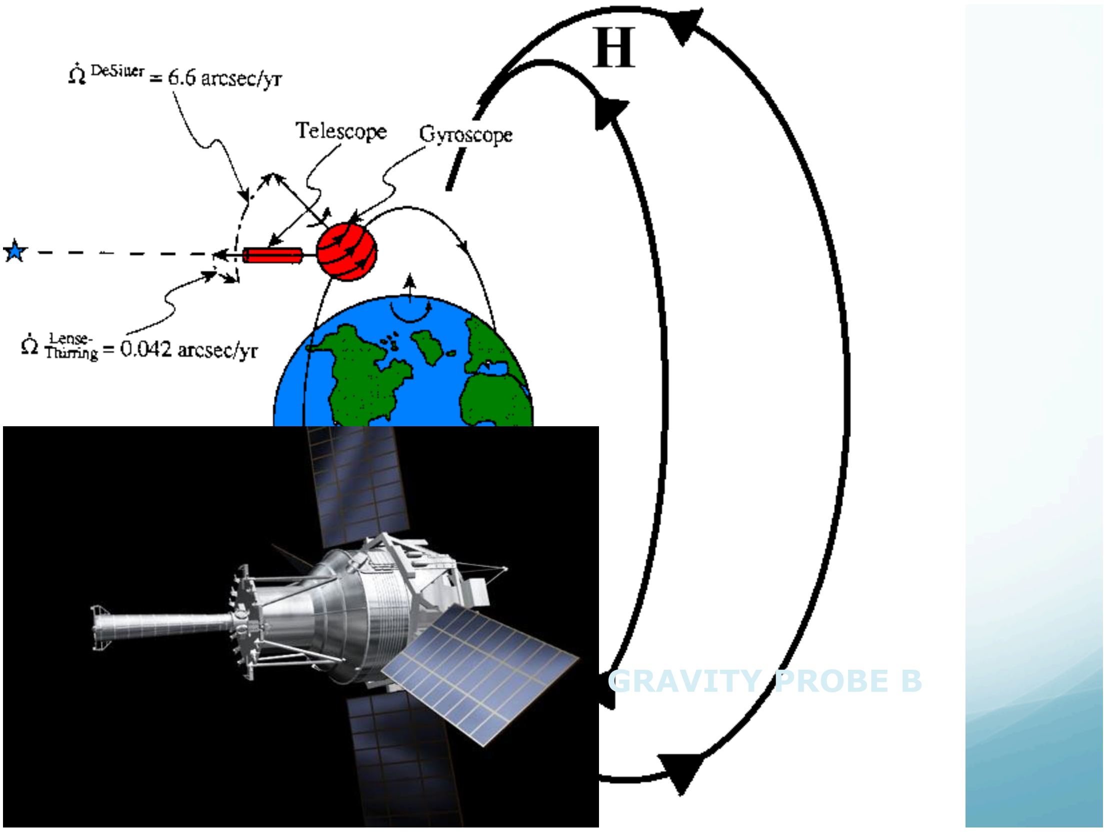
$\dot{\Omega}^{DeSitter} = 6.6$ arcsec/yr
Telescope
Gyroscope
H
$\dot{\Omega}_{Lense-Thirring} = 0.042$ arcsec/yr
GRAVITY PROBE B

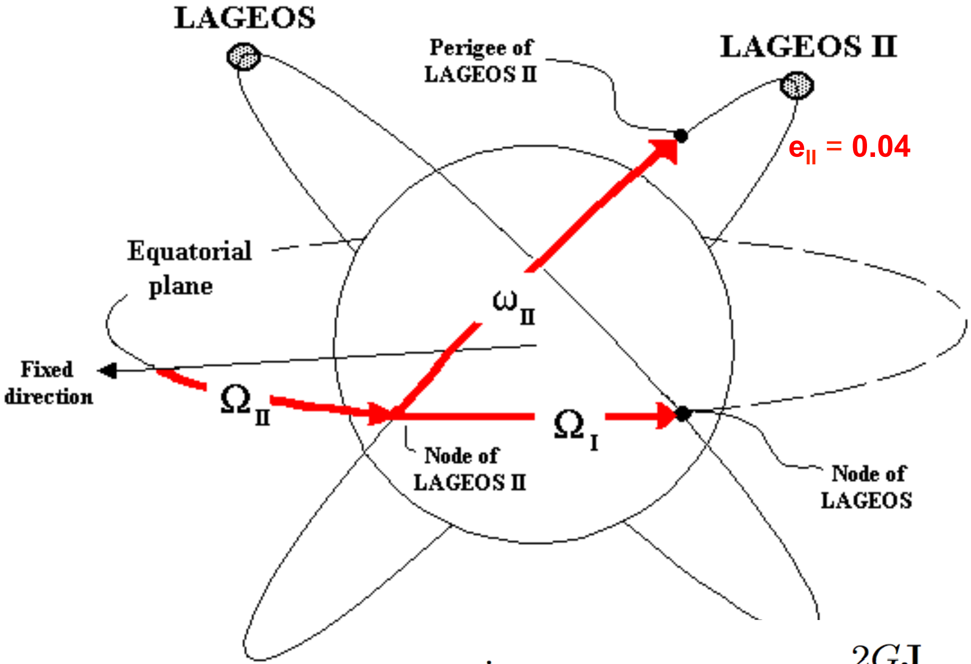

By integrating the Lorentz force equation, we get:

$$\dot{\Omega}_{Lense-Thirring} = \frac{2GJ}{c^2 a^3 (1-e^2)^{3/2}}$$

Chern-Simons Gravity, String Theory and Frame-Dragging

- Can we distinguish between the **intrinsic gravitomagnetic field** generated by the **angular momentum of a central body**, that is, the "drag" of a gyroscope due to the curvature generated by the rotation of a central body (or by a **current of mass-energy**), e.g., by the **Kerr metric**, and the change of orientation of a gyroscope due to the motion of a gyroscope in a static gravitational field, e.g., Schwarzschild metric, that is **B** = γ (**v** x **E)** ?

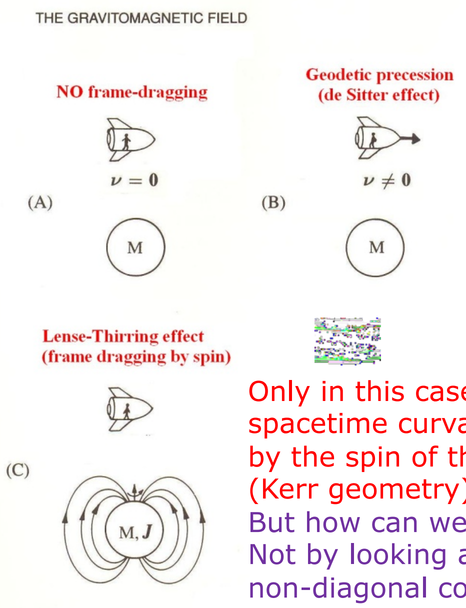

$$-\frac{3}{2}\mathbf{v}\times\mathbf{r}\,\frac{M}{r^3}$$

Geodetic precession: accurately measured by LLR and GP-B

Only in this case (c) additional spacetime curvature is generated by the spin of the central body (Kerr geometry).
But how can we define it?
Not by looking at the g_{0k} non-diagonal components of the metric, nor by simply looking at the magnetic-like components of the Riemann tensor R_{i0kl}

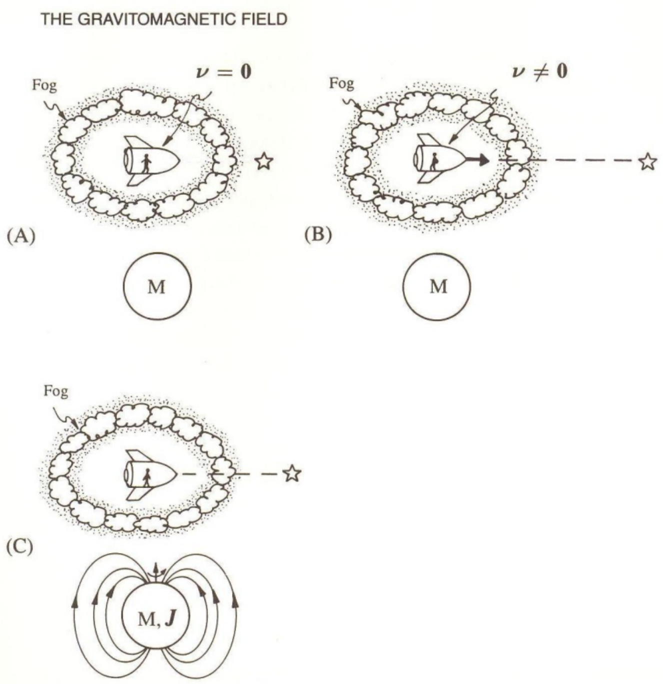

INVARIANT CHARACTERIZATION of "INTRINSIC" GRAVITOMAGNETISM

Gravitomagnetism can be defined without approximations by the Riemann tensor in a local Fermi frame (Matte-1953).

By explicit spacetime invariants built with the Riemann tensor (I.C. 1994, I.C. and Wheeler 1995):

Let us use the Pontryagin pseudo-invariant, that for the Kerr metric is:

$$\tfrac{1}{2}\, \varepsilon_{\alpha\beta\sigma\rho}\, R^{\sigma\rho}{}_{\mu\nu}\, R^{\alpha\beta\mu\nu} = 1536\, J\, M \cos\theta\, (r^5 r^{-6} - r^3 r^{-5} + 3/16\, r\, r^{-4})$$

In weak-field and slow-motion:

$$^{*}R \cdot R = 288\, (J\, M)/r^7 \cos\theta \; + \cdots$$

J = aM = angular momentum

*R · R similar to ***F · F** in electrodynamics. Similarly ***R · R** is different from zero in the case of two **massive** bodies moving with respect to each other (calculated using the PPN metric).

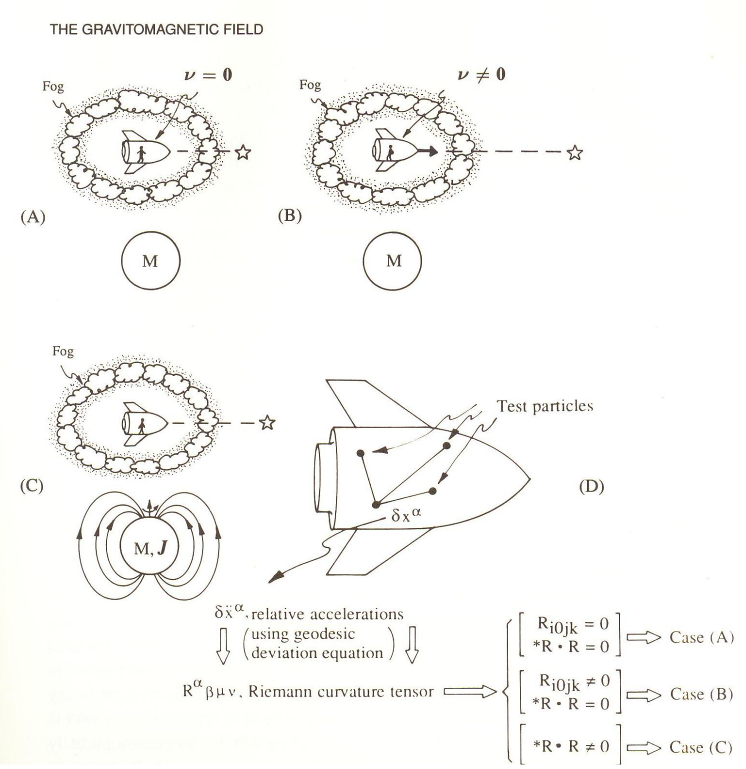

ACTION of CHERN-SIMONS GRAVITY

$$S = \int d^4x\sqrt{-g}\left[-\frac{1}{2\kappa^2}R + \frac{\ell}{12}\theta R\tilde{R} - \frac{1}{2}(\partial\theta)^2 - V(\theta) + \mathcal{L}_{\rm mat}\right],$$

$R\tilde{R} \equiv R^{\beta}{}_{\alpha}{}^{\gamma\delta}\tilde{R}^{\alpha}{}_{\beta\gamma\delta}$, is the Pontryagin pseudoscalar, θ is a scalar field, g the determinant of the metric, R the Ricci scalar, l is a new length parameter, $\mathcal{L}_{mat}$ the matter Lagrangian density and $k^2 = 8\pi G$.

In Smith, Erickcek, Caldwell and Kamionkowski, Phys. Rev D 2008 is shown that the 4-D string action for a type of string theory may reduce to this action.
See also: Yagi K., Yunes N. and Tanaka T., Phys. Rev. D., 86 (2012) 044037 and references therein.

The modified gravitational field equation is:

$$G^{ab} + lC^{ab} = 8\pi T^{ab},$$

where C^{ab} is the Cotton-York tensor. Then, in the weak field approximation, we get a modified Ampere-Maxwell equation:

$$\vec{\nabla}\times\vec{B} - \frac{\partial\vec{E}}{\partial t} - \frac{1}{m_{\rm cs}}\Box\vec{B} = 4\pi G\vec{J},$$

where:

$$A_\mu \equiv -\frac{1}{4}\bar{h}_{\mu\nu}t^\nu = -\frac{1}{4}\bar{h}_{\mu 0}.$$

$$E^i = \partial_i A_0 - \partial_0 A_i,$$
$$B^i = \epsilon^{0ijk}\partial_j A_k,$$

Where **H** of the previous formula is here: **H** = - 4 **B**

The gravitomagnetic potential ***A*** for a sphere rotating with angular velocity ω, including the Chern-Simons contribution, is:

$$\vec{A}_{\rm AY} = \vec{A}_{\rm GR} - \frac{4\pi G\rho R^3}{m_{\rm cs} R}\left[\frac{2R^3}{15r^3}\vec{\omega} + \frac{R^3}{5r^3}\hat{r}\times(\hat{r}\times\vec{\omega})\right]$$

Then by integrating the Lorentz force equation for a test particle:

$$\vec{a} = -\vec{E} - 4\vec{v}\times\vec{B},$$

We find the ratio of the nodal drag of Chern-Simons gravity and General Relativity:

$$\frac{\dot{\Omega}_{\rm CS}}{\dot{\Omega}_{\rm GR}} = 15\frac{a^2}{R^2}j_2(m_{\rm CS}R)y_1(m_{\rm CS}a),$$

Where j_2 and y_l are spherical Bessel functions and m_{cs} is the Chern-Simons mass:

$$m_{cs} = -3 \,/\, k^2\, \theta^2$$

- **Chern-Simons gravity is equivalent to some type of String Theory (Smith et al. 2008).**
- **On the basis of our 2004-2010 measurements of frame-dragging, using the LAGEOS satellites, in 2008, Smith, Erickcek, Caldwell and Kamionkowski (Phys. Rev. D 77, 024015, 2008) have placed limits on some possible low-energy consequences of string theory that may be related to dark energy and quintessence.**
- **See also: S. Alexander and N. Yunes "Chern-Simon Modified General Relativity", Physics Reports, Volume 480, 2009, p. 1-55.**
- **T. Clifton, P.Ferreira, A. Padilla and C. Skordis, "Modified Gravity and Cosmology".**
- **K. Yagi, N. Yunes and T. Tanaka, Phys. Rev. D., 86 (2012) 044037.**

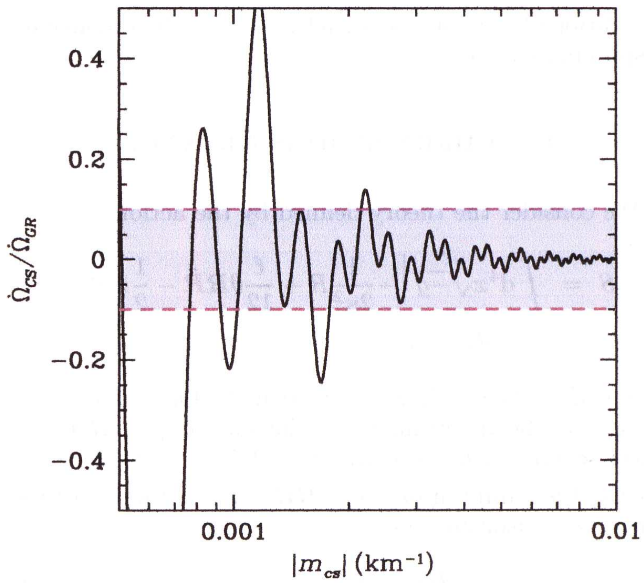

FIG. 1: The ratio $\dot{\Omega}_{\rm CS}/\dot{\Omega}_{\rm GR}$ for the LAGEOS satellites orbiting with a semimajor axis of $a \approx 12,000$ km. A 10% verification of general relativity [16] (the shaded region) leads to a lower limit on the Chern-Simons mass of $|m_{\rm cs}| \gtrsim 0.001\ \text{km}^{-1}$. A 1% verification of the Lense-Thirring drag will improve this bound on $m_{\rm cs}$ by a factor of roughly five.

$m_{cs} \geq 2 \times 10^{-22}$ GeV

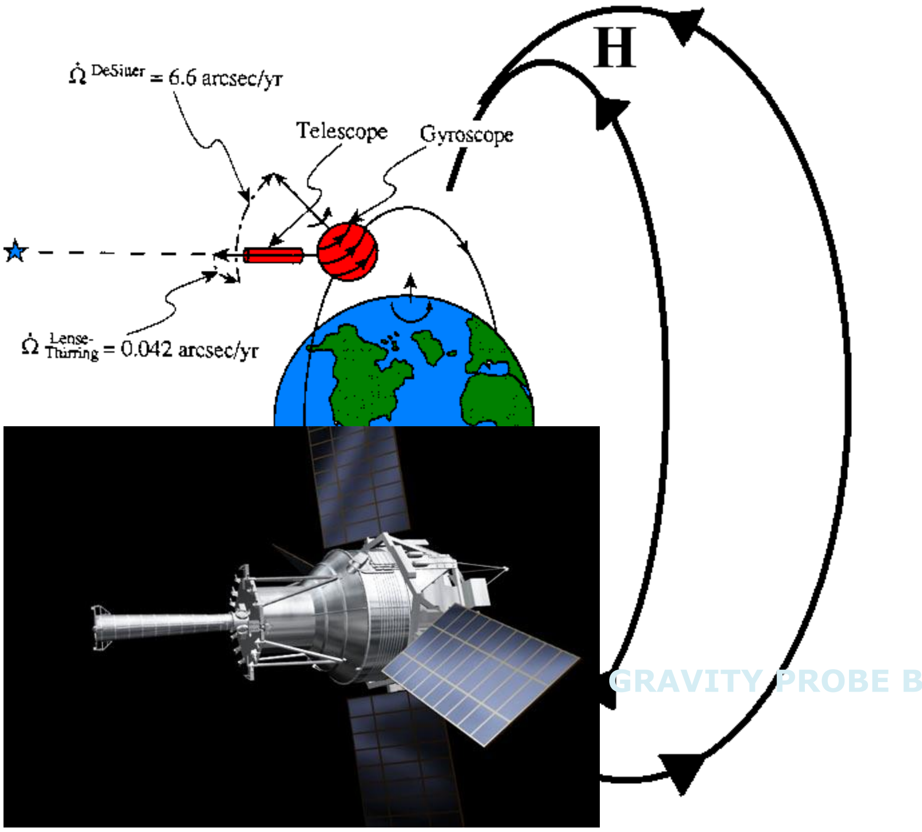

Problems with the GP-B data analysis have been outlined, see, for example: **R. F. O'Connell "Gravito-Magnetism in one-body and two-body systems: Theory and Experiment", in, "Atom Optics and Space Physics", Proc. of Course CLXVIII of the International School of Physics "Enrico Fermi", Varenna, Italy, 2007, ed. E. Arimondo, W. Ertmer and W. Schleich, (2009).**

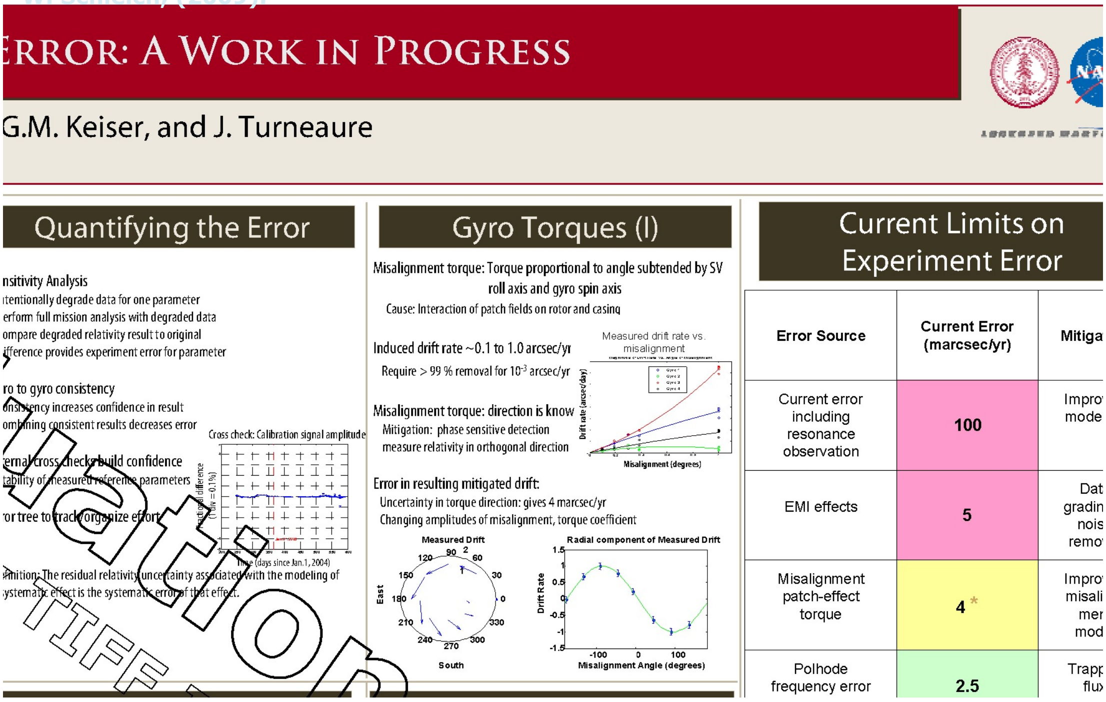

GRAVITY PROBE B was launched in 2004

- **After the data collection (for a few months after the launch) GP-B had systematic errors for over 300 % of the frame-dragging effect.**
- **On 4 May 2011, after over 5 years of data analysis, they announced a reduction of the systematic errors from 300% to 19% by some modelling of the systematic errors and then published a measurement of frame-dragging claiming an error of about 19 %.**

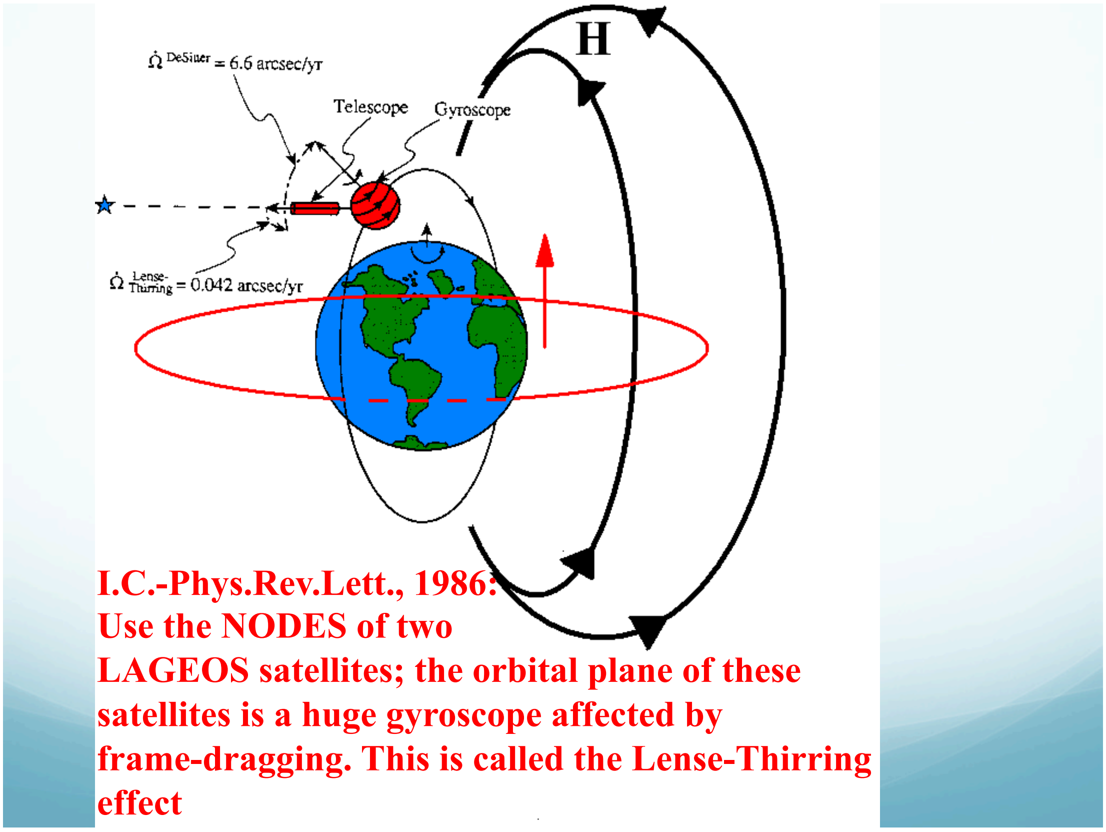

More than 25 years ago in the office of John Archibald Wheeler

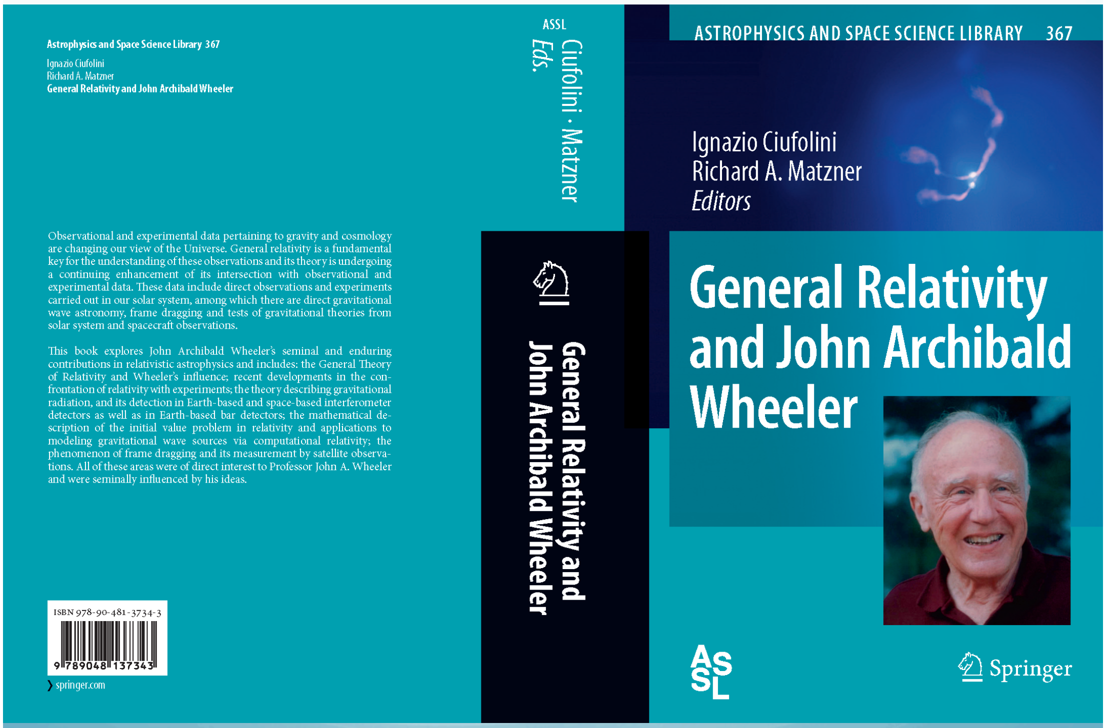

Satellite Laser Ranging

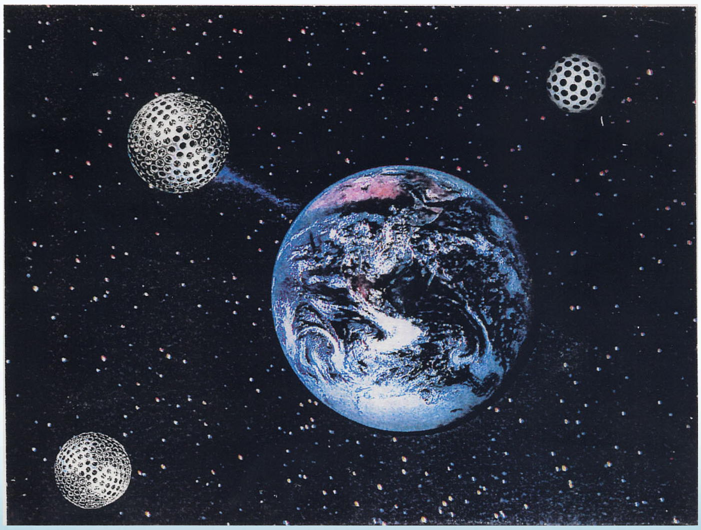

l=3, m=1

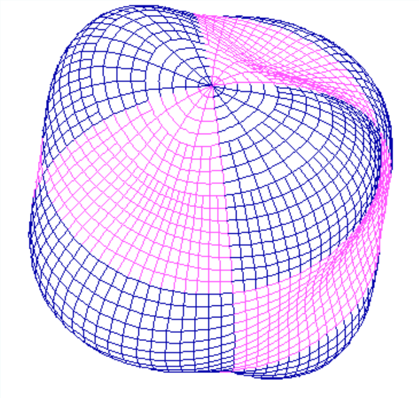

We need to eliminate the errors due to the lowest degree even zonal harmonics.

EVEN ZONAL HARMONICS

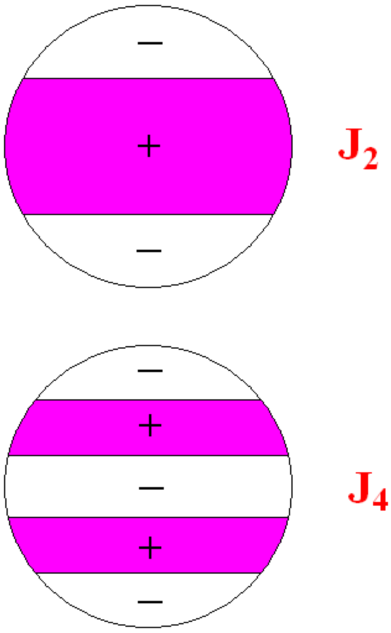

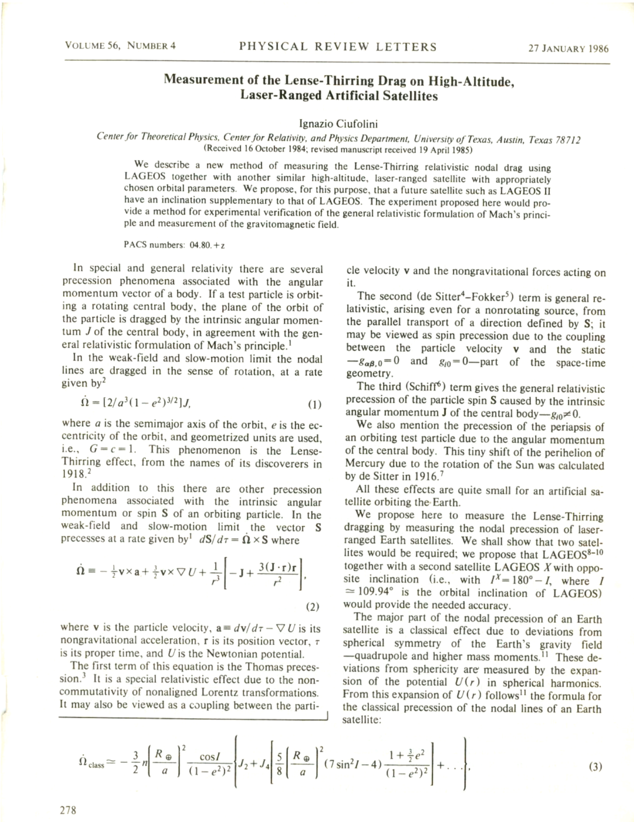
VOLUME 56, NUMBER 4 PHYSICAL REVIEW LETTERS 27 JANUARY 1986

Measurement of the Lense-Thirring Drag on High-Altitude, Laser-Ranged Artificial Satellites

Ignazio Ciufolini
Center for Theoretical Physics, Center for Relativity, and Physics Department, University of Texas, Austin, Texas 78712
(Received 16 October 1984; revised manuscript received 19 April 1985)

We describe a new method of measuring the Lense-Thirring relativistic nodal drag using LAGEOS together with another similar high-altitude, laser-ranged satellite with appropriately chosen orbital parameters. We propose, for this purpose, that a future satellite such as LAGEOS II have an inclination supplementary to that of LAGEOS. The experiment proposed here would provide a method for experimental verification of the general relativistic formulation of Mach's principle and measurement of the gravitomagnetic field.

PACS numbers: 04.80.+z

In special and general relativity there are several precession phenomena associated with the angular momentum vector of a body. If a test particle is orbiting a rotating central body, the plane of the orbit of the particle is dragged by the intrinsic angular momentum J of the central body, in agreement with the general relativistic formulation of Mach's principle.[1]

In the weak-field and slow-motion limit the nodal lines are dragged in the sense of rotation, at a rate given by[2]

$$\dot{\Omega} = [2/a^3(1-e^2)^{3/2}]J, \qquad (1)$$

where a is the semimajor axis of the orbit, e is the eccentricity of the orbit, and geometrized units are used, i.e., $G=c=1$. This phenomenon is the Lense-Thirring effect, from the names of its discoverers in 1918.[2]

In addition to this there are other precession phenomena associated with the intrinsic angular momentum or spin $\mathbf{S}$ of an orbiting particle. In the weak-field and slow-motion limit the vector $\mathbf{S}$ precesses at a rate given by[1] $d\mathbf{S}/d\tau = \dot{\mathbf{\Omega}} \times \mathbf{S}$ where

$$\dot{\mathbf{\Omega}} \equiv -\tfrac{1}{2}\mathbf{v}\times\mathbf{a} + \tfrac{3}{2}\mathbf{v}\times\nabla U + \frac{1}{r^3}\left[-\mathbf{J} + \frac{3(\mathbf{J}\cdot\mathbf{r})\mathbf{r}}{r^2}\right], \qquad (2)$$

where $\mathbf{v}$ is the particle velocity, $\mathbf{a} \equiv d\mathbf{v}/d\tau - \nabla U$ is its nongravitational acceleration, $\mathbf{r}$ is its position vector, τ is its proper time, and U is the Newtonian potential.

The first term of this equation is the Thomas precession.[3] It is a special relativistic effect due to the noncommutativity of nonaligned Lorentz transformations. It may also be viewed as a coupling between the particle velocity $\mathbf{v}$ and the nongravitational forces acting on it.

The second (de Sitter[4]–Fokker[5]) term is general relativistic, arising even for a nonrotating source, from the parallel transport of a direction defined by $\mathbf{S}$; it may be viewed as spin precession due to the coupling between the particle velocity $\mathbf{v}$ and the static —$g_{\alpha\beta,0}=0$ and $g_{i0}=0$—part of the space-time geometry.

The third (Schiff[6]) term gives the general relativistic precession of the particle spin $\mathbf{S}$ caused by the intrinsic angular momentum $\mathbf{J}$ of the central body—$g_{i0}\neq 0$.

We also mention the precession of the periapsis of an orbiting test particle due to the angular momentum of the central body. This tiny shift of the perihelion of Mercury due to the rotation of the Sun was calculated by de Sitter in 1916.[7]

All these effects are quite small for an artificial satellite orbiting the Earth.

We propose here to measure the Lense-Thirring dragging by measuring the nodal precession of laser-ranged Earth satellites. We shall show that two satellites would be required; we propose that LAGEOS[8–10] together with a second satellite LAGEOS X with opposite inclination (i.e., with $I^X = 180° - I$, where $I \simeq 109.94°$ is the orbital inclination of LAGEOS) would provide the needed accuracy.

The major part of the nodal precession of an Earth satellite is a classical effect due to deviations from spherical symmetry of the Earth's gravity field —quadrupole and higher mass moments.[11] These deviations from sphericity are measured by the expansion of the potential $U(r)$ in spherical harmonics. From this expansion of $U(r)$ follows[11] the formula for the classical precession of the nodal lines of an Earth satellite:

$$\dot{\Omega}_{\text{class}} \simeq -\frac{3}{2}n\left(\frac{R_\oplus}{a}\right)^2 \frac{\cos I}{(1-e^2)^2}\left\{J_2 + J_4\left[\frac{5}{8}\left(\frac{R_\oplus}{a}\right)^2(7\sin^2 I - 4)\frac{1+\frac{3}{2}e^2}{(1-e^2)^2}\right] + \dots\right\}, \qquad (3)$$

IC, PRL 1986: Use of the nodes of two laser-ranged satellites to measure the Lense-Thirring effect

International Journal of Modern Physics A, Vol. 4, No. 13 (1989) 3083 – 3145

A COMPREHENSIVE INTRODUCTION TO THE LAGEOS GRAVITOMAGNETIC EXPERIMENT: FROM THE IMPORTANCE OF THE GRAVITOMAGNETIC FIELD IN PHYSICS TO PRELIMINARY ERROR ANALYSIS AND ERROR BUDGET

IGNAZIO CIUFOLINI

CNR-Istituto di Fisica dello Spazio Interplanetario, Via G. Galilei-CP 27-00044 Frascati, Italy

and

Center for Space Research, The University of Texas at Austin, Austin, Texas 78712, USA

Received 3 May 1988
Revised 7 October 1988

The existence of the gravitomagnetic field, generated by mass currents according to Einstein geometrodynamics, has never been proved. The author of this paper, after a discussion of the importance of the gravitomagnetic field in physics, describes the experiment that he proposed in 1984 to measure this field using LAGEOS (Laser geodynamics satellite) together with another non-polar, laser-ranged satellite with the same orbital parameters as LAGEOS but a supplementary inclination.

The author then studies the main perturbations and measurement uncertainties that may affect the measurement of the Lense-Thirring drag. He concludes that, over the period of the node of ~ 3 years, the maximum error, using two nonpolar laser ranged satellites with supplementary inclinations, should not be larger than ~ 10% of the gravitomagnetic effect to be measured.

Table of Contents

IC IJMPA 1989: Analysis of the orbital perturbations affecting the nodes of LAGEOS-type satellites

(1) Use two LAGEOS satellites with supplementary inclinations

OR:

Use n satellites of LAGEOS-type to measure the first n-1 even zonal harmonics: J_2, J_4, … and the frame-dragging effect (IC IJMPA 1989)

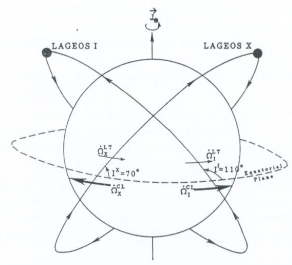

Fig. 5. The LAGEOS and LAGEOS X orbits and their classical and gravitomagnetic nodal precessions. A new[17] configuration to measure the Lense-Thirring effect.

For J_2, this corresponds, from formula (3.2), to an uncertainty in the nodal precession of 450 milliarcsec/year, and similarly for higher J_{2n} coefficients. Therefore, the uncertainty in $\dot{\Omega}^{\text{Class}}_{\text{Lageos}}$ is more than ten times larger than the Lense-Thirring precession.

A solution would be to orbit several high-altitude, laser-ranged satellites, similar to LAGEOS, to measure J_2, J_4, J_6, etc., and one satellite to measure $\dot{\Omega}^{\text{Lense-Thirring}}$.

Another solution would be to orbit polar satellites; in fact, from formula (3.2), for polar satellites, since $I = 90°$, $\dot{\Omega}^{\text{Class}}$ is equal to zero. As mentioned before, Yilmaz proposed the use of polar satellites in 1959.[40,41] In 1976, Van Patten and Everitt[46,47] proposed an experiment with two drag-free, guided, counter-rotating, polar satellites to avoid inclination measurement errors.

A new solution[15,16,17,21,22,23] would be to orbit a second satellite, of LAGEOS type, with the same semimajor axis, the same eccentricity, but the inclination supplementary to that of LAGEOS (see Fig. 5). Therefore, "LAGEOS X" should have the following orbital parameters:

$$I^X \cong \pi - I^I \cong 70°\,, \qquad a^X \cong a^I\,, \qquad e^X \cong e^I\,. \tag{3.3}$$

With this choice, since the classical precession $\dot{\Omega}^{\text{Class}}$ is linearly proportional to $\cos I$, $\dot{\Omega}^{\text{Class}}$ would be equal and opposite for the two satellites:

$$\dot{\Omega}^{\text{Class}}_X = -\dot{\Omega}^{\text{Class}}_I\,. \tag{3.4}$$

By contrast, since the Lense-Thirring precession $\dot{\Omega}^{\text{Lense-Thirring}}$ is independent of the inclination (Eq. (3.1)), $\dot{\Omega}^{\text{Lense-Thirring}}$ will be the same in magnitude and sign for both satellites:

IL NUOVO CIMENTO Vol. 109 A, N. 12 Dicembre 1996

On a new method to measure the gravitomagnetic field using two orbiting satellites

I. Ciufolini
IFSI-CNR - Frascati, Italy
Dipartimento Aerospaziale, Università di Roma «La Sapienza» - Roma, Italy

(ricevuto il 20 Settembre 1996; approvato il 15 Novembre 1996)

Summary. — We describe a new method to obtain the first direct measurement of the Lense-Thirring effect, or dragging of inertial frames, and the first direct detection of the gravitomagnetic field. This method is based on the observations of the orbits of the laser-ranged satellites LAGEOS and LAGEOS II. By this new approach one achieves a measurement of the gravitomagnetic field with accuracy of about 25%, or less, of the Lense-Thirring effect in general relativity.

PACS 11.90 – Other topics in general field and particle theory.
PACS 04.80.Cc – Experimental test of gravitational theories.

1. – The gravitomagnetic field, its invariant characterization and past attempts to measure it

Einstein's theory of general relativity [1, 2] predicts the occurrence of a «new» field generated by mass-energy currents, not present in classical Galilei-Newton mechanics. This field is called the gravitomagnetic field for its analogies with the magnetic field in electrodynamics.

In general relativity, for a stationary mass-energy current distribution $\varrho_m \boldsymbol{v}$, in the weak-field and slow-motion limit, one can write [2] the Einstein equation in the Lorentz gauge: $\Delta \boldsymbol{h} \cong 16\pi\varrho_m \boldsymbol{v}$, where $\boldsymbol{h} \equiv (h_{01}, h_{02}, h_{03})$ are the $(0i)$-components of the metric tensor; $\boldsymbol{h}$ is called the gravitomagnetic potential. For a localized, stationary mass-energy distribution, in the weak-field and slow-motion limit, we can then write: $\boldsymbol{h} \cong -2((\boldsymbol{J} \times \boldsymbol{x})/r^3)$, where $\boldsymbol{J}$ is the angular momentum of the central body. In general relativity, one can also define [2] a gravitomagnetic field $\boldsymbol{H}$ given by $\boldsymbol{H} = \nabla \times \boldsymbol{h}$.

The Lense-Thirring effect is a consequence of the gravitomagnetic field and consists of a tiny perturbation of the orbital elements of a test particle due to the angular momentum of the central body. To characterize the gravitomagnetic field generated by the angular momentum of a body, and the Lense-Thirring effect, and distinguish it from other relativistic phenomena, such as the de Sitter effect, due to the

1709

IC NCA 1996:
use the node of LAGEOS and the node of LAGEOS II to measure the Lense-Thirring effect

However, in 1996 the two nodes were not enough to measure the Lense-Thirring effect

2002

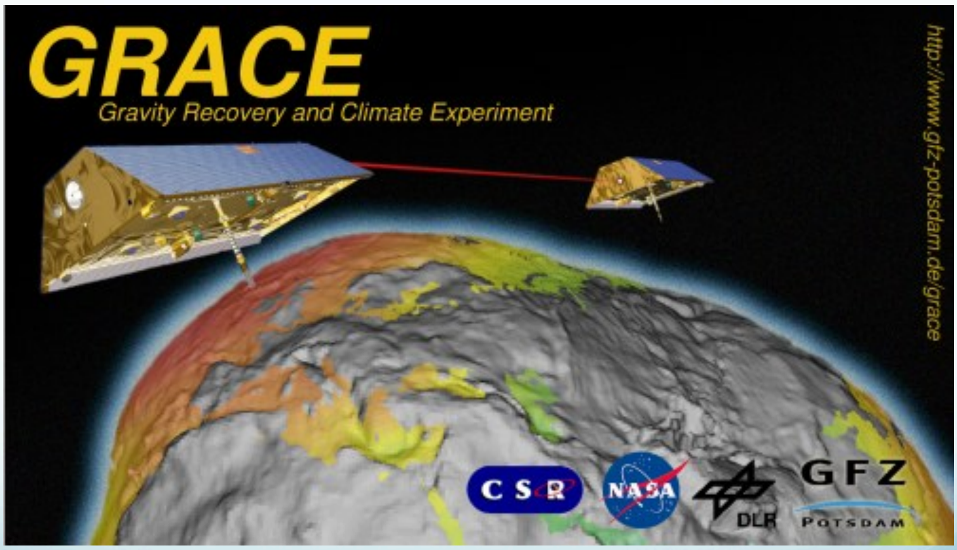

Use of GRACE to test Lense-Thirring at a few percent level:
J. Ries et al. 2003 (1999),E. Pavlis 2002 (2000)

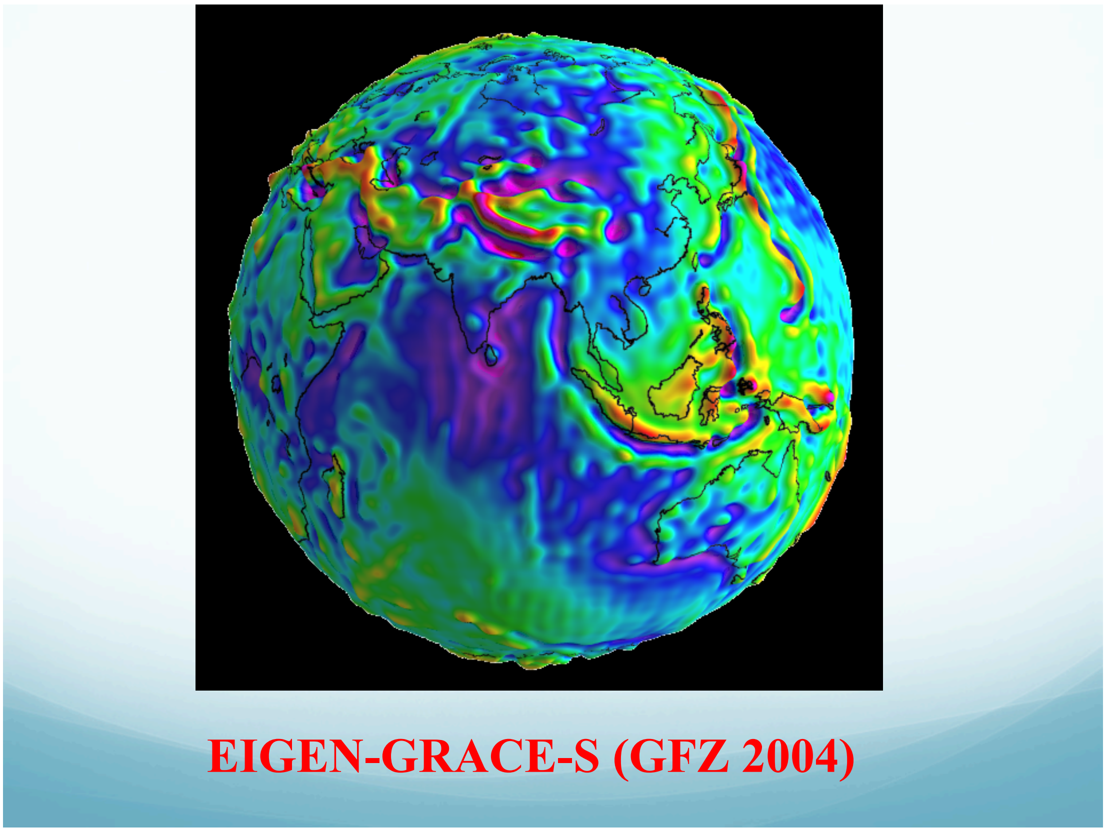
EIGEN-GRACE-S (GFZ 2004)

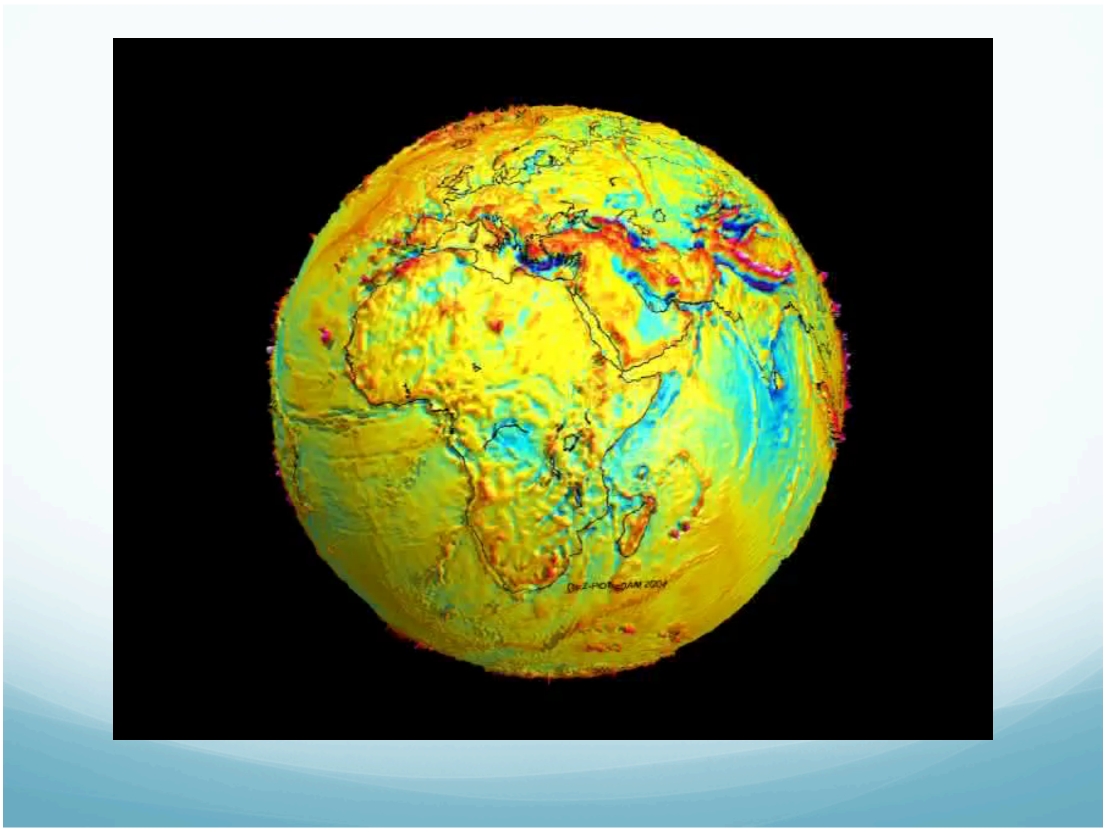

EVEN ZONAL HARMONICS

Using LAGEOS +LAGEOS 2 and the GRACE determinations of the Earth gravitational field we can measure the frame-dragging effect and eliminate the uncertainties in J2.

Even zonal harmonics, of degree even and zero order, are the axially symmetric deviations of the Earth potential (of even degree) from spherical symmetry also symmetric With respect to the Earth's Equatorial plane.

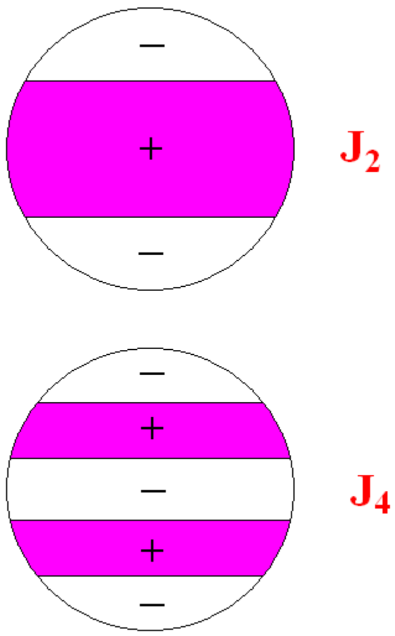

EIGEN-GRACE02S Model and Uncertainties

Even zonals lm	Value $\cdot 10^{-6}$	Uncertainty	Uncertainty on node I	Uncertainty on node II	Uncertainty on perigee II
20	−484.16519788	$0.53 \bullet 10^{-10}$	$1.59\ \Omega_{LT}$	$2.86\ \Omega_{LT}$	$1.17\ \omega_{LT}$
40	0.53999294	$0.39 \bullet 10^{-11}$	$0.058\ \Omega_{LT}$	$0.02\ \Omega_{LT}$	$0.082\ \omega_{LT}$
60	−.14993038	$0.20 \bullet 10^{-11}$	$0.0076\ \Omega_{LT}$	$0.012\ \Omega_{LT}$	$0.0041\ \omega_{LT}$
80	0.04948789	$0.15 \bullet 10^{-11}$	$0.00045\ \Omega_{LT}$	$0.0021\ \Omega_{LT}$	$0.0051\ \omega_{LT}$
10,0	0.05332122	$0.21 \bullet 10^{-11}$	$0.00042\ \Omega_{LT}$	$0.00074\ \Omega_{LT}$	$0.0023\ \omega_{LT}$

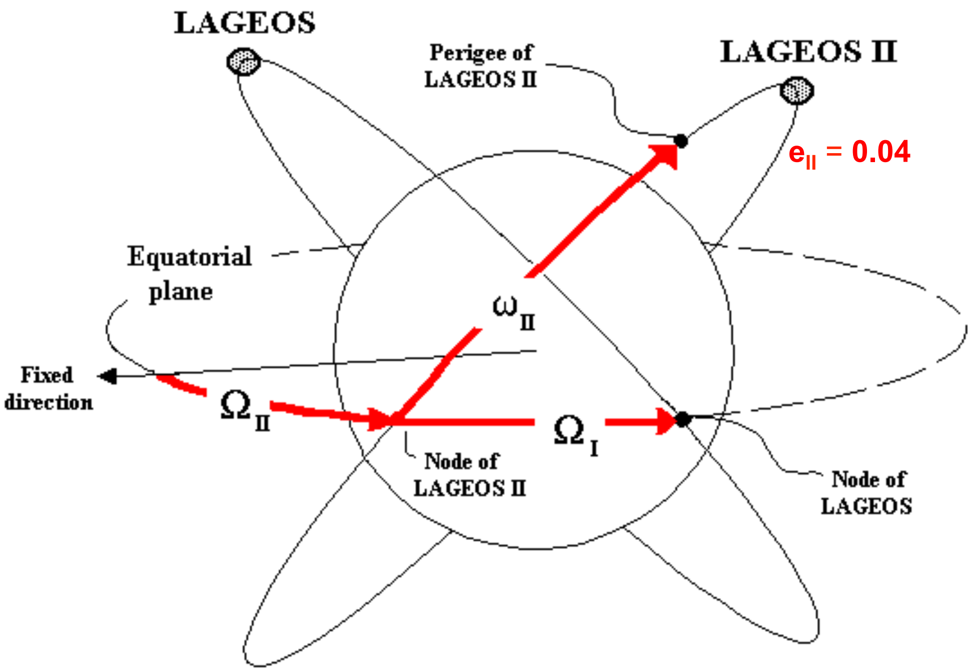
LAGEOS
Perigee of LAGEOS II
LAGEOS II
e_{II} = 0.04
Equatorial plane
ω_{II}
Fixed direction
Ω_{II}
Ω_{I}
Node of LAGEOS II
Node of LAGEOS

I.C., NC A, 1996

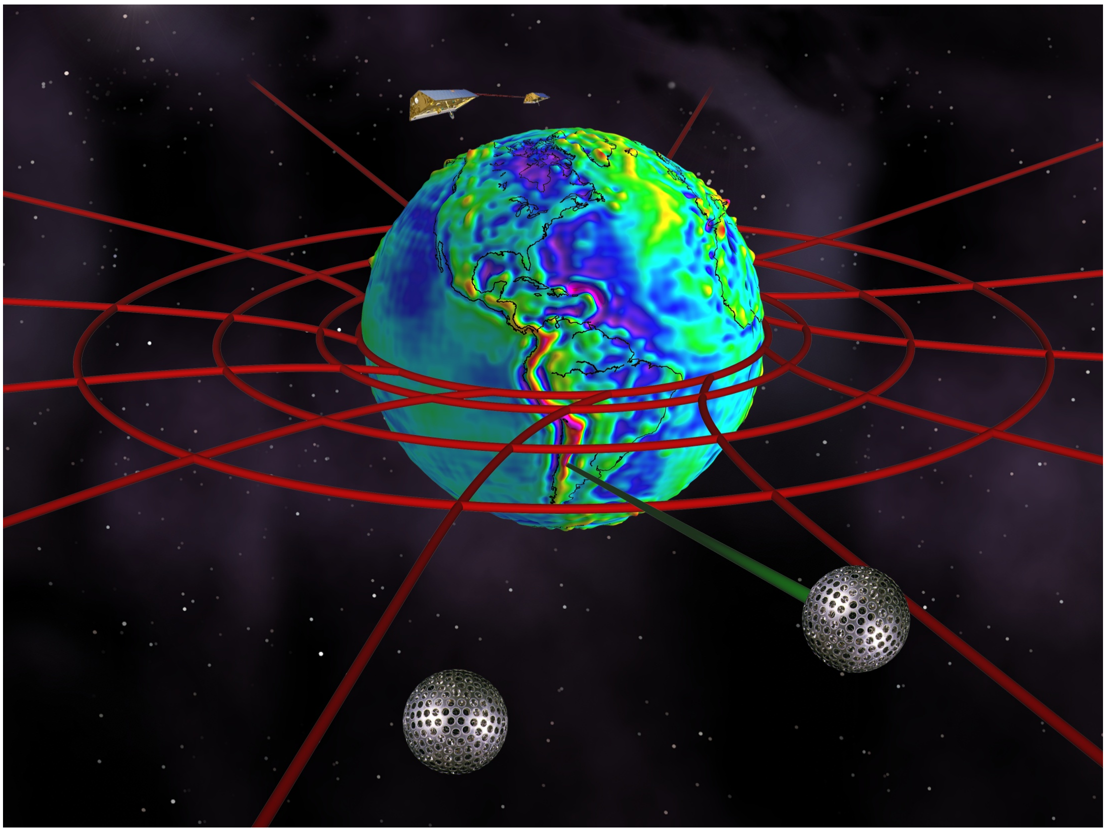

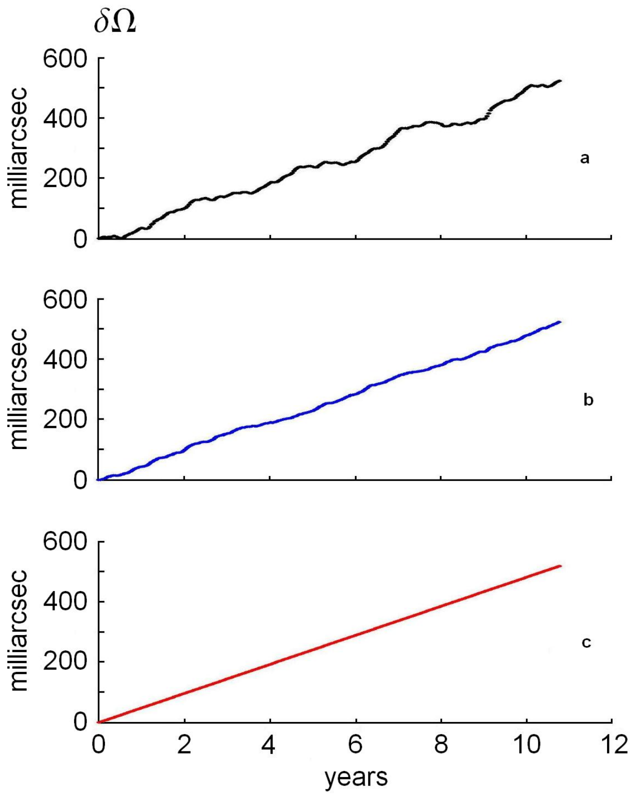

Figure 2

Observed value of Lense-Thirring effect using The combination of the LAGEOS nodes.

Observed value of Lense-Thirring effect = 99% of the general relativistic prediction. Fit of linear trend plus 6 known frequencies

General relativistic Prediction = 48.2 mas/yr

I.C. & E.Pavlis, Letters to NATURE, 431, 958, 2004.

The result was published in Nature Letters in 2004

2006-2007 ANALYSIS OF THE LAGEOS ORBITS USING THE GFZ ORBITAL ESTIMATOR **EPOS**

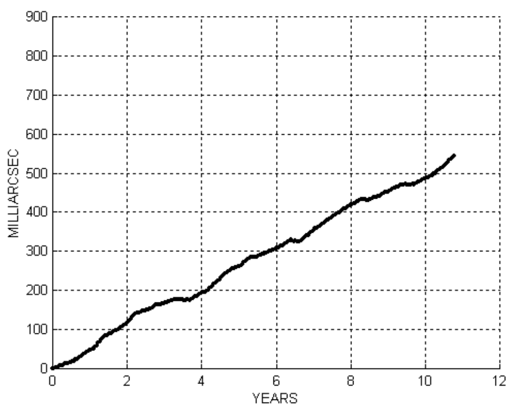

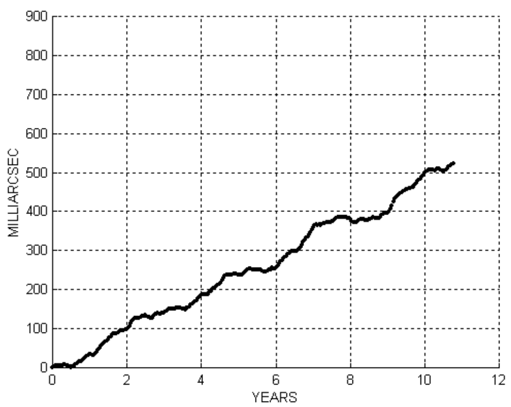

*by adding the geodetic precession of the orbital plane of an Earth satellite in the EPOS orbital estimator.

OLD 2004 ANALYSIS OF THE LAGEOS ORBITS USING THE NASA ORBITAL ESTIMATOR **GEODYN**

Each point corresponds to a different GRACE Earth gravity model

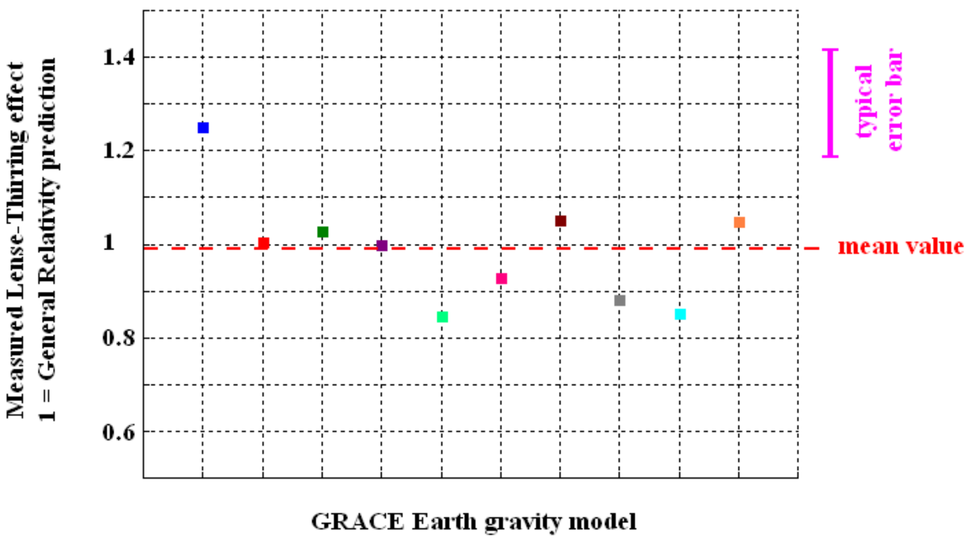

In 2008 Ries et al. presented *independent* results for the measurement of frame.draggging by spin using LAGEOS, LAGEOS 2 and the GRACE Earth's gravity models.
John Ries (UT Austin) error budget is of about 12 %.

Recent Analysis with Geodetic Satellites Summary

- LT measurements:

Totally ndependent Analysis by GFZ-Potsdam

Model	LT (mas/a)	Error (%)
EIGEN-6C	44.9 ± 0.2	6.9
EIGEN-6C w/o TVG	46.5 ± 0.2	3.5
EIGEN-6Sp.34	44.5 ± 0.2	7.6
EIGEN-51C	42.1 ± 0.2	12.7
EIGEN-GRACE03S	51.4 ± 0.2	6.6

USING THE 3 OBSERVABLES PROVIDED BY THE 3 NODES OF *LAGEOS, LAGEOS 2* AND *LARES* WE ELIMINATE THE 2 UNCERTAINTIES DUE TO *J2* AND *J4* AND MEASURE FRAME-DRAGGING

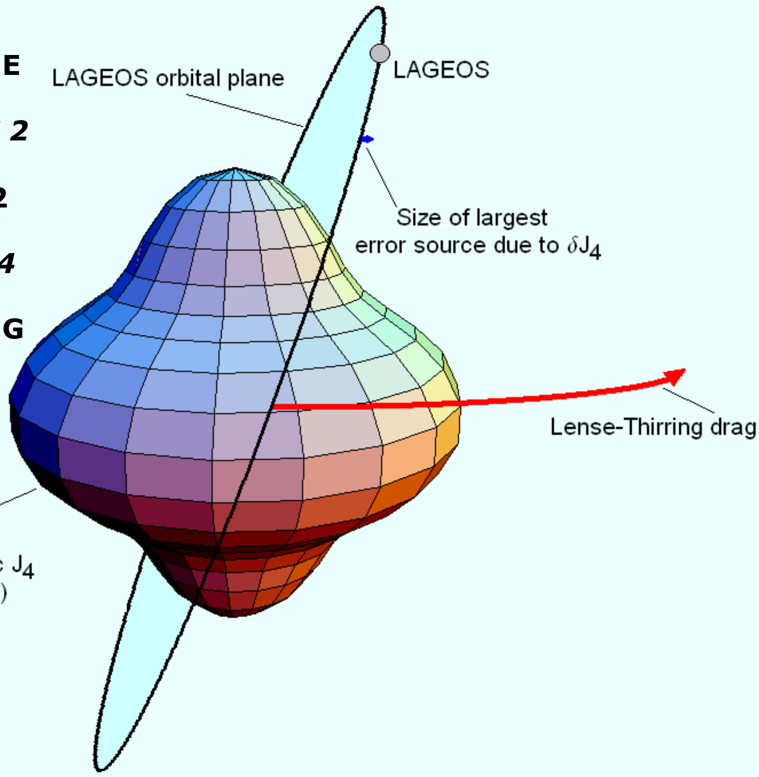

Using LARES +LAGEOS, LAGEOS 2 and the GRACE determinations of the Earth gravitational field we can measure the frame-dragging effect and eliminate the uncertainties in J2 and J4.

Even zonal harmonics, of degree even and zero order, are the axially symmetric deviations of the Earth potential (of even degree) from spherical symmetry.

EVEN ZONAL HARMONICS

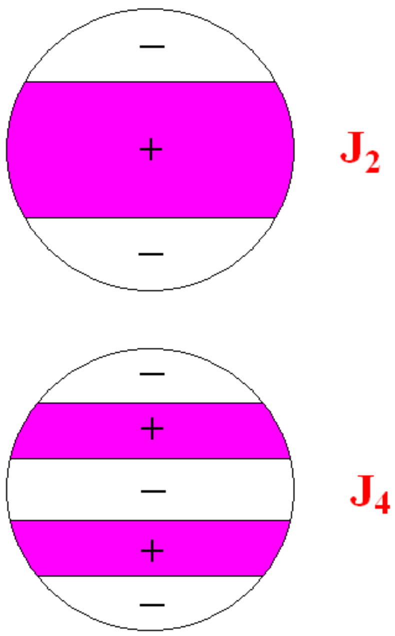

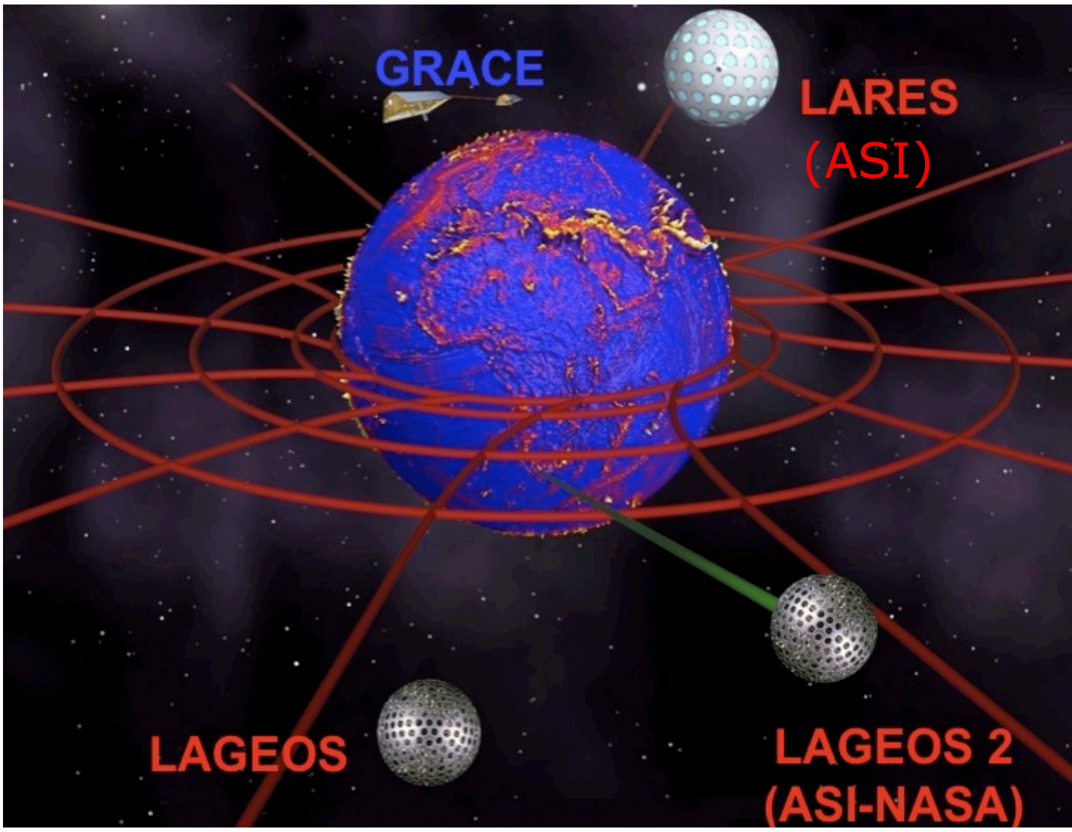

Equation describing the classical rate of change of the node of a satellite as a function of its orbital parameters, a,I, e, and Earth's parameters: mass, radius and even zonal harmonics J2, J4, ...

$$\dot{\Omega}_{Class} = -\frac{3}{2}\, n\, \frac{\cos I}{(1-e^2)^2} \left\{ J_2 \left(\frac{R_\oplus}{a}\right)^2 + J_4 \left(\frac{R_\oplus}{a}\right)^4 \left[\frac{5}{8}\,(7\,\sin^2 I - 4)\,\frac{(1+\frac{3}{2}e^2)}{(1+e^2)^2}\right]\right\}$$

In order to measure the Lense-Thirring effect this classical node precession must be accurately enough modeled (i.e., its behavior must be predicted on the basis of the available physical models), i.e., it must be modeled at the level of a milliarcsec compared to the Lense-Thirring effect (of size of about 31 milliarcsec

Every quantity in this equation can be determined accurately enough via satellite laser ranging to LAGEOS, LAGEOS 2 and LARES for a 1 % measurement of the Lense-Thirring effect, apart from the even zonal harmonics J2, J4, … ,

GRAVITATIONAL ERRORS

Using the Earth gravitational model EIGEN-GRACE02S (February 2004), based on 111 days of GRACE observations, i.e., propagating the uncertainties of EIGEN-GRACE02S published by GFZ Potsdam on the nodes of LAGEOS, LAGEOS 2 and LARES and their combination, we find a total error of 1.4 %.

In particular we have calculated the error induced by the uncertainty of each even zonal harmonic up to degree 70: after degree 26 the error is negligible.

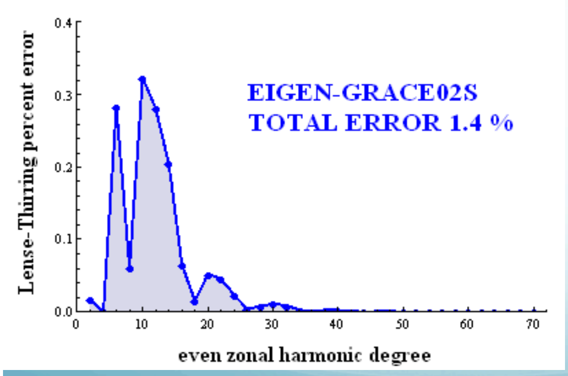

By the time of the LARES data analysis (2012-2015) we can assume an improvement in the GRACE Earth gravity field models of about one order of magnitude, thanks to much longer GRACE observations with respect to 110 days of EIGEN-GRACE02S and also to GOCE (2008).

GRAVITATIONAL ERRORS

Standard technique in space geodesy to estimate the reliability of the published uncertainties of an Earth gravity model: take the difference between each harmonic coefficient of that model with the same harmonic coefficient of a differnt model and compare this difference with the published uncertainties. Let us take difference between each harmonic of the EIGEN-GRACE02S (GFZ Potsdam) model minus the same harmonic in the GGM02S (CSR Austin) model. CAVEAT: in order to use this technique, one must difference models of comparable accuracy, i.e., models that are indeed comparable, or use this method to only evaluate the less accurate model!

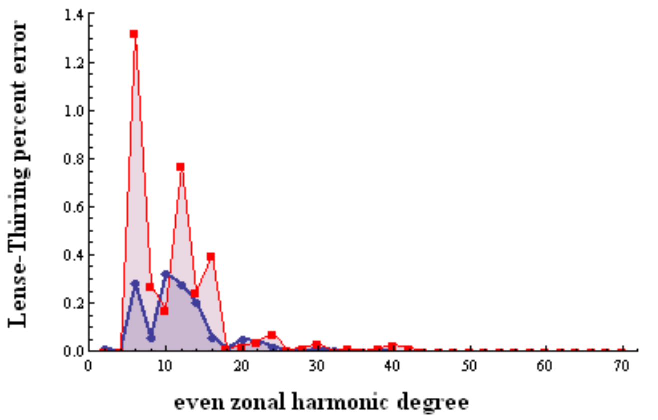

In Blue: percent errors in the measurement of the Lense-Thirring effect for EIGEN-GRACE02S for each even zonal

In Red: percent errors in the measurement of the Lense-Thirring effect using the difference between EIGEN-GRACE02S and GGM02S for each even zonal

GRAVITATIONAL ERRORS

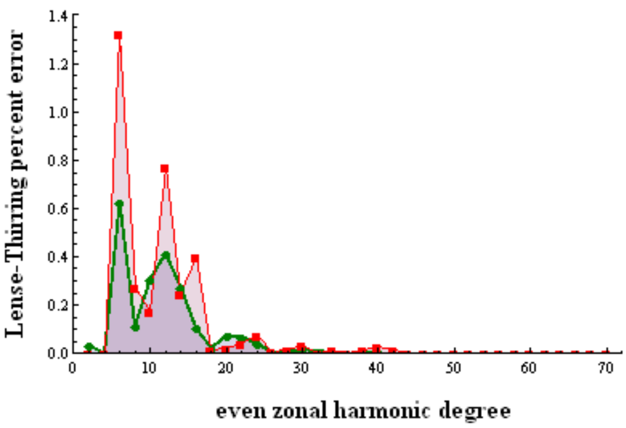

In Green: percent errors in the measurement of the Lense-Thirring effect for GGM02S for each even Zonal harmonic

In Red: percent errors in the measurement of the Lense-Thirring effect Using the difference between EIGEN-GRACE02S and GGM02S for each even zonal harmonic

Parameter	Nominal value	1-Sigma
GM	0.3986004415E+15	8E+05
C20	-.484165112E-03	2.5E-10
C40	0.539968941E-06	0.12280000E-11
C60	-.149966457E-06	0.73030000E-12
C80	0.494741644E-07	0.53590000E-12
C10 0	0.533339873E-07	0.43780000E-12
C20-dot	0.116275500E-10	0.01790000E-11
C40-dot	0.470000000E-11	0.33000000E-11
Cr LAGEOS 1	1.13	0.00565
Cr LAGEOS 2	1.12	0.0056
Cr LARES	Cr_L	0.0054

Main parameters of the Monte Carlo simulations (100 simulations) GFZ
I. C. et al., Class. and Quantum Grav., 2013

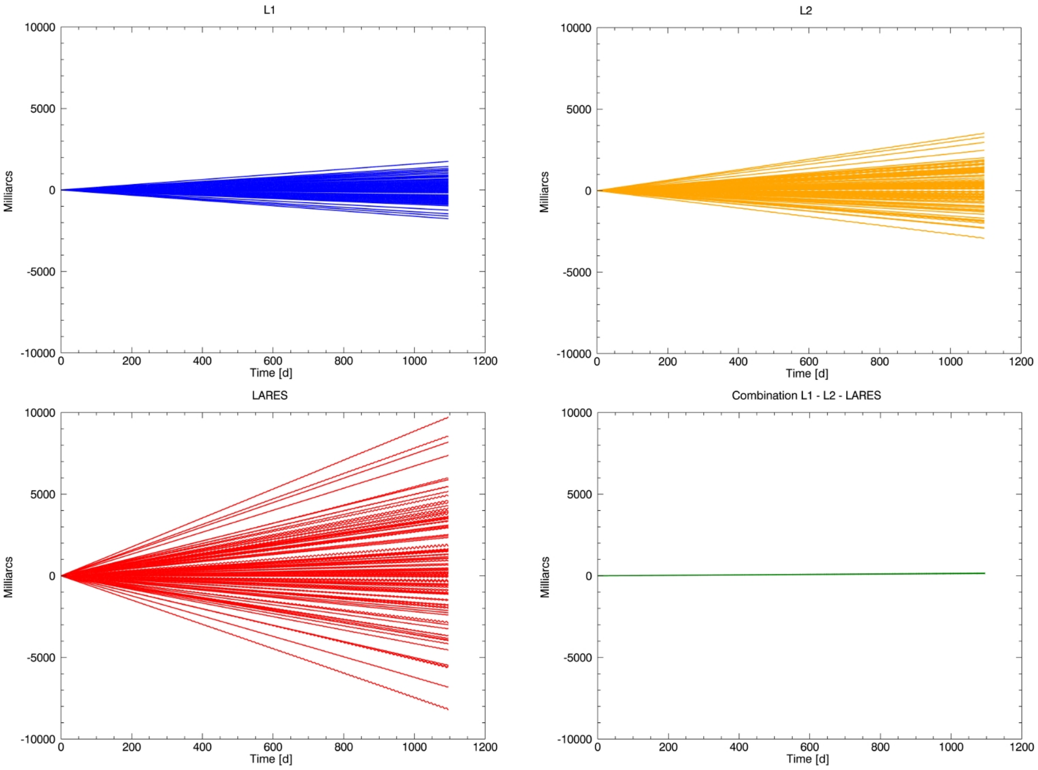
L1
L2
LARES
Combination L1 - L2 - LARES
Milliarcs
Time [d]

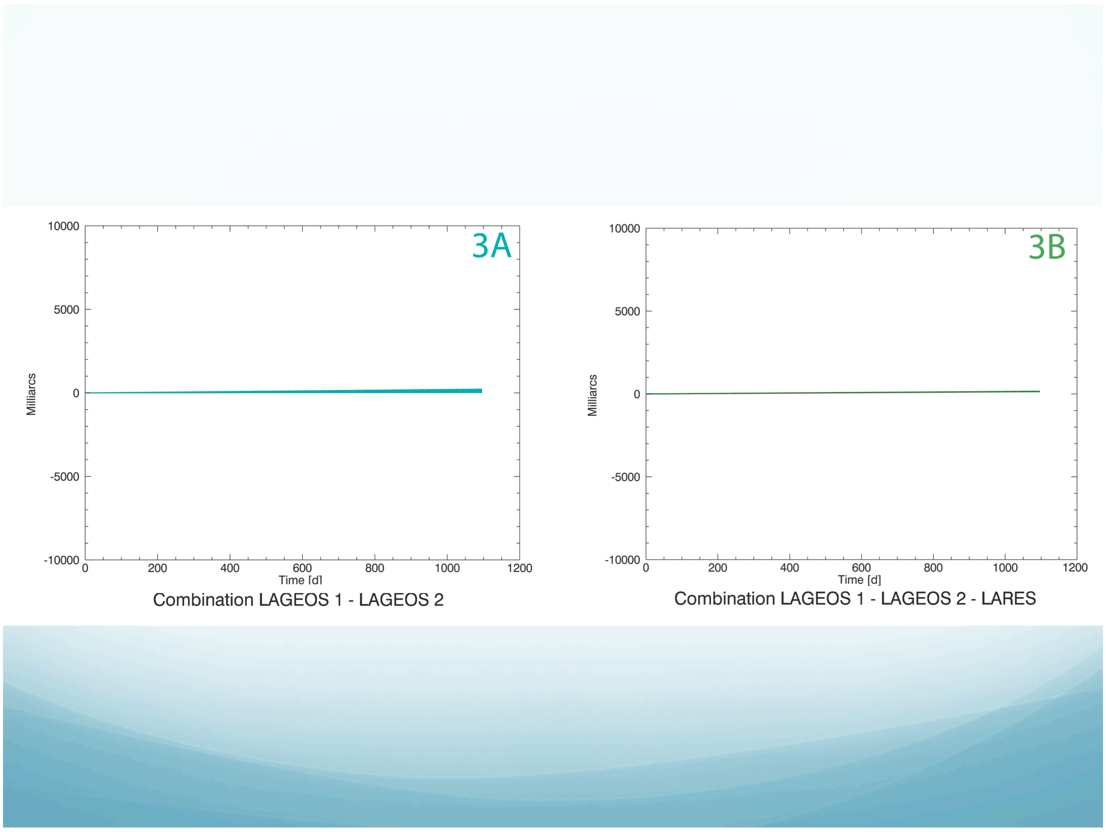
3A
3B
Milliarcs
Time [d]
Combination LAGEOS 1 - LAGEOS 2
Combination LAGEOS 1 - LAGEOS 2 - LARES

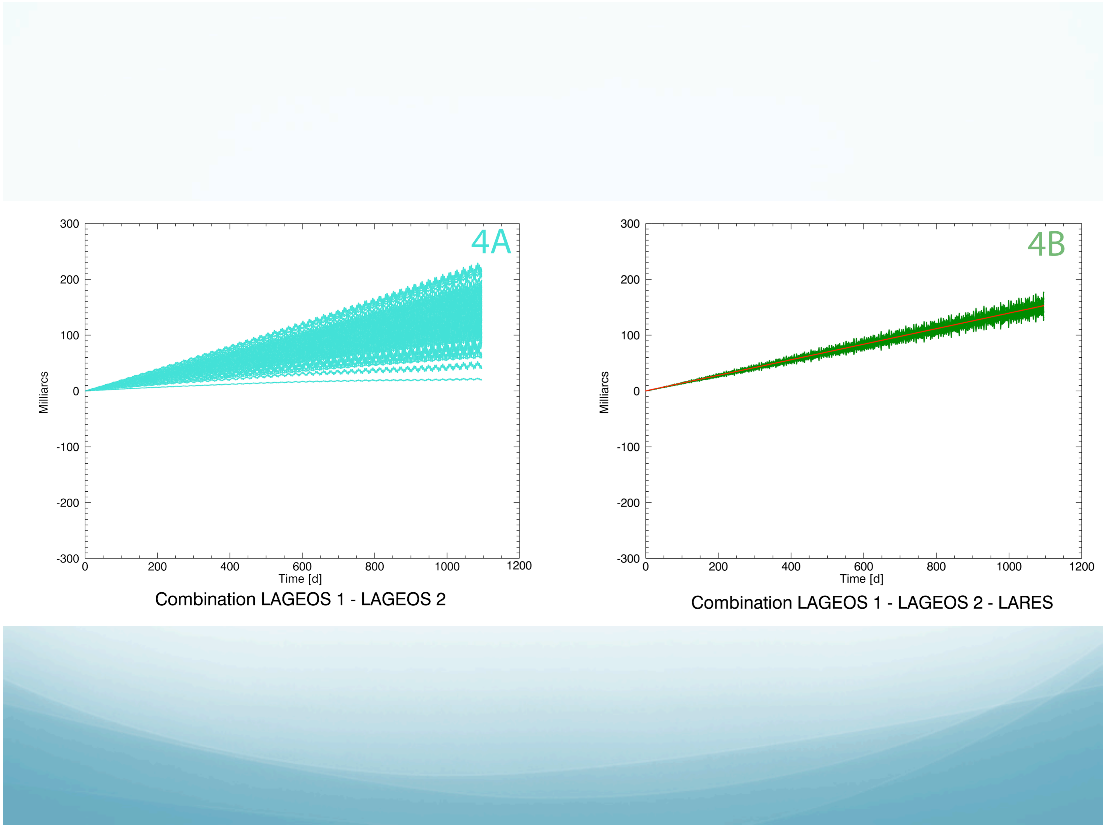
4A
4B
Milliarcs
Time [d]
Combination LAGEOS 1 - LAGEOS 2
Combination LAGEOS 1 - LAGEOS 2 - LARES

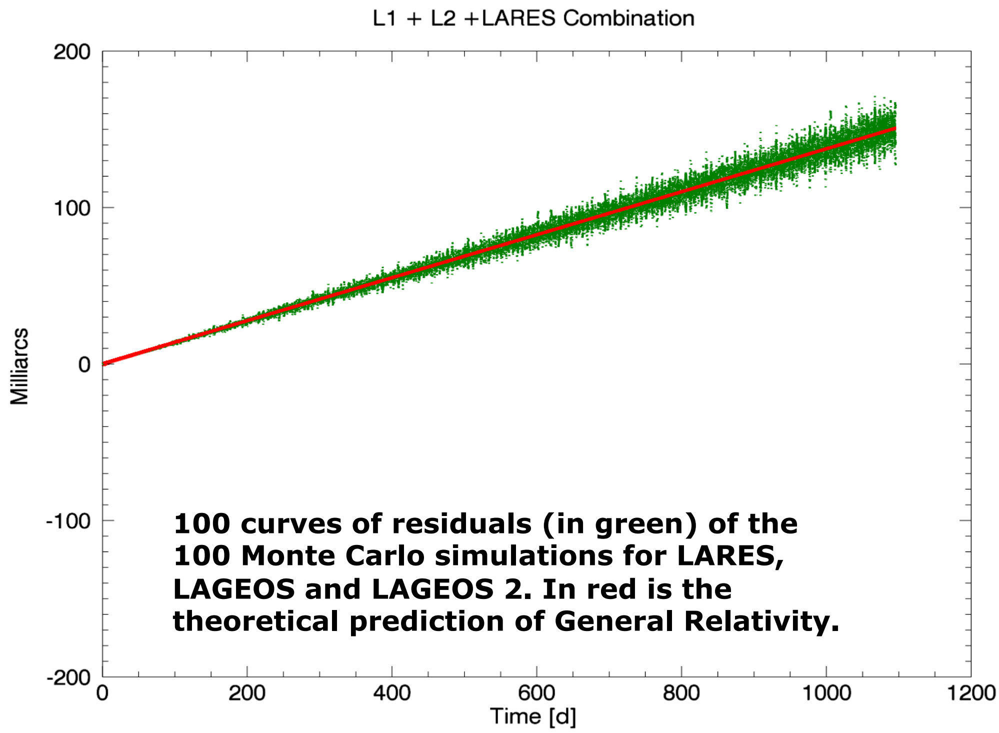
L1 + L2 +LARES Combination
Milliarcs
Time [d]
100 curves of residuals (in green) of the
100 Monte Carlo simulations for LARES,
LAGEOS and LAGEOS 2. In red is the
theoretical prediction of General Relativity.

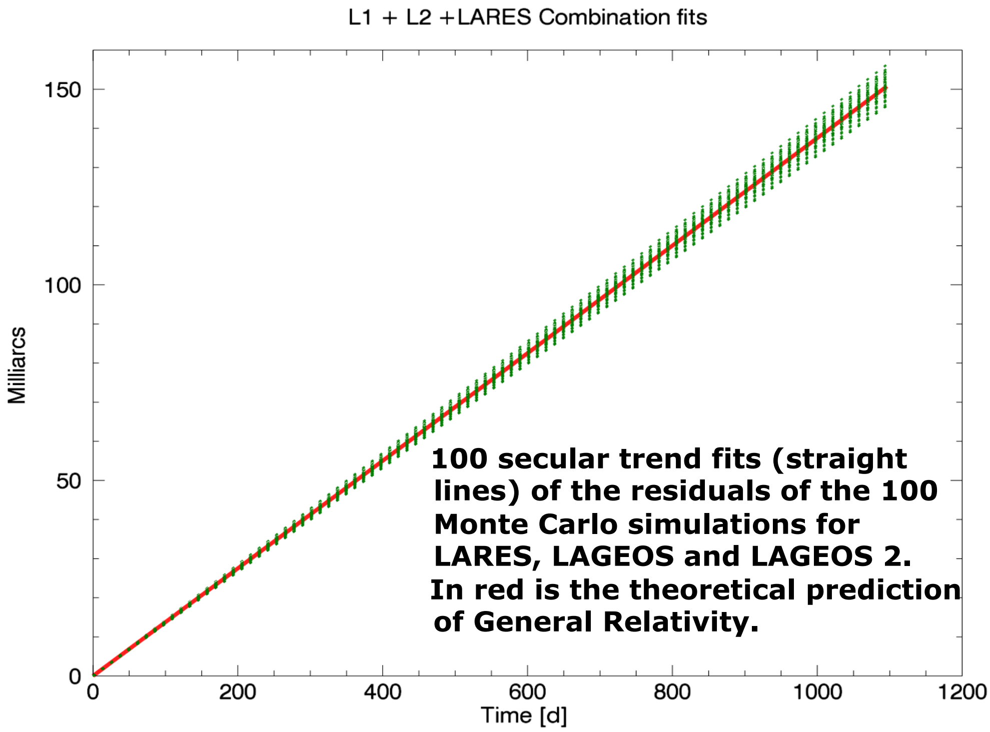
L1 + L2 +LARES Combination fits
Milliarcs
Time [d]
0
50
100
150
0
200
400
600
800
1000
1200
100 secular trend fits (straight lines) of the residuals of the 100 Monte Carlo simulations for LARES, LAGEOS and LAGEOS 2.
In red is the theoretical prediction of General Relativity.

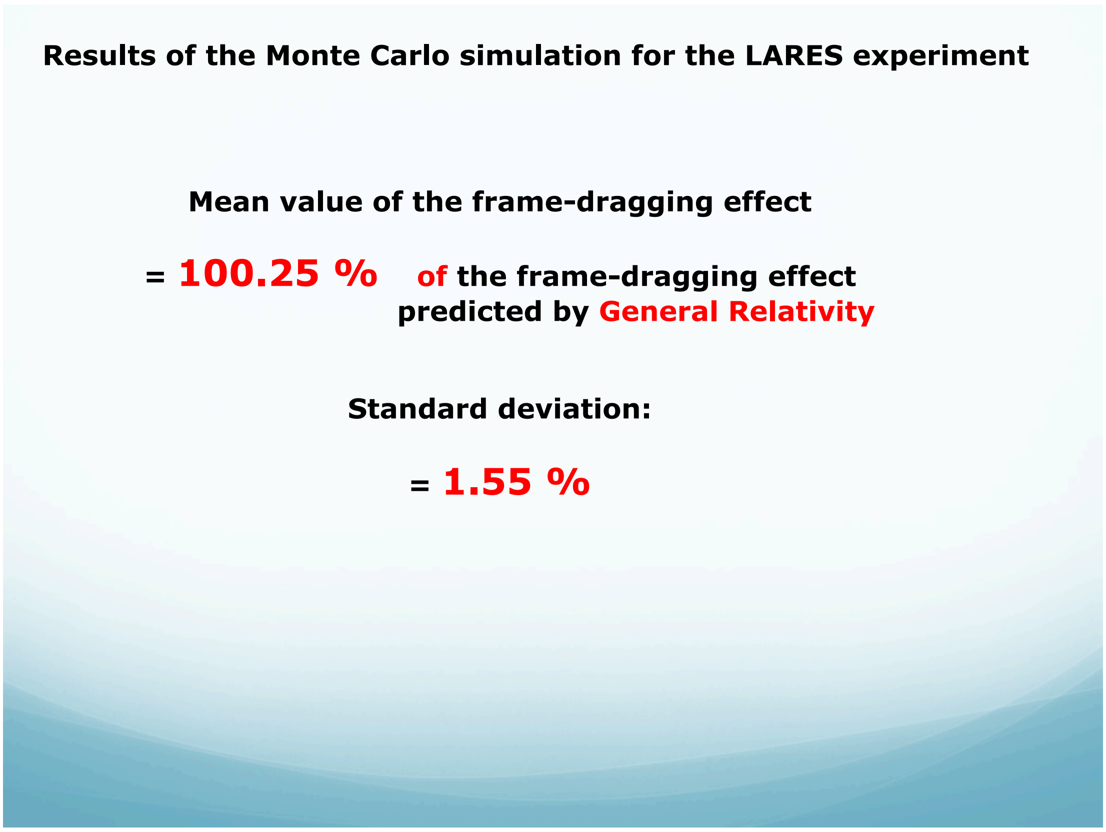
Results of the Monte Carlo simulation for the LARES experiment
Mean value of the frame-dragging effect
= 100.25 % of the frame-dragging effect
predicted by General Relativity
Standard deviation:
= 1.55 %

Current orbital analyses of the LARES observations

I.C. et al., Eur. Phys. J. Plus (2012) 127: 133

Before LARES, with a *residual mean* along-track acceleration of less than 4 × 10^{-13} m/s^2, the smallest residual mean accelerations were measured on the LAGEOS satellites. The *mean residual* along-track acceleration was on the LAGEOS satellites at a level of about 10 to 20 × 10^{-13} m/s^2. The orbit of the LAGEOS satellites is mainly affected by thermal thrust accelerations, i.e., by the Yarkovsky effect and by the Earth-Yarkovsky or Rubincam-Yarkovsky effect. For a comparison, the *mean residual* acceleration of the Starlette laser-ranged satellite is of the order of 400 × 10^{-13} m/s^2.

The best drag-free satellite is at a level of the order of 500 x 10^{-13} m/s^2.

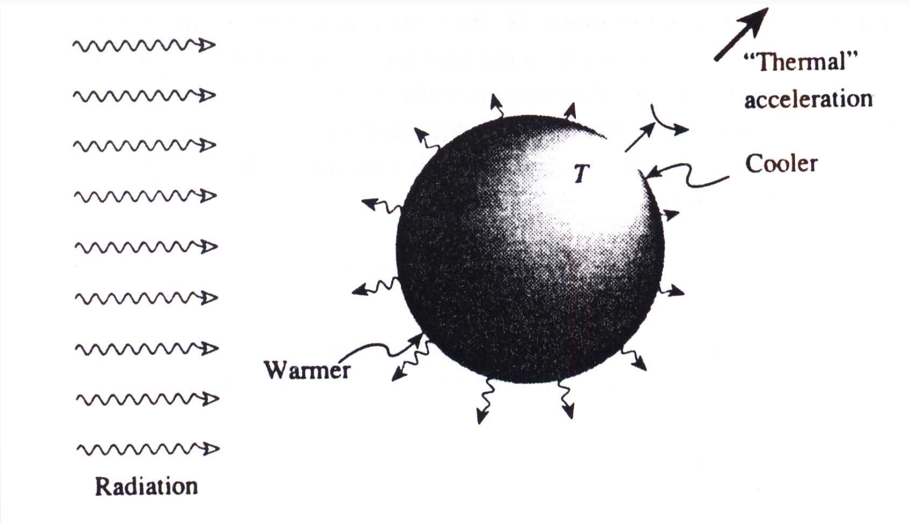

Yarkovsky effect or thermal acceleration: thermal thrust resulting from the anisotropic latitudinal temperature distribution over the satellite's surface caused by solar heating.

Earth Yarkovsky or Rubincam-Yarkovsky effect: infrared radiation from Earth is absorbed by the retro-reflectors; due to their thermal inertia and to the rotation of the satellite, a latitudinal temperature gradient develops. The corresponding thermal radiation causes an along-track acceleration in the direction opposite to the satellite's (LAGEOS) motion.

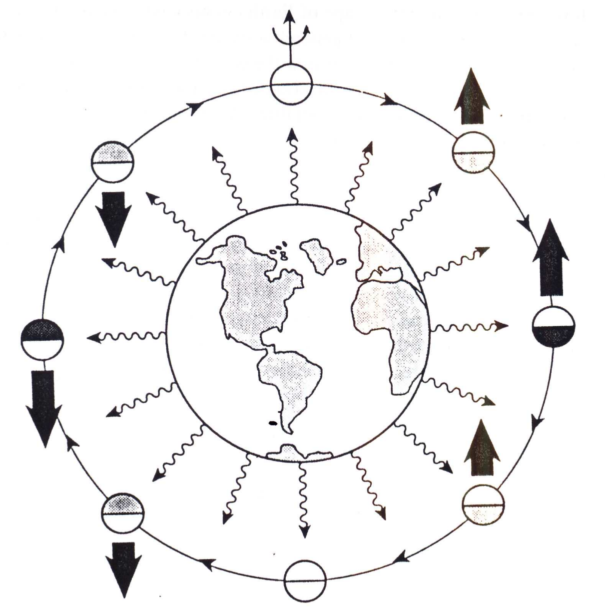

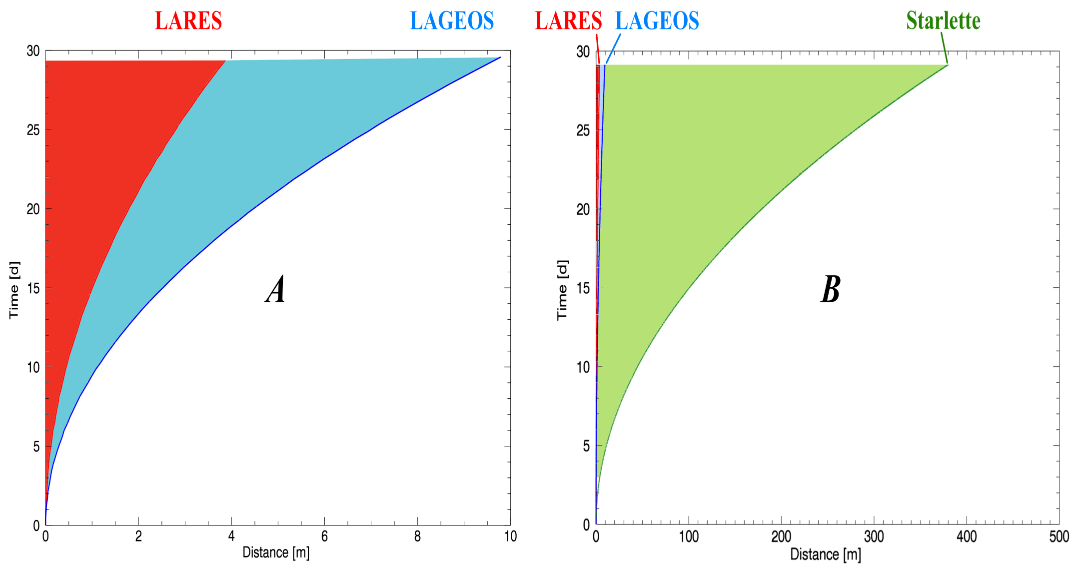

Along-track displacement from an ideal geodesic orbit, after modeling non-gravitational perturbations, due to the *residual mean* along-track accelerations observed on LARES, LAGEOS and STARLETTE.

Current orbital analyses of the LARES observations

I.C. et al., Eur. Phys. J. Plus (2012) 127: 133

The smaller residual mean acceleration of LARES, in spite of the larger effects of atmospheric drag, has been achieved by minimizing the effect of thermal thrust. This has been achieved by the LARES special design, because:

(1) LARES has the smallest cross-sectional-area to mass ratio than other artificial satellite and even of LAGEOS (a factor almost 3 times smaller than LAGEOS). LARES is the single orbiting body in the Solar System with highest mean density.

(2) LARES is much smaller than LAGEOS (18 cm radius versus 30 cm radius for LAGEOS)

(3) LARES has higher thermal conductivity, since it is a solid one-piece sphere. In contrast, LAGEOS is constructed from three separate pieces that decrease thermal conductivity.

(4) The effect of the thermal acceleration due to the retro-reflectors (which are the main source of Earth and solar Yarkovsky effects) is smaller because the surface area of the retro-reflectors relative to the total area is smaller on LARES (about 26% of the total surface area) than on LAGEOS (about 43%).

Current orbital analyses of the LARES observations

I.C. et al., Eur. Phys. J. Plus (2012) 127: 133

- After removing the known LARES orbital perturbations, its orbit shows the smallest deviations than any other satellite from the geodesic motion, i.e., the purely gravitational orbit predicted by General Relativity. These deviations are due to *un-modelled* or *mismodelled* non-gravitational forces acting on a satellite.

- **Geodesic motion is at the very basis of General Relativity.**

LARES is already being used (by CSR-UT Austin) to improve the determination of the 'classical' part of the Earth gravitational field, i.e., to improve some of lowest degree harmonics describing the 'shape' of the Earth gravitational field.

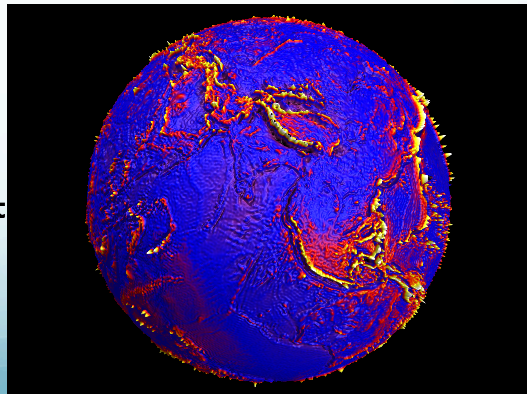

Conclusions

LAGEOS and LAGEOS 2, with GRACE, measured frame-dragging with an accuracy of about 10%. This was used to set limits on the Chern-Simons mass and related String Theories.

LARES already shows an outstanding behaviour for testing General Relativity and gravitational physics. LARES-type satellites could well test other fundamental physics effects and much improve the existing limits on C-S mass.

After a few years of laser-ranging data of the LARES satellite, together with LAGEOS and LAGEOS 2 and with the future improved Earth's gravity models, we would be able to measure the frame-dragging effect with accuracy of about 1%, with other implicational for fundamental physics such as improving the limits on C-S mass and placing further limits on String Theories equivalent to Chern-Simon gravity.

Some of the main papers published since 2004 on the measurement of frame-dragging with LAGEOS and LAGEOS 2.

Ciufolini and E. Pavlis, "A confirmation of the general relativistic prediction of the Lense–Thirring effect", **Nature (Letters),** 431, 958-960 (2004).

Ciufolini, "Frame-Dragging and Its Measurement" *I SIGRAV School on General Relativity*, Villa Mondragone Monte Porzio Catone, Roma, Italy September, 2002. Ciufolini et al. eds. Institute of Physics Publishing, 27, 2004. **Invited (Plenary)**.

Lucchesi, I. Ciufolini, et al., "LAGEOS II perigee rate and eccentricity vector excitations residuals and the Yarkovsky–Schach effect", **Planetary and Space Science** 52, 699-710 (2004).

Ciufolini, A. Paolozzi, D.G. Currie and E.C. Pavlis "LARES/WEBER-SAT, Frame-Dragging and Fundamental Physics", Proceedings of *Frontier Science 2004*, Physics and Astrophysics in Space, Frascati, Italy 2004. INFN Pub., Frascati, 499, 2004. **Invited Plenary Talk**.

Ciufolini, E. Pavlis and R. Peron, "Determination of Frame–Dragging Using the Earth Gravity Models From Champ and Grace", **New Astronomy**, 11, 527-550, 2006.

Ciufolini and E. Pavlis, "On the Measurement of the Lense-Thirring effect using the nodes of the LAGEOS satellites, **New Astronomy**, 10, 636-651, 2005.

Ciufolini, "Gravitomagnetism" in Towards New Milestones in Our Quest to go Beyond the Standard Model, Proc. of the 43th International School of Subnuclear Physics 2005, Erice, Italy, August-September, 2005. (World Scientific, 2007) 146-197. **Invited Plenary Talk.**

Pavlis, I. Ciufolini and R. Koenig, "Recent Results from SLR Experiments in Fundamental Physics", Proc. 15th International Laser Ranging Workshop, Canberra, Australia, 2006. 1-10. **Invited talk.**

Ciufolini, "On the orbit of the LARES satellite", to be published (http://xxx.lanl.gov/abs/gr-qc/0609081), 2007.

Ciufolini, "Dragging of Inertial Frames", **Nature (Review),** 449, 41-47 (2007).

Ignazio Ciufolini, Antonio Paolozzi, Erricos C. Pavlis, John C. Ries, Rolf Koenig, Richard A. Matzner, Giampiero Sindoni and Hans Neumayer, "*Towards a One Percent Measurement of Frame-Dragging by Spin with Satellite Laser Ranging to LAGEOS, LAGEOS 2 and LARES and GRACE Gravity Models*", ***Space Science Reviews***, **148**, 71-104 (2009).

J.C. Ries. Relativity in satellite laser ranging. In Bulletin of the American Astronomical Society. IAU Symposium 261. American Astronomical Society, 2009. Presentation number 14.02.

J.C. Ries, R.J. Eanes, and M.M. Watkins. Confirming the frame-dragging effect with satellite laser ranging. In Proceedings of the 16th International Workshop on Laser Ranging, Vol. 1. Edited by S. Schillak. Space Research Centre, Polish Academy of Sciences, Warszawa, 2009. p. 128.

J.C. Ries and R.J. Eanes. Confirming the Lense–Thirring “frame-dragging” effect with satellite laser ranging and grace gravity models. In Bulletin of the American Astronomical Society. DDA 42nd Meeting, Austin, Texas. Presentation number 03.02. American Astronomical Society. 2011.

J.C. Ries and R.J. Eanes. Confirming the Lense–Thirring orbital precession with satellite laser ranging to the lageos satellites and grace gravity models. In Bulletin of the American Astronomical Society. AAS 219th Meeting, Austin, Texas. Presentation number 122.04. American Astronomical Society. 2012.

Ignazio Ciufolini, *“Lunar Laser Ranging, Gravitomagnetism and Frame-Dragging”,* ***New Astronomy***, **15**, 332-337 (2010).

Ignazio Ciufolini, Erricos C. Pavlis, John C. Ries, Rolf Koenig, Giampiero Sindoni, Antonio Paolozzi and Hans Neumayer, “Test of Gravitomagnetism with the LAGEOS and GRACE Satellites”, in: *General Relativity and John Archibald Wheeler*, I. Ciufolini and R. Matzner eds., 371-434 (***Springer***, 2010).

Ignazio Ciufolini, Antonio Paolozzi, Erricos C. Pavlis, John C. Ries, Rolf Koenig and Richard Matzner, “The LARES Relativity Experiment”, in: *General Relativity and John Archibald Wheeler*, I. Ciufolini and R. Matzner eds., 467-492 (***Springer***, 2010).

Antonio Paolozzi, Ignazio Ciufolini and Cristian Vendittozzi, *“Engineeristic and Scientific Aspects of LARES Satellite”*, ***Acta Astronautica,*** 69, 127-134, 2011.

Ciufolini and R. Matzner *“Chapter I, Introduction to Frame-Dragging, Gravitational Waves and Gravitational Tests”*, in *General Relativity and John Archibald Wheeler*, I. Ciufolini and R. Matzner eds., 1-6 (***Springer***, 2010). http://www.springer.com/astronomy/general+relativity/book/978-90-481-3734-3

Ignazio Ciufolini, Antonio Paolozzi, Erricos C. Pavlis, John Ries, Rolf Koenig, Richard Matzner, Giampiero Sindoni and Hans Neumayer, “Testing Gravitational Physics with Satellite Laser Ranging”, **The European Physical Journal Plus**, **126**, 72 (2011).

J. C. Ries, I. Ciufolini, E. C Pavlis, A. Paolozzi, R. Koenig, R. A. Matzner, G. Sindoni and H. Neumayer, The Earth’s frame-dragging via laser-ranged satellites, **European Physics Letters 96,** 30002--1-5 (2011).

Ignazio Ciufolini, Antonio Paolozzi, Erricos C. Pavlis, John Ries, Rolf Koenig, Richard Matzner, “LARES, Laser-Ranged Satellite for Testing General Relativity”, **Space Research Today 182**, 11-25 (2011).

Ignazio Ciufolini, Antonio Paolozzi, Claudio Paris, Overview of the LARES Mission: orbit, error analysis and technological aspects, **Journal of Physics, 354** 012002 (2012).

Ignazio Ciufolini, Erricos C. Pavlis, Antonio Paolozzi, John Ries, Rolf Koenig, Richard Matzner, Giampiero Sindoni, Karl Hans Neumayer, “Phenomenology of the Lense-Thirring effect in the Solar System: Measurement of frame-dragging with laser ranged satellites”, **New Astronomy**, **17**, 341-346 (2012).

Ignazio Ciufolini, Antonio Paolozzi,Erricos Pavlis,John Ries,Vahe Gurzadyan,Rolf Koenig,Richard Matzner, Roger Penrose,Giampiero Sindoni “Testing General Relativity and gravitational physics using the LARES satellite” **The European Physical Journal Plus 127**:133 (2012).

V. G. Gurzadyan, I. Ciufolini, S. Sargsyan, G. Yegorian, S. Mirzoyan and A. Paolozzi, Satellite probing General Relativity and its extensions and Kolmogorov analysis, **Eur. Phys. Lett., 102**, 60002 (2013)

A. Paolozzi and I. Ciufolini, LARES succesfully launched in orbit: satellite and mission description. **Acta Astronautica** (2013) http://dx.doi.org/10.1016/j.actaastro.2013.05.011 .

I. Ciufolini, Time travel, clock puzzles and their experimental tests. **Eur. Phys. J.** Web of Conferences **58**, 01005 (2013) http://dx.doi.org/10.1051/epjconf/20135801005 .

I. Ciufolini, Moreno Monge B., Paolozzi A., Koenig R., Sindoni G., Michalak G., and Pavlis E. Monte Carlo simulations of the LARES space experiment to test general relativity and fundamental physics **Classical and Quantum Gravity 30** (235009) (2013) doi:10.1088/0264-9381/30/23/235009 .

Ignazio Ciufolini, Antonio Paolozzi, Rolf Koenig, Erricos C. Pavlis, John Ries, Richard Matzner, Vahe Gurzadyan, Roger Penrose, Giampiero Sindoni, Claudio Paris, Fundamental Physics and General Relativity with the LARES and LAGEOS satellites. **Nuclear Physics B** (Proc. Suppl.) **243–244,** 180–193 2013.

THE END

Thank you to the organizers for inviting me at this interesting conference on General Relativity and Gravitation in Hirosaki.

IC

“Quantum interferometry in Chern-Simons gravity”

by Kei Yamada

[JGRG23(2013)110602]

Quantum Interferometry in Chern-Simons Gravity

Kei Yamada (Hirosaki Univ.)

w/ Okawara-san & Asada-san

Contents

Contents

- COW experiment &
  Chern-Simons metric at 1PN order
- Method for Neutron interferometry
- Phase shift by Chern-Simons gravity
- Summary

Introduction

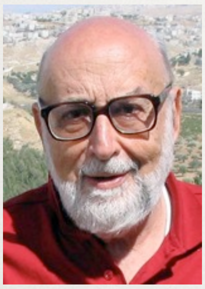 

Higgs boson was detected by ATLAS & CMS.

However

Particle accelerator energy is nearly saturated.

Non-accelerator Experiments

COW Experiment

"Observation of Gravitationally Induced Quantum Interference"
R. Colella, A. W. Overhauser, & S. A. Werner

Measuring the phase difference
between two paths in Newton Gravity

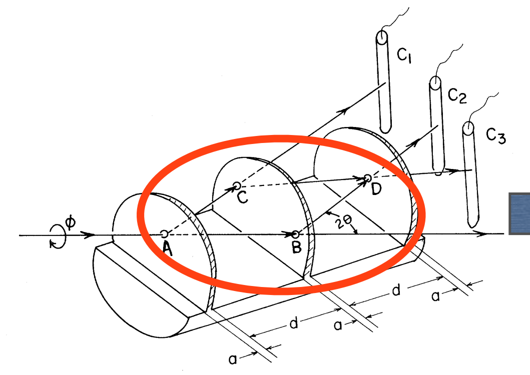

FIG. 1. Schematic diagram of the neutron interferometer and ^{3}He detectors used in this experiment.

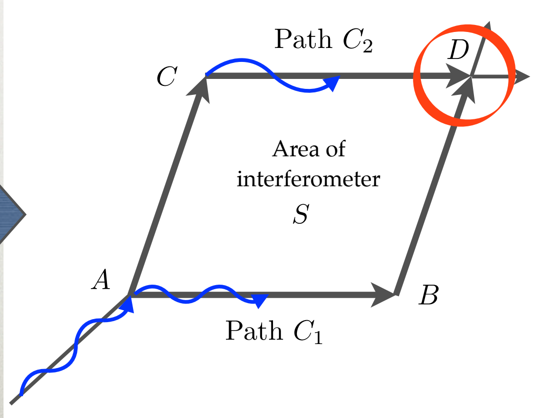

Previous Works

- L. A. Page, Phys. Rev. Lett. 35, 543 (1975)
- J. Anandan, Phys. Rev. D 15, 1448 (1977)
- M. Dresden and C. N. Yang, Phys. Rev. D 20, 1846 (1979)
- J. J. Sakurai, Phys. Rev. D 21, 2993 (1980)
- L. Parker, Phys. Rev. D 22, 1922 (1980)
- Y. N. Obukhov, Phys. Rev. Lett. 86, 192 (2001)
- X. Huang and L. Parker, Phys. Rev. D 79, 024020 (2009)
- K. Konno and R. Takahashi, Phys. Rev. D 85, 061502(R) (2012).
- J. Kuroiwa, M. Kasai, and T. Futamase, Phys. Lett. A 182, 330 (1993).
- S. Wajima, M. Kasai, and T. Futamase, Phys. Rev. D 55, 1964 (1997). etc.

Hirosaki Papers!

Chern-Simons Gravity

- Correction to the Einstein-Hilbert action

$$S_{\rm CS} = \frac{1}{16\pi G}\int d^4x \frac{1}{4} f R^\star R \qquad f\text{: Time-dependent}$$

- New PPN term at 1PN order (Non-dynamical CS gravity)

$$g_{0i}^{\rm (CS)} \equiv g_{0i} - g_{0i}^{\rm (GR)}$$

$$\boxed{g_{0i}^{\rm (CS)} \simeq 2\sum_A \frac{\dot{f}}{r_A}\left[\frac{m_A}{r_A}(v_A \times n_A)^i - \frac{J_A^i}{2r_A^2} + \frac{3}{2}\frac{(J_A \cdot n_A)}{r_A^2} n_A^i\right]}$$

[S. Alexander & N. Yunes, PRL 99, 241101 (2007)]

What happens to phase shift by CS gravity

Sun-Earth System

A=2 (Solar system)

v_S and J_S are zero

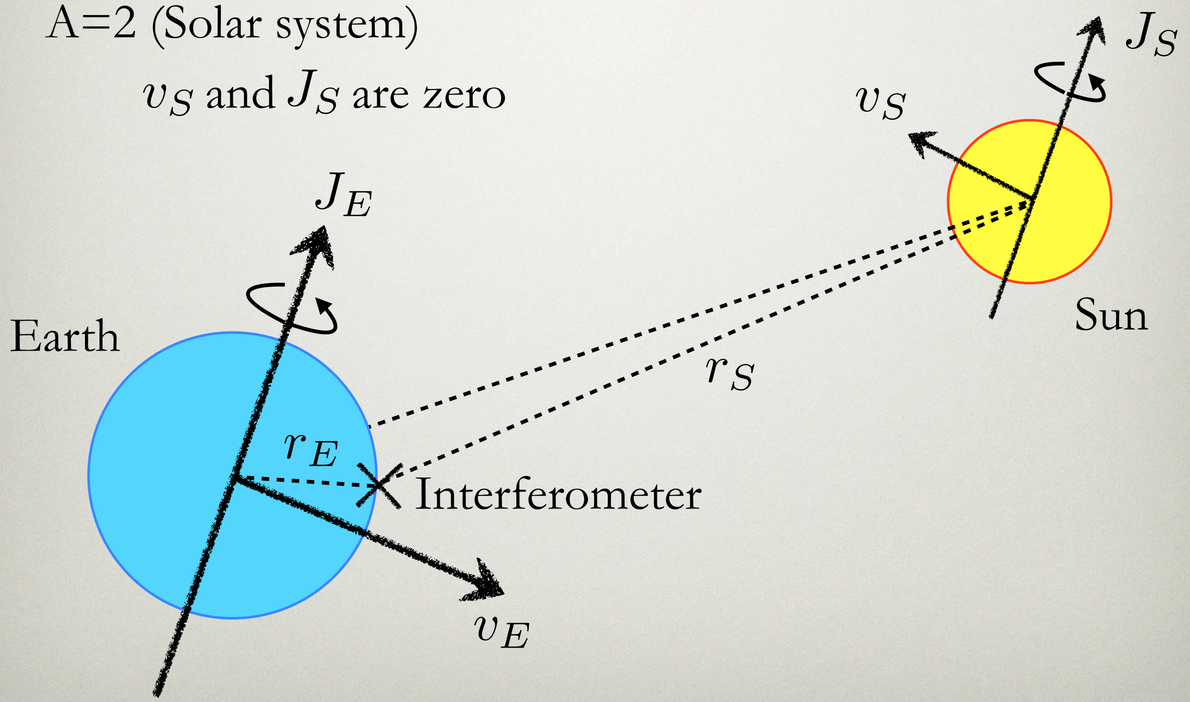

Goal of Study

- Quantum interference effects by CS gravity.
  - Daily & Seasonal variations
  - Latitude effect
- Place a constraint on CS gravity

Contents

- COW experiment &
  Chern-Simons metric at 1PN order
- Method for Neutron interferometry
- Phase shift by Chern-Simons gravity
- Summary

Hamiltonian of Particle

- Weak-field approx.

$$g_{\mu\nu} = \eta_{\mu\nu} + h_{\mu\nu}$$

- Slow-motion approx.

$$L = -mc^2 \left(1 + \frac{1}{2}h_{00} + h_{0i}\frac{\dot{x}^i}{c} - \frac{1}{2}\frac{(\dot{x}^i)^2}{c^2}\right) + \mathrm{O}(c^{-3})$$

- Hamiltonian

$$H = mc^2 + \frac{1}{2m}\left(\vec{p} + mc\vec{h}_0\right)^2 + \frac{1}{2}mc^2 h_{00}$$

$$\vec{h}_0 = h_{0i}, \quad \vec{p} = m\dot{x}^i$$

Wave Function

$$H = mc^2 + \frac{1}{2m}\left(\vec{p} + mc\vec{h}_0\right)^2 + \frac{1}{2}mc^2 h_{00}$$

- Schrödinger Eq.

$$i\hbar\frac{\partial}{\partial t}\psi = \left(\frac{1}{2m}\left(\vec{p} + mc\vec{h}_0\right)^2 + \frac{1}{2}mc^2 h_{00}\right)\psi$$

- Wave function

$$\psi = \psi_0 \exp\left[\left(-i\frac{mc^2}{2\hbar}\int h_{00}dt\right) + \underbrace{\left(-i\frac{mc}{\hbar}\int \vec{h}_0 \cdot d\vec{r}\right)}_{\text{Frame dragging}}\right]$$

Phase Difference

$$\psi = \psi_0 \exp\left[\left(-i\frac{mc^2}{2\hbar}\int h_{00}dt\right) + \left(-i\frac{mc}{\hbar}\int \vec{h}_0\cdot d\vec{r}\right)\right]$$

$$\Delta_{00} = \frac{mc^2}{2\hbar}\left(\int_{C_1} h_{00}dt - \int_{C_2} h_{00}dt\right)$$

$$\begin{aligned}\Delta &= \frac{mc}{\hbar}\left(\int_{C_1}\vec{h}_0\cdot d\vec{r} - \int_{C_2}\vec{h}_0\cdot d\vec{r}\right)\\ &= \frac{mc}{\hbar}\oint_C \vec{h}_0\cdot d\vec{r}\\ &= \frac{mc}{\hbar}\int_S (\vec{\nabla}\times\vec{h}_0)\cdot d\vec{S}\end{aligned}$$

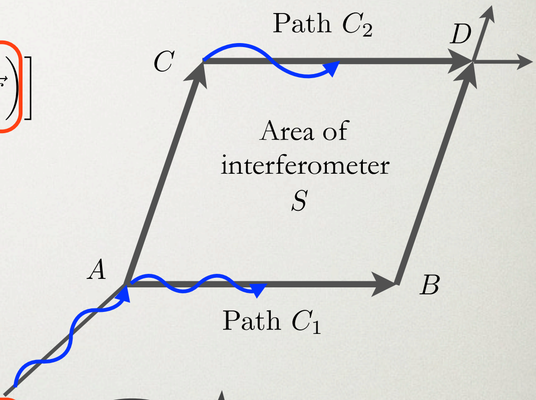

Analogy in Aharonov-Bohm effect

$$\propto \oint_C \vec{A}\cdot d\vec{r} = \int_S (\vec{\nabla}\times\vec{A})\cdot d\vec{S}$$

Contents

- COW experiment &
  Chern-Simons metric at 1PN order
- Method for Neutron interferometry
- Phase shift by Chern-Simons gravity
- Summary

Phase Shift by CS Gravity

Phase difference of vector part: $\Delta = \dfrac{mc}{\hbar}\displaystyle\int_S \boxed{(\vec{\nabla}\times\vec{h}_0)}\cdot d\vec{S}$

$$g_{\mu\nu} = \eta_{\mu\nu} + h^{(\mathrm{GR})}_{\mu\nu} + h^{(\mathrm{CS})}_{\mu\nu} \ @1PN$$

$$h^{(\mathrm{CS})}_{\mu\nu} = g^{(\mathrm{CS})}_{0i} \simeq 2\sum_A \frac{\dot{f}}{r_A}\left[\frac{m_A}{r_A}(v_A\times n_A)^i \boxed{-\frac{J^i_A}{2r_A^2} + \frac{3}{2}\frac{(J_A\cdot n_A)}{r_A^2}n^i_A}\right]$$

$$\nabla\times\left[-\frac{J^i_A}{2r_A^2} + \frac{3}{2}\frac{(J_A\cdot n_A)}{r_A^2}n^i_A\right] = 0.$$

$$\nabla\times g^{(\mathrm{CS})}_{0i} = \sum_A \dot{f}\frac{m_A}{r_A^3}\left[3(v_A\cdot n_A)n^i_A - v^i_A\right]$$

[S. Alexander & N. Yunes, PRL 99, 241101 (2007)]

Phase Shift by CS Gravity

Phase difference of vector part: $\Delta = \dfrac{mc}{\hbar}\displaystyle\int_S \boxed{(\vec{\nabla}\times\vec{h}_0)}\cdot d\vec{S}$

$$g_{\mu\nu} = \eta_{\mu\nu} + h^{(\mathrm{GR})}_{\mu\nu} + h^{(\mathrm{CS})}_{\mu\nu} \ @1PN$$

$$h^{(\mathrm{CS})}_{\mu\nu} = g^{(\mathrm{CS})}_{0i} \simeq 2\sum_A \frac{\dot{f}}{r_A}\left[\frac{m_A}{r_A}(v_A\times n_A)^i \boxed{-\frac{J^i_A}{2r_A^2} + \frac{3}{2}\frac{(J_A\cdot n_A)}{r_A^2}n^i_A}\right]$$

$$\nabla\times\left[-\frac{J^i_A}{2r_A^2} + \frac{3}{2}\frac{(J_A\cdot n_A)}{r_A^2}n^i_A\right] = 0.$$

$$\boxed{\nabla\times g^{(\mathrm{CS})}_{0i} = 2\sum_A \dot{f}\frac{m_A}{r_A^3}\left[3(v_A\cdot n_A)n^i_A - v^i_A\right]}$$

[H. Okawara, KY, & H. Asada, PRL 109, 231101 (2012)]

Phase Shift by CS Gravity

Phase difference of vector part: $\Delta = \frac{mc}{\hbar}\int_S \boxed{(\vec{\nabla}\times\vec{h}_0)}\cdot d\vec{S}$

$$\boxed{\nabla \times g_{0i}^{(\mathrm{CS})} = 2\sum_A \dot{f}\frac{m_A}{r_A^3}[3(v_A\cdot n_A)n_A^i - v_A^i]}$$

$r_E \gg \sqrt{S}$

$$\boxed{\Delta_{(\mathrm{CS})} \simeq 2\dot{f}\frac{mGM_E S}{\hbar c^2 r_E^3}[3(\vec{v}_E\cdot\vec{n}_E)\vec{n}_E - \vec{v}_E]\cdot\vec{N}_I}$$

[H. Okawara, KY, & H. Asada, PRL 109, 231101 (2012)]

Phase Shift by CS Gravity

$$\boxed{\Delta_{(\mathrm{CS})} \simeq 2\dot{f}\frac{mGM_E S}{\hbar c^2 r_E^3}\underline{[3(\vec{v}_E\cdot\vec{n}_E)\vec{n}_E - \vec{v}_E]\cdot\vec{N}_I}}$$

change with time

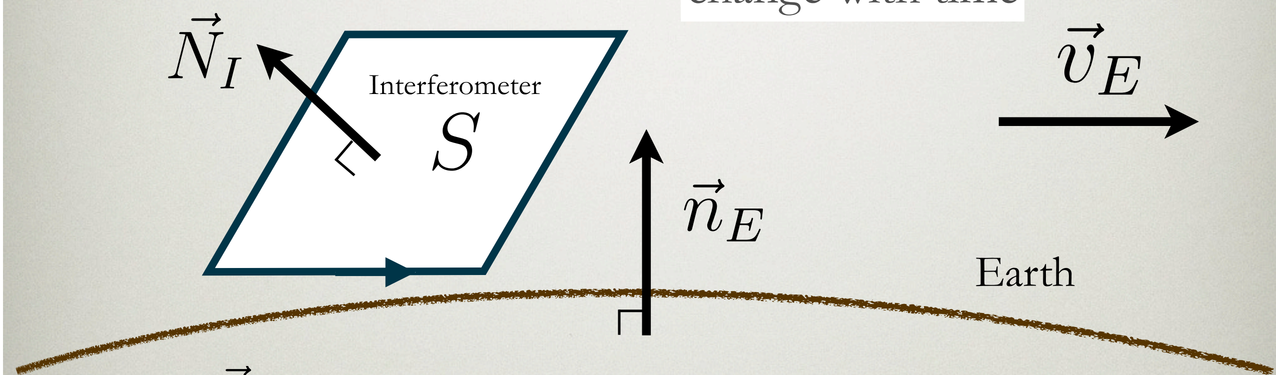

$\vec{v}_E$: Orbital velocity of Earth

$\vec{n}_E$: Vertical unit vector at the interferometer

$\vec{N}_I$: Normal unit vector of the interferometer

Time Dependence

$$[3(\vec{v}_E \cdot \vec{n}_E)\vec{n}_E - \vec{v}_E] \cdot \vec{N}_I = (\boxed{R(t)^{-1}}\vec{v}_E)^T \boxed{[3(\vec{n}_{E0} \cdot \vec{N}_{I0})\vec{n}_{E0} - \vec{N}_{I0}]}$$

Initial condition

$t = 0$: Midnight of Winter solstice

$$R(t)^{-1} = (R(\varphi))^{-1}(R(\omega_E))^{-1}(R(\Omega_E))^{-1}R(I_E)R(\Omega_E)$$

Time variation $\quad I_E \simeq 23^\circ \quad \omega_E = \frac{2\pi}{1\ \text{day}} \quad \Omega_E = \frac{2\pi}{1\ \text{year}}$

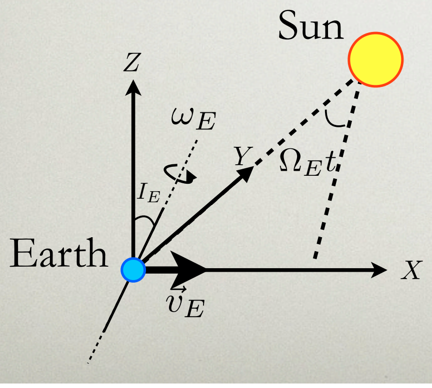

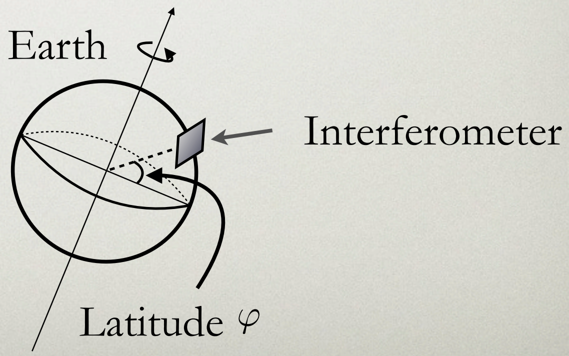

Time Dependence

$$R(t)^{-1} = \underbrace{(R(\varphi))^{-1}}_{\text{Latitude effect}}\underbrace{(R(\omega_E))^{-1}}_{\text{Daily variation}}\underbrace{(R(\Omega_E))^{-1}R(I_E)R(\Omega_E)}_{\text{Seasonal variation}}$$

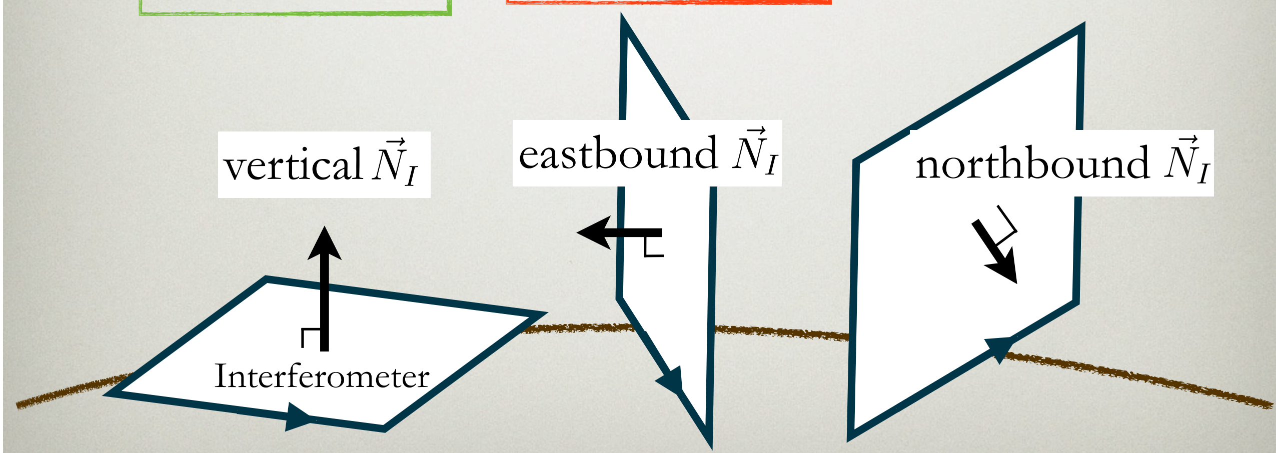

Daily variation

Phase difference at the equator $\varphi = 0^\circ$

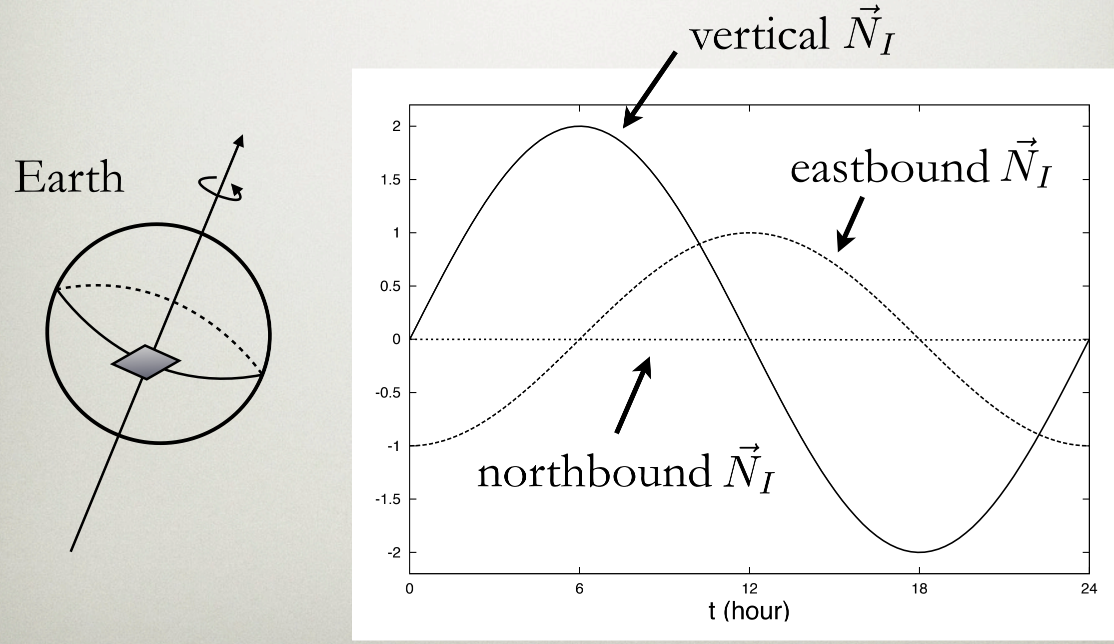

Daily variation

Phase difference at $\varphi = 45^\circ$

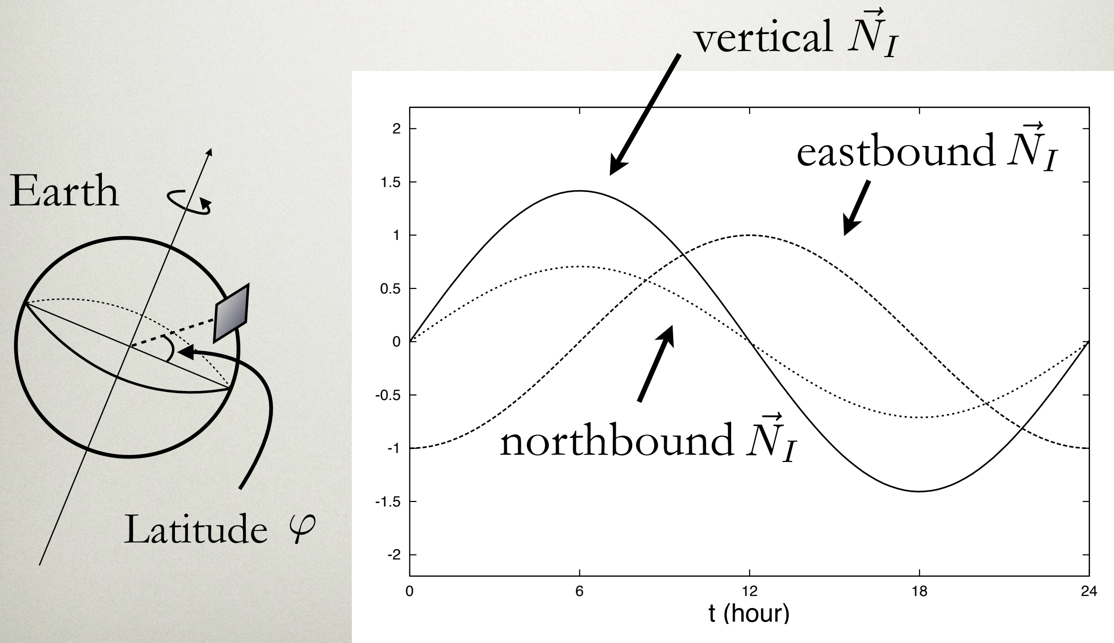

Seasonal variation

Phase difference at $\varphi = 0^\circ$ for vertical $\vec{N}_I$

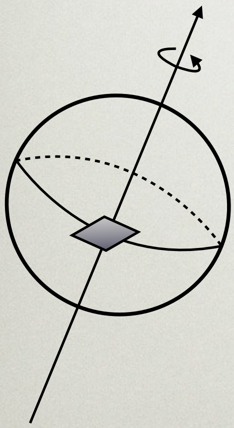

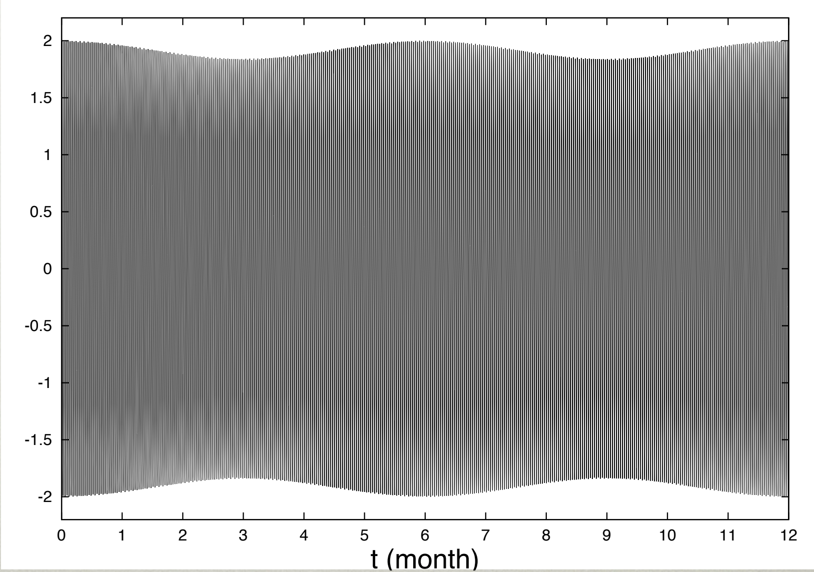

Seasonal variation

Phase difference at $\varphi = 45^\circ$ for vertical $\vec{N}_I$

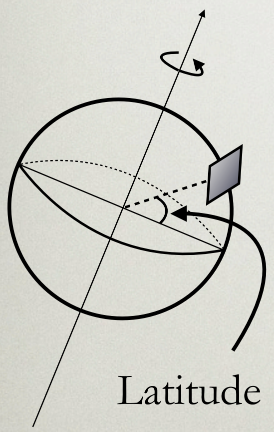

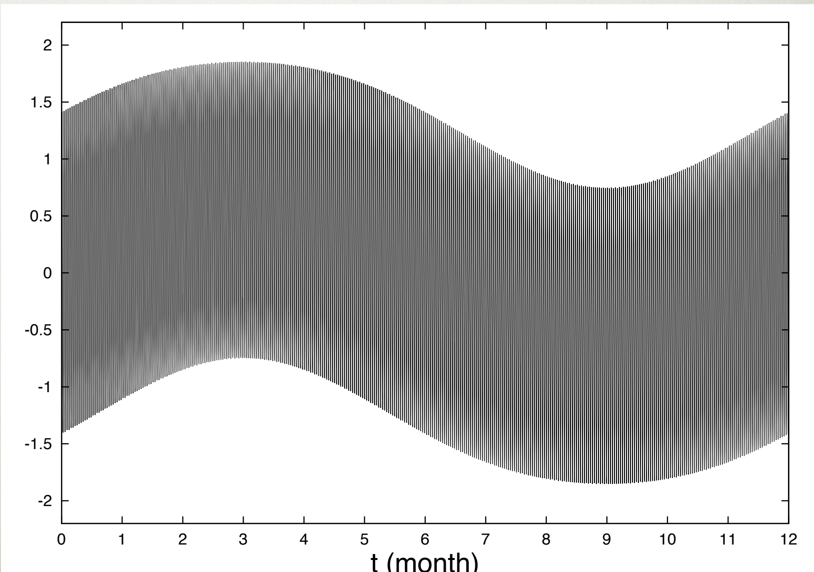

Possible constraint on $\dot{f}$

$\dot{f}$ induces the phase shift

$$|\Delta_{CS}| \sim 4 \underbrace{\left(\frac{mc^2}{\hbar}\right)} \left(\frac{\dot{f}}{c} \underbrace{\frac{GM_E}{c^2 r_E} \frac{v_E}{c}\right) \left(\frac{S}{r_E^2}\right)}$$

$\boxed{\textbf{CS gravity by Earth}} \sim 10^{-27}$ tiny

$\boxed{\textbf{Quantum Effect}} \sim 10^{24}$ huge

$$\sim 10^{-3}[\,\mathrm{s}^{-1}\,] \times \left(\frac{mc^2}{1\mathrm{GeV}}\right) \left(\frac{\dot{f}}{c}\right) \left(\frac{S}{0.4\mathrm{m}^2}\right)$$

Current neutron interferometry $\sim \mathrm{O}(10^{-3})$ $\Rightarrow$ $\boxed{\dot{f}c^{-1} < 10^0 s}$

Classical Experiments

Current neutron interferometry $\sim \mathrm{O}(10^{-3})$ $\Rightarrow$ $\boxed{\dot{f}c^{-1} < 10^0 s}$

- LAGEOS and Gravity Probe B
- Lense-Thirring effect (No deviation)

[I. Ciufolini and E.C. Pavlis, Nature 431, 958(2004).
C. W. F. Everitt, et al., PRL 106, 221101 (2011).]

$\boxed{\text{3 digits}}$

$$\Downarrow$$

$$\dot{f}c^{-1} < 10^{-3}s$$

[S. Alexander & N. Yunes, PRL 99, 241101 (2007).
T. L. Smith, et al., PRD 77, 024015 (2008).]

Possible constraint on $\dot{f}$

$$|\Delta_{CS}| \sim 10^{-3}[\,\mathrm{s}^{-1}\,] \times \left(\frac{mc^2}{1\mathrm{GeV}}\right)\left(\frac{\dot{f}}{c}\right)\left(\frac{S}{0.4\mathrm{m}^2}\right)$$

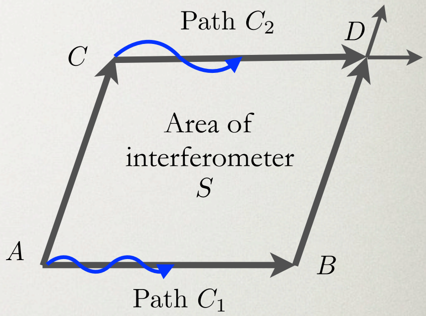

- Arm Length 0.6 m → 5 m => S larger by two digits
  [H.Rauch, and S.A. Werner, Neutron Interferometry, (Clarendon Press, Oxford, 2000)]
- Phase accuracy $O(10^{-3})$ => $O(10^{-4})$
  [S. A. Werner, and A. G. Klein, J. Phys. A: Math. Theor. 43, 354006 (2010)]
- Current $\dot{f}c^{-1} < 10^0 s$ $\longrightarrow$ $\boxed{\dot{f}c^{-1} < 10^{-3}s}$

Contents

- COW experiment &
  Chern-Simons metric at 1PN order
- Method for Neutron interferometry
- Phase shift by Chern-Simons gravity
- Summary

Summary

- Prediction of time variation and Latitude effect.
- Possible constraints on CS gravity by neutron interferometry.
- Current $\dot{f}c^{-1} < 10^{0}s$
  $\rightarrow \boxed{\dot{f}c^{-1} < 10^{-3}s}$ in the future

Future Work

- How about Null geodesic?
  - Sagnac interferometer
- How about Dynamical CS?

Thank You for Your Attention

Appendix

Why Neutron Interferometry?

$$\Delta_{(\mathrm{CS})} \simeq 2f \frac{mGM_E S}{\hbar c^2 r_E^3}[3(\vec{v}_E \cdot \vec{n}_E)\vec{n}_E - \vec{v}_E] \cdot \vec{N}_I$$

- Phase shift $\propto\ m$
  - Atom interferometry is advantageous.
- However, atoms have electric charges.
  - Other effects (e.g. Lorentz force).
- Neutron is affected by only gravitational force.

Michelson Interferometer?

$$\Delta_{(\mathrm{CS})} \simeq 2f \frac{mGM_E S}{\hbar c^2 r_E^3}[3(\vec{v}_E \cdot \vec{n}_E)\vec{n}_E - \vec{v}_E] \cdot \vec{N}_I$$

- Phase shift $\propto S$
- Michelson interferometer (e.g. KAGRA)

$$S = 0 \ (\because\ \text{L-shaped})$$

- Michelson interferometer cannot measure that.
- eLISA & DECIGO may be interesting.

Seasonal variation

Phase difference at $\varphi = 0^\circ$ for eastbound $\vec{N}_I$

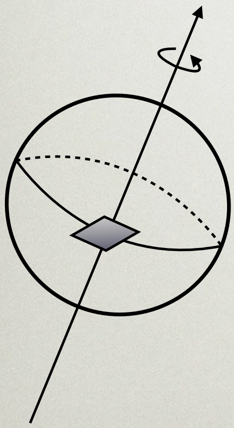

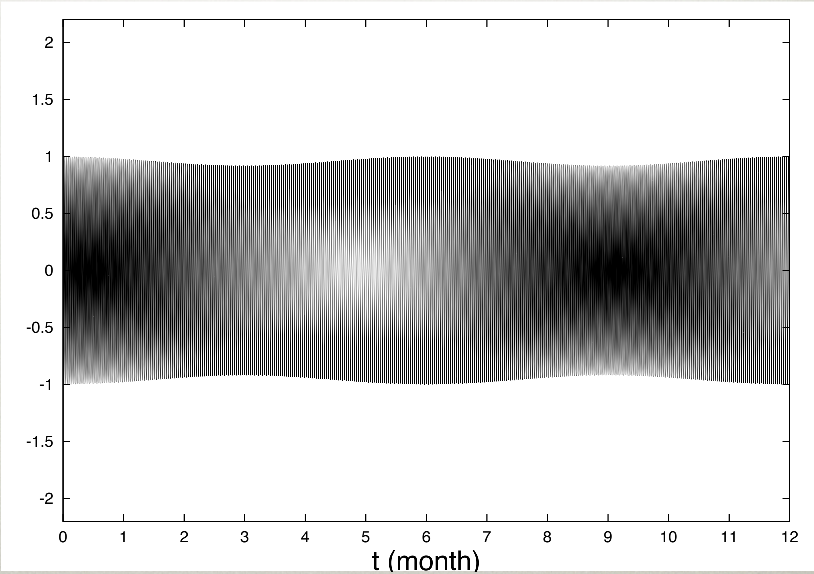

Seasonal variation

Phase difference at $\varphi = 0^\circ$ for northbound $\vec{N}_I$

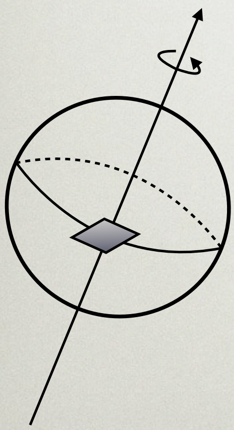

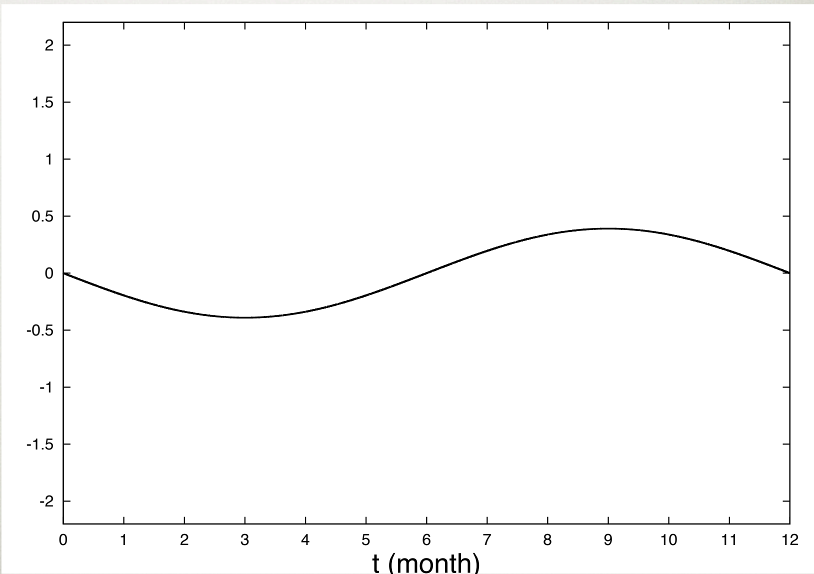

Seasonal variation

Phase difference at $\varphi = 45^\circ$ for eastbound $\vec{N}_I$

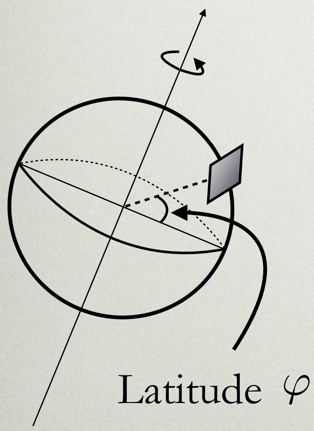

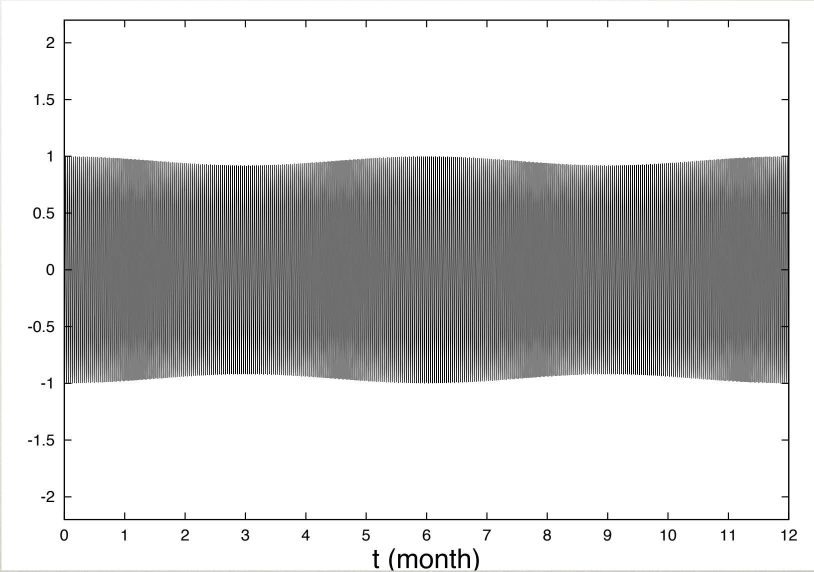

Seasonal variation

Phase difference at $\varphi = 45^\circ$ for northbound $\vec{N}_I$

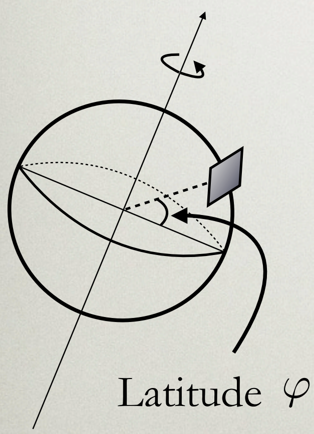

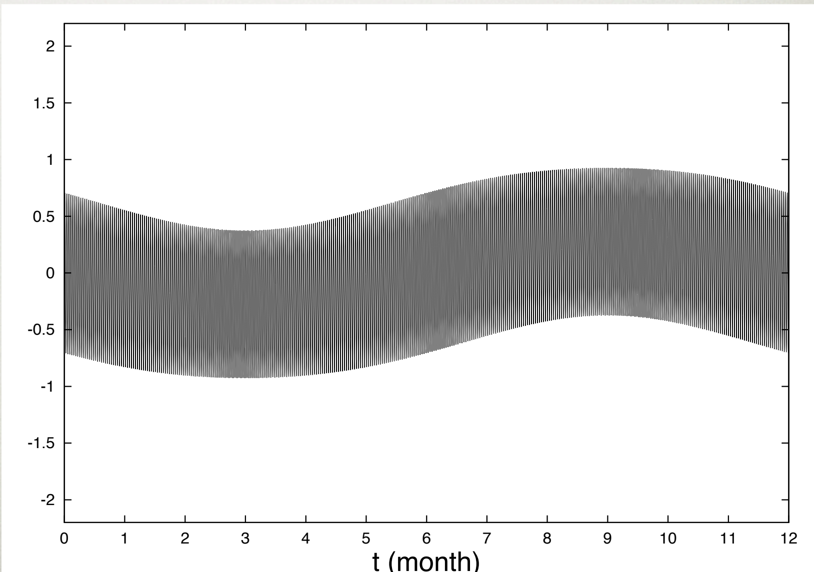

“Hydrostatic equilibrium of gas distribution in Coma cluster and a test of chameleon gravity model”

by Ayumu Terukina

[JGRG23(2013)110603]

Hydrostatic equilibrium of gas distribution in Coma cluster and a test of chameleon gravity model

Hiroshima University

Ayumu Terukina

Collaborators

K. Yamamoto (Hiroshima University)

K. Koyama, D. Bacon, R. C. Nicol, L. Lombriser (Portsmouth University)

Introduction

Chameleon Gravity Model

- Equation for scalar field

$$\nabla^2\phi = V_{,\phi} + \frac{\beta}{M_{\rm Pl}}\rho e^{\frac{\beta\phi}{M_{\rm Pl}}}$$

$V(\phi)$: Potential β : Coupling constant ρ : Matter density

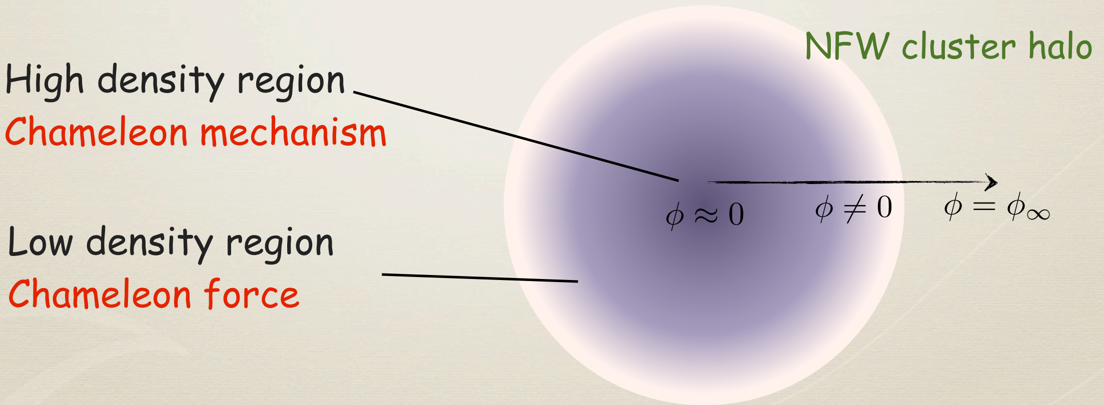

Scalar Field Configuration

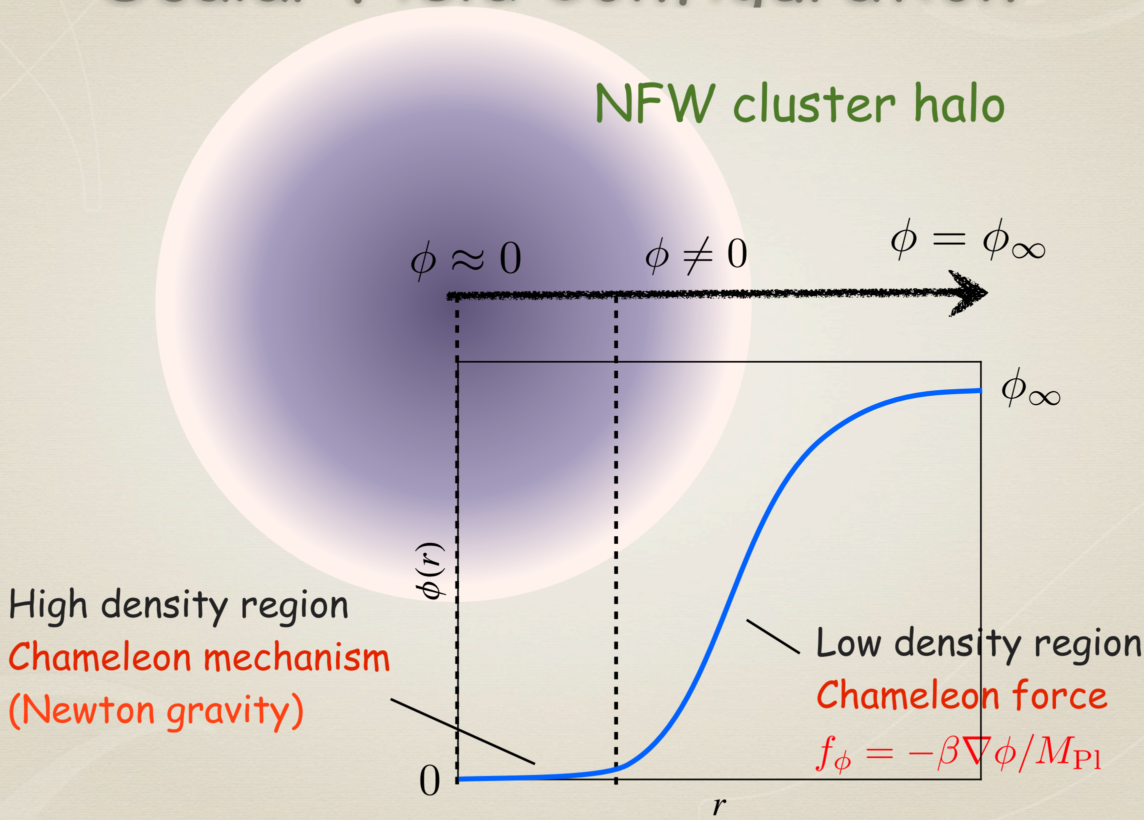

Previous Work

AT & K. Yamamoto, 2012

Analytical derivation of the gas distribution profiles.

Assumptions

- Hydrostatic equilibrium

gravitational force, chameleon force

$$\rho_{\rm gas}^{-1}\frac{dP_{\rm gas}}{dr} = -\frac{GM(<r)}{r^2} - \frac{\beta}{M_{\rm Pl}}\frac{d\phi}{dr}$$

- NFW dark matter density profile
- Polytropic equation of state

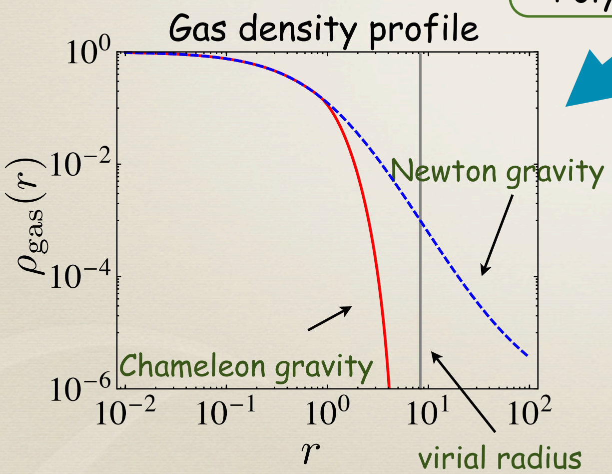

* Gas density profile decreases faster compared with the case of Newtonian gravity.

* Large deviation from Newtonian gravity is not consistent with an X-ray observation.

✳ Multiwavelength observations of cluster of galaxies

- X-ray surface brightness
- X-ray temperature
- Sunyaev-Zel'dovich (SZ) effect
- Gravitational lensing

Coma Cluster Observations

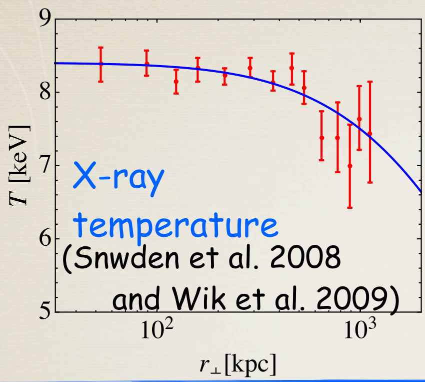

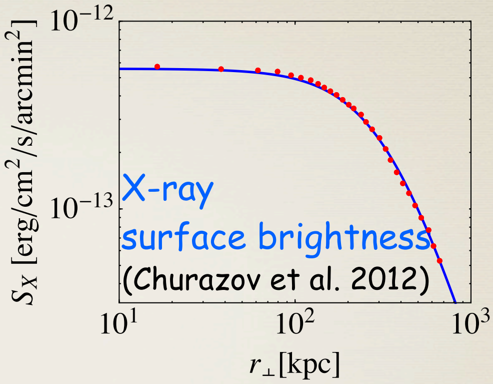

3D density , 3D temperature

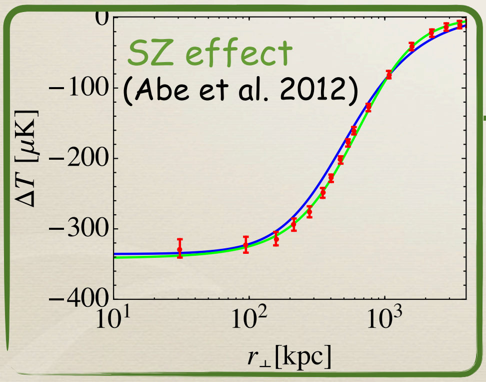

3D pressure

Weak lensing (NFW) (Okabe et al. 2010)

$$M_{\rm vir} = 8.92^{+20}_{-5} \times 10^{14} h^{-1} M_\odot$$

$$c = 3.50^{+2.56}_{-1.79}$$

Reconstruct 3D Profiles

3D profiles

Gas temperature

$$T_{\rm gas}^{(X)}(r) = T_0 \left[1 + A_1 \left(\frac{r}{r_0}\right)\right]^{\beta_0}$$

Electron number density

$$n_{\rm e}^{(X)}(r) = n_0 \left[1 + \left(\frac{r}{r_1}\right)^2\right]^{\beta_1}$$

Electron pressure

$$P_{\rm e}^{(SZ)}(r) = \frac{P_0}{(r/r_2)^{\beta_2}(1+(r/r_2)^{\beta_3})^{\beta_4}}$$

projected profiles

X-ray temperature

$$T_X(r_\perp) = \frac{\int dz \lambda_{\rm c}(r) n_{\rm e}^2(r) T_{\rm gas}(r)}{\int dz \lambda_{\rm c}(r) n_{\rm e}^2(r)}$$

X-ray surface brightness

$$S_X(r_\perp) = \int dz \lambda_{\rm c}(r) n_{\rm e}^2(r)$$

Sunyaev-Zel'dovich effect

$$\frac{\Delta T(r_\perp)}{T_{\rm CMB}} = -2\frac{\sigma_{\rm T}}{m_{\rm e}} \int dz P_{\rm e}(r)$$

* Approach 1 :
  Test of the validity of hydrostatic equilibrium.
  (Comparing hydrostatic mass with lensing mass.)

* Approach 2 :
  Constraint on the chameleon gravity model.
  (Comparing theoretical model with multiwavelength observations using MCMC analysis.)

Approach 1

Test of the validity of hydrostatic equilibrium

Hydrostatic Mass

- Hydrostatic equilibrium

$$\rho_{\rm gas}^{-1}\frac{dP_{\rm gas}}{dr} = -\frac{GM(<r)}{r^2} - \frac{\beta}{M_{\rm Pl}}\frac{d\phi}{dr}$$

chameleon force

gravitational force

$\rho_{\rm gas}$: density
$P_{\rm gas}$: pressure
$T_{\rm gas}$: temperature

- Mass Profile (Hydrostatic mass)

X-ray

SZ effect

$$M_{\rm HE}(<r) = -\frac{r^2}{G\rho_{\rm gas}}\frac{dP_{\rm gas}}{dr} - \frac{\beta r^2}{GM_{\rm Pl}}\frac{d\phi}{dr} \qquad \left(P_{\rm gas} = \frac{\rho_{\rm gas}}{\mu m_{\rm p}}kT_{\rm gas}\right)$$

$$= -\frac{kT_{\rm gas}r}{\mu m_{\rm p}G}\left(\frac{d\ln\rho_{\rm gas}}{d\ln r} + \frac{d\ln T_{\rm gas}}{d\ln r}\right) - \frac{\beta r^2}{GM_{\rm Pl}}\frac{d\phi}{dr}$$

X-ray

We test the validity of hydrostatic equilibrium

$M_{\rm WL}$: Weak lensing mass

Mass Profiles in the Coma Cluster

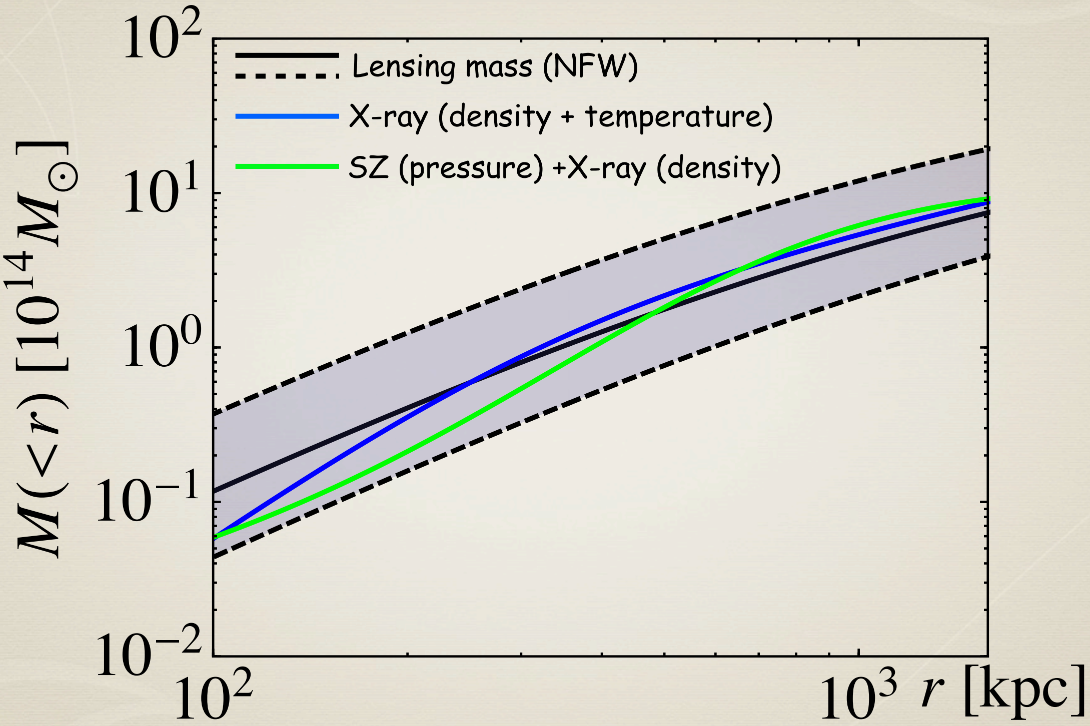

Hydrostatic equilibrium is good assumption

Mass Profiles in the Coma Cluster

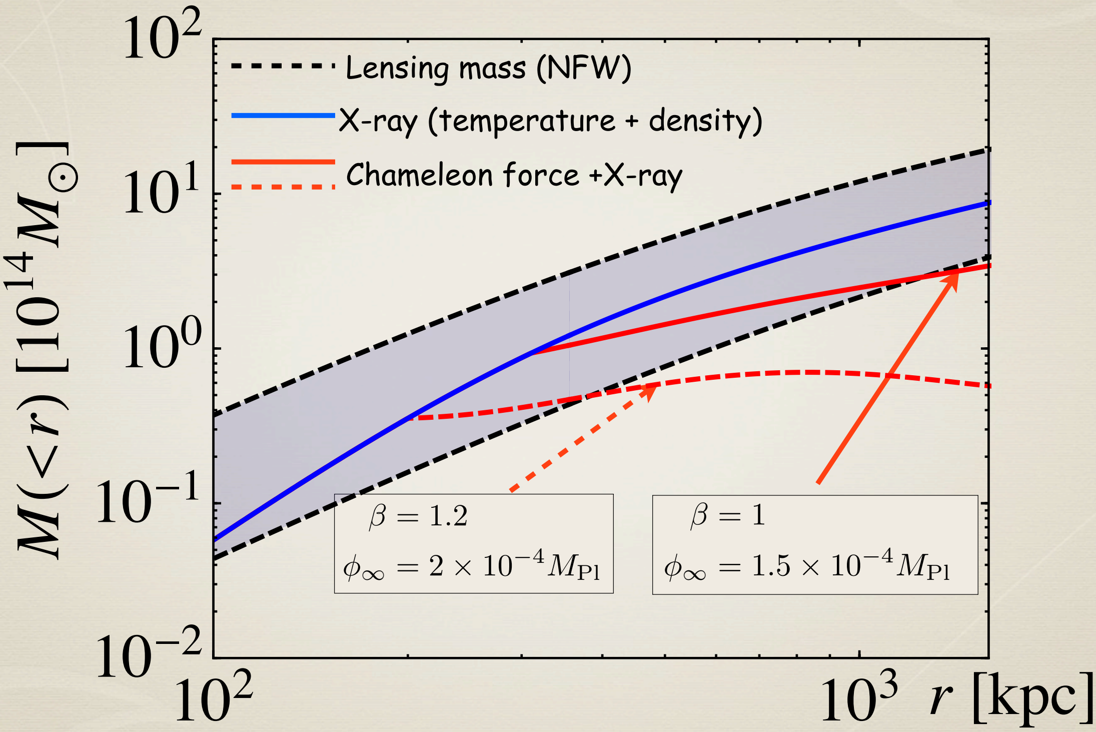

Hydrostatic mass becomes small due to the chameleon force.

Approach 2

Constraint on the chameleon gravity model

Gas Distribution Profiles

Assumptions

Hydrostatic equilibrium

$$\rho_{\rm gas}^{-1}\frac{dP_{\rm gas}}{dr} = -\frac{GM(<r)}{r^2} - \frac{\beta}{M_{\rm Pl}}\frac{d\phi}{dr}$$

Electron number density

$$n_{\rm e}(r) = n_0\left[1+\left(\frac{r}{r_1}\right)^2\right]^{\beta_1}$$

EoS of the gas

$$P_{\rm gas} = \rho_{\rm gas} kT_{\rm gas}/\mu m_{\rm p}$$

3D profiles

$$P_{\rm gas} = n_0 T_0 + \mu m_{\rm p}\int_0^r n_{\rm e}\left(\frac{GM}{r^2} - \frac{\beta}{M_{\rm Pl}}\frac{d\phi}{dr}\right)dr$$

$$\rho_{\rm gas} = \frac{5\mu m_{\rm p}}{2+\mu} n_{\rm e}$$

$$kT_{\rm gas} = \frac{\mu m_{\rm p} P_{\rm gas}}{\rho_{\rm gas}}$$

Projected profiles and cluster mass profile

X-ray temperature

$$T_X(r_\perp) = \frac{\int dz \lambda_{\rm c}(r) n_{\rm e}^2(r) T_{\rm gas}(r)}{\int dz \lambda_{\rm c}(r) n_{\rm e}^2(r)}$$

X-ray surface brightness

$$S_X(r_\perp) = \int dz \lambda_{\rm c}(r) n_{\rm e}^2(r)$$

SZ effect

$$\frac{\Delta T(r_\perp)}{T_{\rm CMB}} = -2\frac{\sigma_{\rm T}}{m_{\rm e}}\int dz P_{\rm e}(r) = -2y(r_\perp)$$

Weak lensing (NFW)

$$M(<r) = 4\pi\int_0^r \rho_{\rm NFW}(r) r^2 dr$$

Comparison with Observations

X-ray temperature   X-ray surface brightness   SZ effect

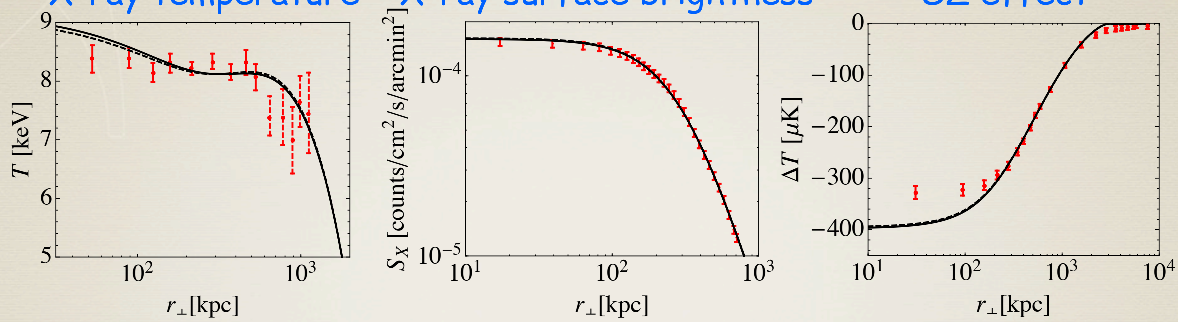

$$\chi^2_{XT} = \sum_i \frac{(T_X(r_{\perp,i}) - T^{\rm obs.}_{X,i})^2}{(\Delta T^{\rm obs.}_{X,i})^2} \qquad \chi^2_{SB} = \sum_i \frac{(S_X(r_{\perp,i}) - S^{\rm obs.}_i)^2}{(\Delta S^{\rm obs.}_i)^2}$$

$$\chi^2_{SZ} = \sum_i \frac{(y(r_{\perp,i}) - y^{\rm obs.}_i)^2}{(\Delta y^{\rm obs.}_i)^2} \qquad \chi^2_{WL} = \frac{(M_{\rm vir} - M_{WL})^2}{(\Delta M_{WL})^2} + \frac{(c - c_{WL})^2}{(\Delta c_{WL})^2}$$

$$\Rightarrow \chi^2_{\rm XT+SB+SZ+WL}(M_{\rm vir}, c, T_0, n_0, b_1, r_1, \underline{\beta, \phi_\infty})$$

coupling constant, background scalar field

Constraint on the Model Parameters (MCMC)

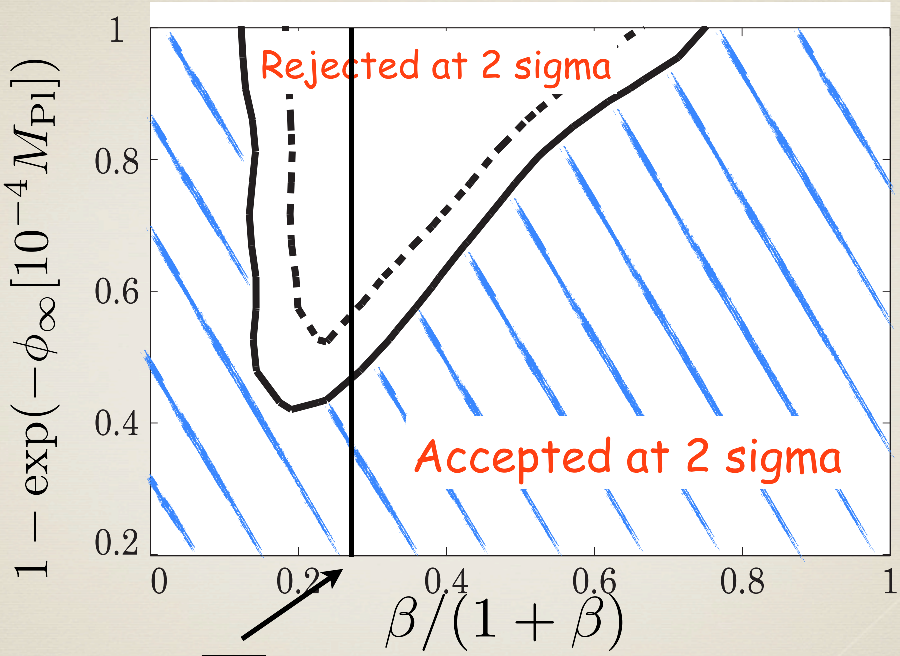

f(R) Model $\beta = \sqrt{1/6}$

$$\phi_\infty \lesssim 0.6\times 10^{-4} M_{\rm Pl} \Longleftrightarrow |f_{R0}| \lesssim 0.5\times 10^{-4}$$

Summary

* Using multiwavelength observations of the Coma cluster, we obtained the following 3 results.

1. The hydrostatic equilibrium approximately holds in the outer region of the Coma cluster.

2. Presence of chameleon force requires the estimation of low hydrostatic mass.

3. Comparing theoretical model with multiwavelengs observations gave us useful constraint on the chameleon gravity model parameters.

For an f(R) model, $|f_{R0}| \lesssim 0.5\times 10^{-4}$

“The temporally enhanced curvature perturbation from the shift-symmetry breaking of a galileon field”

by Yi-Peng Wu

[JGRG23(2013)110604]

JGRG23 @ Hirosaki University, Hirosaki

The temporally enhanced curvature perturbation from the shift symmetry breaking of a galileon field

with Jun'ichi Yokoyama, in preparation

Yi-Peng Wu
Research Center for the Early Universe, the University of Tokyo
National Tsing Hua University

$R_{\mu\nu} - \frac{1}{2}g_{\mu\nu}R = 8\pi G T_{\mu\nu}$

RESCEU

東京大学大学院理学系研究科附属ビッグバン宇宙国際研究センター
Research Center for the Early Universe

outline

We study the curvaton mechanism of a single field from a purely kinematic origin and its cosmological implications.

$\cancel{V(\phi)}$

Coherent oscillations of ϕ

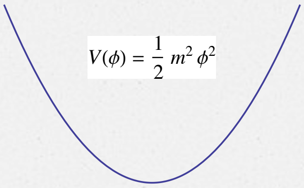

$$\rho_\phi \propto a^{-3}$$

$$\rho_\phi \propto a^{-4}$$

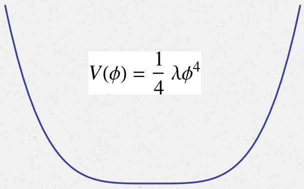

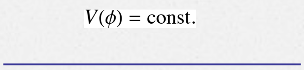

$$\rho_\phi \propto a^{-6}$$

Coherent oscillations of ϕ

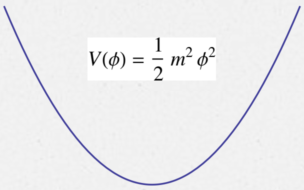

$$\rho_\phi \propto a^{-3}$$ curvaton candidates

$$\rho_\phi \propto a^{-4}$$

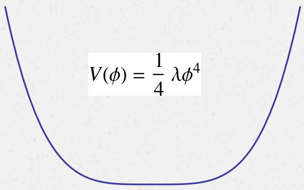

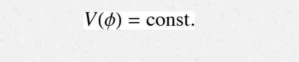

$$\rho_\phi \propto a^{-6}$$

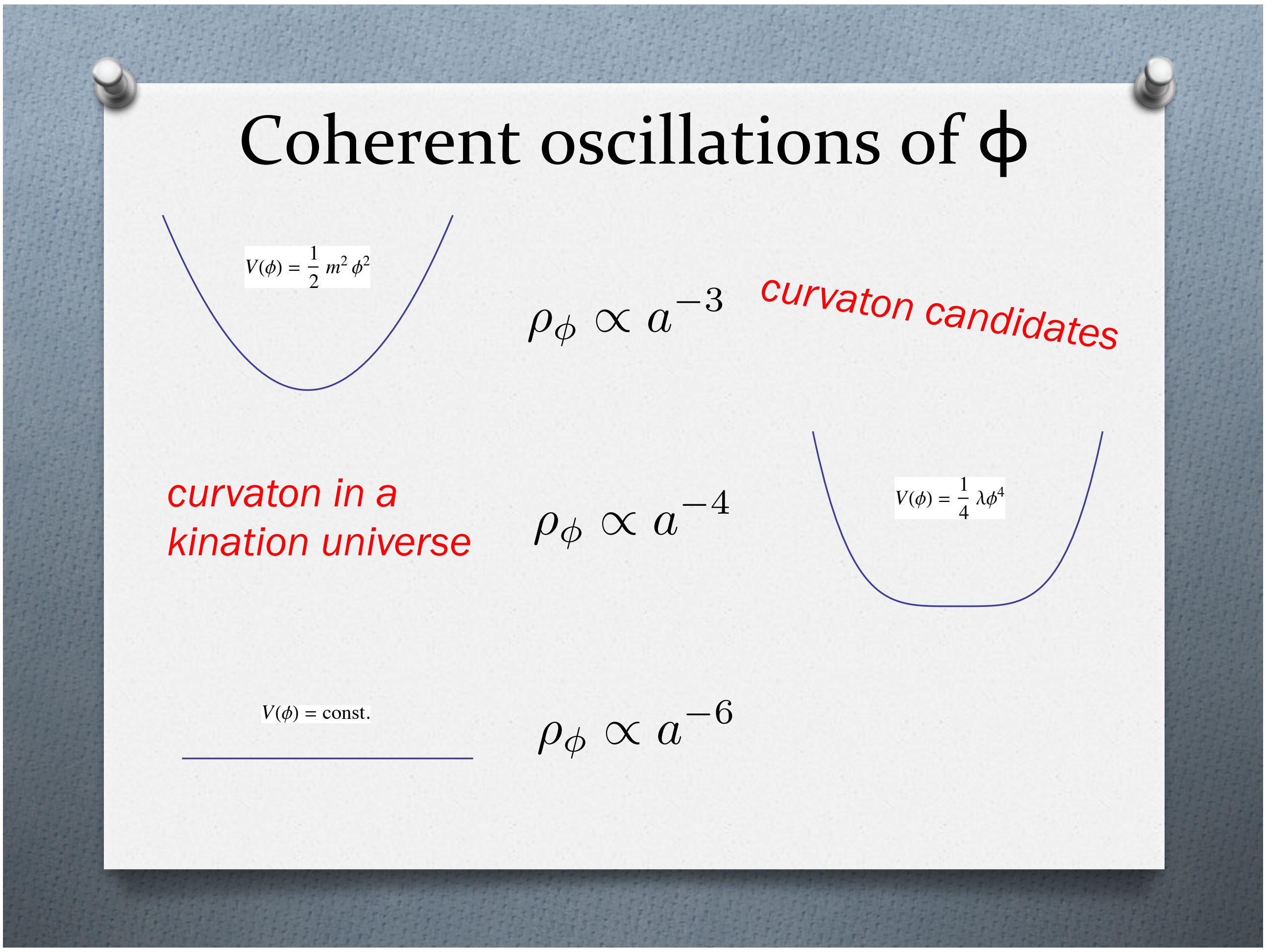
Coherent oscillations of ϕ
$V(\phi) = \frac{1}{2} m^2 \phi^2$
$\rho_\phi \propto a^{-3}$
curvaton candidates
curvaton in a
kination universe
$\rho_\phi \propto a^{-4}$
$V(\phi) = \frac{1}{4} \lambda \phi^4$
$V(\phi) = \text{const.}$
$\rho_\phi \propto a^{-6}$

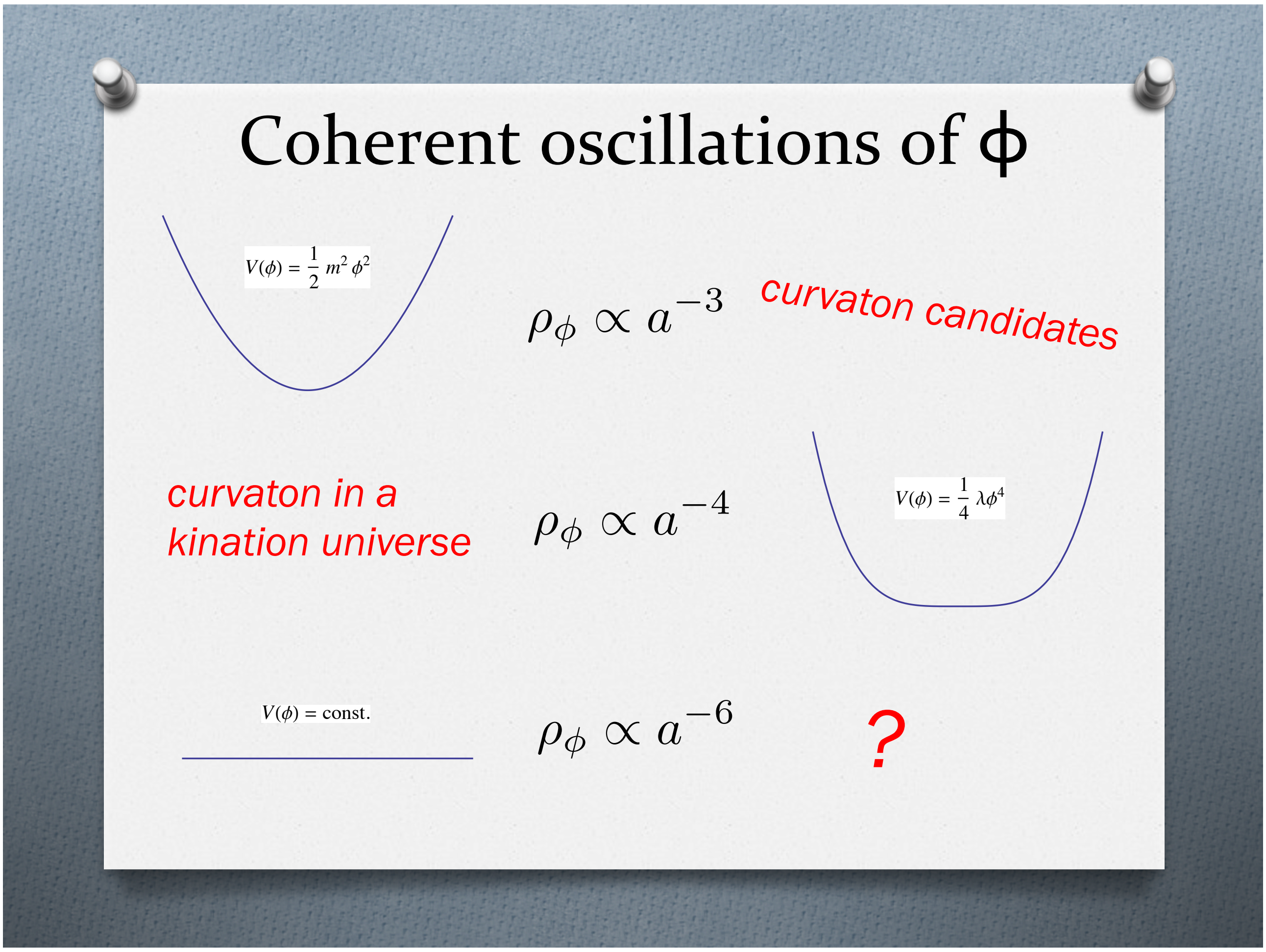
Coherent oscillations of ϕ
$V(\phi) = \frac{1}{2} m^2 \phi^2$
$\rho_\phi \propto a^{-3}$
curvaton candidates
curvaton in a
kination universe
$\rho_\phi \propto a^{-4}$
$V(\phi) = \frac{1}{4} \lambda \phi^4$
$V(\phi) = \text{const.}$
$\rho_\phi \propto a^{-6}$
?

- Can a free scalar field with subsidiary energy density during inflation be relevant to the large scale curvature perturbation?

The curvaton scenario

$$\zeta = (1 - r_\sigma)\,\zeta_r + r_\sigma\,\zeta_\sigma$$

Lyth et. al (2003)

The density fluctuations generated either by inflaton or curvaton are constant on the large scales

$$\begin{aligned} \zeta_r &\sim \delta_r = const. \\ \zeta_\sigma &\sim \delta_\sigma = const. \end{aligned}$$

The evolution of the total curvature perturbation is governed by the weight function of the energy density, which is monotonic in time

$$r_\sigma(t) = \frac{3\rho_\sigma(1+w_\sigma)}{4\rho_r + 3\rho_\sigma(1+w_\sigma)}$$

$$\begin{aligned} \rho_r &\propto a^{-4} \\ \rho_\sigma &\propto a^{-3} \end{aligned}$$

The curvaton scenario

$$\zeta = (1 - r_\sigma)\,\zeta_r + r_\sigma\,\zeta_\sigma$$

Lyth et. al (2003)

The density fluctuations generated either by inflaton or curvaton are constant on the large scales

$$\begin{aligned} \zeta_r &\sim \delta_r = const. \\ \zeta_\sigma &\sim \delta_\sigma = const. \end{aligned}$$

The evolution of the total curvature perturbation is governed by the weight function of the energy density, which is monotonic in time

$r_\sigma(t) =$

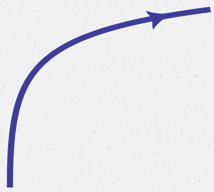

$$\begin{aligned} \rho_r &\propto a^{-4} \\ \rho_\sigma &\propto a^{-3} \end{aligned}$$

The curvaton scenario

$$\zeta = (1 - r_\sigma)\,\zeta_r + r_\sigma\,\zeta_\sigma$$

Given a monotonic increasing weight function,
there are only two possibility :

I. $\zeta_\sigma > \zeta_r$ II. $\zeta_\sigma < \zeta_r$

$\zeta =$

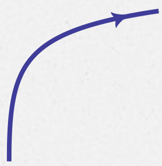

The curvaton scenario

$$\zeta = (1 - r_\sigma)\,\zeta_r + r_\sigma\,\zeta_\sigma$$

Given a monotonic increasing weight function,
there are only two possibility :

I. $\zeta_\sigma > \zeta_r$ II. $\zeta_\sigma < \zeta_r$

$\zeta =$

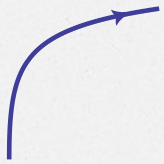

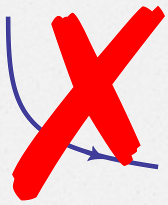

Does not happen in the
single curvaton scenario

A temporally enhanced ζ ?

$$\zeta = (1 - r_\sigma)\,\zeta_r + r_\sigma\,\zeta_\sigma$$

If there are two curvatons σ_1, σ_2 :

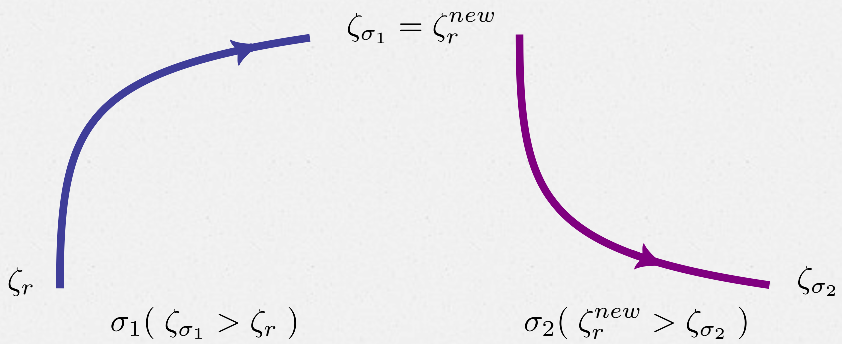

➔ Multi-curvaton scenario is essential to realize a temporal enhancement of the curvature perturbation
➔ Closely related to PBH and GW formations

Suyama & Yokoyama (2011)

- Can a free scalar field with subsidiary energy density during inflation be relevant to the large scale curvature perturbation?

- How does the curvature perturbation evolve in a curvaton scenario with a general weight function?

$$r_\sigma(t) \neq$$

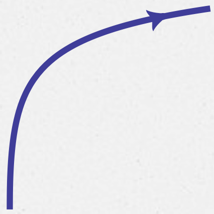

A massless and self-interacting free scalar

$$\mathcal{L}_\phi = K(\phi, X) - \epsilon X \Box \phi$$

Deffayet et. al (2010)

Kobayashi et. al (2010)

- $K = 0 \;\text{ when }\; X = 0$
- $\epsilon \Box \phi \ll 1$

Wu & Yokoyama in prep.

The energy density and pressure :

$$\rho_\phi = 2XK_X - K + 3\epsilon H \dot{\phi}^3,$$
$$p_\phi = K - 2\epsilon X \ddot{\phi}.$$

The Noether current of the constant shift $(\phi \to \phi + c)$

$$J_\mu = K_X \nabla_\mu \phi + \epsilon(\nabla_\mu \nabla_\nu \phi \nabla^\nu \phi - \Box \phi \nabla_\mu \phi)$$

The equation of motion :

$$\nabla_\mu J^\mu = K_\phi \qquad \dot{J}_0 + 3HJ_0 = K_\phi$$

$$J_0 = \dot{\phi}(K_X + 3\epsilon H \dot{\phi})$$

A massless and self-interacting free scalar

$$\mathcal{L}_\phi = K(\phi, X) - \epsilon X \Box \phi$$

Deffayet et. al (2010)
Kobayashi et. al (2010)

- $K = 0 \text{ when } X = 0$
- $\epsilon \Box \phi \ll 1$

Wu & Yokoyama in prep.

The energy density and pressure :

$$\rho_\phi = 2XK_X - K + 3\epsilon H \dot{\phi}^3,$$
$$p_\phi = K - 2\epsilon X \ddot{\phi}.$$

The shift symmetry limit

$$K_\phi = 0 \qquad \dot{J}_0 + 3HJ_0 = 0 \qquad J_0 \propto \frac{1}{a^3} \to 0$$

$$J_0 = \dot{\phi}(K_X + 3\epsilon H \dot{\phi}) = 0$$

The non-trivial solution

$$K_X + 3\epsilon H \dot{\phi} = 0$$

A massless and self-interacting free scalar

$$\mathcal{L}_\phi = K(\phi, X) - \epsilon X \Box \phi$$

Deffayet et. al (2010)
Kobayashi et. al (2010)

- $K = 0 \text{ when } X = 0$
- $\epsilon \Box \phi \ll 1$

Wu & Yokoyama in prep.

The energy density and pressure :

$$\rho_\phi = 2\cancel{X}K_X - K + 3\cancel{\epsilon}H \dot{\phi}^3,$$
$$p_\phi = K - 2\epsilon X \ddot{\phi}.$$

$$w_\phi \approx -1$$

The shift symmetry limit

$$K_\phi = 0 \qquad \dot{J}_0 + 3HJ_0 = 0 \qquad J_0 \propto \frac{1}{a^3} \to 0$$

$$J_0 = \dot{\phi}(K_X + 3\epsilon H \dot{\phi}) = 0$$

The non-trivial solution

$$\boxed{K_X + 3\epsilon H \dot{\phi} = 0}$$

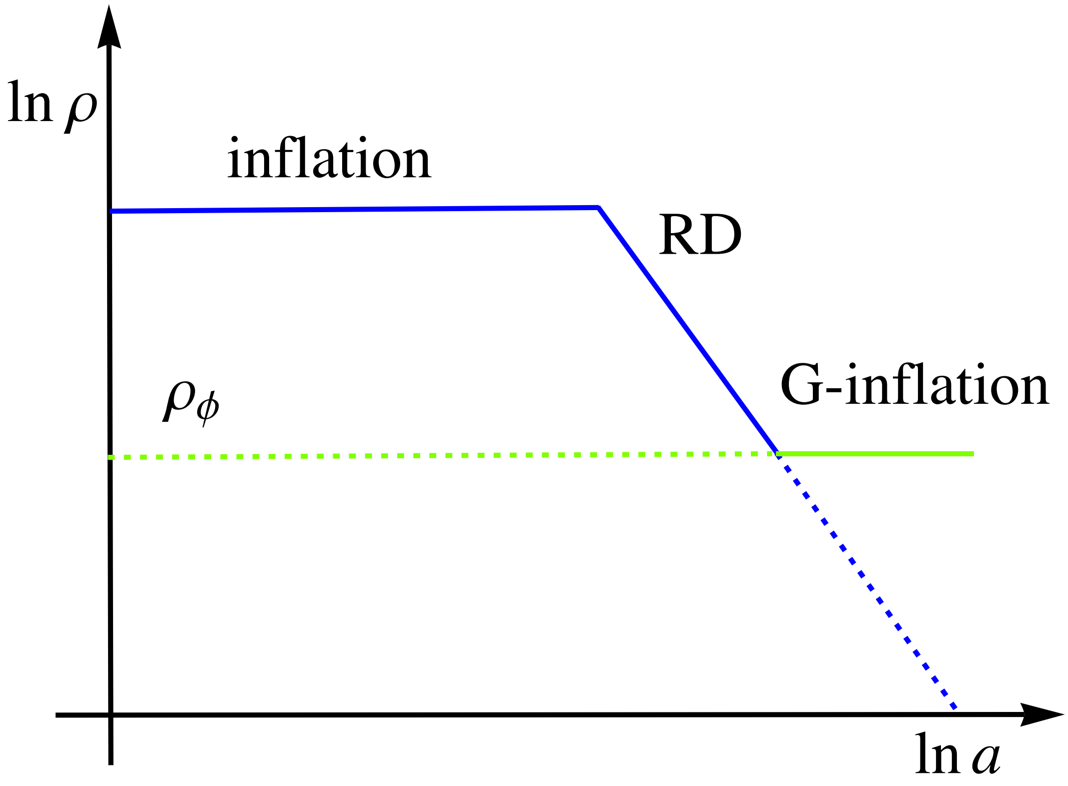

To escape from a secondary inflation…

$$\mathcal{L}_\phi = K(\phi, X) - \epsilon X \Box \phi$$

$*\quad K = 0$ when $X = 0$

$*\quad \epsilon \Box \phi \ll 1$

The shift symmetry must be temporarily broken

We consider $K(\phi, X) = -A(\phi)X + \frac{X^2}{2M^4}, \quad \epsilon = \frac{1}{M^3}$

$$A(\phi) = \tanh\left(\frac{\phi_c - \phi}{\mu}\right)$$

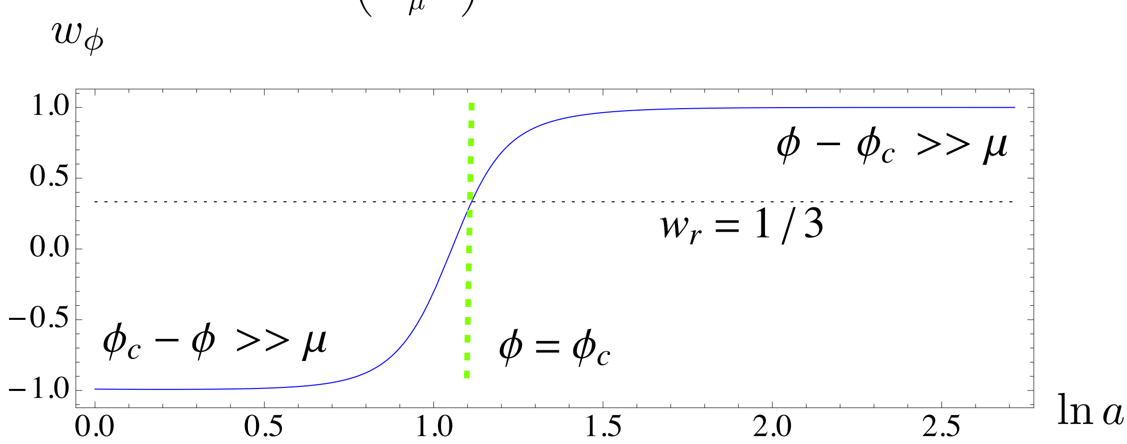

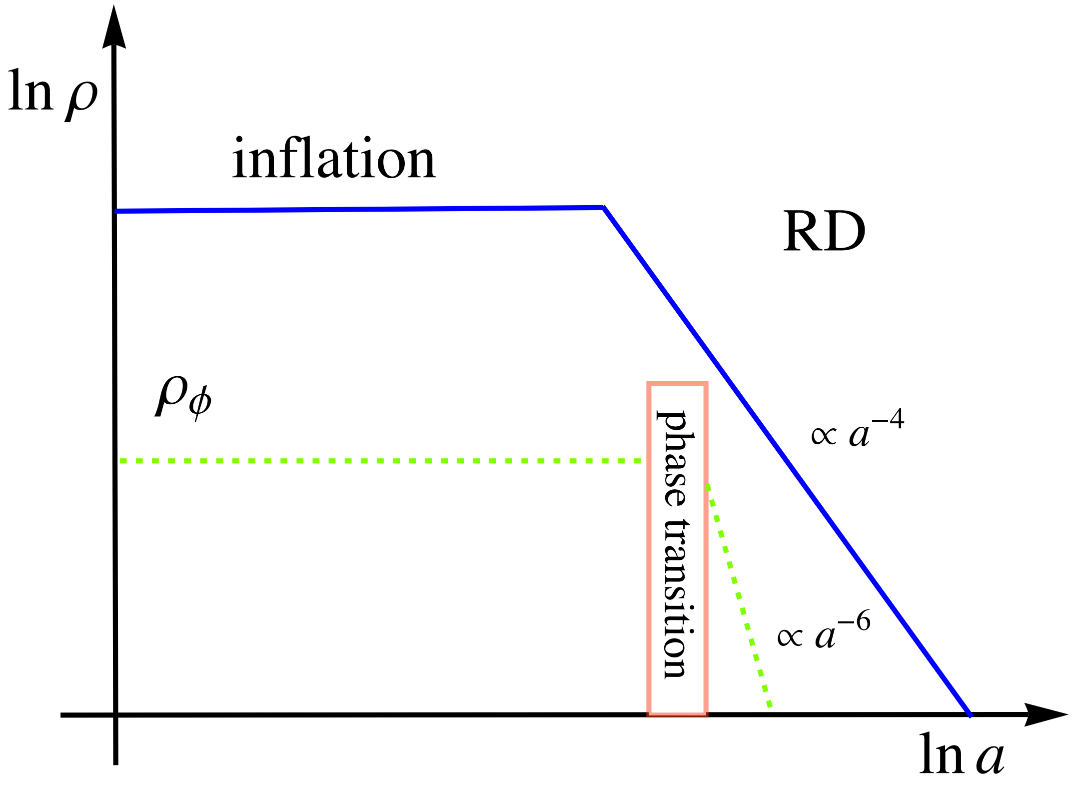

$w_\phi =$

$\Omega_\phi =$

$r_\phi =$

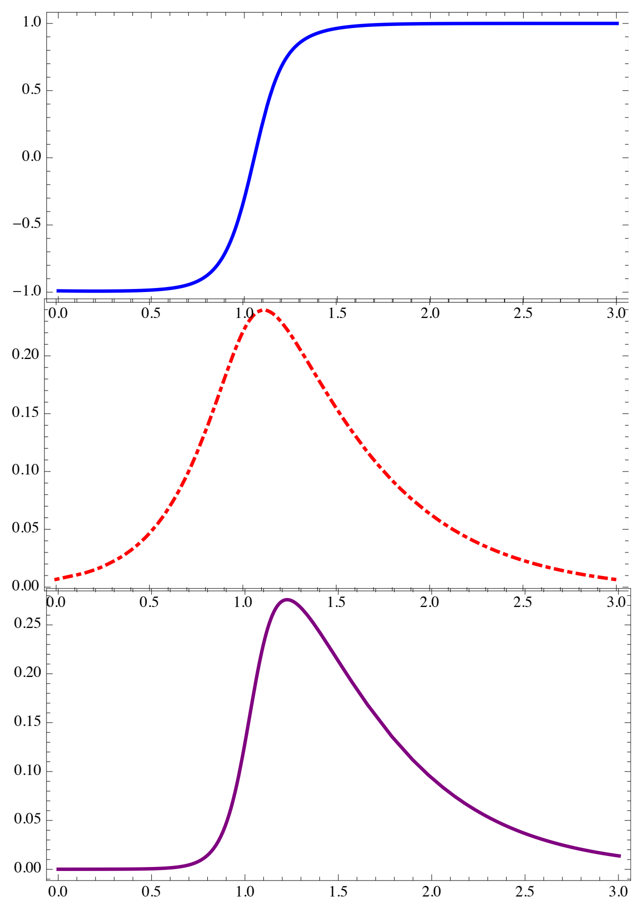

How is the curvature perturbation generated through this scenario?

The galileon field perturbation:

$$\delta\ddot{\phi} + \left(3 + \frac{\dot{D}}{HD}\right) H\delta\dot{\phi} - \frac{c_s^2}{a^2}\nabla^2\delta\phi + M_{\rm eff}^2\delta\phi = 0$$

Wang et. al (2012)

We have an additional friction, a time varying sound speed, and an effective mass term:

$$\begin{aligned} D &= -A + \frac{3X}{M^4} + \frac{6H\dot{\phi}}{M^3}, \\ c_s^2 &= \frac{-AM^4 + X + 2M(\ddot{\phi} + 2H\dot{\phi})}{-AM^4 + 3X + 6MH\dot{\phi}}, \\ M_{\rm eff}^2 &= -A_\phi\left(\ddot{\phi} + 3H\dot{\phi}\right) - XA_{\phi\phi}. \end{aligned}$$

The spectrum is given at the time the cosmological scale leaves the horizon during the shift-symmetry regime:

$(\phi_c - \phi \gg \mu)$

$$\boxed{\begin{aligned} D &\approx 2, \\ c_s^2 &\sim \Box\phi/M^3 \sim H/M, \\ M_{\rm eff}^2 &= 0. \end{aligned}}$$

The galileon field perturbation:

$$\delta\ddot{\phi} + \left(3 + \cancel{\frac{\dot{D}}{HD}}\right) H\delta\dot{\phi} - \frac{c_s^2}{a^2}\nabla^2\delta\phi + \cancel{M_{\rm eff}^2}\delta\phi = 0$$

$<< 1$

We have an additional friction, a time varying sound speed, and an effective mass term:

$$\begin{aligned} D &= -A + \frac{3X}{M^4} + \frac{6H\dot{\phi}}{M^3}, \\ c_s^2 &= \frac{-AM^4 + X + 2M(\ddot{\phi} + 2H\dot{\phi})}{-AM^4 + 3X + 6MH\dot{\phi}}, \\ M_{\rm eff}^2 &= -A_\phi\left(\ddot{\phi} + 3H\dot{\phi}\right) - XA_{\phi\phi}. \end{aligned}$$

The spectrum is given at the time the cosmological scale leaves the horizon during the shift-symmetry regime:

$(\phi_c - \phi \gg \mu)$

$$\begin{aligned} D &\approx 2, \\ c_s^2 &\sim \Box\phi/M^3 \sim H/M, \\ M_{\rm eff}^2 &= 0. \end{aligned}$$

$$\Rightarrow \text{scale-invariant spectrum} \quad \mathcal{P}_{\delta\phi} = \frac{H_*^2}{4\pi c_s^3 D}$$

The galileon field perturbation:

$$\delta\ddot{\phi} + \left(3 + \frac{\dot{D}}{HD}\right) H\delta\dot{\phi} - \frac{c_s^2}{a^2}\nabla^2\delta\phi + M_{\rm eff}^2\delta\phi = 0$$

During phase transition, the effective mass becomes important and the field perturbation is evolving : $(|\phi_c - \phi| \sim \mu)$

$$\delta\phi = \lambda(t)\delta\phi_*$$

The galileon field perturbation can convert to the adiabatic curvature perturbation when the shift symmetry is severely broken :

$$\begin{aligned} \zeta_\phi &= \frac{\delta\rho_\phi}{3\rho_\phi(1+w_\phi)} \\ \delta\rho_\phi &= \rho_{\phi,\phi}\delta\phi \end{aligned}$$

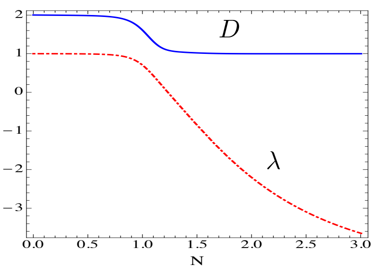

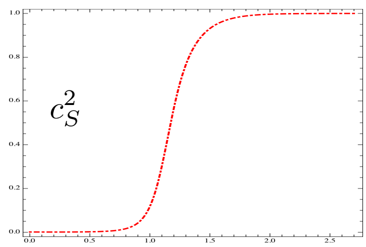

The curvature perturbation is temporally enhanced:

$$\zeta(x) = (1 - r_\phi(t))\zeta_r(\mathbf{x}) + \Theta(t)\delta\phi_*(\mathbf{x})$$

$$\Theta(t) = \frac{r_\phi \lambda}{M_p} \frac{\rho_{\phi,\phi}}{3\rho_\phi(1 + w_\phi)}$$

$$\mathcal{P}_\zeta(k) = (1 - r_\phi)^2 \mathcal{P}_{\zeta_r}(k) + \Theta^2 \mathcal{P}_{\delta\phi}(k)$$

$$\boxed{\mathcal{P}_{\delta\phi} \gg \mathcal{P}_{\zeta_r}}$$

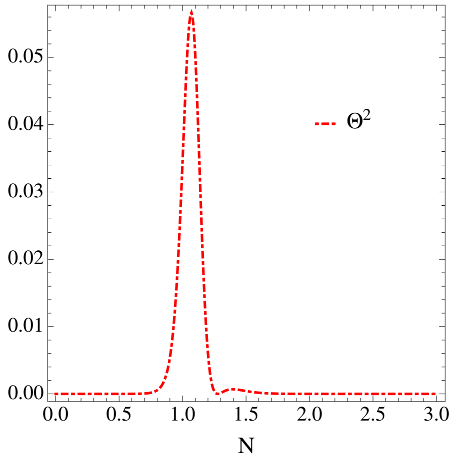

$\Rightarrow$ The resulting power spectrum:

$$\mathcal{P}_\zeta(t = t_c) \simeq 0.05 \times \mathcal{P}_{\delta\phi}$$

$$\mathcal{P}_\zeta(t \gg t_c) = \mathcal{P}_\zeta(t = t_0) = \mathcal{P}_{\zeta_r}$$

Summary

We study a curvaton model with time varying curvature perturbation generated in the radiation dominated epoch.

The spectrum of the curvature perturbation can be temporarily enhanced to an appreciable value.

This cosmological phenomenon is observationally desirable (PBH, GW, ...).

The PBH formation in the temporal enhancement:

Suyama & Yokoyama (2011)

It is enough to consider a toy spectrum in a ''top-hat'' type peaked at the critical scale $k_c = a_c H_c$

Saito & Yokoyama (2009)

$$\mathcal{P}_\psi(k) = \begin{cases} \frac{\mathcal{A}^2}{2\Delta} & \text{for } \ |\ln(k/k_c)| < \Delta, \\ 0 & \text{otherwise,} \end{cases}$$

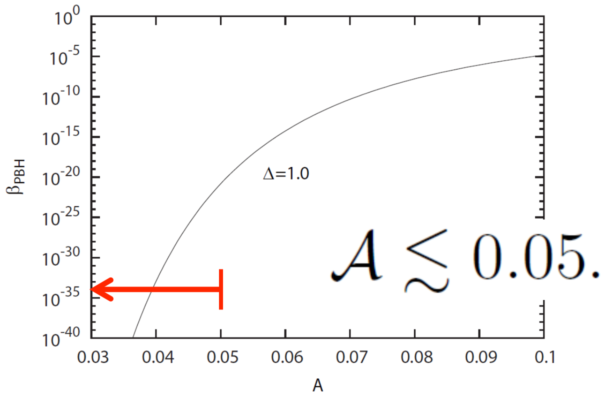

$$\mathcal{A} \lesssim 0.05.$$

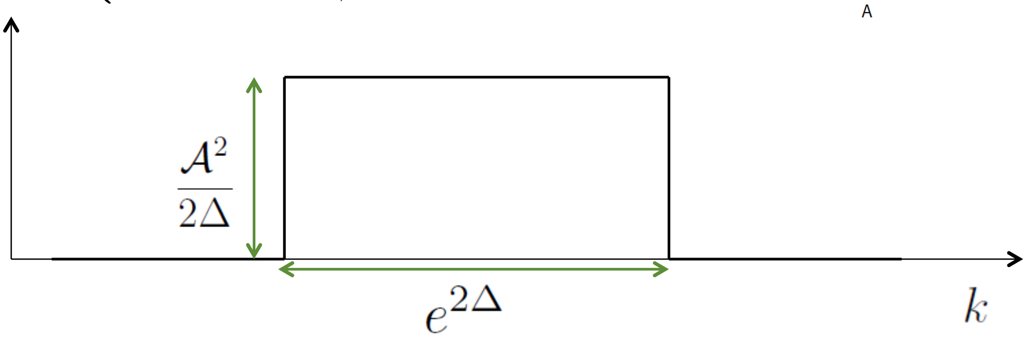

“An Inflationary Universe in Weyl Gauge Theory of Gravitation”

by Masa-aki Watanabe

[JGRG23(2013)110605]

An inflationary universe in Weyl-Cartan gauge theory of gravitation

Masa-aki WATANABE(Kyoto U.),

Jiro SODA(Kobe U.)

Ref:
[1]Charap&Tait Roy.Soc.Lon.Proc.A. **340** 249(1974)
[2]Nieh Phys.Lett.A **88** 388(1982)
[3] MW & JS in prep.

§ 0-1.Motivation

- The **principles** of gravitation(Einstein)
  - Principle of General relativity
  - Principle of Equivalence

General Gauge Principle
(Yang,Millls,Utiyama 1950s)

- **Poincare Gauge theory of Gravitation (PG)**
  (Kibble 1961)

…Einstein gravity is understood as a certain limit of a PG model!

§ 0-2.extention to Weyl group

- The symmetry group of gravitation is really the Poincare?

  What if not Poincare?

- a simplest extension:
  Weyl-Cartan Gauge theory of gravitation(WG)
  (§ 1 , Charap&Tait 1974 [1])

  (Weyl group) = (Poincare group) **x (dilation)**

- However, the **dilation** (scale transformation) symmetry **must be broken** for mass scales to appear.

§ 0-3.Observational signatures

- Spontaneous breakdown of the dilation symmetry (§ 2, Nieh 1982 [2])
  - Broken by ``dilaton'' $\langle \varphi \rangle \neq 0$

YIELDS

PG + massive vector ``conformon'' A_μ
that is **decoupled** to Dirac fields
``It will not be physically significant.''

- Our question:
  ``Can **inflation cosmology** shed the light of **modern precise observation** on the Weyl-Cartan gauge theory of gravitation? (through **inflaton-conformon** interaction)''

§ 0-4.Outline

§ 1. Weyl-Cartan gauge theory of gravitation[1]

- -1.define **global Weyl** transformation
- -2.**localize** the Weyl transformation
- -3.compose **covariant derivative**
- -4.construct an **invariant action** integral

§ 2. Spontaneous **breakdown** of **dilation** sym.[2]

§ 3. dynamics of the **inflationary** universe and its imprints on the **CMB** [3]

§ 1-1.Global (positon independent) Weyl transformation

- Infinitesimal Weyl transformation of x^μ

$$\delta x^\mu = \epsilon^{\mu\nu}\eta_{\nu\lambda}x^\lambda + \epsilon^\mu + \epsilon x^\mu$$

Homogenous Lorentz trans Translation Dilation

- Correspondingly, matter fields, e.g.:

$$\chi = {}^T(\varphi^{(1)}, \phi^{(2)}, A_1^{(0)}, .., A_4^{(0)}, \psi_1^{(3/2)}, .., \psi_4^{(3/2)}, ..etc)$$

are assumed to transform as

$$\delta\chi = \frac{1}{2}\epsilon^{\mu\nu}\mathbf{S}_{\mu\nu}\chi - \epsilon\Delta\chi$$

$\mathbf{S}_{\mu\nu} = -\mathbf{S}_{\nu\mu}$:representation matrix of Lorentz group

Δ:diag. matrix (the A^{th} comp.= ``dilation class” of χ_A)

§ 1-2.Local (position dependent) Weyl transformation.

- **Kibble's idea** to ``localize" spacetime transformations: **to distinguish…**
  - **(external) coordinate transformation and,**
  - **(internal) field transformation**
- Independent variables $\epsilon^{\mu\nu}, \epsilon, \epsilon^{\mu}$ (global)

LOCALIZE
$$\begin{cases} \xi^{\mu}(x) = \delta x^{\mu} = \epsilon^{\mu\nu}(x)\eta_{\nu\lambda}x^{\lambda} + \epsilon^{\mu}(x) + \epsilon(x)x^{\mu} \\ \qquad\qquad\qquad \text{:external(Greek index)} \\ \epsilon^{ij}(x), \epsilon(x) \;\; \text{:internal(Latin index)} \end{cases}$$

- Thus, infinitesimal local Weyl trans. is defined by

$$\delta x^{\mu} = \xi^{\mu}(x), \quad \delta\chi(x) = \tfrac{1}{2}\epsilon^{ij}(x)\mathbf{S}_{ij}\chi - \epsilon(x)\Delta\chi$$

§ 1-3.Covariant derivative

- Out of $\delta(\chi_{,\mu}) = (\delta\chi)_{,\mu} - (\delta x^{\nu})_{,\mu}\chi_{,\nu}$

$$= \left(\tfrac{1}{2}\epsilon^{ij}S_{ij} - \epsilon\Delta\right)\chi_{,\mu} - \xi^{\nu}_{,\mu}\chi_{,\nu} + \tfrac{1}{2}\epsilon^{ij}{}_{,\mu}\mathbf{S}_{ij}\chi - \epsilon_{,\mu}\Delta\chi$$

, we'd like to construct **cov. der.** that obeys the same transformation law as the global one:

$$\delta(\chi_{;k}) = \tfrac{1}{2}\epsilon^{ij}\mathbf{S}_{ij}\chi_{;k} - \epsilon^{i}{}_{k}\chi_{;i} - \epsilon(\Delta+1)\chi_{;k}$$

- **Kibble's idea**: to introduce **2 kinds** of ``gauge fields"

$$\boxed{\chi_{;k} = h^{\mu}_{k}\chi_{|\mu}, \;\; \chi_{|\mu} = \chi_{,\mu} + \tfrac{1}{2}A^{ij}{}_{\mu}\mathbf{S}_{ij}\chi - A_{\mu}\Delta\chi}$$

$$\begin{cases} \delta A^{ij}{}_{\mu} = \epsilon^{i}{}_{k}A^{kj}{}_{\mu} + \epsilon^{j}{}_{k}A^{ik}{}_{\mu} - \xi^{\nu}{}_{,\mu}A^{ij}{}_{\nu} - \epsilon^{ij}{}_{,\mu} \\ \delta A_{\mu} = -\xi^{\nu}{}_{,\mu}A_{\nu} - \epsilon_{,\mu} \end{cases}$$

$$\delta h^{\mu}_{k} = \xi^{\mu}_{,\nu}h^{\nu}_{k} - \epsilon^{i}{}_{k}h^{\mu}_{i} - \epsilon h^{\mu}_{k} \quad \text{:Dilation class 1}$$

§ 1-4.Weyl-invariant action

- The invariant volume element in PG:

$$\mathfrak{H} d^4x = (\det(h_k^\mu)^{-1}) d^4x$$

is no longer invariant in WG, but transforms as:

$$\delta(\mathfrak{H} d^4x) = 4\epsilon(\mathfrak{H} d^4x)$$

,hence for action integral $I = \int L(x)\mathfrak{H} d^4x$ to be Weyl-invariant, Lagrangian must satisfy:

$\delta L = -4\epsilon$: translation & Lorentz invariant but belongs to dilation class 4

§ 1-4.Lagrangian of gauge fields

- For field strengths of gauge fields, we have:
  - □Maxwell tensor: dilation class 2

$$F_{kl} = h_k^\mu h_l^\nu (A_{\nu,\mu} - A_{\mu,\nu})$$

  - □Riemann tensor: dilation class 2

$$R^{ij}{}_{kl} = h_k^\mu h_l^\nu (A^{ij}{}_{\mu,\nu} - A^{ij}{}_{\nu,\mu} - A^i{}_{k\mu} A^{kj}{}_\nu + A^i{}_{k\nu} A^{kj}{}_\mu)$$

  - □Torsion tensor: dilation class 1

$$C^i_{kl} = h_k^\mu h_l^\nu (b^i_{\mu|\nu} - b^i_{\nu|\mu})$$

$$(b^i_{\mu|\nu} = b^i_{\mu,\nu} + A^i_{k\nu} b^k_\mu + A_\nu b^i_\mu,\ b = h^{-1} : \text{inverse matrix})$$

⇒ We only have to construct dilation class 4 Lagrangian out of them.

§ 2.a simple model of spontaneous **breakdown of dilation** symmetry[2]

- Introduce ``dilaton" (scalar field of dilation class 1): φ and consider the Lagrangian:

$$L = \frac{a\varphi^2 R}{2} - \frac{1}{2} D_\mu \varphi D^\mu \varphi - \frac{f^2}{4} F^{\mu\nu} F_{\mu\nu} + \cdots .$$

$$D_\mu \varphi = (\partial_\mu - A_\mu)\varphi$$

a, f : dimensionless coupling constants

- Hyposesis: ``φ has a non-zero value"

⇒ Using the gauge d.o.f. of dilation ϵ, we can choose ``unitary gauge" $\varphi(x) \equiv \frac{1}{\sqrt{8\pi G a}}$

§ 2.**breakdown of dilation** symmetry

- In unitary gauge: $\varphi(x) \equiv \frac{1}{\sqrt{8\pi G a}}$, it yields

$$L = \frac{R}{16\pi G} - \frac{1}{2} \frac{1}{8\pi G a} A_\mu A^\mu - \frac{f^2}{4} F^{\mu\nu} F_{\mu\nu} + \cdots .$$

⇒ PG+massive vector field ``conformon" with mass $M_A = \frac{1}{\sqrt{af}} m_{\mathrm{pl}}$

- However, conformon is **decoupled** to Dirac fields;

$$L_{\mathrm{Dirac}} = \frac{1}{2}\left[\bar{\psi} i\gamma^\alpha h_a^\mu D_\mu \psi - \bar{\psi} \bar{D}_\mu i\gamma^\alpha h_\alpha^\mu \psi\right]$$

is already invariant without…

$$\left.\begin{aligned} D_\mu &= \partial_\mu - \tfrac{1}{4} i A^{ab}{}_\mu \sigma_{ab} - \tfrac{3}{2} A_\mu \\ \bar{D}_\mu &= \partial_\mu + \tfrac{1}{4} i A^{ab}{}_\mu \sigma_{ab} - \tfrac{3}{2} A_\mu \end{aligned}\right\}\text{gauge coupling!}$$

§ 3-1.inflationary model

- Inflaton-conformon coupling yields any observational effect?

$$L_1 = \left[-\frac{1}{2}D_\mu\phi D^\mu\phi - \lambda\phi^4\right]$$

ϕ : inflaton (dilation class 1) $D_\mu\phi = (\partial_\mu - A_\mu)\phi$

- unitary gauge $\varphi(x) \equiv \frac{1}{\sqrt{8\pi G a}}$ makes **WG->PG**.
- Furthermore $\frac{\partial L_1}{\partial A^{ij}{}_\mu} = 0$ makes **PG->Einstein**

$\boxed{\textit{Einstein + conformon } A_\mu \textit{ + coupled inflaton } \phi}$

§ 3-2.background solution

- Homogeneous isotropic ansatz

$$ds^2 = -dt^2 + e^{2\alpha(t)}d\mathbf{x}^2,\ \mathrm{A}_\mu dx^\mu = A_t(t)dt,\ \ \phi = \phi(t)$$

- Solving constraint

$$A_t = \frac{\phi\dot{\phi}}{\frac{1}{8\pi G a} + \phi^2}$$

$$\mathfrak{H}L = e^{3\alpha}\left[-\frac{3}{8\pi G}\dot{\alpha}^2 + \frac{1}{2}\frac{\frac{1}{8\pi G a}}{\frac{1}{8\pi G a} + \phi^2}\dot{\phi}^2 - \lambda\phi^4\right]$$

- For $\frac{1}{8\pi G a} \ll \phi^2$

  canonical variable is given by $\Phi = \frac{\ln\phi}{\sqrt{8\pi G a}}$
  and the *quartic* potential acts as *exponential* (power-law inflation)

§ 3-3.imprints on the CMB

- Evolution of slow-roll parameters

N: e-folding number(horizon exit -> inflation end)

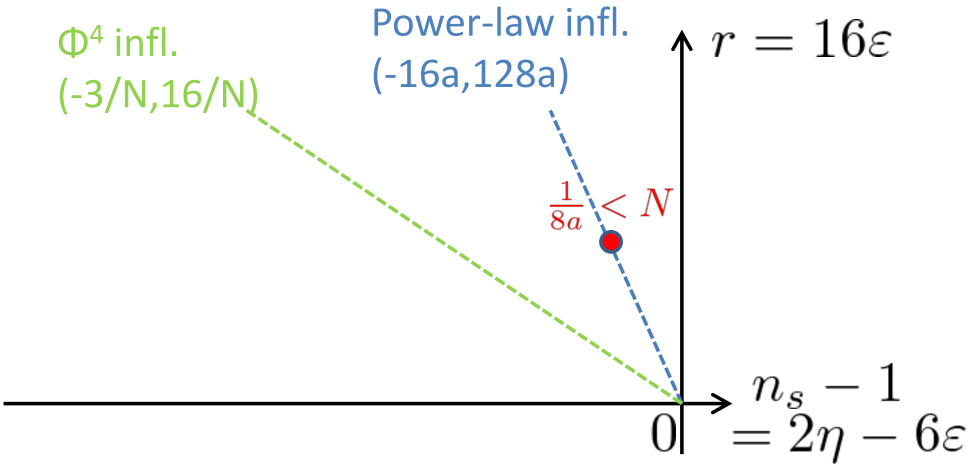

§ 3-3.imprints on the CMB

- Evolution of slow-roll parameters

N: e-folding number(horizon exit -> inflation end)

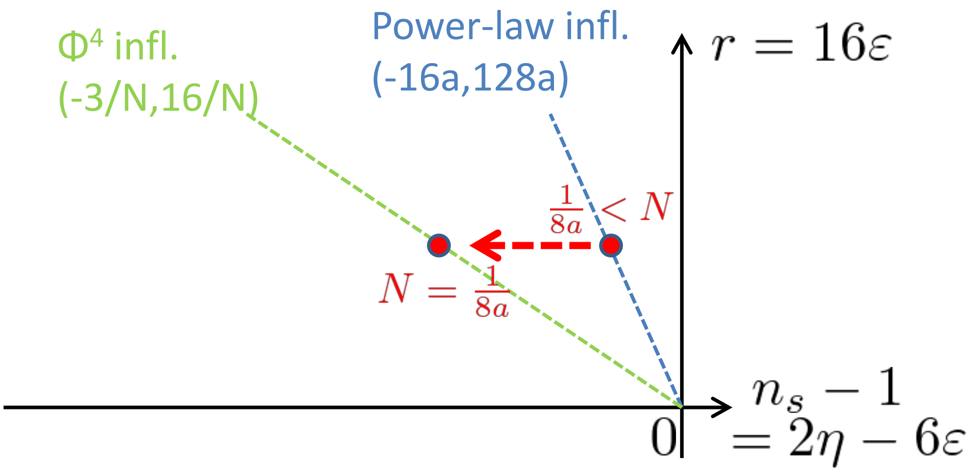

§ 3-3.imprints on the CMB

- Evolution of slow-roll parameters

N: e-folding number(horizon exit -> inflation end)

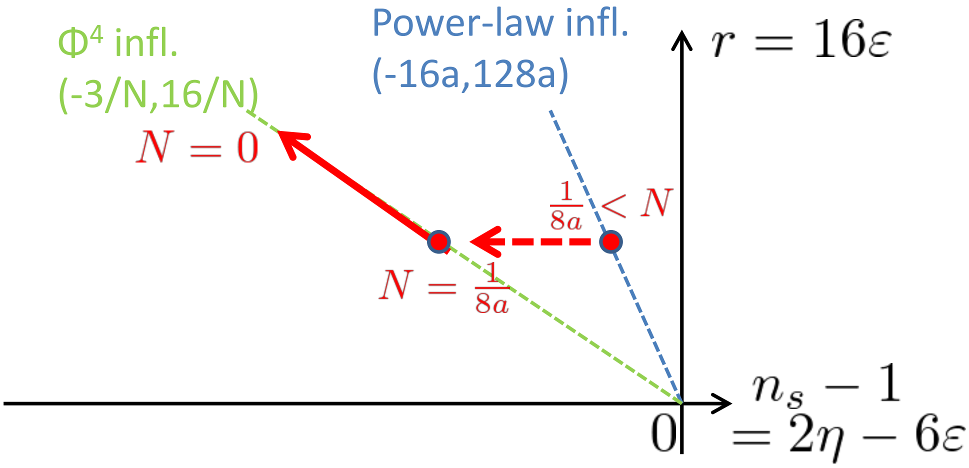

§ 3-3.imprints on the CMB

- Evolution of slow-roll parameters

N: e-folding number(horizon exit -> inflation end)

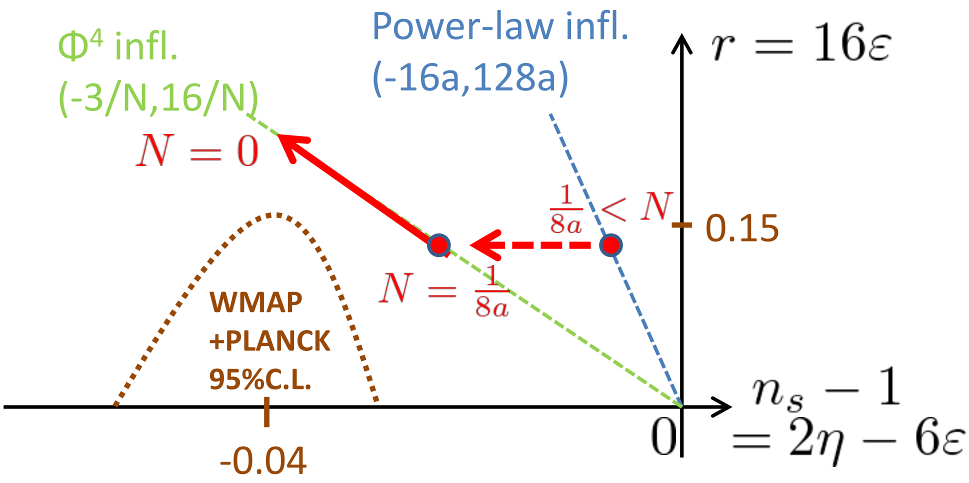

- Excluded by WMAP+PLANCK (>95% C.L.)

§ 3-3.an extension

- e.g.: Inflaton of dilation class 2

$$L_2 = -\frac{1}{2}\varphi^{-2} D_\mu \phi D^\mu \phi - \lambda \phi^2, \;\; D_\mu \phi = (\partial_\mu - 2A_\mu)\phi$$

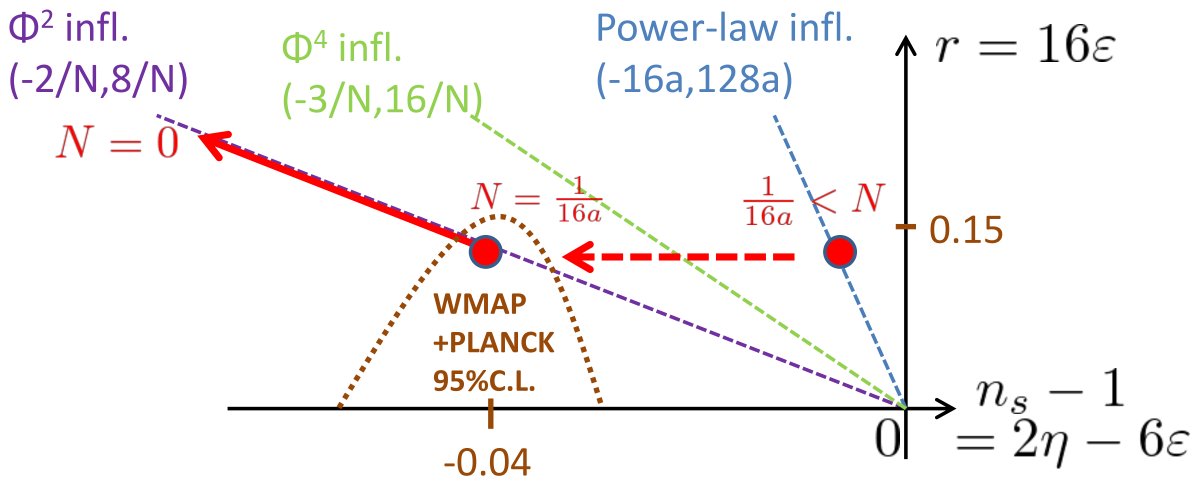

- Dilaton –EH coupling const. is constrained!

$N > 55 \Rightarrow a < \frac{1}{880}$ (WMAP+PLANCK 95%C.L.)

SUMMARY

- To understand better the principles and the symmetries underlying the gravitation, we focused on Weyl-Cartan gauge theory of gravitation.
- Spontaneous breakdown of dilation symmetry yields PG + massive vector field ``conformon" that is, however, decoupled to Dirac fields.
- **Yet, conformon-inflaton interaction may affect the inflationary cosmology, and constrain dilaton-EH coupling constant *a*.**

Thanks for your attention!

“Gravitational particle production and modulated reheating after inflation”

by Yuki Watanabe

[JGRG23(2013)110606]

JGRG23 – The 23rd Workshop on General Relativity and Gravitation in Japan
Hirosaki University, Aomori, Japan, 6 Nov. 2013

Gravitational particle production and modulated reheating after inflation

Yuki Watanabe (RESCEU, U. Tokyo)
Collaborator: J. White (YITP, Kyoto U.)

Work in progress

Refs: PRD 75, 061301(R) (2007); 77, 043514 (2008)
83, 043511 (2011); 87, 103524 (2013)

Outline

- Introduction: Why study reheating?
- Inflationary models with multiple fields and non-minimal gravitational coupling
- Gravitationally induced interactions and decay rates
- The role of Higgs boson during gravitational reheating
- Constraints on perturbation spectra from Planck 2013
- Conclusion

Why Study Reheating?

Inflation saves the Big Bang model.

By exponentially expanding a small region, inflation solves several problems not addressed by the Big Bang model:

- Isotropy of the CMB radiation
- Origin of the cosmic structure, $\delta T/T \sim 10^{-5}$
- Flatness of the Universe, $\Omega_{tot} \sim 1$

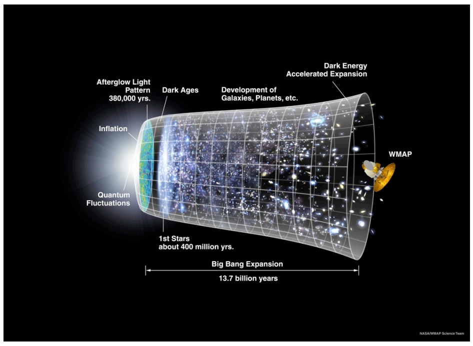

The Universe is left cold and empty after inflation.

⇒ It must heat up to have a hot Big Bang cosmology:

Energy in inflaton must transfer to radiation, and heat the Universe to at least ~10 MeV for successful nucleosynthesis.

Can we constrain this important epoch from observations?

Yes, we can (hopefully in the future).

- Inflationary predictions are on lines and have "theoretical uncertainty."
- Reheating physics tells us a point or shorter line in n_s-r plane.

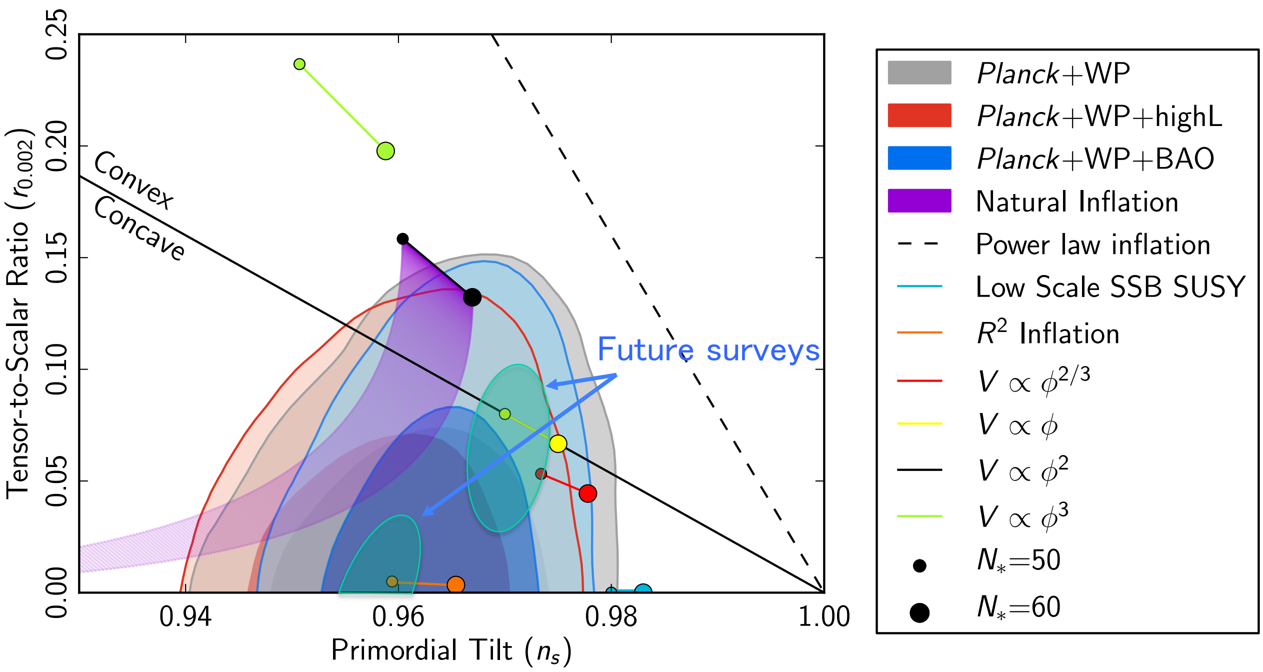

Standard Lore

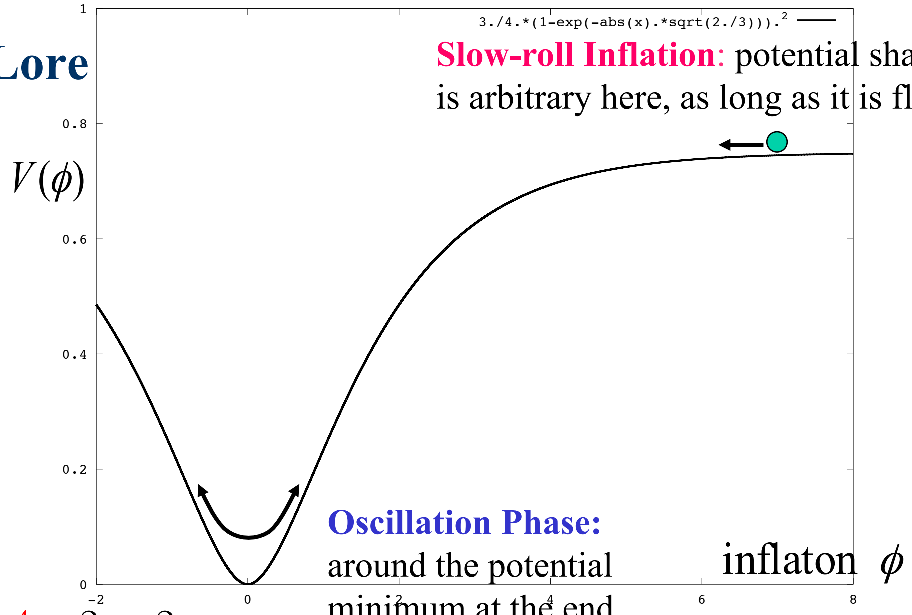

Slow-roll Inflation: potential shape is arbitrary here, as long as it is flat.

Oscillation Phase: around the potential minimum at the end of inflation

Energetics:

$$g^4 V \sim g^4 H^2 M_{pl}^2$$

$$\sim \rho_{rad} \sim T_{rh}^4$$

$$\rightarrow T_{rh} \sim g\sqrt{HM_{pl}}$$

What determines *"energy–conversion efficiency factor", g?*

Yuki Watanabe, Gravitational Modulated Reheating, JGRG, 6 Nov. 2013

Perturbative Reheating

Dolgov & Linde (1982); Abbott, Farhi & Wise (1982); Albrecht et al. (1982)

Inflaton decays and the Universe is thermalized through the tree-level interactions like:

$$L_{\text{int}} = -\left(g_\psi \phi\bar{\psi}\psi + g_\chi \phi\chi^2 + g^2\phi^2\chi^2 + \cdots\right)$$

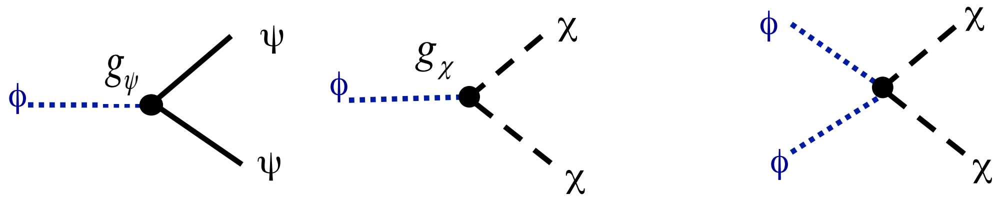

Inflaton can decay, if allowed kinematically, with the widths given by

$$\Gamma(\phi \to \chi\chi) = \frac{N_\chi g_\chi^2}{8\pi m_\phi}\left(1 - \frac{4m_\chi^2}{m_\phi^2}\right)^{1/2} \coth\left(\frac{m_\chi}{4T}\right) C_\chi$$

$$\Gamma(\phi \to \bar{\psi}\psi) = \frac{N_\psi g_\psi^2 m_\phi}{8\pi}\left(1 - \frac{4m_\psi^2}{m_\phi^2}\right)^{3/2} \tanh\left(\frac{m_\psi}{4T}\right) C_\psi$$

Bose condensate

Pauli blocking

Thermal medium effect

Reheating Temperature from Energetics

$$\ddot{\phi} + (3H + \Gamma_{tot})\dot{\phi} + m_\phi^2 \phi = 0 \qquad H_{\inf} >> H_{osc} \propto a^{-3/2}$$

$3H_{osc} > \Gamma_{tot} \Rightarrow$ Inflaton dominates the energy density.

$3H_{osc} < \Gamma_{tot} \Rightarrow$ Decay products dominate the energy density.

$$\rho_{rad}(t_{rh}) = 3M_{Pl}^2 H_{osc}^2 = \frac{M_{Pl}^2 \Gamma_{tot}^2}{3} = \frac{\pi^2}{30} g_*(T_{rh}) T_{rh}^4$$

$$\Longrightarrow \quad T_{rh} = \frac{\sqrt{M_{Pl}\Gamma_{tot}}}{(10\pi^2)^{1/4}} \left(\frac{g_*(T_{rh})}{100} \right)^{-1/4}$$

Coupling constants determine the decay width, Γ.

But, what determines coupling constants and how strong are they?

Fine-tuning Problem?

$$g^4 V \sim g^4 H_{inf}^2 M_{pl}^2$$

$$\sim \rho_{rad} \sim T_{rh}^4$$

$$\rightarrow T_{rh} \sim g\sqrt{H_{inf} M_{pl}}$$

If $T_{rh} = 10^{-10} M_{Pl}$ and $H_{\inf} = 10^{-4} M_{Pl}$,

then $\underline{g \sim 10^{-8}}$.

To relax fine-tuning, one needs:

(a) High reheat temperature

- unwanted relics (e.g., topological defects),

(b) Very low-scale inflation (H ~ 10^{-18} M_{pl} ~ 1 GeV for g ~ 0.1)

- worse fine-tuning, or

(c) Natural explanation for the smallness of *g*.

What are coupling constants?

Problem: arbitrariness of the nature of inflaton fields

- Reheating works very well as a concept, but we do not understand the nature (including interaction properties) of inflaton.

  e.g. Higgs-like scalar fields, Axion-like fields, Flat directions, RH sneutrino, Moduli fields, Distances between branes, and many more…

- Arbitrariness of inflaton = Arbitrariness of couplings
- Can we say anything generic about reheating? Universal reheating?

Universal coupling?

Gravitational coupling is universal.

➢ too weak to cause reheating with GR only

In the early universe, however, GR would be modified.

→ What happens to "gravitational decay channel", when GR is modified?

Conventional GR during inflation & reheating

$$\mathcal{L} = \sqrt{-g}\left[\underline{\frac{1}{2}M_{\rm Pl}^2 R} - \frac{1}{2}h_{ab}g^{\mu\nu}\partial_\mu\phi^a\partial_\nu\phi^b - V(\phi)\right] + \mathcal{L}_{\rm m}$$

Einstein-Hilbert term generates GR.
Inflaton minimally couples to gravity.

$$L_{\rm int} = -\left(g_\psi \phi\bar{\psi}\psi + g_\chi \phi\chi^2 + g^2\phi^2\chi^2 + \cdots\right)$$

Conventionally one introduces explicit couplings between inflaton and matter.

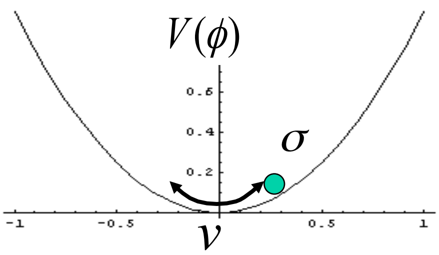

$$\phi = v + \sigma$$

Modifying GR during inflation & reheating

Instead of introducing explicit couplings by hand,

$$L_{\rm int} = -\cancel{\left(g_\psi \phi\bar{\psi}\psi + g_\chi \phi\chi^2 + g^2\phi^2\chi^2 + \cdots\right)}$$

$$\mathcal{L} = \sqrt{-g}\left[\frac{1}{2}\underline{f(\phi)R} - \frac{1}{2}h_{ab}g^{\mu\nu}\partial_\mu\phi^a\partial_\nu\phi^b - V(\phi)\right] + \mathcal{L}_{\rm m}$$

Non-minimal gravitational coupling: common in low-r inflationary models, e.g. R^2, Higgs inflation
In order to ensure GR after inflation, $f(v) = M_{Pl}^2$

Matter (all standard model particles) completely decouples from inflaton and coupled to gravity minimally.

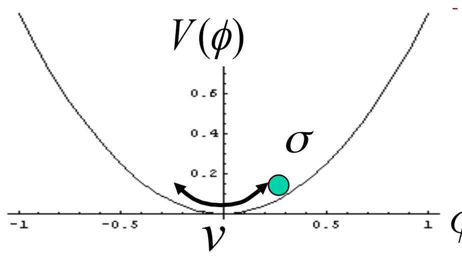

$$\phi = v + \sigma$$

Yuki Watanabe, Gravitational Modulated Reheating, JGRG, 6 Nov. 2013

Induced decay channel through "scalar gravity waves"

$$g_{\mu\nu} = \bar{g}_{\mu\nu} + \tilde{h}_{\mu\nu} - \frac{f_A}{M_{\rm Pl}^2}\bar{g}_{\mu\nu}\alpha^A \qquad \phi^a - \phi^a_{\rm vev} = \sigma^a = \alpha^A e^a_A$$

Fermion matter:

Yukawa interaction

$$\mathcal{L}_\psi = -\bar{e}\bar{\psi}[\bar{e}^{\mu\alpha}\gamma_\alpha\bar{D}_\mu + m_\psi]\psi + \cdots + \bar{e}\underbrace{\frac{f_A m_\psi}{2M_{\rm Pl}^2}}_{=\, g_\psi}\alpha^A\bar{\psi}\psi$$

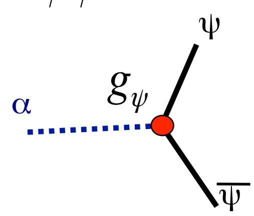

Scalar matter:

$$\mathcal{L}_\chi = -\frac{1}{2}\bar{e}\Big[\bar{g}^{\mu\nu}\partial_\mu\chi\partial_\nu\chi + 2U(\chi) + \cdots - \frac{f_A}{2M_{\rm Pl}^2}\alpha^A\{2m_\chi^2\chi^2 + (\partial\chi)^2\}\Big]$$

Trilinear interaction

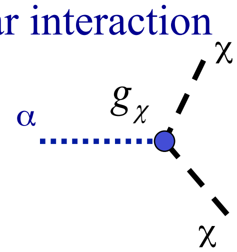

$$m_\chi^2 = U''(\chi) \qquad g_\chi \equiv \frac{f_A(2m_\chi^2 + m_{\hat{A}}^2)}{4M_{\rm Pl}^2}$$

Magnitude of the Induced Couplings

$$g_\psi = \frac{f_a e^a_A}{2M^2_{\rm Pl}} m_\psi$$

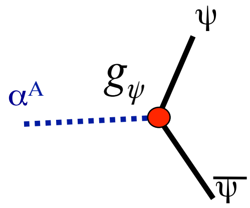

- For $f(\phi) = M^2+\xi\phi^2$, $h(\phi)=1$, $g_\psi = \xi(1+6\xi)^{-1/2}(v/M_{pl})(m_\psi/M_{pl})$
  ⇒ Natural to obtain a small Yukawa coupling, $g_\psi \sim 10^{-8}$, for $\xi \sim 1$, $m_\psi \sim 10^{-8} M_{pl}$
- The induced Yukawa interaction vanishes for massless fermions: **conformal invariance of massless fermions**

- Massless, minimally-coupled scalar fields are **not conformally invariant**. Therefore, the trilinear interaction does not vanish even for massless scalar fields:

$$g_\chi = \frac{f_a e^a_A}{4M^2_{\rm Pl}} (m^2_{\hat{A}} + 2m^2_\chi)$$

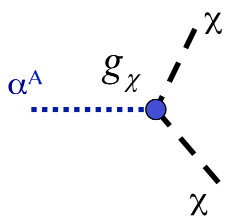

Yuki Watanabe, Gravitational Modulated Reheating, JGRG, 6 Nov. 2013

Gravitational Particle Production Rate in the SM

Top Quarks $\quad m_t^2 = y_t^2 h^2$

$$\Gamma(\alpha^A \to \bar{\psi}_t \psi_t) \simeq \frac{N_t f_A^2 m_{\hat{A}} y_t^2 h^2}{64\pi M^4_{Pl}}$$

Higgs Bosons $\quad h = \sqrt{\langle h^2 \rangle} + \chi, \quad m_h^2 = 3\lambda h^2$

$$\Gamma(\alpha^A \to \chi\chi) \simeq \frac{f_A^2 m^3_{\hat{A}}}{128\pi M^4_{Pl}} \left(1 + \frac{6\lambda h^2}{m^2_{\hat{A}}}\right)$$

Weak Bosons (longitudinal modes of W^+, W^-, Z) $\quad m_w^2 = g^2 h^2$

$$\Gamma(\alpha^A \to W_L W_L) \simeq \frac{N_w f_A^2 m^3_{\hat{A}}}{128\pi M^4_{Pl}} \left(1 + \frac{2g^2 h^2}{m^2_{\hat{A}}}\right)$$

Modulated Reheating [Dvali, Gruzinov & Zaldarriaga 2004; Kofman 2003]

The decay rate of inflatons depends on a light scalar field, h.

$$\Gamma = \Gamma(h) = a + bh^2$$

SM Higgs condensate may modulate the gravitational decay rate!

During inflation, [Starobinsky & Yokoyama 1994; Kunimitsu & Yokoyama 2012]

$$h = \sqrt{\langle h^2 \rangle} + \delta h, \quad \langle h^2 \rangle \approx 0.132 \frac{H_J^2}{\sqrt{\lambda}}, \quad \delta h \approx \sqrt{S^{hh}} \frac{H}{2\pi}$$

$$\Gamma(h) = \Gamma(\langle h^2 \rangle) + \delta\Gamma \qquad T_{\rm rh} \propto \Gamma^{1/2} \Rightarrow \frac{\delta T_{\rm rh}}{T_{\rm rh}} = \frac{1}{2}\frac{\delta\Gamma}{\Gamma}$$

Reheating time is modulated due to the Higgs.
How does this lead to the curvature perturbation?

Curvature Perturbation from Modulated Reheating

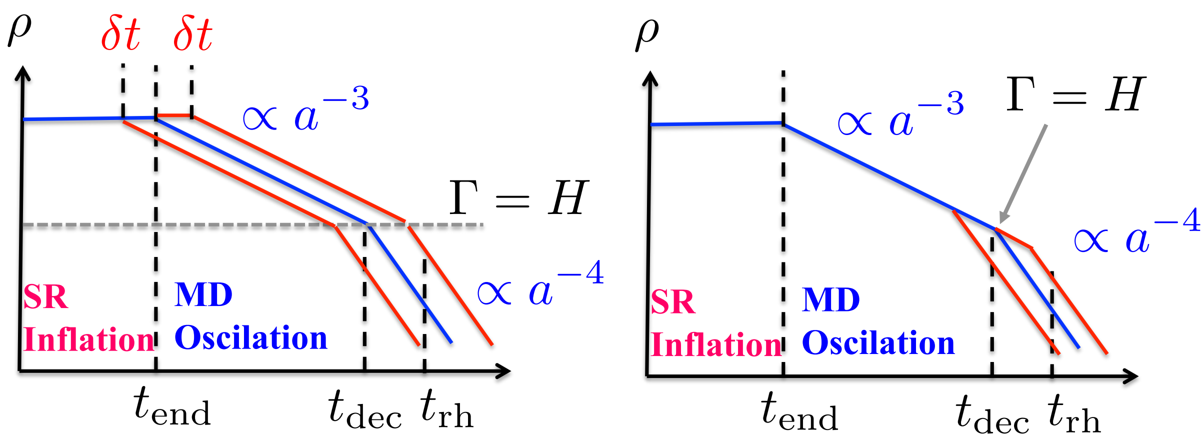

On flat gauge

$$\rho(t_{\rm rh}) = \rho_* \left(\frac{a_{\rm dec}}{a_{\rm end}}\right)^{-3} \left(\frac{a_{\rm rh}}{a_{\rm dec}}\right)^{-4} = \rho_* \left(\frac{a_{\rm end}}{a_{\rm rh}}\right)^{4} \left(\frac{\Gamma}{H_*}\right)^{-2/3}$$

$$\frac{\delta\rho(t)}{\rho(t)} = \frac{\delta a_{\rm dec}}{a_{\rm dec}} = -\frac{2}{3}\frac{\delta\Gamma}{\Gamma} \qquad \zeta = \frac{1}{4}\frac{\delta\rho(t)}{\rho(t)} = -\frac{1}{6}\frac{\delta\Gamma}{\Gamma} = -\frac{1}{3}\frac{\delta T_{\rm rh}}{T_{\rm rh}}$$

Curvature Perturbation and its Spectral Properties

[Zaldarriaga 2004; Suyama & Yamaguchi 2008; White & YW in prep.]

When instant decay approximation is not valid,

$$\tilde{N} = \tilde{N}^{(i)} - \frac{1}{2}\ln\left(\frac{\tilde{H}(t_{\rm rh})}{\tilde{H}(t_{\rm osc})}\right) + Q\left(\frac{\tilde{\Gamma}(\bar{h})}{\tilde{H}(t_{\rm osc})}\right)$$

$$\delta\tilde{N} = \tilde{N}_a^{(i)}\delta\phi_*^a + \tilde{N}_{ab}^{(i)}\delta\phi_*^a\delta\phi_*^b + xQ'\frac{\tilde{\Gamma}_h}{\tilde{\Gamma}}\delta h + \frac{1}{2}\left[x^2Q''\left(\frac{\tilde{\Gamma}_h}{\tilde{\Gamma}}\right)^2 + xQ'\frac{\tilde{\Gamma}_{hh}}{\tilde{\Gamma}}\right]\delta h\delta h$$

$$\mathcal{P}_\zeta = \mathcal{P}_{inf} + \mathcal{P}_{reh} = \tilde{N}_a^{(i)}\tilde{N}_b^{(i)}S^{ab}\left(\frac{\tilde{H}_*}{2\pi}\right)^2 + \left(A(x)\frac{\tilde{\Gamma}_h}{\tilde{\Gamma}}\right)^2\left(\frac{h(\tilde{N})}{h_*}\right)^{12}S^{hh}\left(\frac{\tilde{H}_*}{2\pi}\right)^2$$

$$\simeq \left(A(x)\frac{\tilde{\Gamma}_h}{\tilde{\Gamma}}\right)^2\left(\frac{h(\tilde{N})}{h_*}\right)^{12}\left(\frac{H_*}{2\pi}\right)^2\frac{1+\Upsilon}{\Upsilon},$$

$$\Upsilon = \frac{\mathcal{P}_{reh}}{\mathcal{P}_{inf}} \qquad A(x) = xQ' \qquad B(x) = x^2Q''$$

Curvature Perturbation and its Spectral Properties

[Zaldarriaga 2004; Suyama & Yamaguchi 2008; White & YW in prep.]

$$\tilde{n}_s - 1 = \frac{(\tilde{n}_s-1)^{(i)}}{1+\Upsilon} + \frac{\Upsilon}{1+\Upsilon}\left(\frac{df/d\tilde{t}}{f\tilde{H}_*} + \frac{2M_{pl}^2V_{hh}}{3\tilde{H}_*^2 f} - 2\tilde{\epsilon}\right)$$

$$(\tilde{n}_s-1)^{(i)} = -2\tilde{\epsilon} - \frac{2}{\tilde{N}^a\tilde{N}_a} + \frac{2\tilde{N}^a\tilde{N}^b}{3\tilde{H}^2\tilde{N}_e\tilde{N}^e}\left[\tilde{\nabla}_a\tilde{\nabla}_b\tilde{V} + \tilde{R}_{acbd}\frac{d\phi^c}{d\tilde{t}}\frac{d\phi^d}{d\tilde{t}}\right]$$

$$r = \frac{8S_{hh}\Upsilon}{M_{pl}^2(1+\Upsilon)}\left(A(x)\frac{\tilde{\Gamma}_h}{\tilde{\Gamma}}\right)^{-2}\left(\frac{h(\tilde{N})}{h_*}\right)^{-12}$$

$$f_{NL} = \frac{5}{6}\frac{\tilde{N}_a^{(i)}\tilde{N}_b^{(i)}\tilde{\nabla}_c\tilde{\nabla}_d S^{ac}S^{bd} + \frac{1}{2}\tilde{N}_h\tilde{N}_h\frac{f_a}{f}\tilde{N}_c^{(i)}S^{ac}S^{hh}}{\left[\tilde{N}_h\tilde{N}_h S^{hh}\frac{1+\Upsilon}{\Upsilon}\right]^2}$$

$$+\frac{5}{6}\frac{\Upsilon^2}{A(x)(1+\Upsilon)^2}\left[\frac{B(x)}{A(x)} + \frac{\tilde{\Gamma}\tilde{\Gamma}_{hh}}{\tilde{\Gamma}_h^2} + \frac{\tilde{\Gamma}}{\tilde{\Gamma}_h}\frac{12}{5h_*}\left[\frac{h_*}{h(N)} - \left(\frac{h_*}{h(N)}\right)^6\right]\right]$$

Constraints from Observations [White & YW in prep.]

$$\mathcal{P}_\zeta = 2.06 \times 10^{-4} \Theta^2 \frac{(1+\Upsilon)}{\Upsilon} \left(\frac{1}{\mu_1}\right)^5 \left(\frac{A(x)}{0.089}\right)^2 \left(\frac{\sqrt{\lambda}}{0.1}\right) \left(\frac{0.132}{\kappa^2}\right)$$

$$\mu_1 = \left[1 + \frac{0.242}{1.242}\left(\left(\frac{\kappa^2}{0.132}\right)\left(\frac{\sqrt{\lambda}}{0.1}\right)\left(\frac{\tilde{N}_f - \tilde{N}_*}{55}\right) - 1\right)\right]$$

$$f_{NL} \simeq \frac{5}{6} \frac{\Upsilon^2}{(1+\Upsilon)^2} \frac{4.08}{\Theta} \qquad \Theta = \frac{bh^2}{a + bh^2}$$

Planck: $\mathcal{P}_\zeta = 2.2 \times 10^{-9}$ ⇒ $\Theta^2 \simeq 1.07 \times 10^{-5} \frac{\Upsilon}{1+\Upsilon}$

$-8.9 < f_{NL} < 14.3 \quad (95\%\mathrm{CL})$ ⇒ $\frac{\Upsilon}{1+\Upsilon} \lesssim 5.7 \times 10^{-2}$

$$\Theta \lesssim 7.8 \times 10^{-4}$$

$$\left(\frac{H_*}{m_A}\right)^2 \lesssim 1.1 \times 10^{-2}$$

Conclusion

- Reheating by gravitational particle production with non-minimal gravity and non-trivial field-space metric:
  - Inflaton quanta inevitably decay into any non-conformal fields (spin-0, ½, 1) without explicit interactions in the original Lagrangian.
  - Conformal invariance must be broken at the tree-level or by loops.
  - Heavy fields contribute through gauge trace anomaly.
- Reheating modulated by SM Higgs condensate
  - General formulas for perturbations are derived.
  - Curvature perturbation from GMR is subdominant.
  - Inflaton mass during reheating can be constrained by observational data.

“I-ball formation with log potential”

by Naoyuki Takeda

[JGRG23(2013)110607]

13年11月6日水曜日

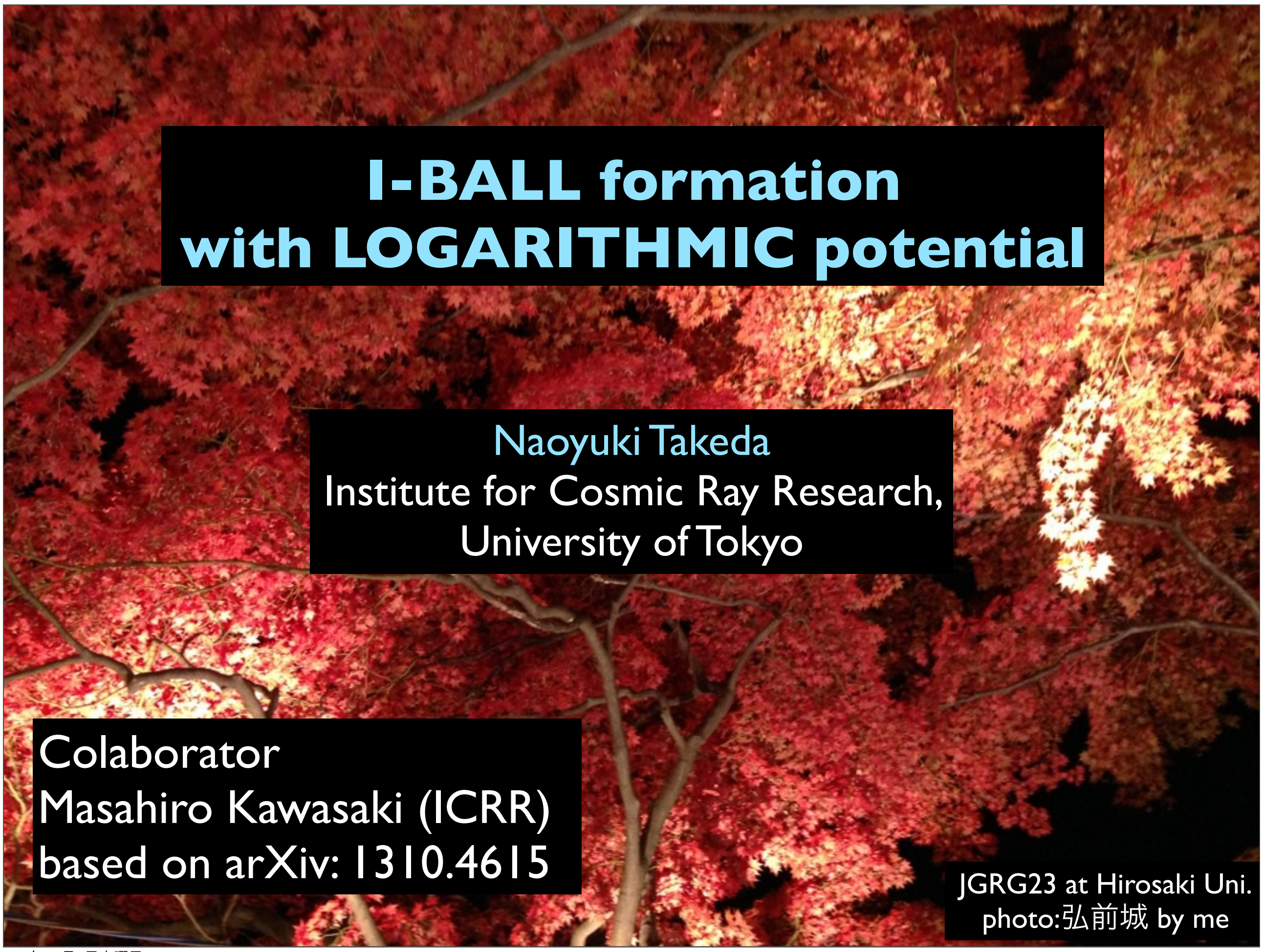

13年11月6日水曜日

CONTENTS

- INTRODUCTION
- MODEL
- RESULT
- CONCLUSION

13年11月6日水曜日

Introduction

SOLITON

In the early Universe, the scalar field fragments into soliton, when a conserved invariant exists.

The soliton affetcs the scenario of the cosmology.

topological number $\longrightarrow$ topological defect

U(1) charge $\longrightarrow$ Q-BALL

Even if no conserved invariants, the soliton could be formed through coherent oscillation

I-BALL(OSCILLON)

13年11月6日水曜日

Introduction **Adiabatic Invariant**

classical mechanics

when the motion of the system is quasi-periodic motion,
the area of the track in the phase space is conserved. (ex. Landau)

$$\frac{\dot\lambda}{\lambda} \ll \frac{1}{T} \longrightarrow I \equiv \frac{1}{2\pi}\oint pdq : \text{ CONST}$$

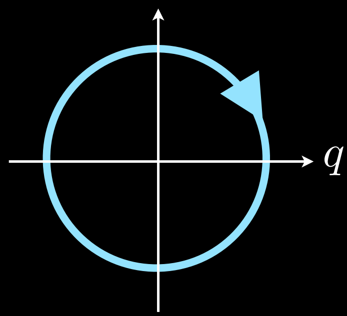

field theory

$\frac{\dot\lambda}{\lambda} \ll \frac{1}{T}, \frac{\nabla\lambda}{\lambda} \ll \frac{1}{T}$ in V

$$\boxed{I \equiv \frac{1}{2m}\int d^3x\, \bar{\dot\phi}^2 : \text{ CONST}}$$

$\longrightarrow$ quasi stable soliton I-BALL

Kasuya Takahashi and Kawasaki '03

Introduction **I-BALL**

$$\ddot\phi - \nabla^2\phi + V' = 0$$

$$V = \frac{1}{2}m^2 + \delta V$$

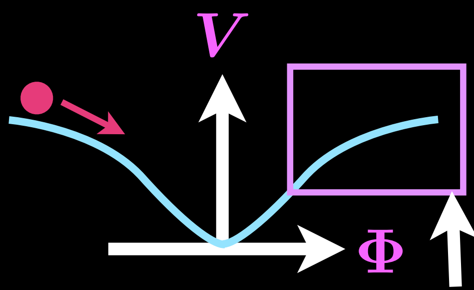

Necessary condition for I-ball formation $V'' < m^2$

Far away from the minimum ,
V should be shallower than quadratic

$$V = \frac{m^2}{2}\phi^2 - \frac{\lambda}{4}\phi^4 + \frac{g}{6}\phi^6$$ '10 M.Amin

Time for formation is excessively larger than the typical scale 1/m.
Confirmation of the formation needs numerical simulation.

MODEL

$$\boldsymbol{V} = \boldsymbol{M}^4 \log\left[\mathbf{1} + \left(\frac{\boldsymbol{\Phi}}{\boldsymbol{M}}\right)^2\right]$$

Thermal correction for inflaton in mind (Mukaida and Nakayam '12), we confirm the I-ball formation with logarithmic potential.

setting

E.O.M.

$$\ddot{\phi} + H\dot{\phi} - \frac{\nabla^2}{a^2}\phi + \frac{\partial V}{\partial \phi} = 0$$

$a \propto t^{2/3}$ with lattice simulation

initial value

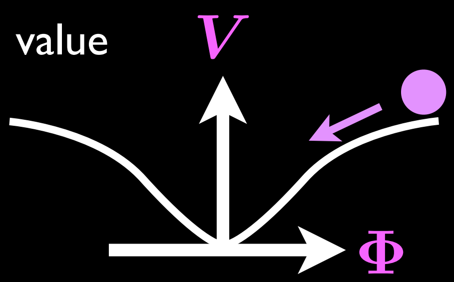

RESULT

13年11月6日水曜日

lattice simulation

M^2

lattice simulation

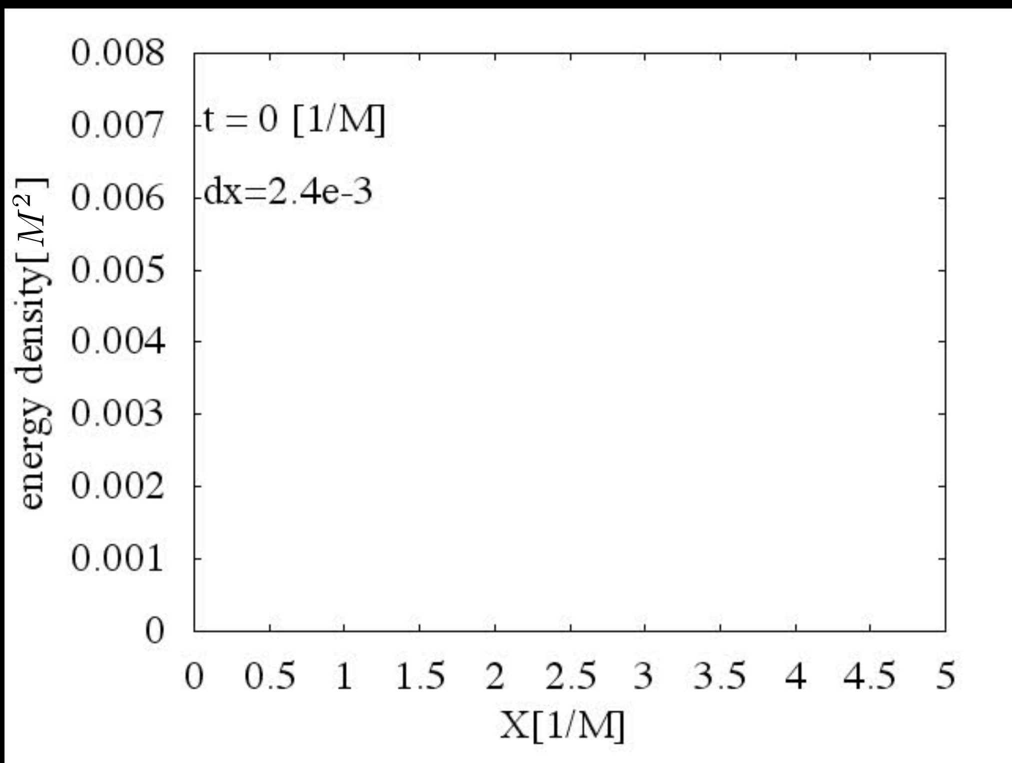

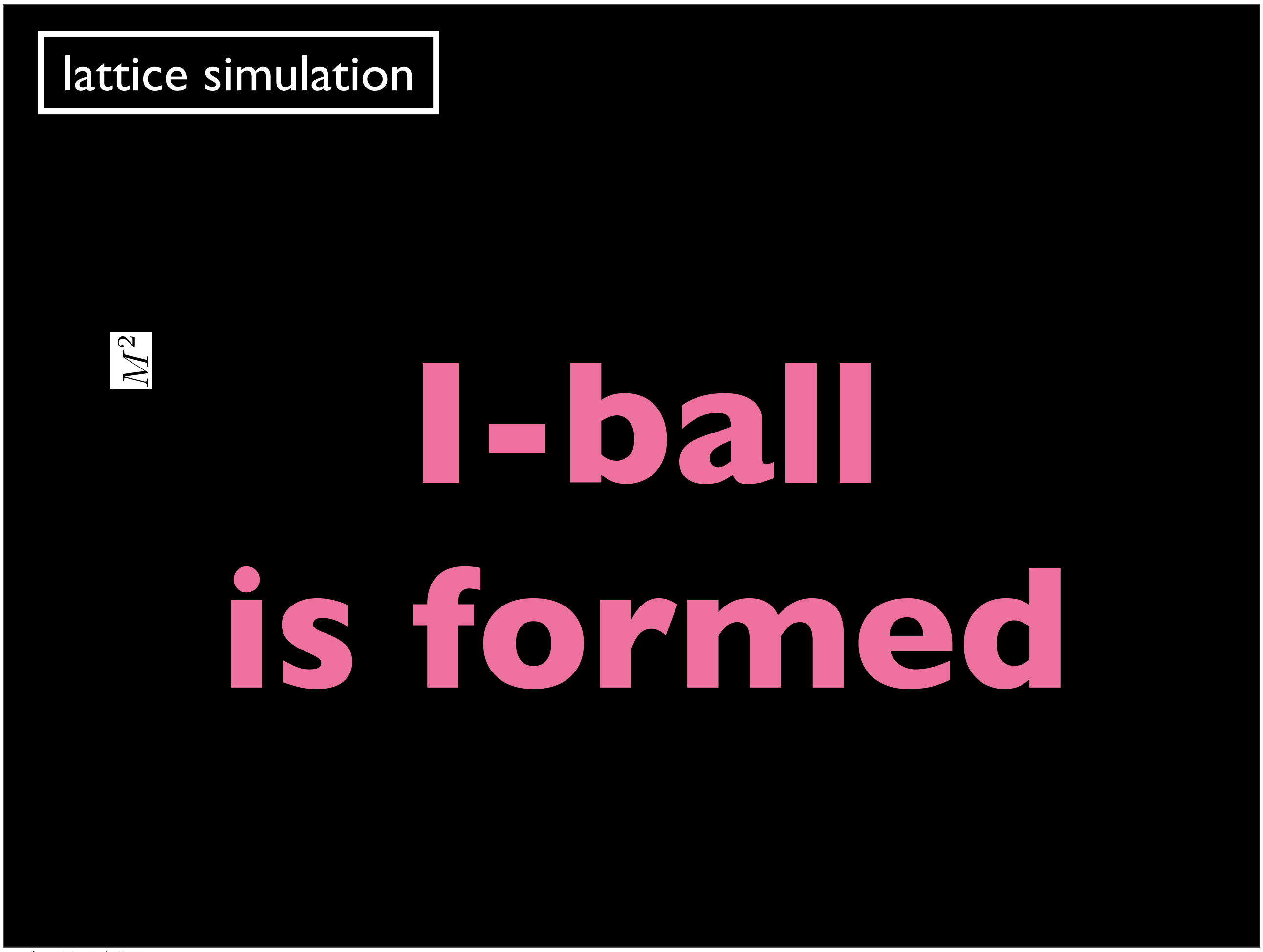

13年11月6日水曜日

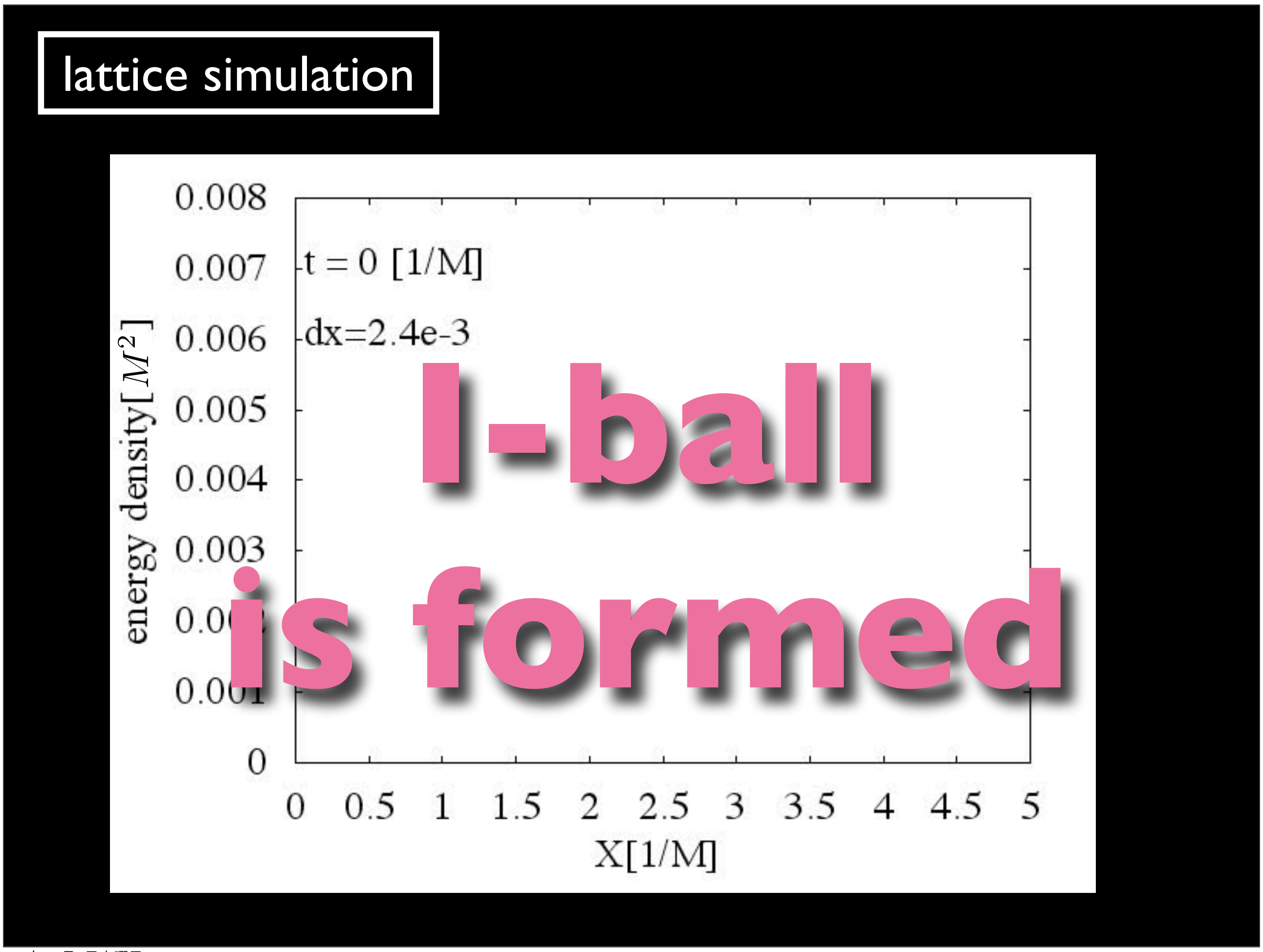

13年11月6日水曜日

PROFILE

We estimate the configuration of the I-ball,
using Lagrange multiplier assuming the I is conserved.

$$E_\omega = \bar{E} + \omega\left[I - \frac{1}{2M}\int dx\overline{\dot{\phi}^2}\right]$$

$$\delta E = 0$$

$$\longrightarrow \quad \nabla^2\Phi + \omega M\Phi - V'(\Phi) = 0$$

$$V(\Phi)' \simeq 2M^{(}1 - \Phi^2/2)\Phi$$

$$\longrightarrow \quad \boxed{\Phi(r) = \Phi(0)\mathrm{sech}\left(\frac{\Phi(0)}{\sqrt{2}}r\right) \qquad R \sim \frac{2}{\Phi(0)}\frac{1}{M}}$$

comparison the ana. to simu.

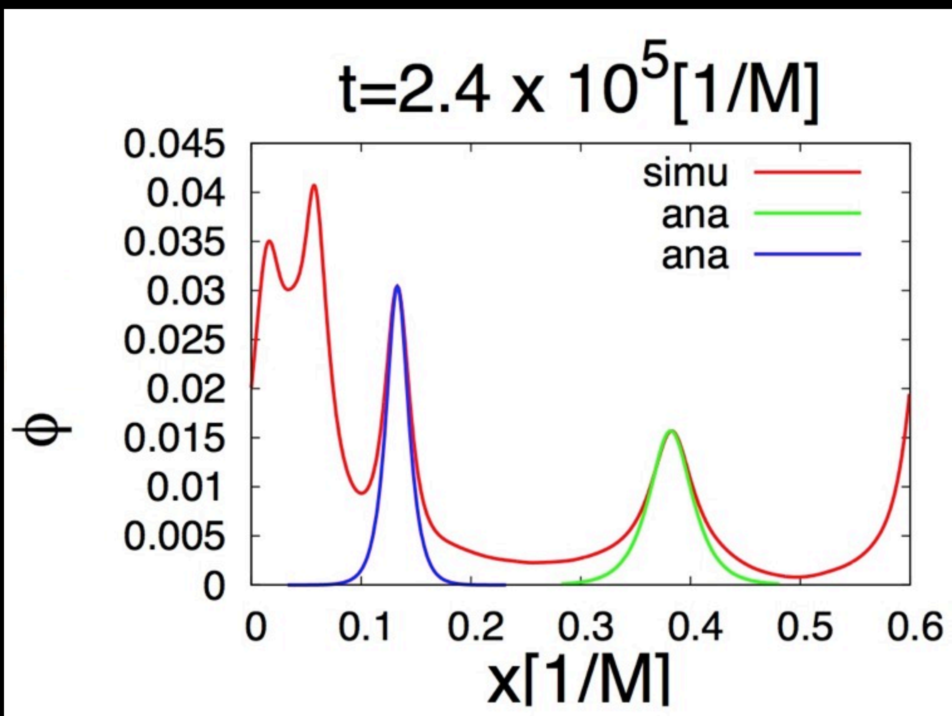

lattice simulation

Formation time and amplitude of I-ball for each initial amplitude

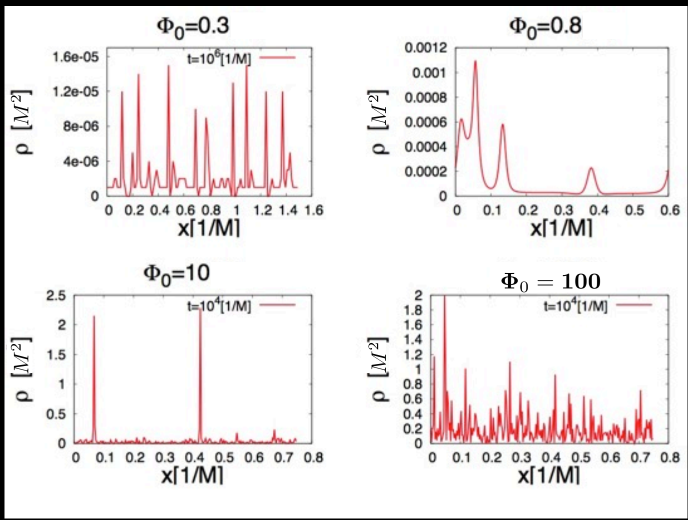

ϕ_0	0.3	0.8	10	100
Time[1/M]	10^6	10^5	10^4	10^4
amplitude	10^{-3}	10^{-1}	1	1

CONCLUSION

We have confirmed the coherently oscillating scalar filed fragments into I-ball.

The amplitude of formed I-ball is limited to O(1) from above.

The accordance of the estimate of the configuration with numerical simulations suggest the crucial role of the adiabatic invariant for I-ball formation.

This logarithmic potential appears in the various situation in the early Universe, hence I-ball formation would affect the cosmological scenario, which will be studied in a forthcoming paper.

13年11月6日水曜日

Instability mode

Oscilating amplitude of the I-ball induce the enhancement of the fluctuation by paraametric resonance

$$\delta\ddot{\phi}_k + \left[k^2 + (2 - 2\phi_0^2(t))M^2\right]\delta\phi_k = 0$$

$$\phi_0(t) = \Phi\cos(\sqrt{2}Mt)$$

→ Mathieu equation

$$\boxed{\frac{d^2}{d\tau^2}\delta\phi_k + \left[\underbrace{\frac{k^2+(2-\Phi^2)}{2}M^2}_{} - \frac{\Phi^2}{2}M^2\cos(2M\tau)\right]\delta\phi_k = 0}$$

instability at ~1

$$\tau \equiv \sqrt{2}t$$

Instability mode $\boxed{\frac{1}{k} \sim \frac{1}{\Phi(0)}\frac{1}{M}}$

gradient pressure is supported by the enhanced flucuations

lattice simulation

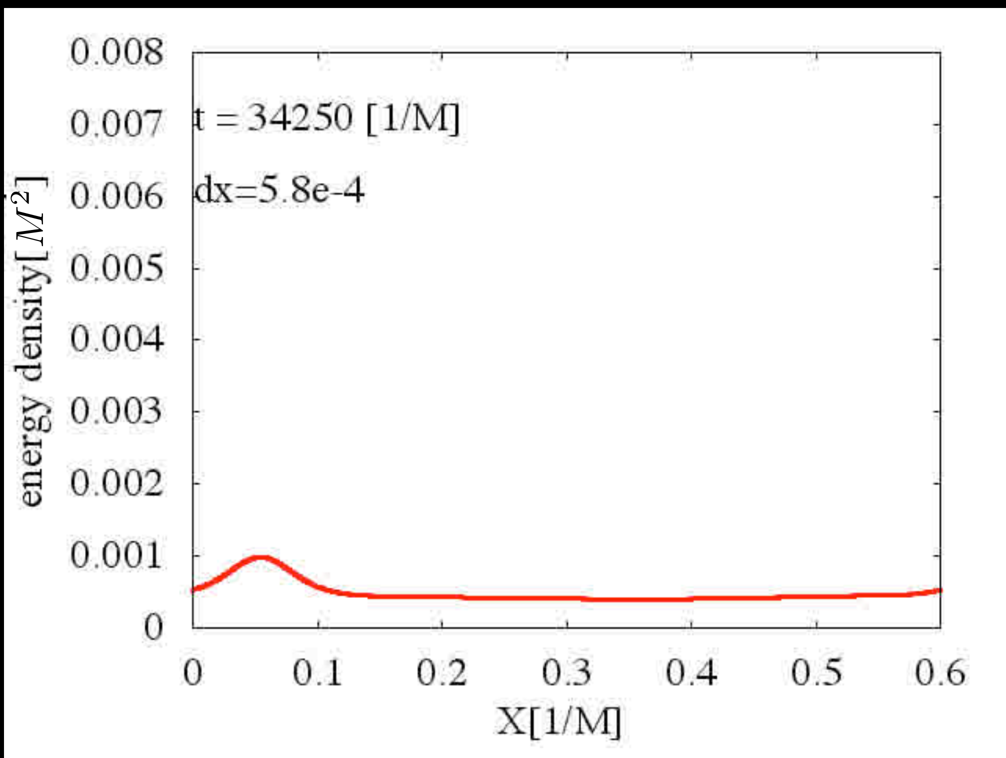

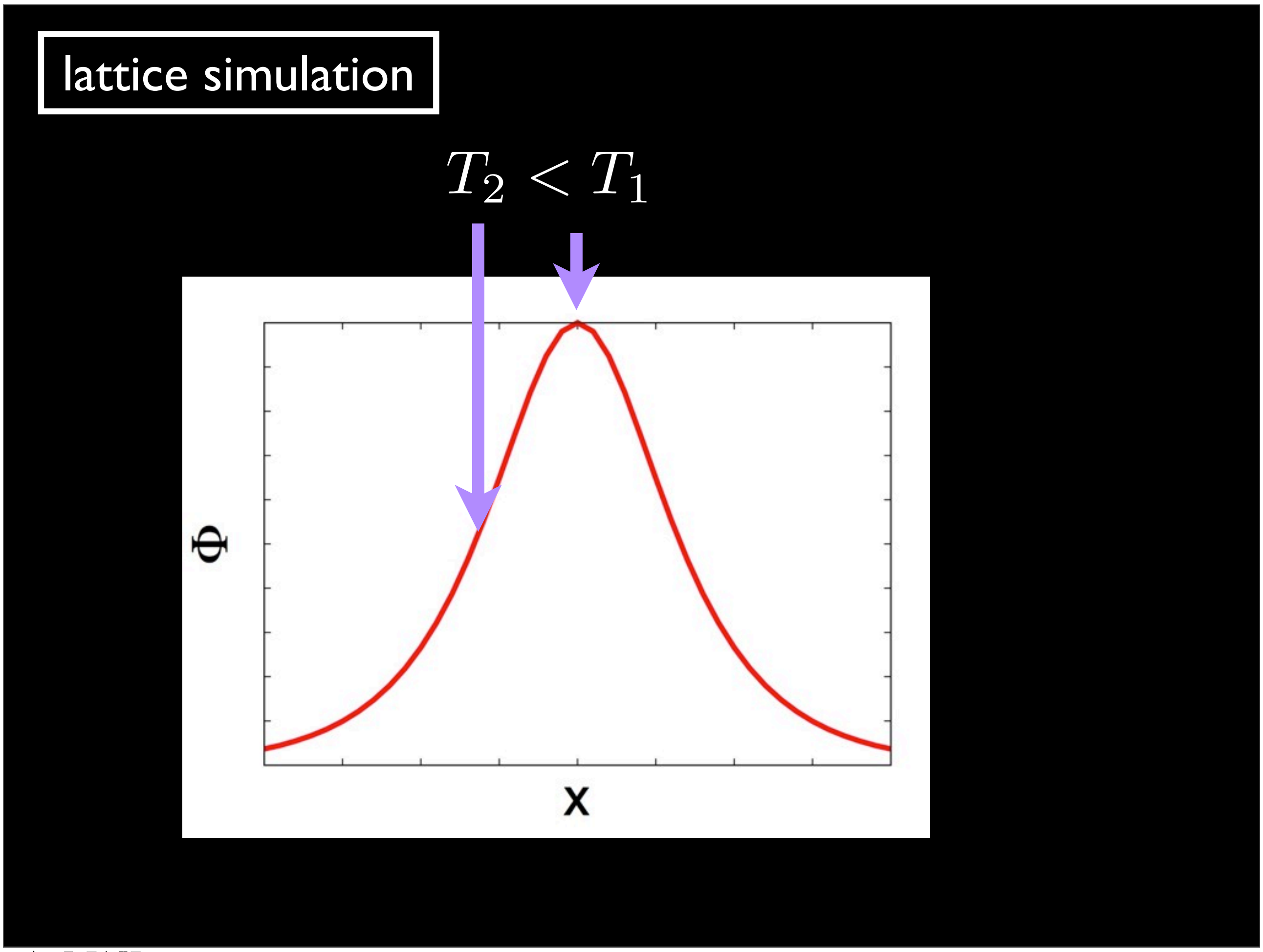

13年11月6日水曜日

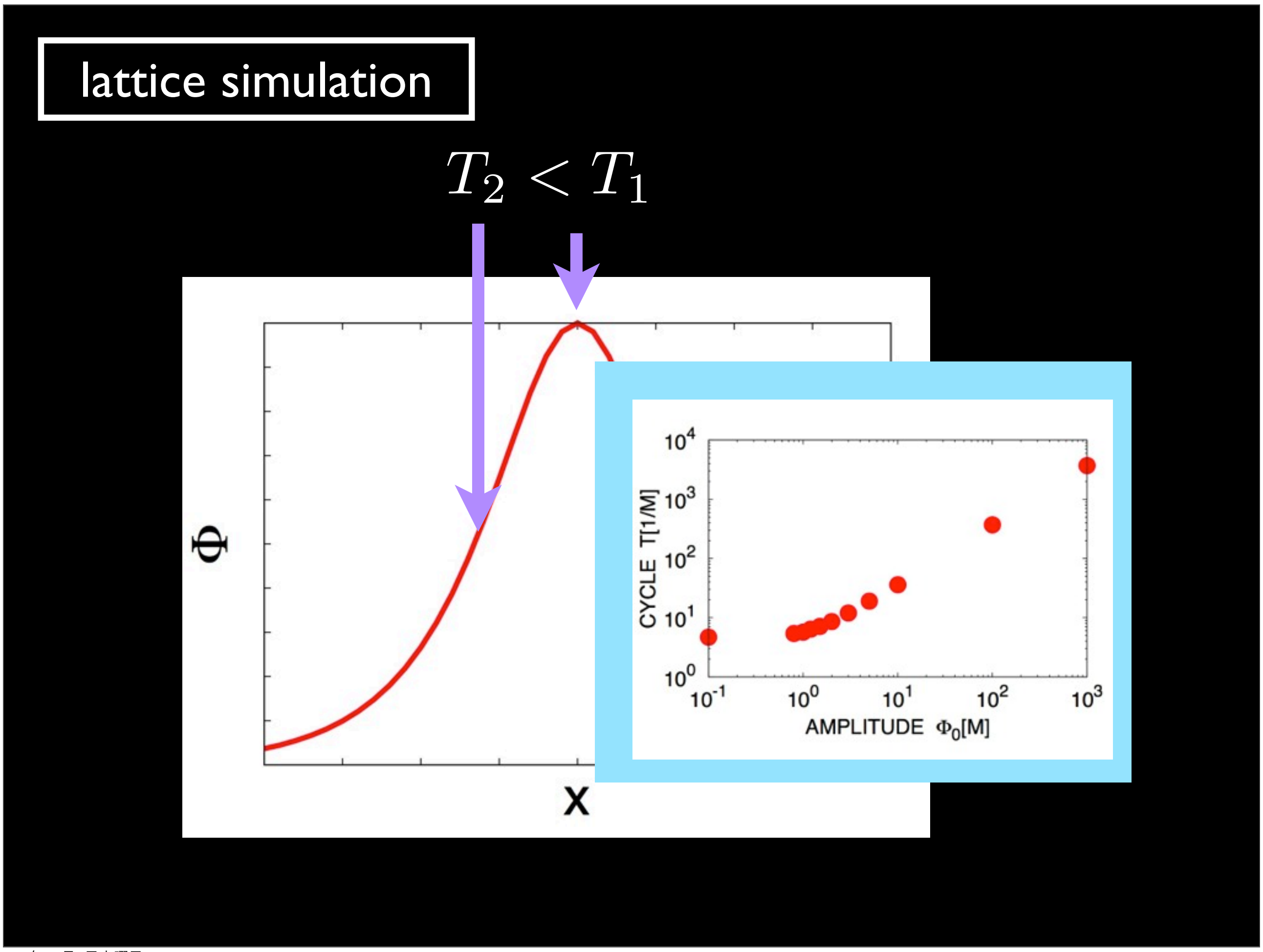

13年11月6日水曜日

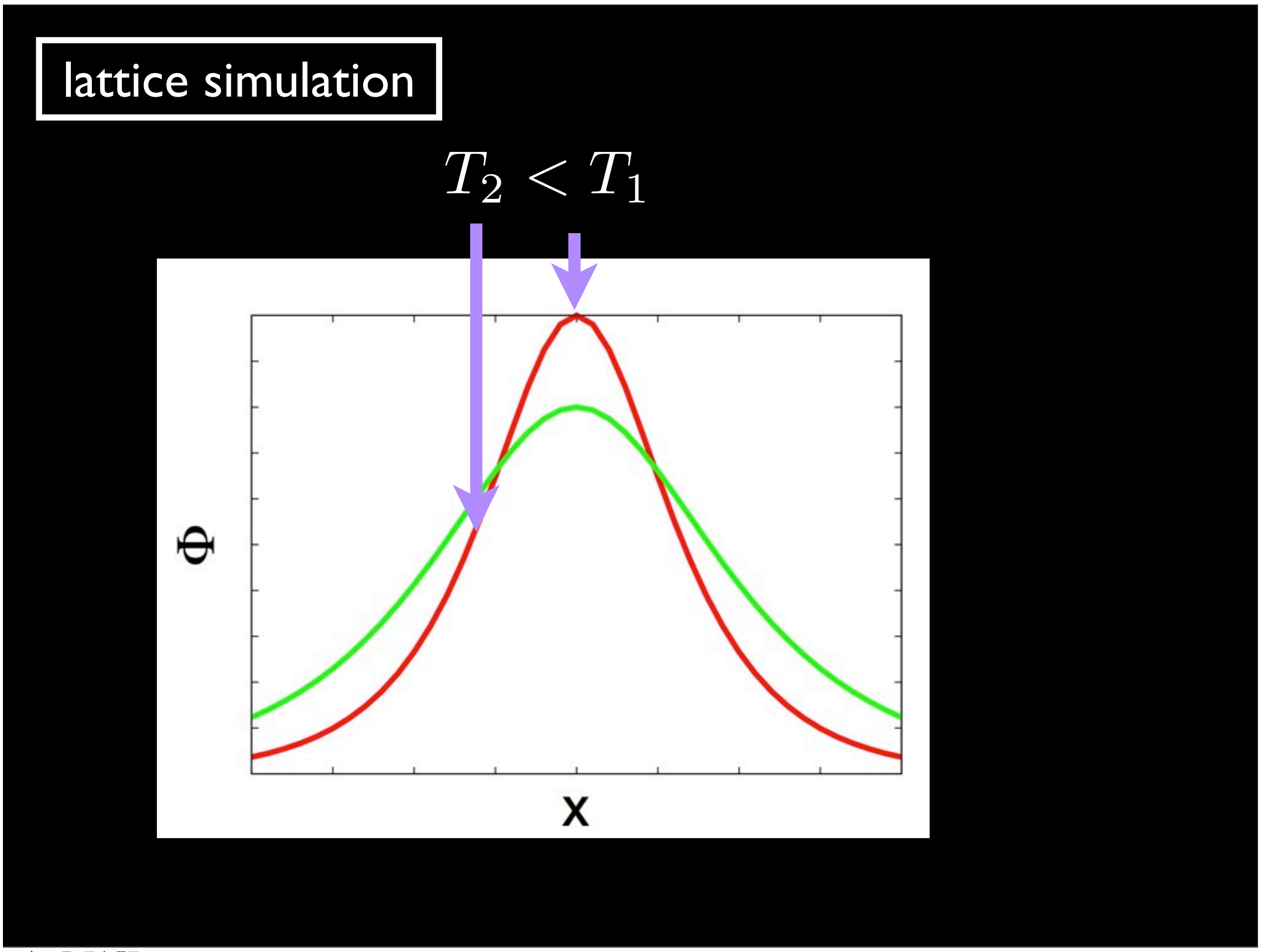
lattice simulation
$T_2 < T_1$
Φ
x

“Cosmology in ghost-free bigravity theory with twin matter fluid”

by Katsuki Aoki

[JGRG23(2013)110608]

Cosmology in ghost-free bigravity with twin matter fluid

Nov. 6th, 2013

@JGRG23, Hirosaki Univ.

Waseda University

Katsuki Aoki

With K. Maeda

in preparation

Introduction

・Our universe shows accelerating expansion!

Cosmological constant ? → Fine-tuning problem

Dark energy VS $\boxed{\text{Modified gravity}}$

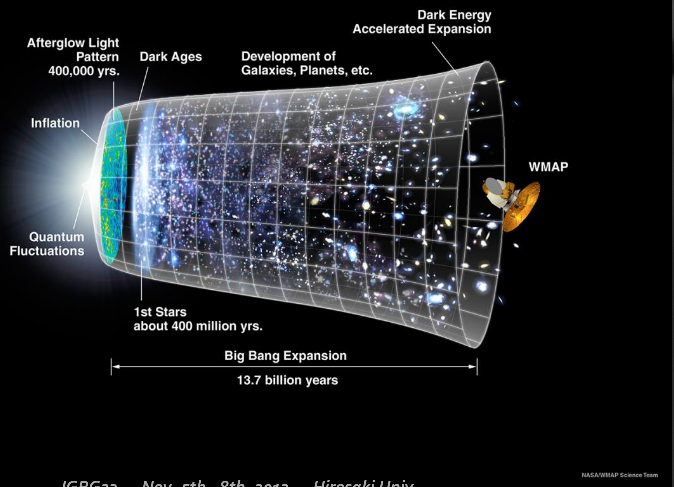

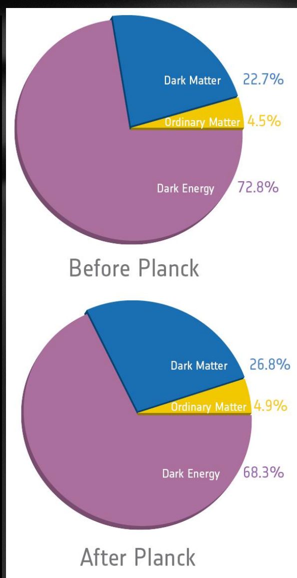

Massless or Massive ?

Graviton is thought as massless spin 2 particle in General Relativity (GR).

◆ Can graviton have a mass?

→ Massive gravity

Linear theory (Fierz and Pauli (1939))

Non-linear theory (de Rham, Gabadadze and Tolley (2011))

Bimetric extension (Hassan and Rosen (2011))

Main motivation is to explain accelerating expansion with bigravity.

Cosmology in bigravity

◆ This theory involves two metrics $g_{\mu\nu}$ and $f_{\mu\nu}$.

The interaction between two metrics gives mass term.

◆ There are two type solutions in cosmology

Reference metric is

(1) Isotropic case Koyama et al. '11, Chamseddine et al '11, D'Amico et al. '11, Gumrukcuoglu et al. '11 Volkov '11,'12, Gratia et al. '12, Kobayashi et al '12.

➡ Cosmological constant is mimicked (same as GR).

(2) Homogeneous and isotropic case Volkov '11, von Strauss et al. '11, Cristosomi et al. '11. Y. Akrami et al. '13

➡ Although cosmic evolution is difference from GR in general, this shows acceleration

Cosmology in bigravity

◆ This theory involves two metrics $g_{\mu\nu}$ and $f_{\mu\nu}$.

The interaction be

◆ There are two typ

Reference metric

(1) Isot

C

(2) Hor

A

i

tosomi et al. '11.

However these solutions are assumed the matter couples only $g_{\mu\nu}$.

Bigravity theory supposes twin metrics.

So, do you think the bigravity theory with twin matter is more natural?

Cosmology in bigravity with twin matter

◆ We assumed two metrics are homogeneous and isotropic and with twin matter fluid.

◆ Main topics are

(1) Does the accelerating solution naturally exists or not?

➡ **Accelerating solution does not always exist, but it naturally exists!**

(2) Can we get any observational constraints for f-matter?

➡ **We can get constraint from observation!**

Outline

1.Introduction

2.Review of bigravity

3.Cosmology in bigravity with twin matter

- -Example solutions
- -Details

4.Observational constraint

5.Conclusions

Outline

1.Introduction

2.Review of bigravity

3.Cosmology in bigravity with twin matter

- -Example solutions
- -Details

4.Observational constraint

5.Conclusions

Bigravity theory (S. F. Hassan and R. A. Rosen, 2011)

◆ The action $\kappa^2 = \kappa_g^2 + \kappa_f^2$

$$S = \frac{1}{2\kappa_g^2}\int d^4x\sqrt{-g}R(g) + \frac{1}{2\kappa_f^2}\int d^4x\sqrt{-f}\mathcal{R}(f)$$
$$-\frac{m^2}{\kappa^2}\int d^4x\sqrt{-g}\,\mathscr{U}(g,f) + S^{[\mathrm{m}]}(g,f)$$

◆ Interaction term

$$\mathscr{U}(\gamma) = \sum_{k=0}^{4} b_k \mathscr{U}_k(\gamma)$$
$$\gamma^\mu{}_\nu = \pm\sqrt{g^{\mu\lambda}f_{\lambda\nu}}$$

Coupling constants

b_0, b_1, b_2, b_3, b_4

$$\mathscr{U}_0(\gamma) = -\frac{1}{4!}\epsilon_{\mu\nu\rho\sigma}\epsilon^{\mu\nu\rho\sigma},$$
$$\mathscr{U}_1(\gamma) = -\frac{1}{3!}\epsilon_{\mu\nu\rho\sigma}\epsilon^{\alpha\nu\rho\sigma}\gamma^\mu{}_\alpha,$$
$$\mathscr{U}_2(\gamma) = -\frac{1}{4}\epsilon_{\mu\nu\rho\sigma}\epsilon^{\alpha\beta\rho\sigma}\gamma^\mu{}_\alpha\gamma^\nu{}_\beta,$$
$$\mathscr{U}_3(\gamma) = -\frac{1}{3!}\epsilon_{\mu\nu\rho\sigma}\epsilon^{\alpha\beta\gamma\sigma}\gamma^\mu{}_\alpha\gamma^\nu{}_\beta\gamma^\rho{}_\gamma,$$
$$\mathscr{U}_4(\gamma) = -\frac{1}{4!}\epsilon_{\mu\nu\rho\sigma}\epsilon^{\alpha\beta\gamma\delta}\gamma^\mu{}_\alpha\gamma^\nu{}_\beta\gamma^\rho{}_\gamma\gamma^\sigma{}_\delta$$

JGRG23, Nov. 5th - 8th, 2013, Hirosaki Univ.

Bigravity theory (S. F. Hassan and R. A. Rosen, 2011)

◆ The action $\kappa^2 = \kappa_g^2 + \kappa_f^2$

$$S = \frac{1}{2\kappa_g^2}\int d^4x\sqrt{-g}R(g) + \frac{1}{2\kappa_f^2}\int d^4x\sqrt{-f}\mathcal{R}(f)$$
$$-\frac{m^2}{\kappa^2}\int d^4x\sqrt{-g}\,\mathscr{U}(g,f) + S^{[\mathrm{m}]}(g,f)$$

◆ Interaction term

We also use c_0, c_1, c_2, c_3, c_4

◆ Normalization

$$c_2 = b_2 + 2b_3 + b_4 = -1$$

◆ Minkowski space is vacuum solution

$$c_0 = c_1 = 0$$

Coupling constants

b_0, b_1, b_2, b_3, b_4

$$\mathscr{U}_4(\gamma) = -\frac{1}{4!}\epsilon_{\mu\nu\rho\sigma}\epsilon^{\alpha\beta\gamma\delta}\gamma^\mu{}_\alpha\gamma^\nu{}_\beta\gamma^\rho{}_\gamma\gamma^\sigma{}_\delta$$

JGRG23, Nov. 5th - 8th, 2013, Hirosaki Univ.

EOM for twin matter bigravity

Contribution from interaction (= dark energy?)

$$G^{\mu}{}_{\nu} = \kappa_g^2 \left(\boxed{T_g^{[\gamma]\mu}{}_{\nu}} + \boxed{T_g^{[\mathrm{m}]\mu}{}_{\nu}} \right),$$
$$\mathcal{G}^{\mu}{}_{\nu} = \kappa_f^2 \left(\boxed{\mathcal{T}_f^{[\gamma]\mu}{}_{\nu}} + \boxed{\mathcal{T}_f^{[\mathrm{m}]\mu}{}_{\nu}} \right)$$

Contribution from matter

◆Assuming g-matter only couples $g_{\mu\nu}$, similarly $f_{\mu\nu}$.

$$\overset{(g)}{\nabla}{}_{\mu} T_g^{[\mathrm{m}]\mu}{}_{\nu} = 0, \quad \overset{(f)}{\nabla}{}_{\mu} \mathcal{T}_f^{[\mathrm{m}]\mu}{}_{\nu} = 0,$$

It is not doubly-coupled! Doubly-coupled case is breaking Einstein's equivalence principle and conservation in a metric.

Outline

1. Introduction
2. Review of bigravity
3. Cosmology in bigravity with twin matter
   - -Example solutions
   - -Details
4. Observational constraint
5. Conclusions

Set up

◆ Both metrics are homogeneous and isotropic

$$ds_g^2 = -dt^2 + a_g^2(t)\left(\frac{dr^2}{1-kr^2} + r^2 d\Omega^2\right),$$

$$ds_f^2 = -A^2(t)dt^2 + a_f^2(t)\left(\frac{dr^2}{1-kr^2} + r^2 d\Omega^2\right)$$

◆ Because we concern present universe, we assume twin matter consist of only non-relativistic matter (dust).

The matter coupling $g_{\mu\nu}$

$$\kappa_g^2 \rho_g = \frac{c_{g,\mathrm{m}}}{a_g^3}, \kappa_f^2 \rho_f = \frac{c_{f,\mathrm{m}}}{a_f^3}$$

The matter coupling $f_{\mu\nu}$

Basic equations

$$ds_g^2 = -dt^2 + a_g^2(t)\left(\frac{dr^2}{1-kr^2} + r^2 d\Omega^2\right),$$

$$ds_f^2 = -A^2(t)dt^2 + a_f^2(t)\left(\frac{dr^2}{1-kr^2} + r^2 d\Omega^2\right)$$

$$m_g^2 = m^2\kappa_g^2/\kappa^2, m_f^2 = m^2\kappa_f^2/\kappa^2$$

◆ EOM for scale factors ($\dot{} = d/dt$)

$$3\left(\frac{\dot{a}_g^2}{a_g^2} + \frac{k}{a_g^2}\right) = m_g^2\left(b_0 + 3b_1\frac{a_f}{a_g} + 3b_2\frac{a_f^2}{a_g^2} + b_3\frac{a_f^3}{a_g^3}\right) + \frac{c_{g,\mathrm{m}}}{a_g^3}$$

$$3\left(\frac{\dot{a}_f^2}{A^2 a_f^2} + \frac{k}{a_f^2}\right) = m_f^2\left(b_4 + 3b_3\frac{a_g}{a_f} + 3b_2\frac{a_g^2}{a_f^2} + b_1\frac{a_g^3}{a_f^3}\right) + \frac{c_{f,\mathrm{m}}}{a_f^3}$$

Interaction term

◆ Bianchi identity

$$\underbrace{\left(\frac{\dot{a}_f}{\dot{a}_g} - A\right)}_{\text{Interaction term} \Rightarrow \text{dynamical}} \underbrace{\left(b_1 + 2b_2\frac{a_f}{a_g} + b_3\frac{a_f^2}{a_g^2}\right)}_{\text{Interaction term} \Rightarrow \text{constant}} = 0$$

Cosmological solutions: examples

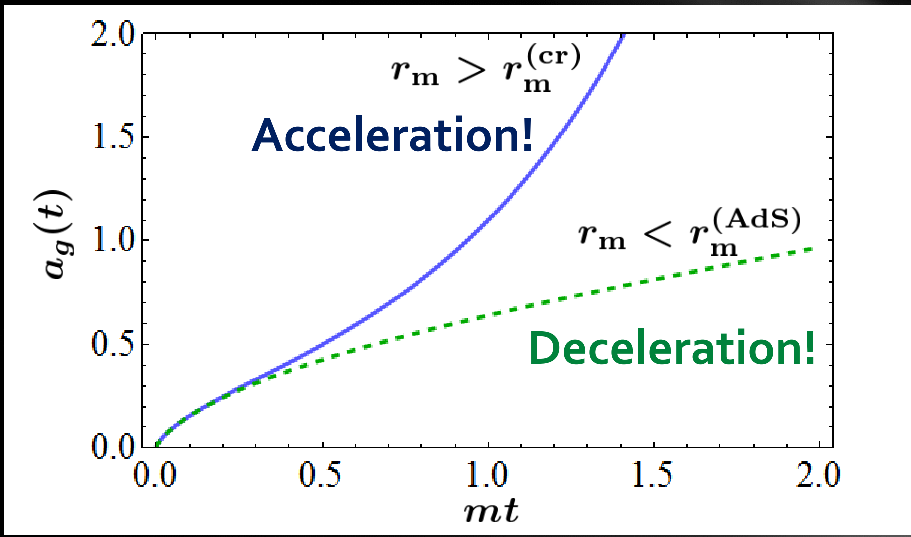

Two examples are chosen same coupling constants,
only difference is the matter ratio $r_{\mathrm{m}} = c_{f,\mathrm{m}}/c_{g,\mathrm{m}}$

$$\kappa_g^2 \rho_g = \frac{c_{g,\mathrm{m}}}{a_g^3}, \kappa_f^2 \rho_f = \frac{c_{f,\mathrm{m}}}{a_f^3}$$

Details

- Analyzing EOM for scale factor is very complex…, however, analyzing EOM for scale factor's ratio is comparatively easy!
  (All variables can be written by scale factor's ratio, so, we only have to calculate it.)
- EOM for scale factor's ratio

$$\dot{B}^2 + V_g = 0, V_g = V_g(B; \kappa_f/\kappa_g, b_i, r_{\mathrm{m}})$$

where $B = a_f/a_g, r_{\mathrm{m}} = c_{f,\mathrm{m}}/c_{g,\mathrm{m}}$

$$\kappa_g^2 \rho_g = \frac{c_{g,\mathrm{m}}}{a_g^3}, \kappa_f^2 \rho_f = \frac{c_{f,\mathrm{m}}}{a_f^3}$$

Potential for scale factor's ratio

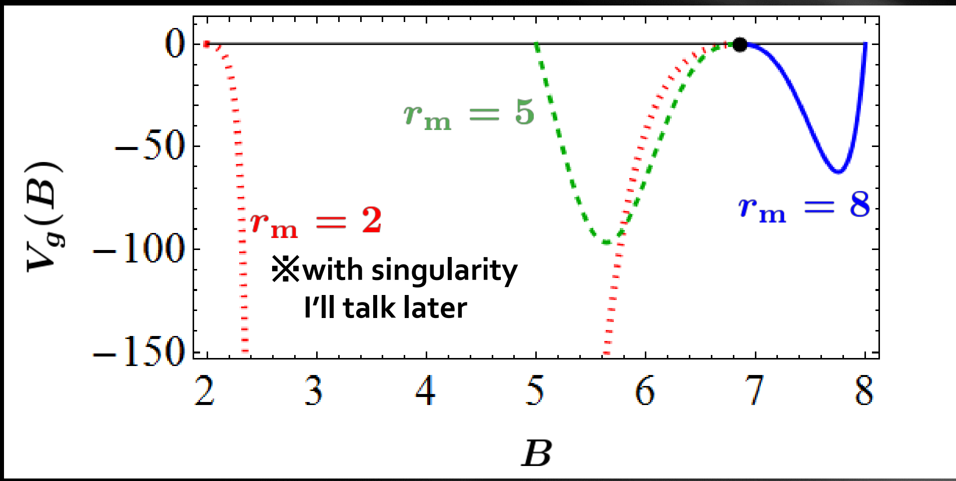

$\kappa_f/\kappa_g = 1, c_0 = c_1 = c_4 = 0, c_2 = c_3 = -1$

- EOM $\dot{B}^2 + V_g = 0, V_g = V_g(B; \kappa_f/\kappa_g, b_i, r_{\mathrm{m}})$

  where $B = a_f/a_g, r_{\mathrm{m}} = c_{f,\mathrm{m}}/c_{g,\mathrm{m}}$ $\kappa_g^2 \rho_g = \frac{c_{g,\mathrm{m}}}{a_g^3}, \kappa_f^2 \rho_f = \frac{c_{f,\mathrm{m}}}{a_f^3}$

Potential for scale factor's ratio

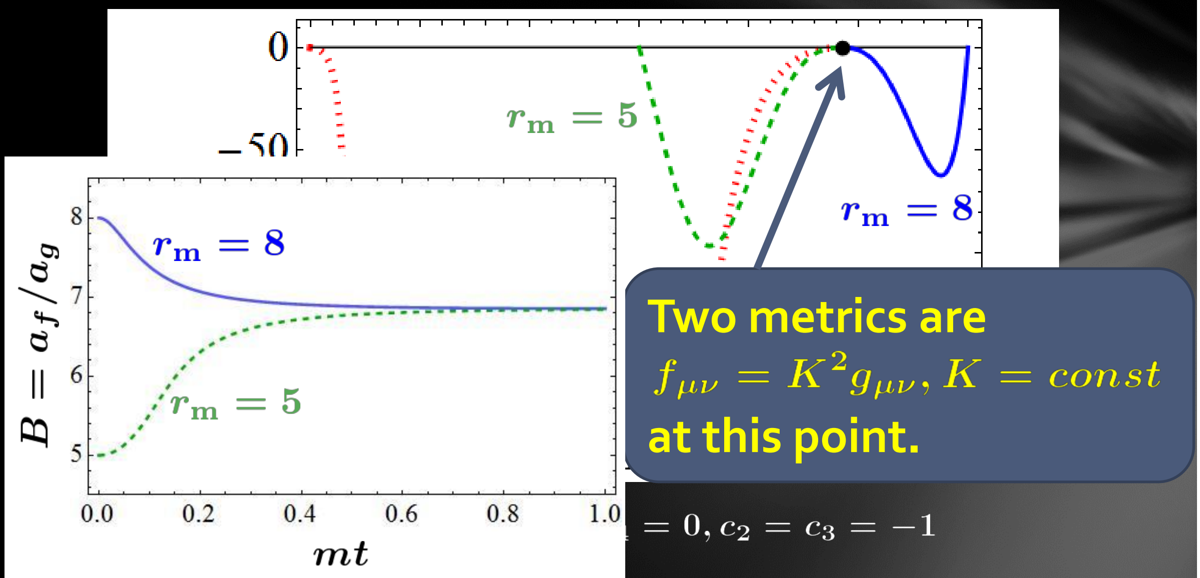

$= 0, c_2 = c_3 = -1$

- EOM $\dot{B}^2 + V_g = 0, V_g = V_g(B; \kappa_f/\kappa_g, b_i, r_{\mathrm{m}})$

  where $B = a_f/a_g, r_{\mathrm{m}} = c_{f,\mathrm{m}}/c_{g,\mathrm{m}}$ $\kappa_g^2 \rho_g = \frac{c_{g,\mathrm{m}}}{a_g^3}, \kappa_f^2 \rho_f = \frac{c_{f,\mathrm{m}}}{a_f^3}$

Homothetic solutions

(K. Maeda and M. S. Volkov '13, Y. Akrami et al. '13)

◆ If two metrics satisfy $f_{\mu\nu} = K^2 g_{\mu\nu}, K = const$,

EOM is the same as GR with a cosmological constant Λ_g.

$$\Lambda_g = m_g^2(b_0 + 3b_1 K + 3b_2 K^2 + b_3 K^3), m_g^2 = \frac{\kappa_g^2 m^2}{\kappa^2}$$

◆ K is given by a quartic equation $C_\Lambda(K; \kappa_g, \kappa_f, b_i) = 0$

K_i	Λ_g	vacuum
-0.523476	$-22.0323 m_g^2$	AdS
1	0	M
1.67319	$-0.394464 m_g^2$	AdS
6.85028	$12.4267 m_g^2$	dS

$\kappa_f/\kappa_g = 1, c_0 = c_1 = c_4 = 0, c_2 = c_3 = -1$

◆ In the $\Lambda_g > 0$ branch,

the vacuum solution is de Sitter spacetime.

Homothetic solutions

◆ If two metrics

EOM is the sa

$\Lambda_g = m_g^2($

◆ K is given by

Our question is whether or not the cosmological solution approaches de Sitter branch.

K_i	Λ_g	vacuum
-0.523476	$-22.0323 m_g^2$	AdS
1	0	M
1.67319	$-0.394464 m_g^2$	AdS
6.85028	$12.4267 m_g^2$	dS

$\kappa_f/\kappa_g = 1, c_0 = c_1 = c_4 = 0, c_2 = c_3 = -1$

◆ In the $\Lambda_g > 0$ branch,

the vacuum solution is de Sitter spacetime.

JGRG23, Nov. 5th - 8th, 2013, Hirosaki Univ.

Does accelerating solution naturally exists?

EOM: $\dot{B}^2 + V_g = 0$

$B = a_f/a_g, r_{\rm m} = c_{f,{\rm m}}/c_{g,{\rm m}}$

$$\kappa_g^2 \rho_g = \frac{c_{g,{\rm m}}}{a_g^3}, \kappa_f^2 \rho_f = \frac{c_{f,{\rm m}}}{a_f^3}$$

Red line = Big Bang singularity

$f_{\mu\nu}$ is singular at $A = 0$

$g_{\mu\nu}$ is singular at $A = \infty$

$$ds_g^2 = -dt^2 + \cdots$$
$$ds_f^2 = -A^2 dt^2 + \cdots$$

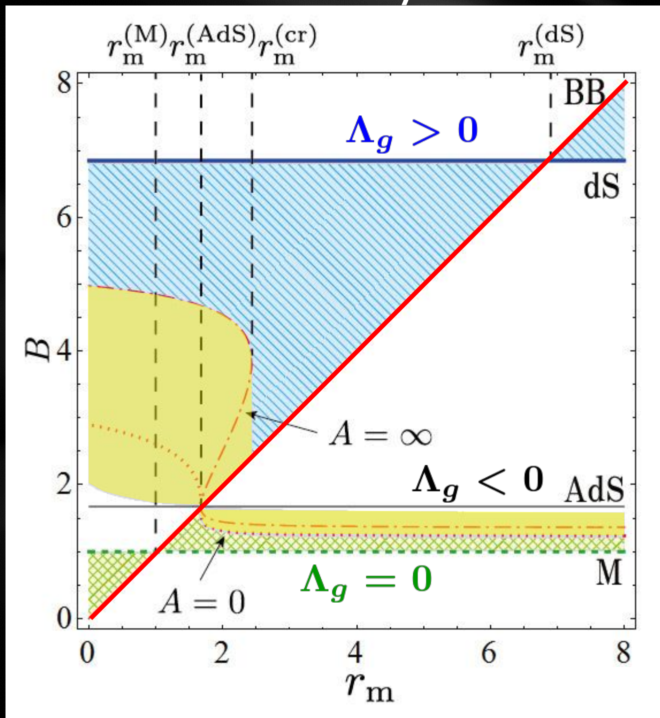

$\kappa_f/\kappa_g = 1, c_0 = c_1 = c_4 = 0, c_2 = c_3 = -1$

Does accelerating solution naturally exists?

EOM: $\dot{B}^2 + V_g = 0$

$B = a_f/a_g, r_{\rm m} = c_{f,{\rm m}}/c_{g,{\rm m}}$

$$\kappa_g^2 \rho_g = \frac{c_{g,{\rm m}}}{a_g^3}, \kappa_f^2 \rho_f = \frac{c_{f,{\rm m}}}{a_f^3}$$

Homothetic solutions

Red line = Big Bang singularity

$f_{\mu\nu}$ is singular at $A = 0$

$g_{\mu\nu}$ is singular at $A = \infty$

$$ds_g^2 = -dt^2 + \cdots$$
$$ds_f^2 = -A^2 dt^2 + \cdots$$

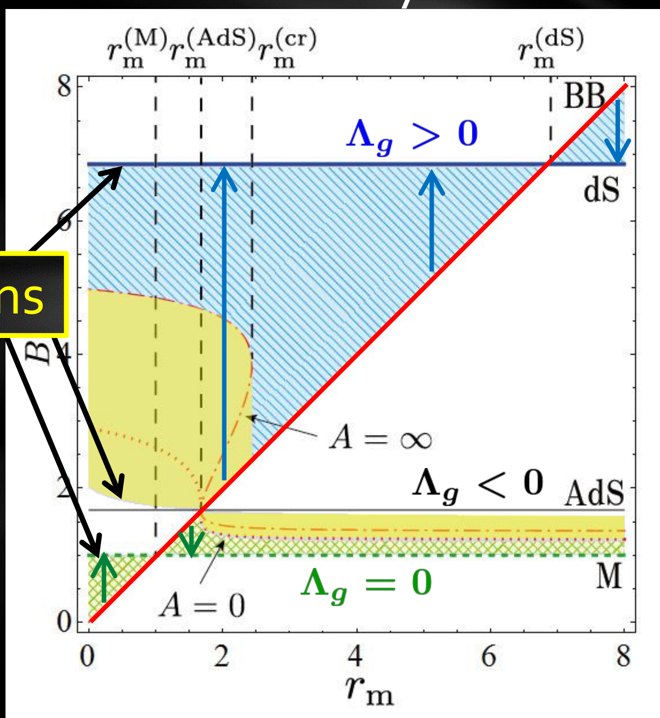

$\kappa_f/\kappa_g = 1, c_0 = c_1 = c_4 = 0, c_2 = c_3 = -1$

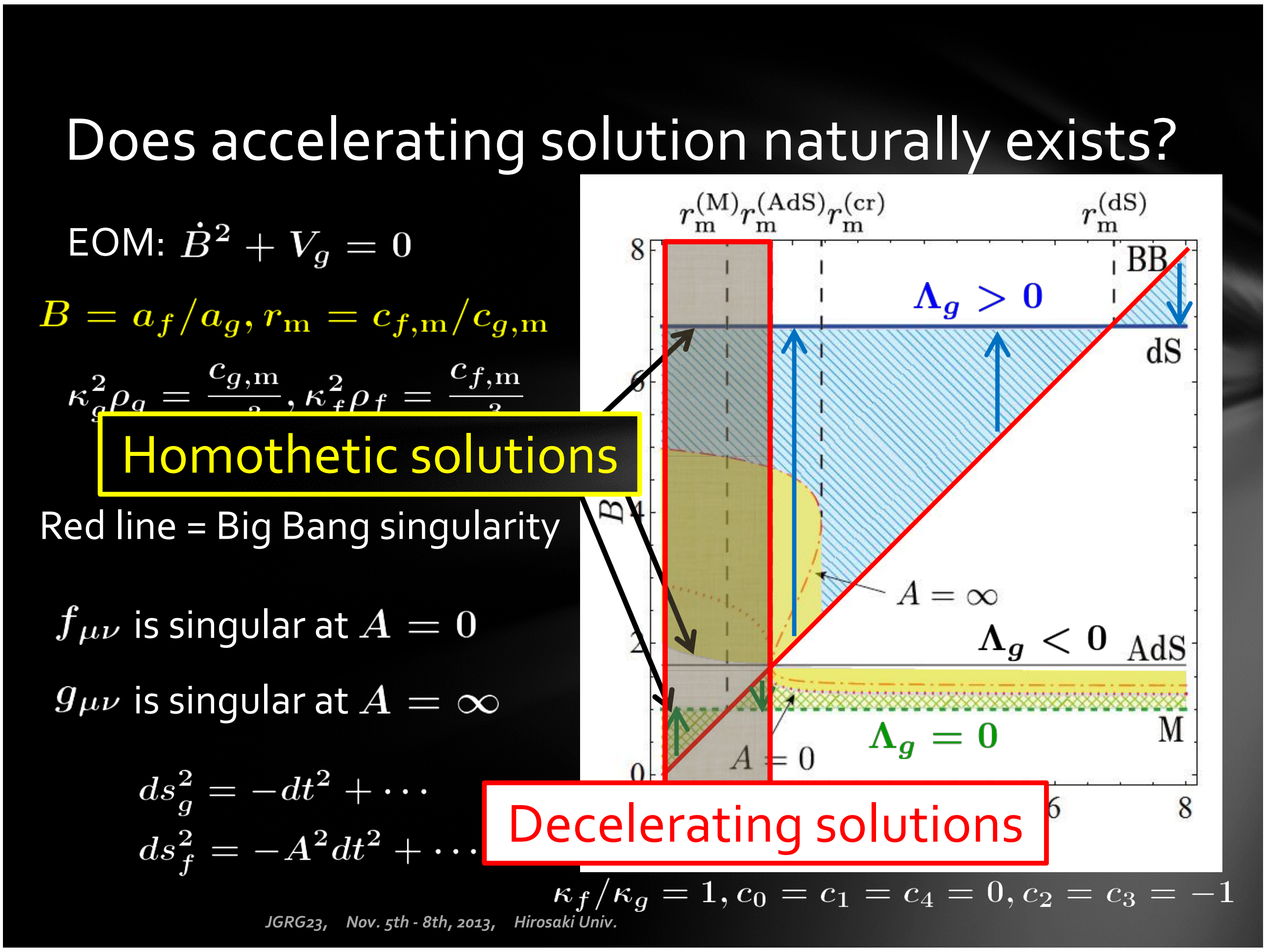
Does accelerating solution naturally exists?
EOM: $\dot{B}^2 + V_g = 0$
$B = a_f/a_g, r_\mathrm{m} = c_{f,\mathrm{m}}/c_{g,\mathrm{m}}$
$\kappa_g^2\rho_g = \frac{c_{g,\mathrm{m}}}{}, \kappa_f^2\rho_f = \frac{c_{f,\mathrm{m}}}{}$
Homothetic solutions
Red line = Big Bang singularity
$f_{\mu\nu}$ is singular at $A = 0$
$g_{\mu\nu}$ is singular at $A = \infty$
$ds_g^2 = -dt^2 + \cdots$
$ds_f^2 = -A^2dt^2 + \cdots$
Decelerating solutions
$r_\mathrm{m}^{(\mathrm{M})} r_\mathrm{m}^{(\mathrm{AdS})} r_\mathrm{m}^{(\mathrm{cr})}$
$r_\mathrm{m}^{(\mathrm{dS})}$
BB
$\Lambda_g > 0$
dS
$A = \infty$
$\Lambda_g < 0$
AdS
$\Lambda_g = 0$
M
$A = 0$
B
0
2
4
6
8
$\kappa_f/\kappa_g = 1, c_0 = c_1 = c_4 = 0, c_2 = c_3 = -1$
JGRG23, Nov. 5th - 8th, 2013, Hirosaki Univ.

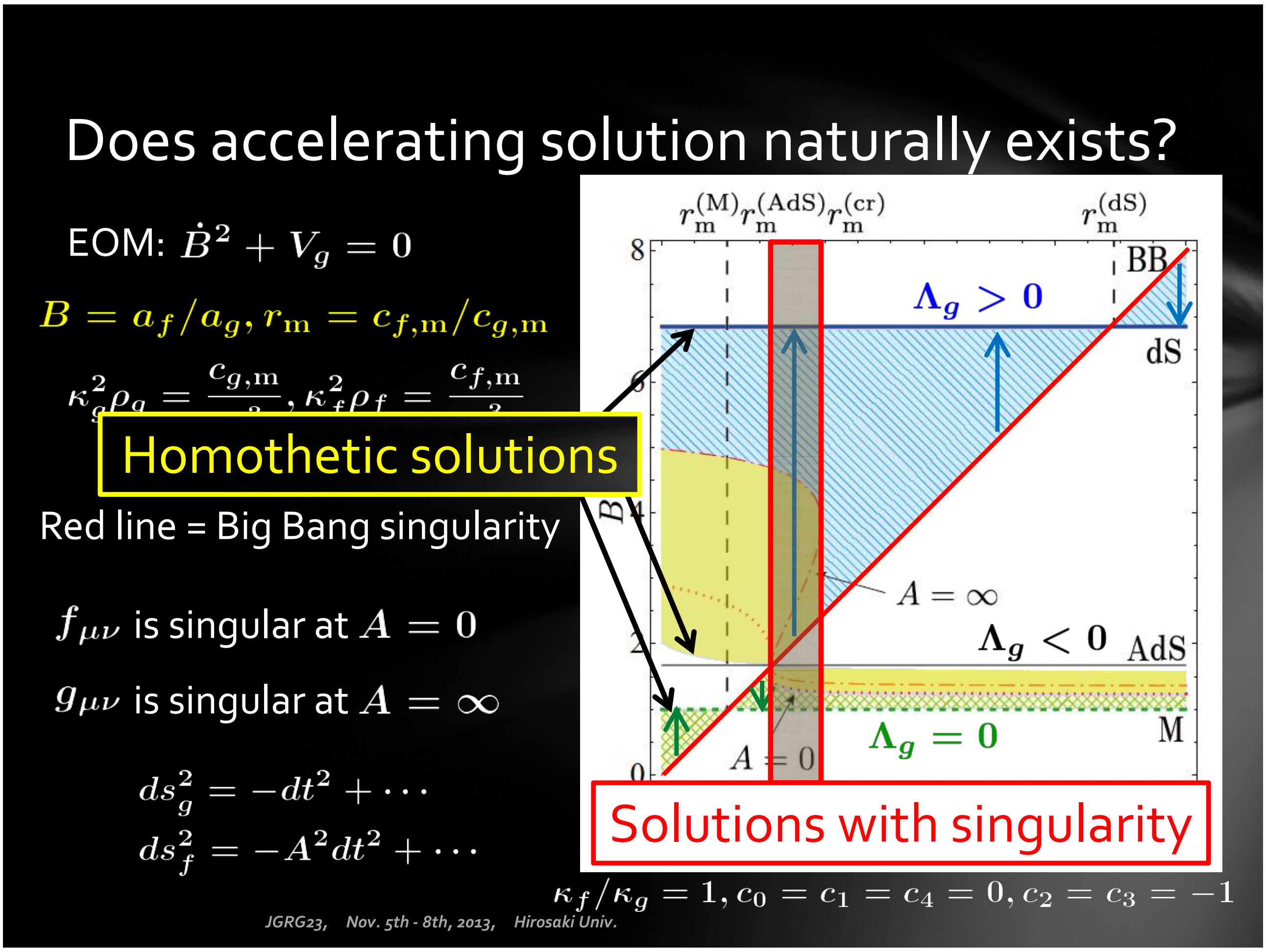
Does accelerating solution naturally exists?
EOM: $\dot{B}^2 + V_g = 0$
$B = a_f/a_g, r_\mathrm{m} = c_{f,\mathrm{m}}/c_{g,\mathrm{m}}$
$\kappa_g^2\rho_g = \frac{c_{g,\mathrm{m}}}{}, \kappa_f^2\rho_f = \frac{c_{f,\mathrm{m}}}{}$
Homothetic solutions
Red line = Big Bang singularity
$f_{\mu\nu}$ is singular at $A = 0$
$g_{\mu\nu}$ is singular at $A = \infty$
$ds_g^2 = -dt^2 + \cdots$
$ds_f^2 = -A^2dt^2 + \cdots$
Solutions with singularity
$r_\mathrm{m}^{(\mathrm{M})} r_\mathrm{m}^{(\mathrm{AdS})} r_\mathrm{m}^{(\mathrm{cr})}$
$r_\mathrm{m}^{(\mathrm{dS})}$
BB
$\Lambda_g > 0$
dS
$A = \infty$
$\Lambda_g < 0$
AdS
$\Lambda_g = 0$
M
$A = 0$
B
0
2
4
6
8
$\kappa_f/\kappa_g = 1, c_0 = c_1 = c_4 = 0, c_2 = c_3 = -1$
JGRG23, Nov. 5th - 8th, 2013, Hirosaki Univ.

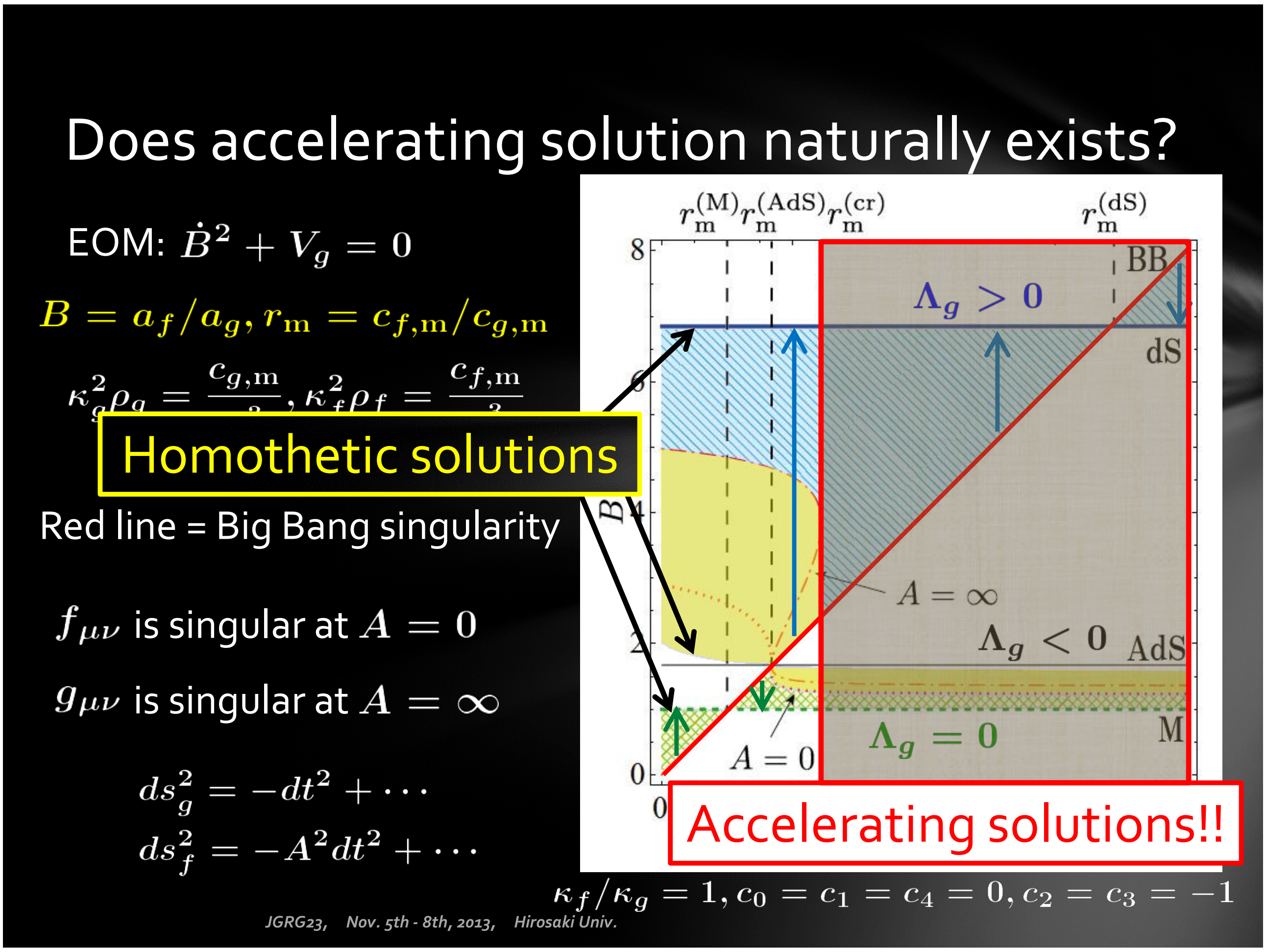
Does accelerating solution naturally exists?
EOM: $\dot{B}^2 + V_g = 0$
$B = a_f/a_g, r_m = c_{f,m}/c_{g,m}$
Homothetic solutions
Red line = Big Bang singularity
$f_{\mu\nu}$ is singular at $A = 0$
$g_{\mu\nu}$ is singular at $A = \infty$
$ds_g^2 = -dt^2 + \cdots$
$ds_f^2 = -A^2 dt^2 + \cdots$
$r_m^{(M)} r_m^{(AdS)} r_m^{(cr)}$
$r_m^{(dS)}$
BB
$\Lambda_g > 0$
dS
$A = \infty$
$\Lambda_g < 0$ AdS
$\Lambda_g = 0$
M
$A = 0$
Accelerating solutions!!
$\kappa_f/\kappa_g = 1, c_0 = c_1 = c_4 = 0, c_2 = c_3 = -1$
JGRG23, Nov. 5th - 8th, 2013, Hirosaki Univ.

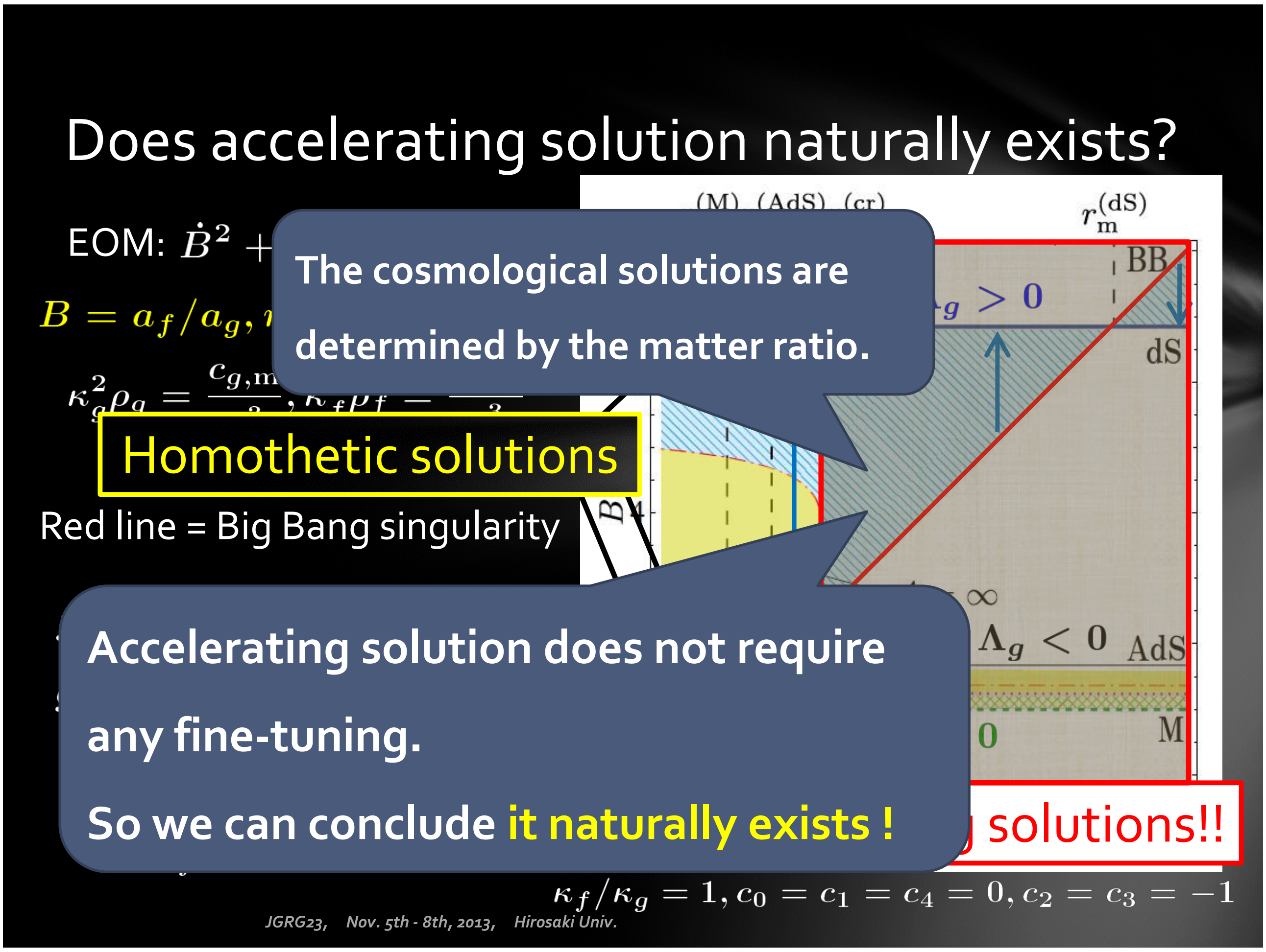
Does accelerating solution naturally exists?
The cosmological solutions are determined by the matter ratio.
Homothetic solutions
Red line = Big Bang singularity
Accelerating solution does not require any fine-tuning.
So we can conclude it naturally exists !
$\kappa_f/\kappa_g = 1, c_0 = c_1 = c_4 = 0, c_2 = c_3 = -1$
JGRG23, Nov. 5th - 8th, 2013, Hirosaki Univ.

Outline

Can we get any observational constraints for f-matter?

$$\kappa_g^2 \rho_g = \frac{c_{g,\mathrm{m}}}{a_g^3}, \kappa_f^2 \rho_f = \frac{c_{f,\mathrm{m}}}{a_f^3}$$

◆ We will focus only accelerating solutions. $r_\mathrm{m} = c_{f,\mathrm{m}}/c_{g,\mathrm{m}}$

If the matter ratio is fine-tuned as $r_\mathrm{m} = r_\mathrm{m}^{(\mathrm{dS})}$,

the cosmic evolution is exactly same as ΛCDM model.

Two metrics are always proportional.
= exact homothetic solution
= GR solution

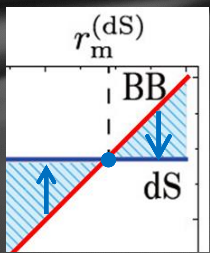

In non-fine-tuning case, how difference of cosmic evolution from ΛCDM model is there?

Can we get any observational constraints for f-matter?

$$\kappa_g^2\rho_g = \frac{c_{g,\mathrm{m}}}{a_g^3},\ \kappa_f^2\rho_f = \frac{c_{f,\mathrm{m}}}{a_f^3}$$

$$r_{\mathrm{m}} = c_{f,\mathrm{m}}/c_{g,\mathrm{m}}$$

◆ EOM for scale factor (in flat)

Contribution from interaction term (= dark energy?)

$$\frac{\dot{a}_g^{\,2}}{a_g^2} = \frac{\kappa_g^2}{3}\rho_g^{[\gamma]} + \frac{\kappa_g^2}{3}\rho_g$$

◆ The dark energy has

Energy: $\rho_g^{[\gamma]}$, Pressure: $P_g^{[\gamma]}$

e.o.s. parameter : $w^{[\gamma]} = \frac{\rho_g^{[\gamma]}}{P_g^{[\gamma]}}$

◆ Present value

$$w_0 = w^{[\gamma]}\Big|_{t=t_0},\ w_{a0} = -\frac{dw^{[\gamma]}}{da_g}\Big|_{t=t_0}$$

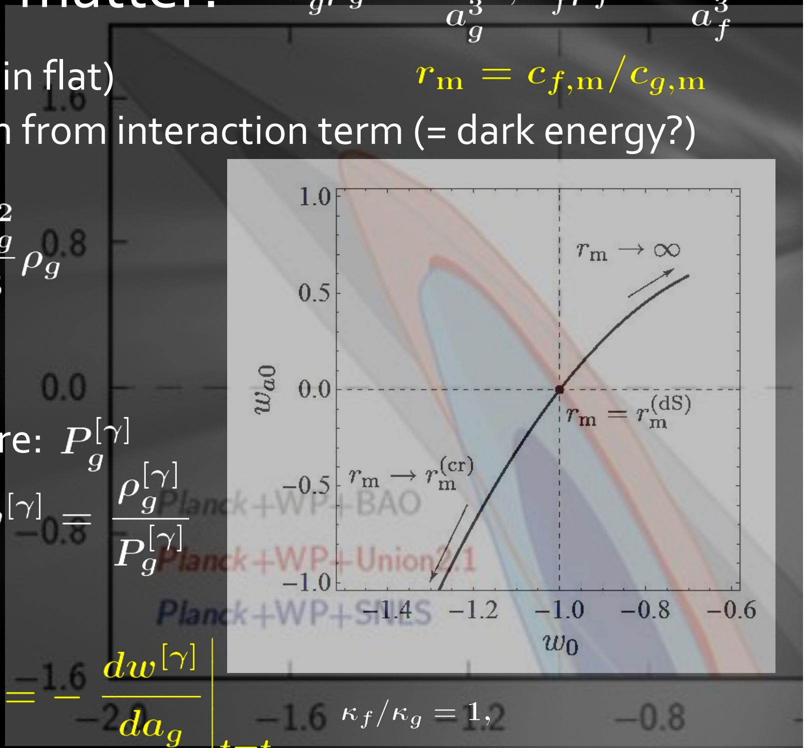

$\kappa_f/\kappa_g = 1,$

$c_0 = c_1 = c_4 = 0, c_2 = c_3 = -1$

Radiation dominant in $f_{\mu\nu}$?

There is no reason that
the f-dust also dominates the universe in $f_{\mu\nu}$.

Analysis is very complex...
But we can get same figure →

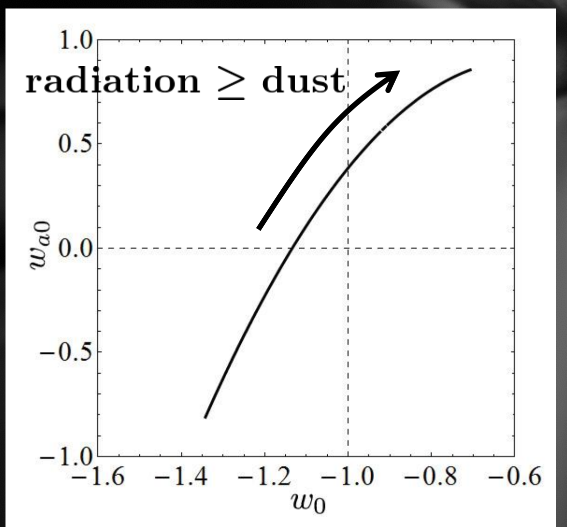

◆ The dark energy has

Energy: $\rho_g^{[\gamma]}$, Pressure: $P_g^{[\gamma]}$

e.o.s. parameter : $w^{[\gamma]} = \frac{\rho_g^{[\gamma]}}{P_g^{[\gamma]}}$

◆ Present value

$$w_0 = w^{[\gamma]}\Big|_{t=t_0},\ w_{a0} = -\frac{dw^{[\gamma]}}{da_g}\Big|_{t=t_0}$$

$\kappa_f/\kappa_g = 1, r_{\mathrm{m}} = 1$

$c_0 = c_1 = c_4 = 0, c_2 = c_3 = -1$

Conclusions

In the present work, we have demonstrated the cosmology in bigravity with twin matter.

◆Cosmological solution is determined by the matter ratio, and accelerating solutions do not need any fine-tuning.

◆We can distinguish bigravity models from ΛCDM model and get the observational constraint for f-matter.

◆It would be important to investigate other phenomena with twin matter fluid. ← get other constraints?

Homothetic solutions (= GR solutions) exist only in twin matter case in non-vacuum. ← stable or unstable?

“Numerical relativity: Application to gravitational-wave science and astrophysics”

by Kenta Hotokezaka (invited)

[JGRG23(2013)110609]

Numerical relativity:
Application to gravitational-wave science and astrophysics

Kenta Hotokezaka (Kyoto U.)

Collaborators:
K. Kiuchi, T. Muransushi, H. Nagakura, Y. Sekiguchi, and M. Shibata (YITP)
K. Kyutoku (UMW), H. Okawa (CENTRA), and K. Taniguchi (U. of Tokyo)
M. Tanaka, S. Wanajo (NAOJ), and K. Ioka (KEK)

Outline

1. Introduction

2. Gravitational waves from compact binaries and EOS
   - ✓ Inspiral phase and tidal effects and EOS
   - ✓ Post-merger and massive neutron star and EOS

3. Electromagnetic signals from compact binary mergers
   - ✓ A golden event: the short GRB 130603B
   - ✓ Kilonova emission

4. Summary

Gravitational-wave Astronomy

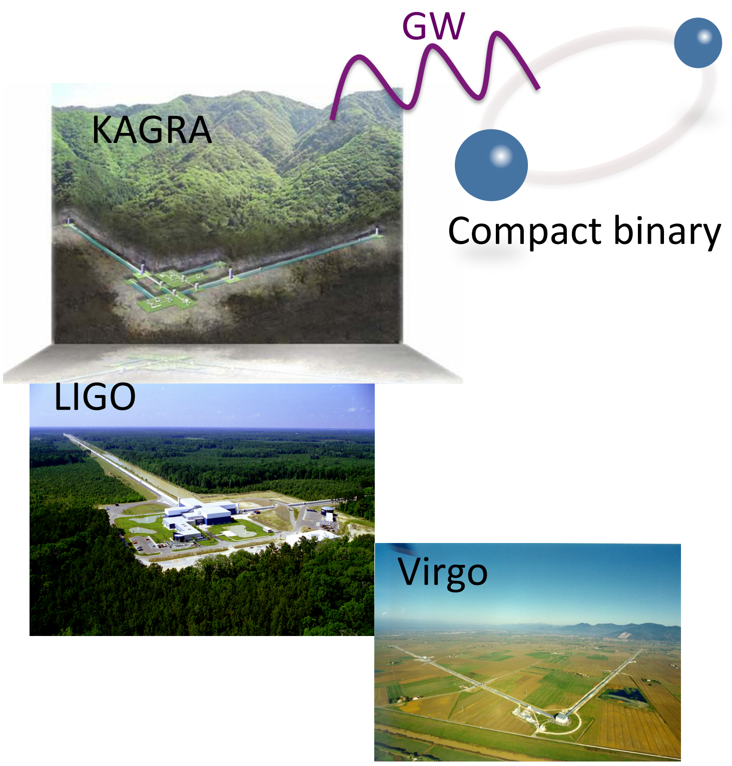

Expected event rate

Several times /yr

Abadie et al 2010

Progress in
  Theory of gravity
  Astrophysics
  High-density physics
  :

Multi-Messenger Astronomy

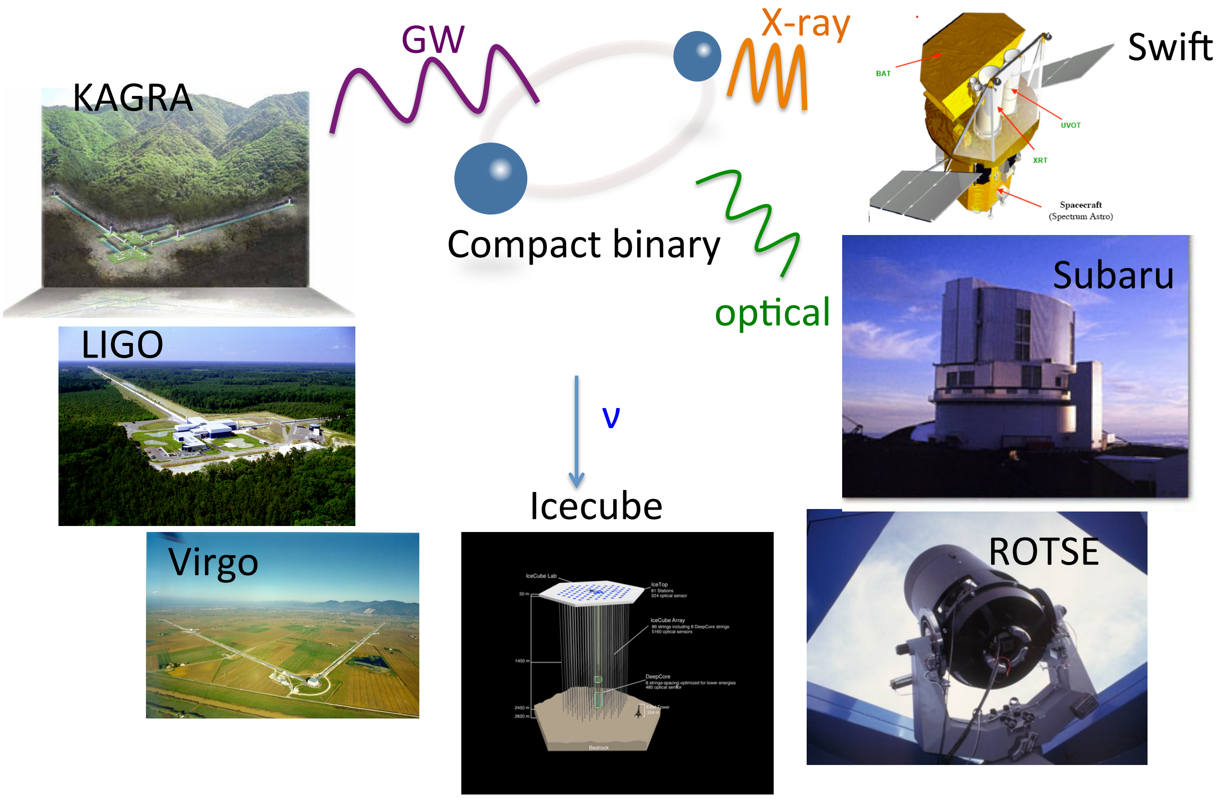

Multi-messenger Astronomy

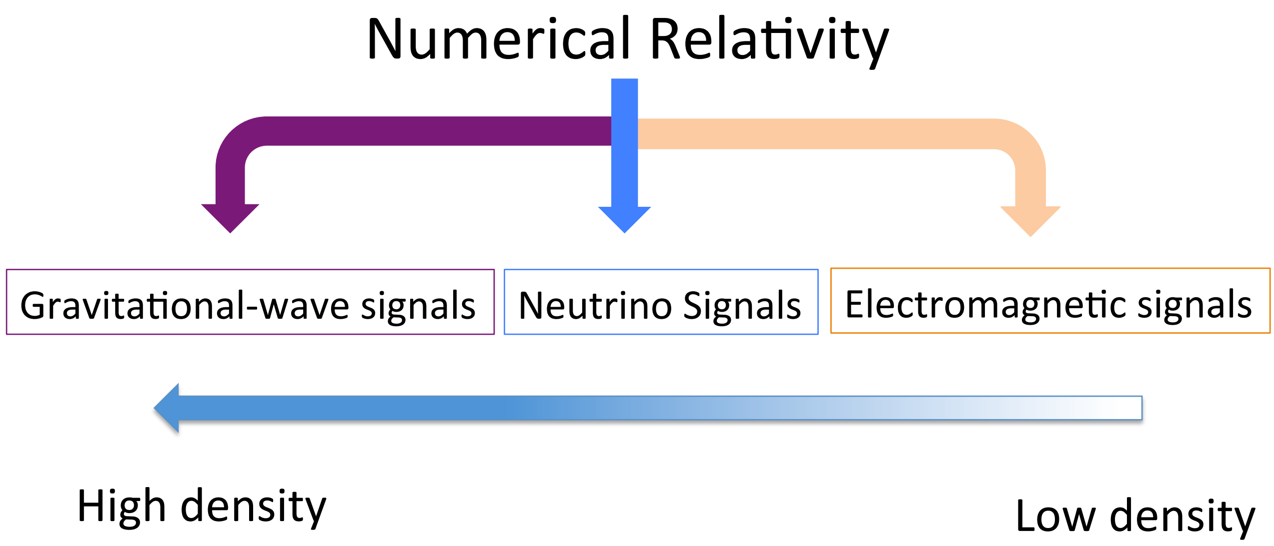

Outline

1. Introduction

2. Gravitational waves from compact binaries and EOS

   ✓ Inspiral phase and tidal effects and EOS
   ✓ Post-merger and massive neutron star and EOS

3. Electromagnetic signals from compact binary mergers

   ✓ A golden event: the short GRB 130603B
   ✓ Kilonova emission

4. Summary

Why NS Equation of State ?

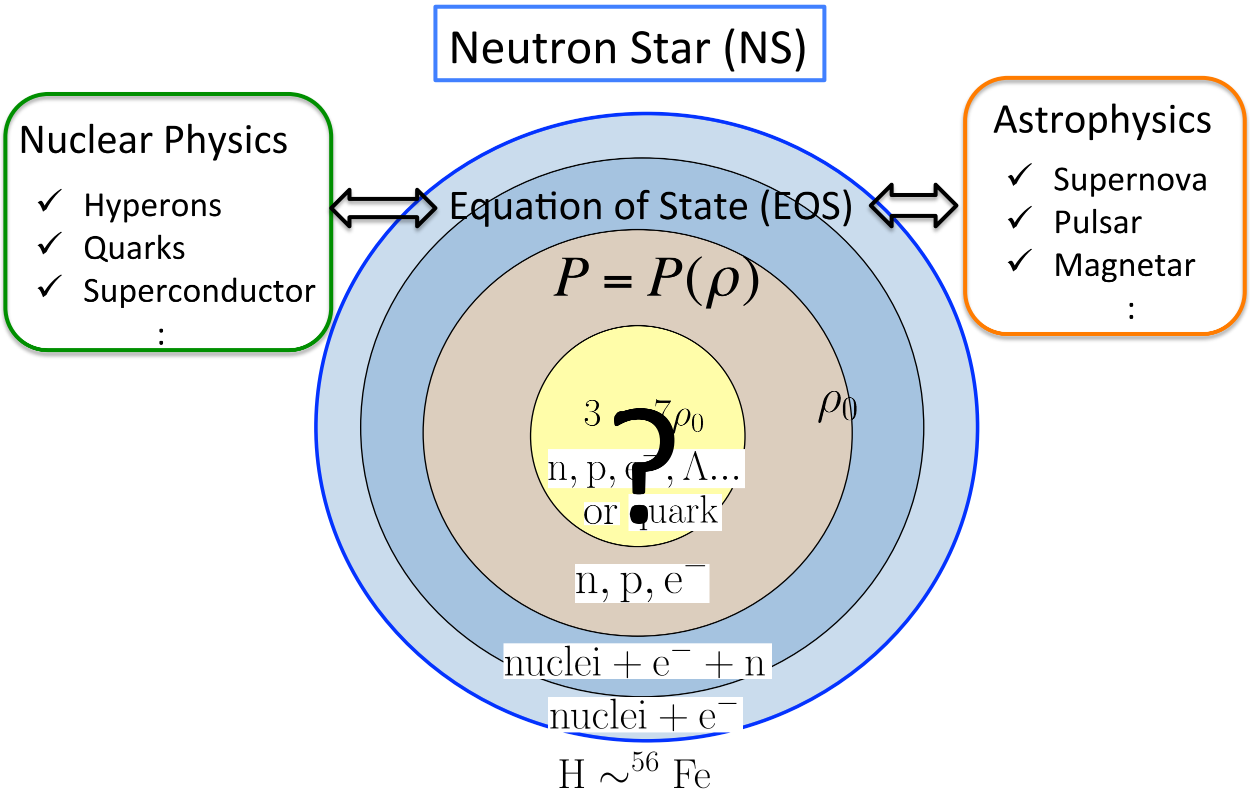

Finite-size of NS and equation of state (EOS)

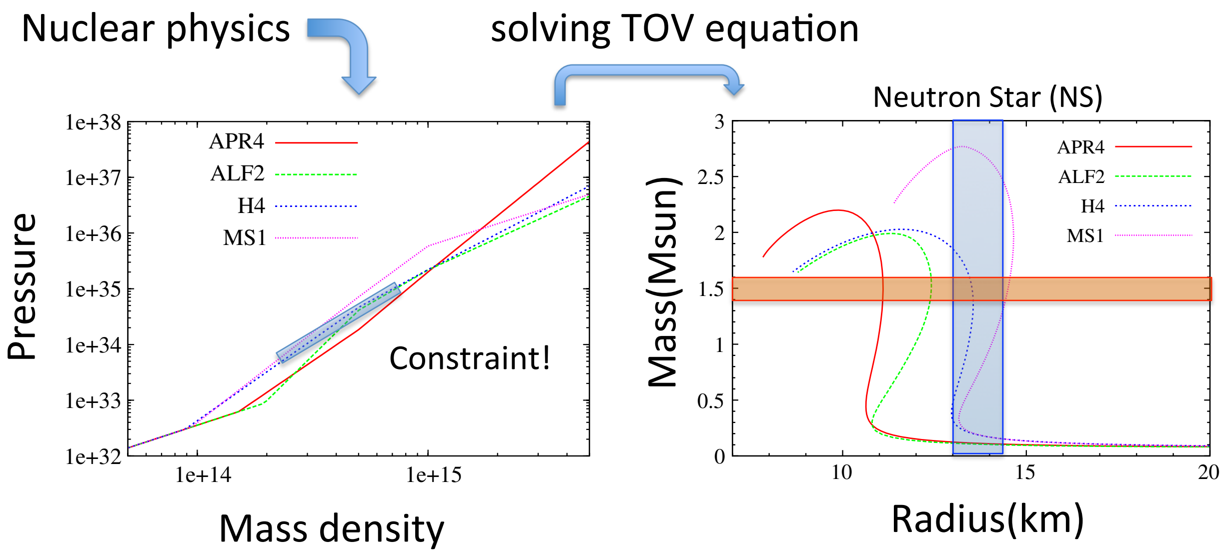

✓One-to-one correspondence: Lindblom(1992)

Equation of State (EOS) <=> M-R of Neutron Star (NS)

A big challenge to measure EOS by gw observation

Binary Neutron Star Merger

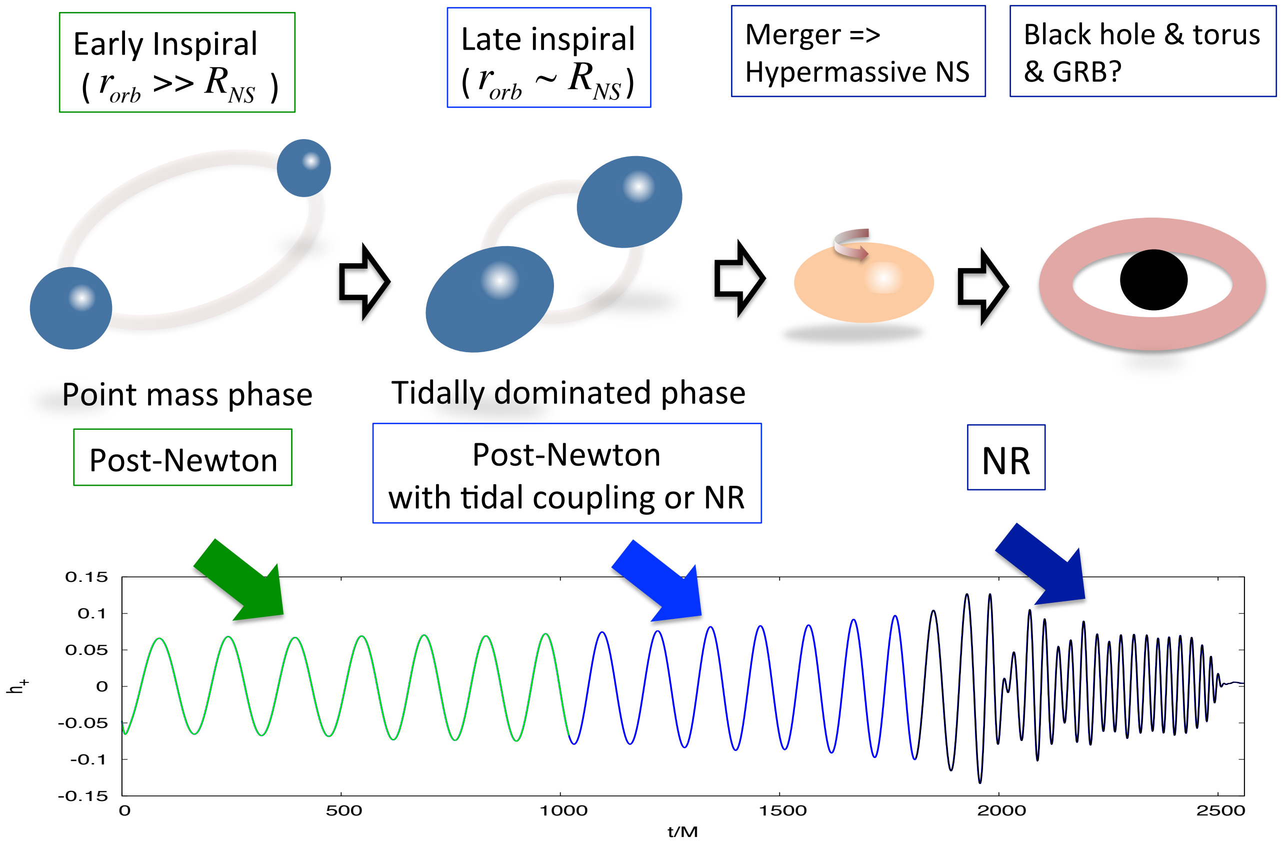

Inspiral Stage of NS-NS binary: measuring tidal Love number

How to measure the finite size of NS?

=>Tidal interaction in the late inspiral

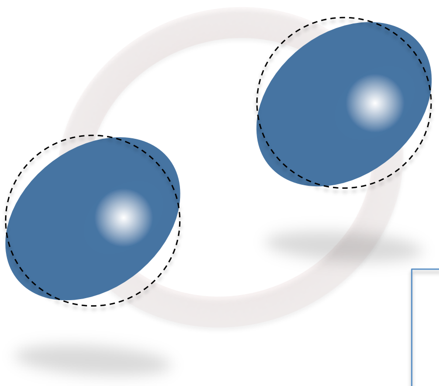

$$M\ddot{z} \sim -\frac{M}{r^2}\left(M + \frac{Q}{r^2} + O(r^{-6})\right)$$

Linear response of NS to tidal fields

$$Q \sim \frac{\Lambda}{r^3} \qquad \Lambda = \frac{2}{3}kR_{NS}^5$$

Λ : tidal deformability
k: Love number

depend on EOS

=> Leading terms of Tidal effects on the GW phase (5PN order)
⇒ Prepare waveform with (M1, M2, Λ1, Λ2)
⇒ EOS can be known through Λ

Flanagan & Hinderer (2008)

Analytic Computation (Effective One-Body)

1.35-1.35 Msun, EOS: MS1 (C~1.38)
without tidal effects
with tidal effects

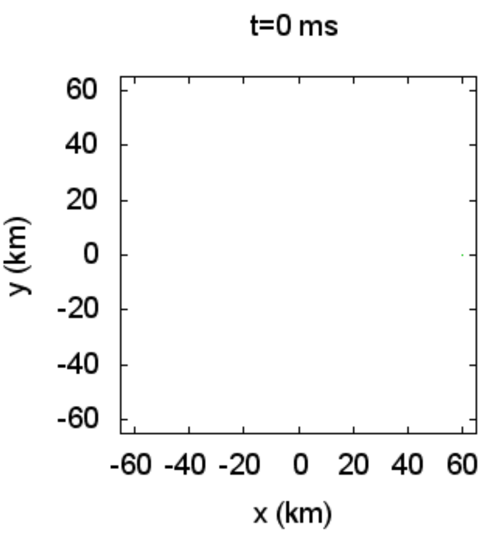

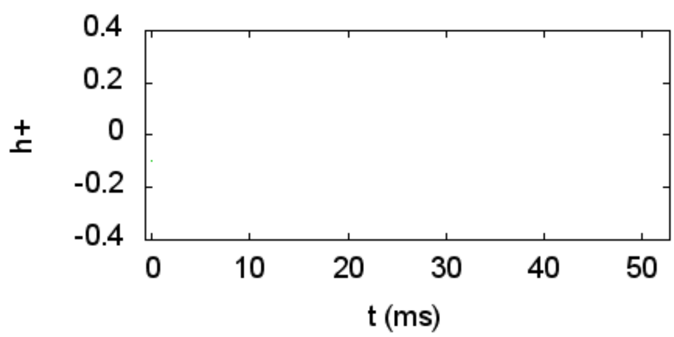

See e.g.,Pan et al., (2011)
Damour et al., (2012)

Two waveforms can be distinguished for NS-NS merger at D=200Mpc.

Post-merger stage of NS-NS binary; measuring NS radius

Evolutionary path of NS-NS merger

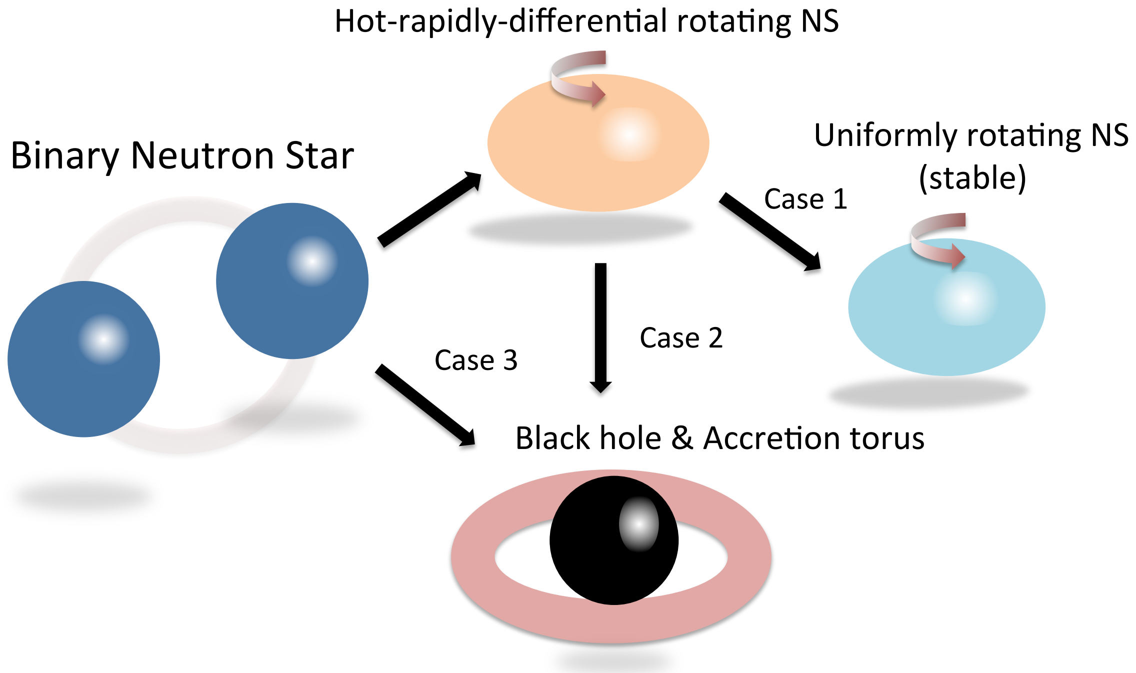

Case 2 : Hypermassive neutron star (HMNS) formation

HMNS/MNS formation

◆ Existence of Heavy Neutron Stars

✓ PSR J1614-2230 : 1.97 (0.04) Msun
✓ PSR J0348+0432 : 2.01 (0.04) Msun

Demorest et al., (2010)
Antoniadis et al,. (2013)

⇨ EOS of NS is very stiff

◆ Average mass of NSs in NS-NS binaries

$$1.33 \pm 0.05 M_{sun}$$

Ozel et al, 2013

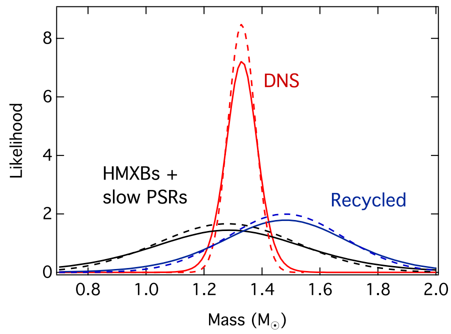

Numerical relativity computation

density

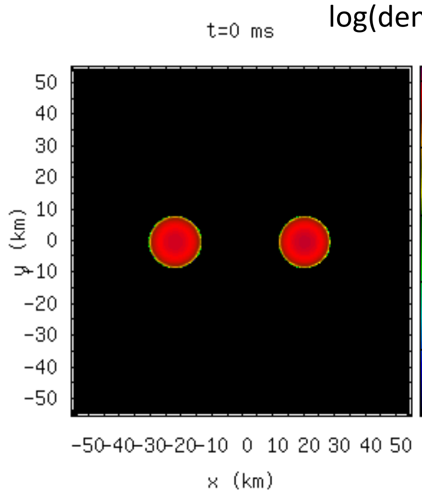

EOS : APR

Hotokezaka, et al. (2013)

$M_1 = 1.4 M_{sun}$ $M_2 = 1.3 M_{sun}$

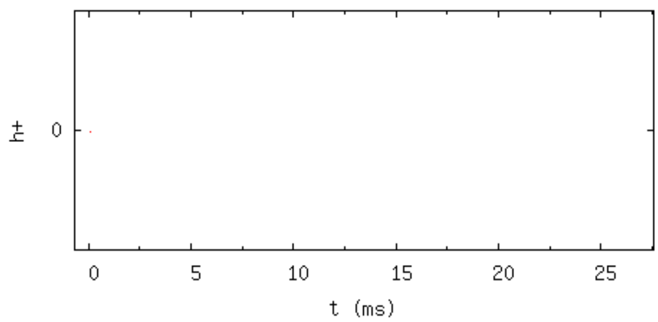

First remnant of NS-NS mergers

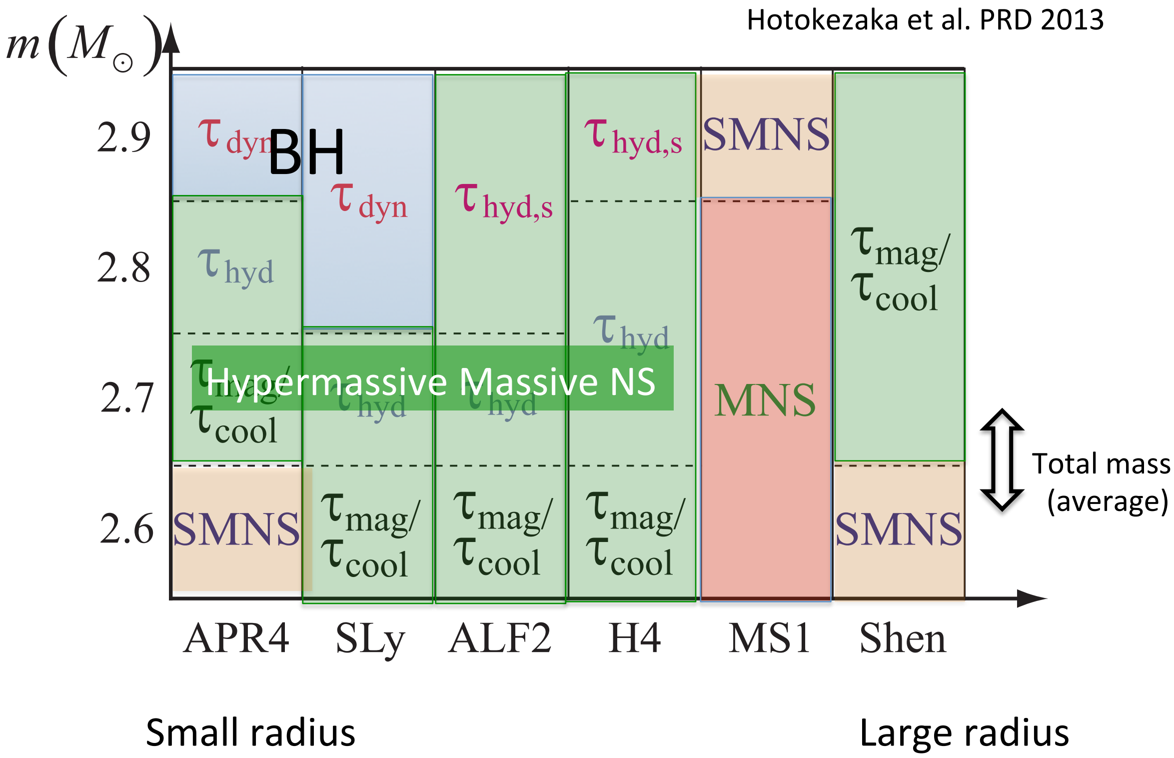

Various Gravitational Waveforms

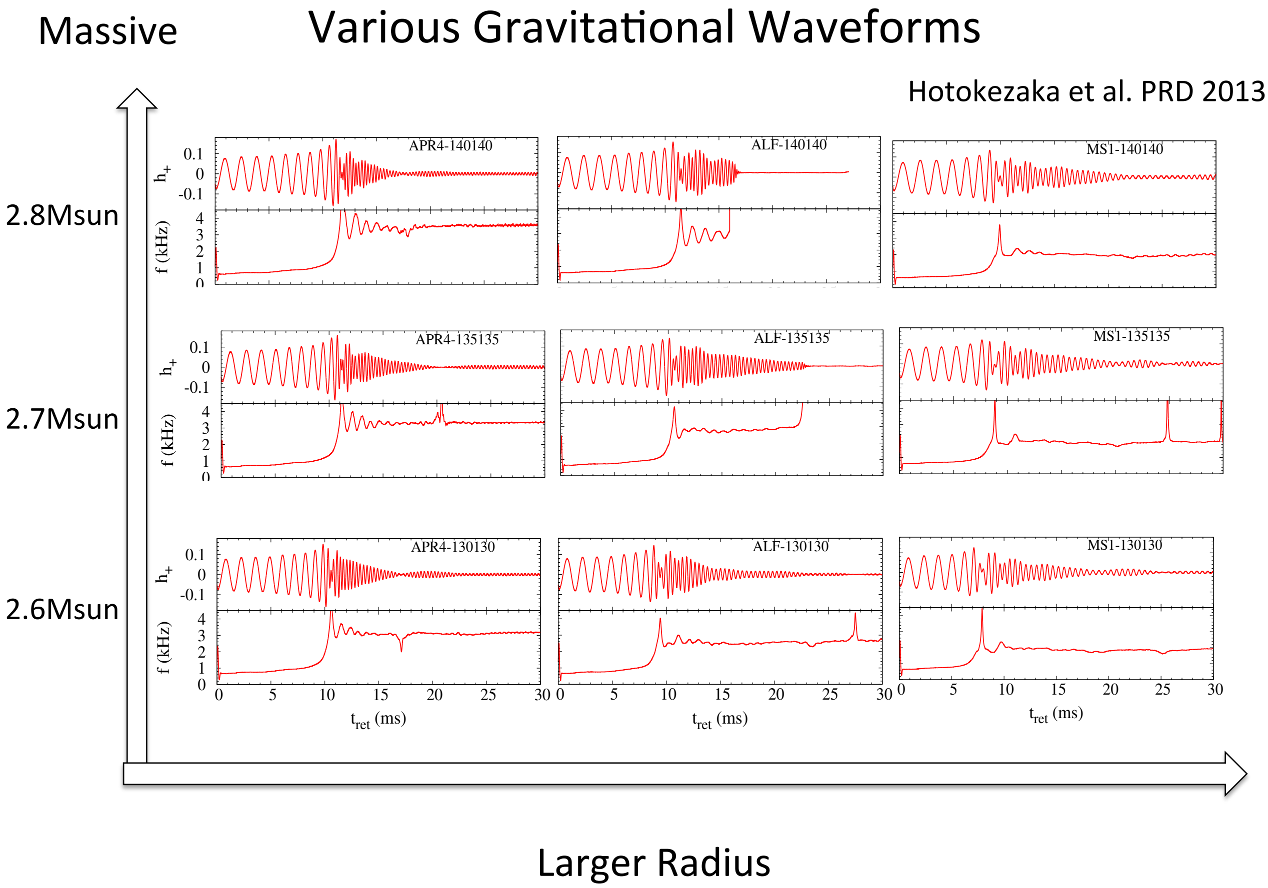

Fourier peak & NS Radius

Bauswein & Janka, PRD 86, 063001 (2012)
Hotokezaka et al, PRD 2013

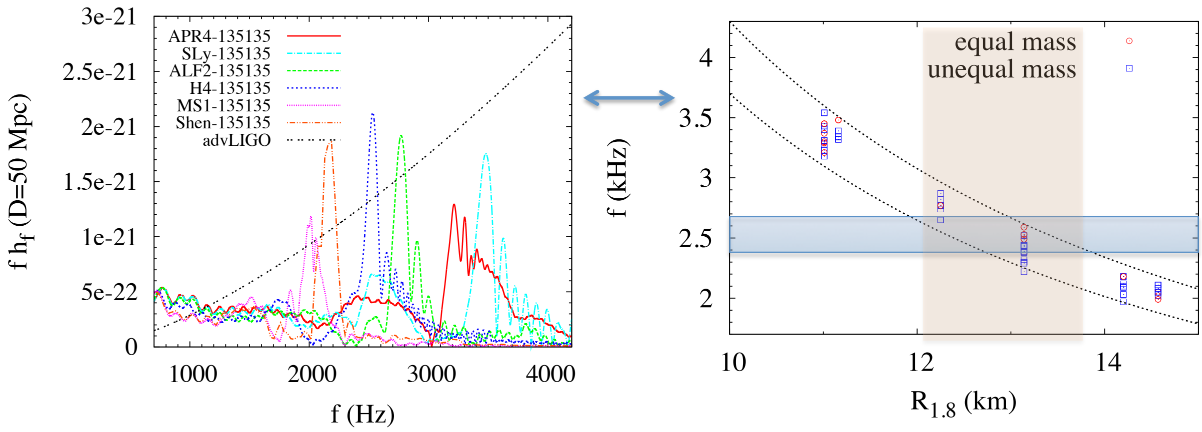

If we could measure the peak frequency,
we can know the NS radius with 1km error.

Measurability of finite-size of NS with gravitational wave signals

	Analytic(tidal)	NR	hybrid waveform
Measurability (10-50% accuracy)	～ 200Mpc	～ 100Mpc	～ 300Mpc

Damour et al., (2012), Read et al., (2013)

※Horizon distance for NS-NS ～445Mpc

But, many uncertainties prevent the measurements.....

A tough way to "EOS"

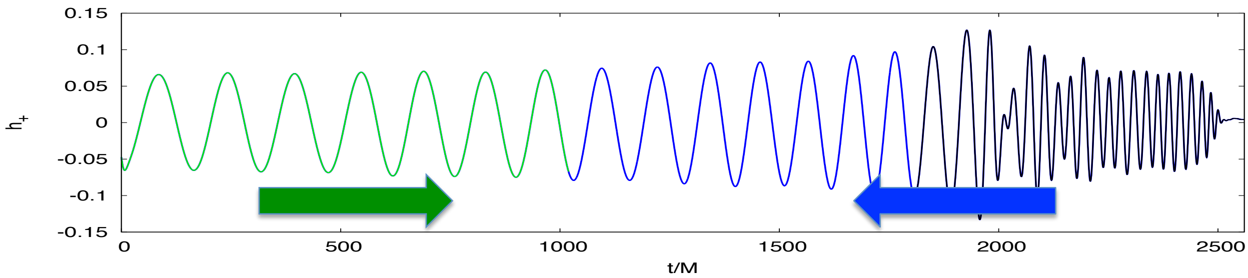

Analytic computation (higher order)
✓ 4PN and 5PN of point-mass should be computed.
(Favata 2013, Yagi and Yunes 2013)
✓ Non-linear finite-size effects. (Read et al, 2013, Hotokezaka et al 2013)

NR computation (control numerical error)
✓ Longer and longer waveforms are needed.
✓ Residual eccentricity has to be reduced as small as possible.
✓ More and more accurate formulations are need.
(beyond BSSN, higher order hydrodynamics)

Outline

1. Introduction
2. Gravitational waves from compact binaries and EOS
   - ✓ Inspiral phase and tidal effects and EOS
   - ✓ Post-merger and massive neutron star and EOS
3. Electromagnetic signals from compact binary mergers
   - ✓ A golden event: the short GRB 130603B
   - ✓ Kilonova emission
4. Summary

Long/Short Gamma-ray bursts

Kouveliotou et al (1993)

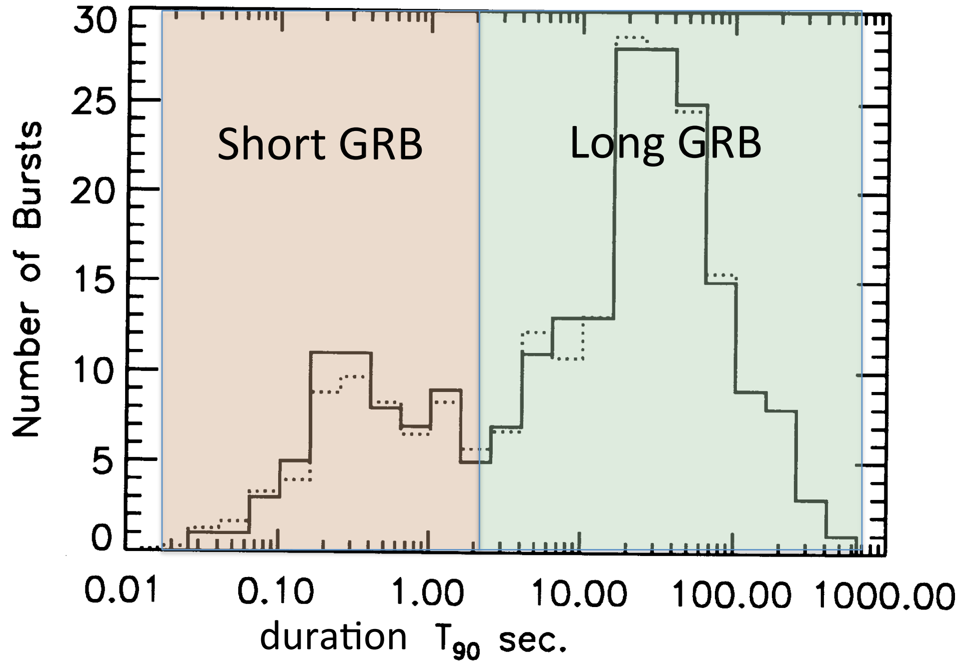

Long GRB => Death of Massive star because of discovery of supernova.
Short GRB => Compact binary merger ? No direct evidence.

A Golden event: the short GRB 130603B
~ Discovery of a "kilonova" ~

- ✓ This could be direct evidence of compact binary merger hypothesis of short GRBs.
- ✓ The time scale, brightness, and color of Kilonova are quite consistent with the NR prediction.
- ✓ Origin of gold is found.
  This event may produces 70 Earth-masses of gold!

The short GRB130603B: Swift BAT/XRT

http://www.swift.ac.uk/burst_analyser/00557310/

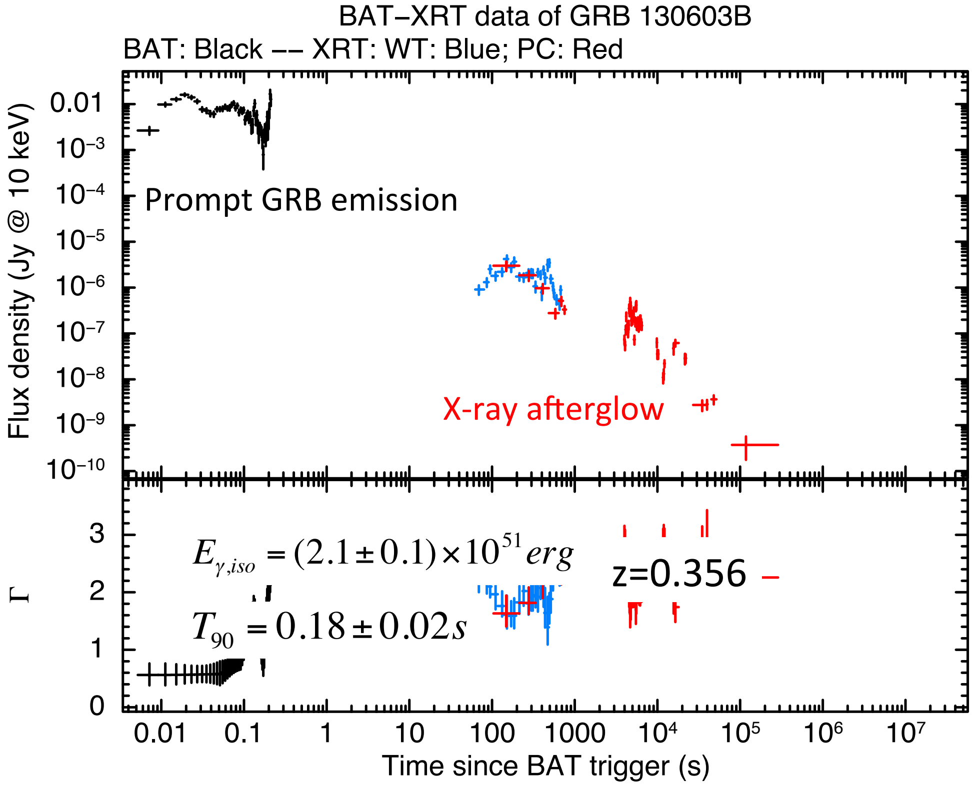

A Kilonova associated with the short GRB 130603B ?

◆ Hubble Space Telescope imaging

Tanvir et al.,Nature,2013
Berger et al., ApJ, 2013

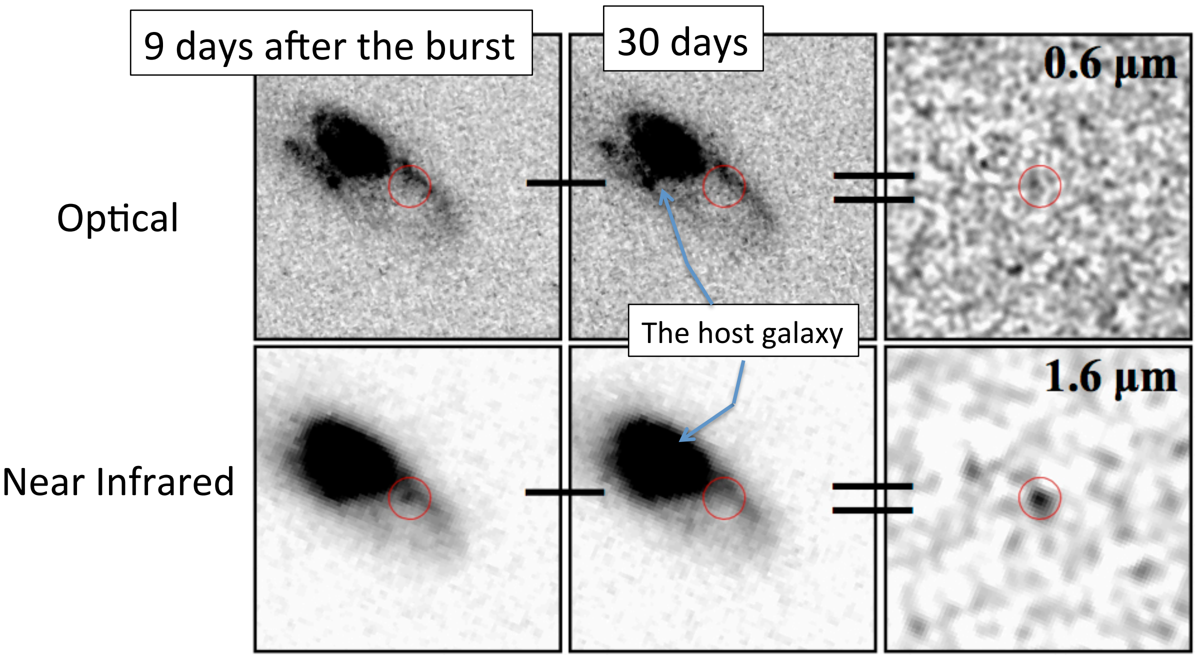

Observed Light curves

Tanvir et al.,Nature,2013
Berger et al., ApJ, 2013
de Ugarte Postigo et al 2013

These straight lines are a model of a GRB afterglow
- X-ray
- Optical
- Near Infrared

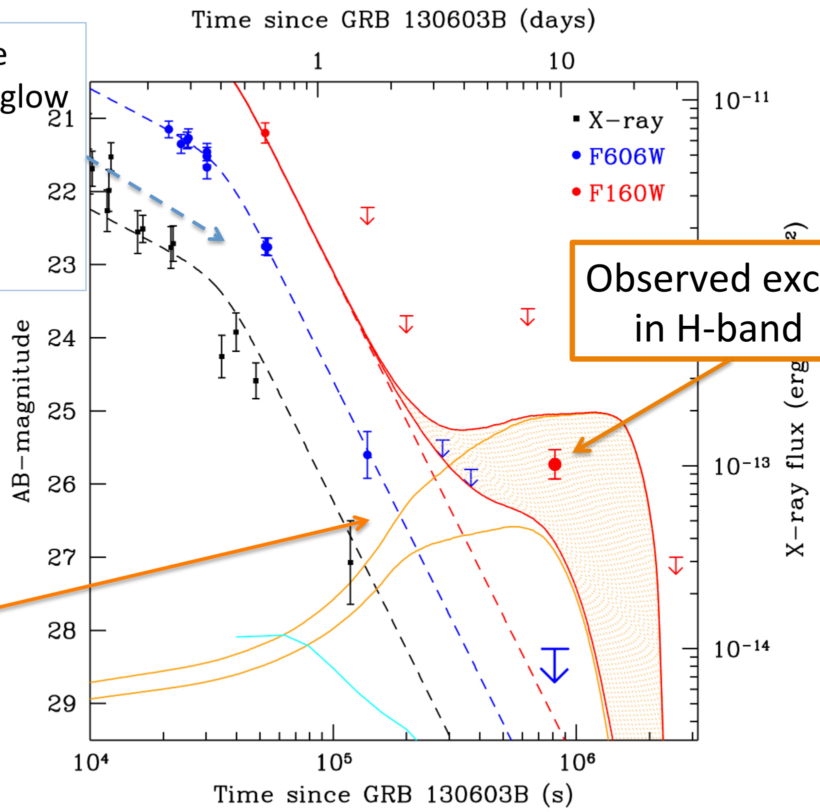

Observed excess in H-band

These bumps are Predicted curves of "Kilonova"
- optical
- Near Infrared

What is "kilonova"

A kilonova is proposed by Li & Paczynski in 1998
as an observable consequence of NS-NS mergers.

Ejected matter of an NS-NS merger

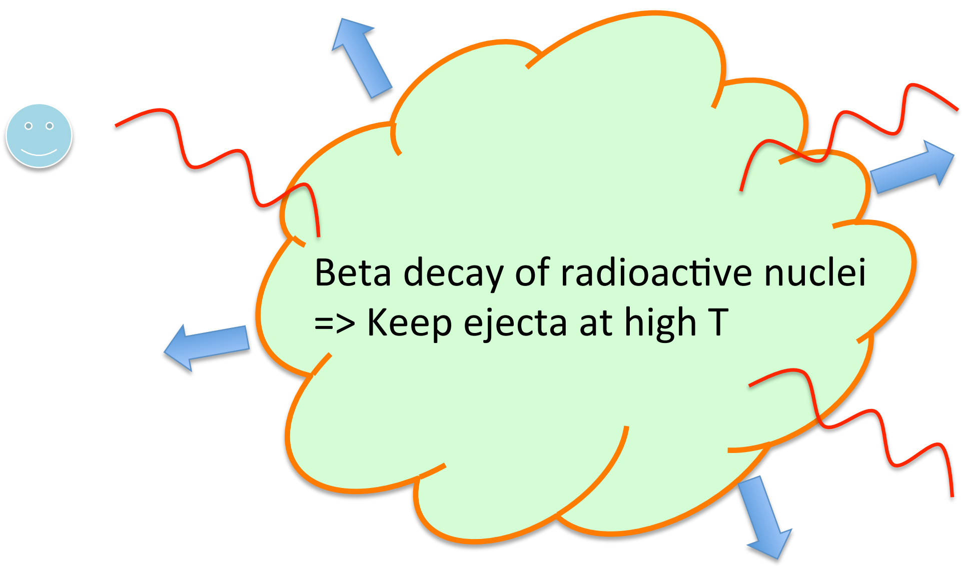

A brief summary of Kilonova emission

At peak luminosity (diffusion time = expansion time)

Hydrodynamics

Microphysics

$$L \sim 5\times 10^{40}\, erg/s \left(\frac{f}{10^{-6}}\right)\left(\frac{M}{0.01M_{sun}}\right)^{\frac{1}{2}}\left(\frac{v}{0.1c}\right)^{-\frac{1}{2}}\left(\frac{\kappa}{10cm^2g^{-1}}\right)^{-\frac{1}{2}}$$

$$t \sim 5days\left(\frac{M}{0.01M_{sun}}\right)^{\frac{1}{2}}\left(\frac{v}{0.1c}\right)^{-\frac{1}{2}}\left(\frac{\kappa}{10cm^2g^{-1}}\right)^{\frac{1}{2}}$$

To specify these parameters, detailed computations are needed.

Computation of Kilonova light curves

Numerical Relativity simulation

NS-NS merger
BH-NS merger → Mass ejection

⇩

Radiative transfer simulation

Photon propagation in expanding ejecta with heating due to radioactive decay

⇩

Light curve and spectrum of kilonova

⇕

Observed light curves of kilonova

Zoom out: Mass ejection at merger

Model : 1.2Msun – 1.5Msun, APR

300 km x 300 km　　　　2400 km x 2400 km

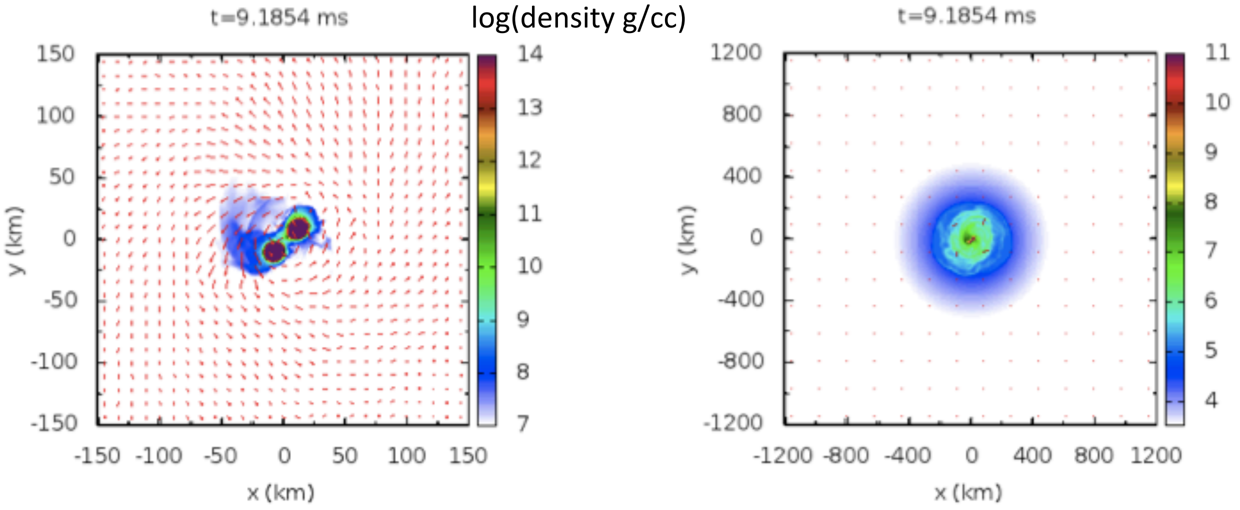

Zoom out: mass ejection at merger

Model : 1.2Msun – 1.5Msun, APR

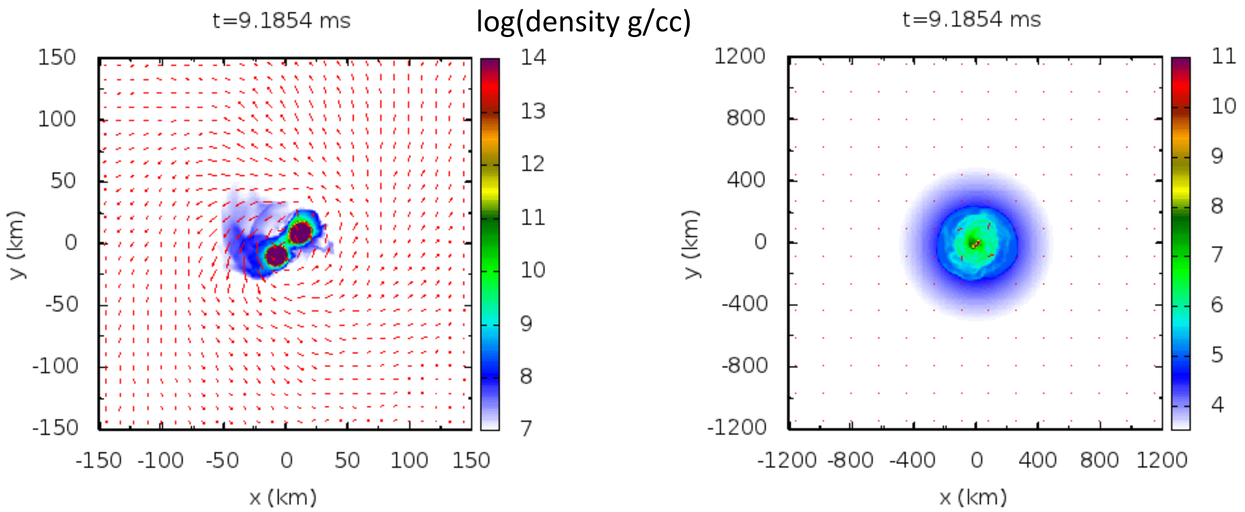

Mass ejection : Mej ~ 0.01Msun, v ~ 0.2c

Mass ejection on the Meridional plane

(x-z plane)

Model : 1.2Msun – 1.5Msun, APR

300 km x 150 km

2400 km x 1200 km

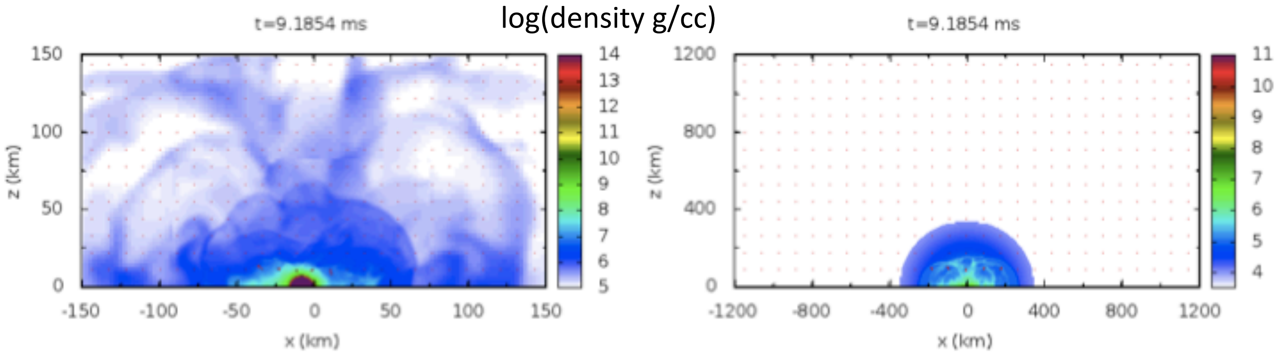

Mass ejection on the Meridional plane

(x-z plane)

Model : 1.2Msun – 1.5Msun, APR

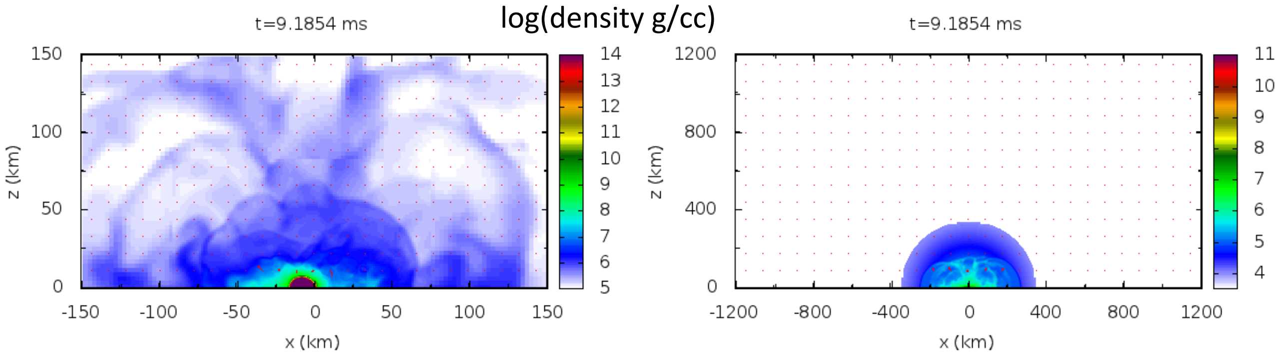

NS-NS Ejecta is spheroidal.

Compor

Nuclear network calculatio

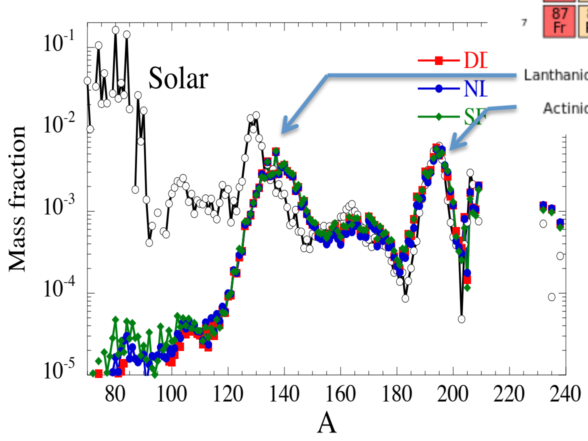

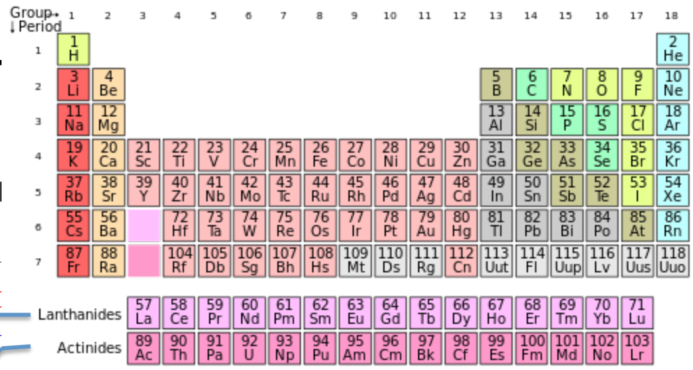

r-process elements
(between 2nd & 3rd peak)

⇒ Opacities of ejecta are significantly enhanced ~ 10 cm^2/g

*For SN Ia, Opacity ~ 0.1 cm^2/g

Bauswain, Goriely, & Janka (2013)
See also Korobkin et al. (2012)

see Kasen et al. (2013), Tanaka & KH (2013)

Transitions of Lanthanides

Kasen, Bandell, and Brase (2013)

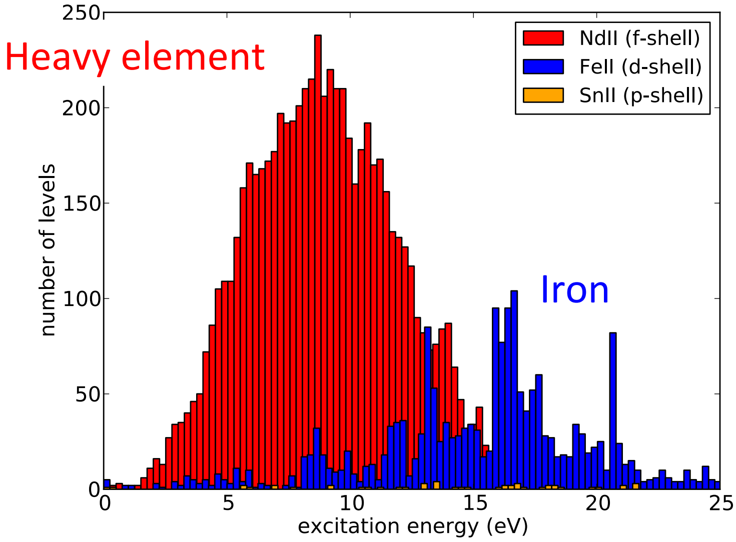

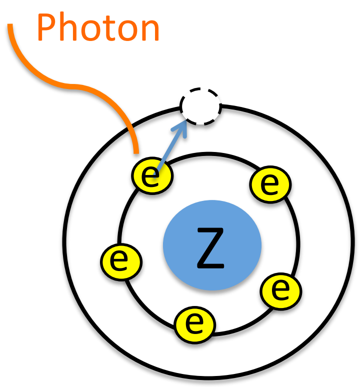

Absorption due to
bound-bound transition

Many transition levels in UV-Visible-IR band
=> We include this bound-bound opacity to solve radiation transfer

Radiation transfer of NS-NS merger ejecta

Opacity @ 3 days after the merger

Tanaka & KH 2013
See also Kasen + 2013

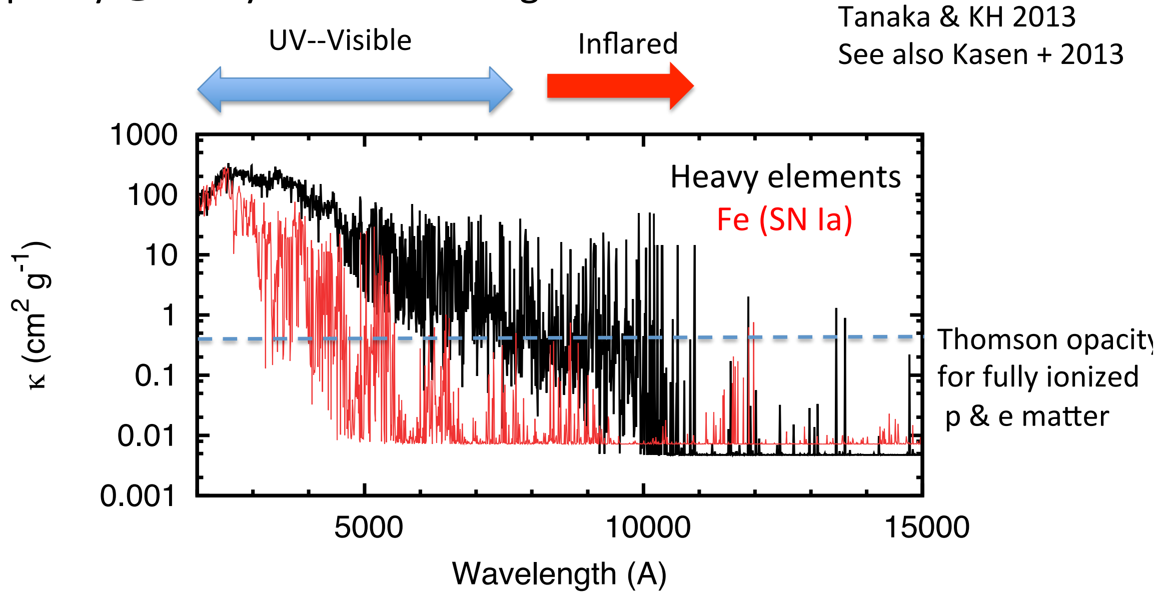

Huge opacity of bound-bound transitions of many elements
=> Photon cannot escape

The first direct comparison of NR results to observation!!

Hotokezaka et al (2013)

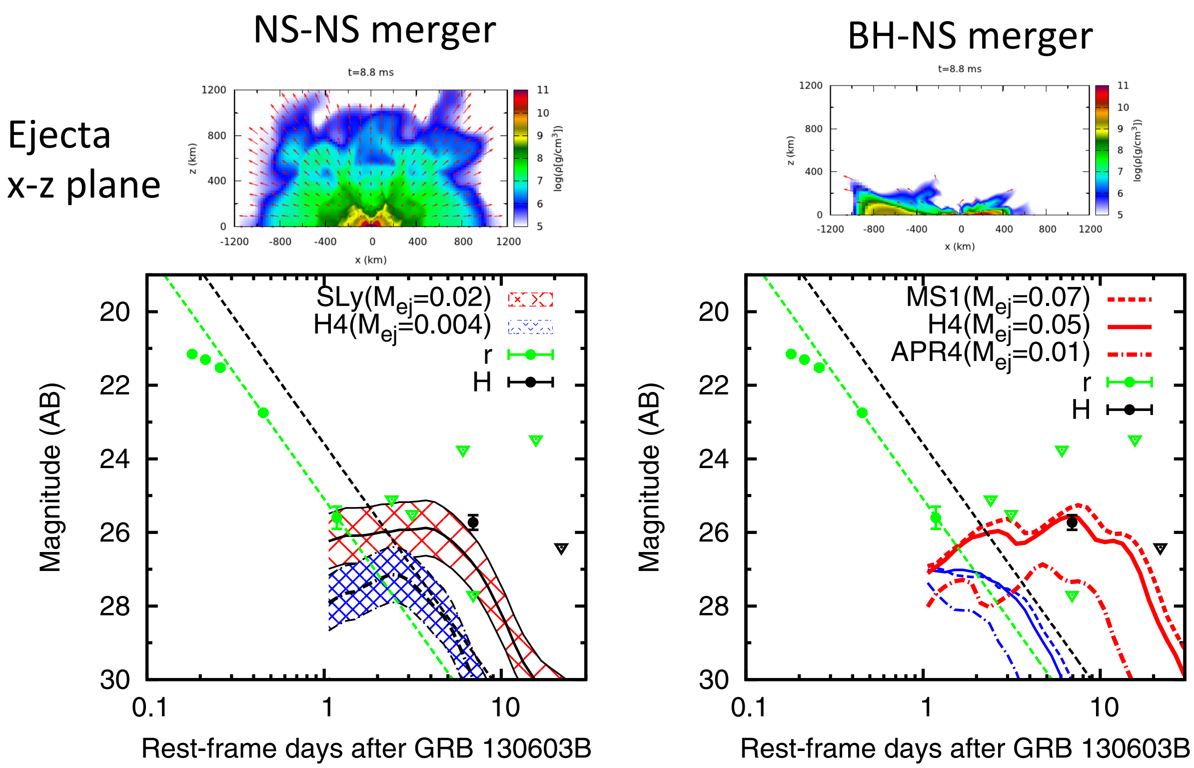

Implications for the progenitor of GRB130603B

Hotokezaka et al (2013)

Allowed region of a progenitor

NS-NS

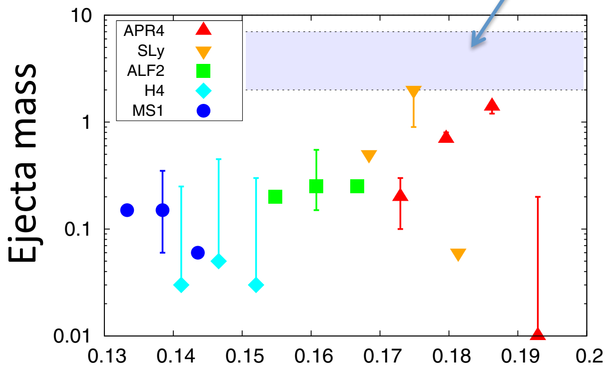

BH-NS

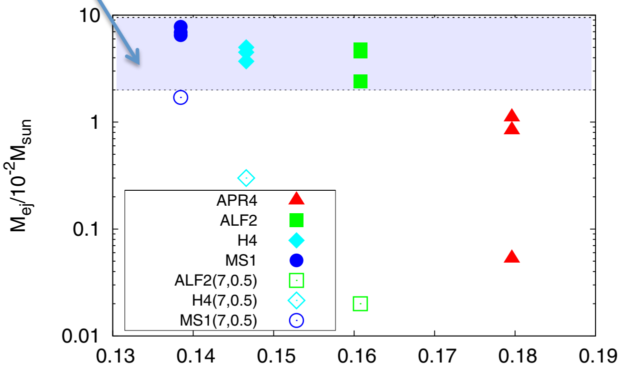

Compactness of NS

Compactness of NS

Favor: Compact NS | Less compact NS

Implication for gravitational-wave counterparts

Shorter wavelength

Longer wavelength

Optical

Near Infrared

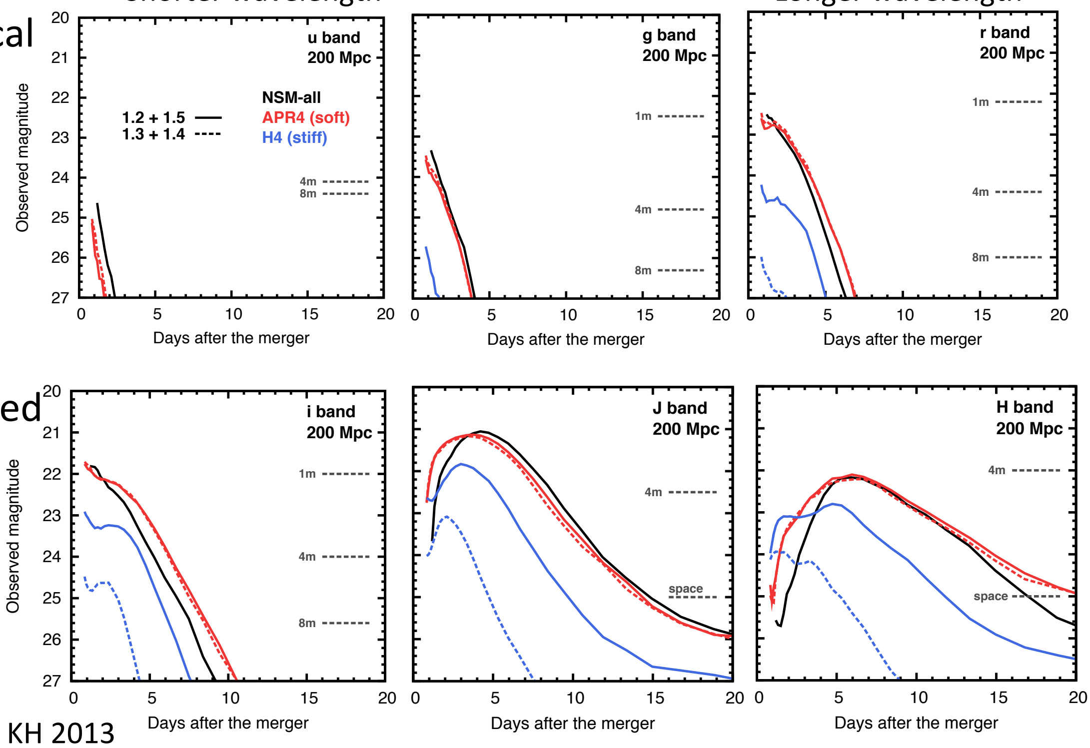

Tanaka & KH 2013

Bright in near infrared at 1 week after the merger

Summary

Neutron Star equation of State can be measured through

- ✓ tidal effects in the late inspiral stage and
- ✓ fourier peak frequency of gws from HMNS.

However, to succeed in measuring the EOS,

- ✓ higher order PN corrections and
- ✓ longer and more accurate NR computation are needed.

GRB 130603B is a golden event

- ✓ This could be direct evidence of compact binary merger hypothesis of short GRBs.
- ✓ The time scale, brightness, and color of Kilonova are quite consistent with the NR prediction.
- ✓ For NS-NS merger models, soft EOSs are favored.
  For BH-NS merger models, stiff EOSs are favored.

Multi-Messenger Astronomy is coming soon !!

Thank you !!

“Binary neutron star merger with a 'soft' equation of state and r-process”

by Yuichiro Sekiguchi

[JGRG23(2013)110610]

The Ministry of Education, Culture, Sports, Science and Technology (MEXT) Grant-in-Aid for Scientific Research on Innovative Areas

科研費 KAKENHI

重力波天体の多様な観測による宇宙物理学の新展開

New development in astrophysics through multimessenger observations of gravitational wave sources

K computer

Binary neutron star merger with a 'soft' equation of state and r-process

Yuichiro Sekiguchi (YITP)

with S. Wanajo, N. Nishimura, K. Kiuchi, K. Kyutoku, M. Shibata

Solar abundance of nuclei

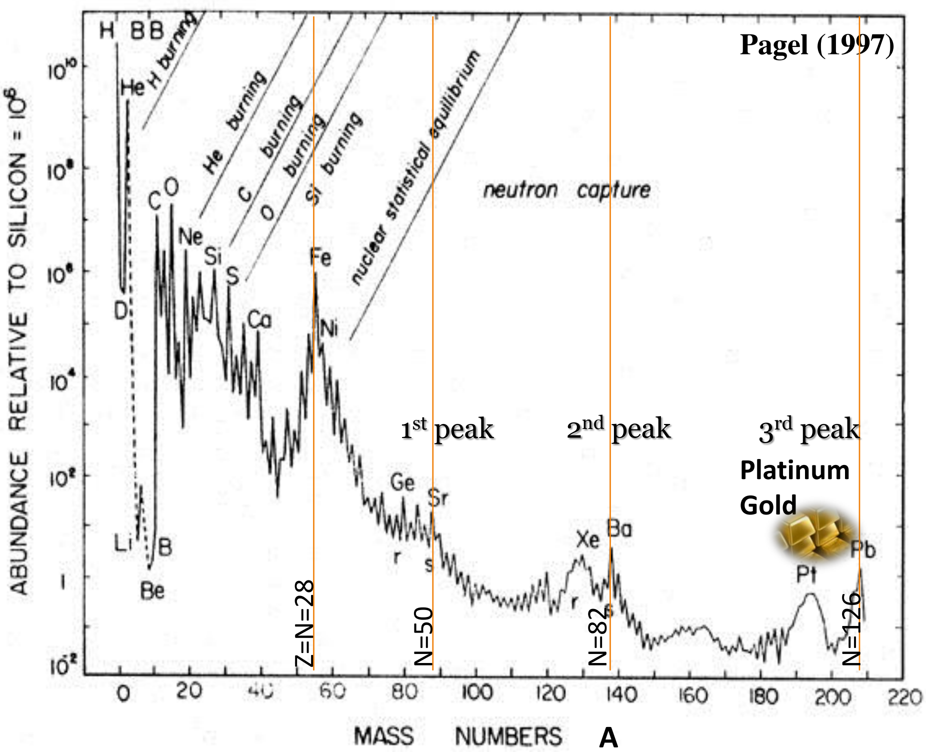

- **Basic feature :** exponential decay with mass number + constant tail
- **Characteristic features:**
- Peak in iron-group
- Deficient of D, Li, Be, and B
- Enhancement of α-nuclei (C, O, Ne, Si,..)
- **Peaks in heavier region associated with n-magic numbers, made by neutron capture processes**

Neutron capture processes

$\boxed{n + (Z,N) \Rightarrow (Z,N+1)}$ $\boxed{(Z,N+1) \Rightarrow (Z+1,N) + e + \bar{\nu}_e}$

n-capture versus **β-decay**

$\tau_n < \tau_\beta$ $\tau_n > \tau_\beta$

rapid neutron-capture process **(r-process)**	slow neutron-capture process **(s-process)**
large neutron densities ➢ Can synthesize all heavy nuclei	moderate neutron densities ➢ does not synthesize all heavy nuclei ➢ terminates at Pb, Bi

To be an alchemist : recipe to cook gold

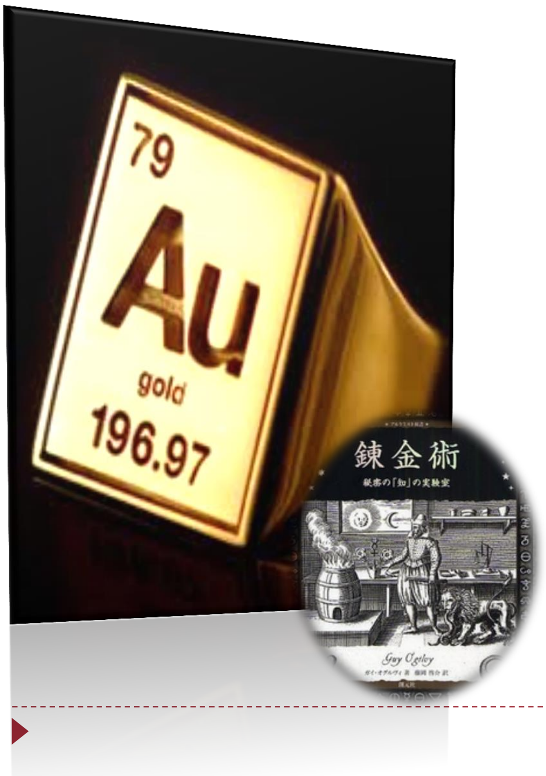

- Neutron capture : packing neutrons into ‘seed’ nuclei $\boxed{n + (Z,N) \Rightarrow (Z,N+1)}$
  - Large neutron/seed ratio required
  - A(gold) – A (seed) ~ 100
- **Low electron fraction Ye**
  - To have a large number of free neutrons
- **Higher entropy per baryon**
  - To slow the seed nuclei production
- **Short expansion timescale**
  - To freeze seed production with rapid decrease of temperature

What is the melting pot for r-process ?

- **<u>Supernova (SN) explosion: theoretically disfavored</u>**
  - Smaller entropy/per baryon than previously expected (e.g., *Janka et al. 1997*)
  - Neutrinos from PNS make the flow proton-rich : $n+\nu \rightarrow p+e$
  - ⇒ only weak r-process (up to 2nd peak, no gold (3rd peak)!) (*Roverts et al. 2011*)
    - <u>Electron capture SN</u> : does not produce nuclei with A >~ 90 (*Hoffman et al. 2008; Wanajo et al. 2009*)
    - <u>(Iron) core collapse SN</u> : outflows are too proton-rich (*Fisher et al. 2010; Hudepohl et al. 2010*) to produce nuclei with A >~ 120 (*Wanajo et al. 2011*)
- **<u>NS-NS/BH binary merger: Observationally disfavored (*Argast et al. 2004*)</u>**
  - delayed appearance of r-process element (long lifetime to merge)
  - large star-to-star scattering (low event rate (~ 10^{-5}/yr/gal) : rock sugar vs. table sugar)
  - A clustering scenario of sub-halos to the Galactic halo overcomes the above issues (*Ishimaru, Wanajo, Prantzos, in prep.*)
    - <u>Parameterized studies</u> (Ye, T are given by hand) (*Freiburghaus et al. 1999; Roberts et al. 2011*)
    - <u>More self-consistent studies</u> with approximate GR (*Goriely et al. 2011; Korobkin et al. 2012*)
- **<u>BH-Torus system :</u>** R-process in <u>hot neutrino driven wind</u> (*Wanajo & Janka 2012*)

Kilo-nova/Macro-nova/r-process-nova

- **EM transients powered by radioactivity of the r-process elements are expected (Li & Paczynski 1998) ⇒ important EM counterpart of GW**
- Recent critical update : <u>Opacities are dominated by lanthanoids : orders of magnitude (~100) larger</u> (Kasen e al. 2013; Tanaka & Hotokezaka 2013)

$$t_{\rm peak} \sim 10\ {\rm days}\left(\frac{v}{0.3c}\right)^{-1/2}\left(\frac{M}{0.01M{\rm solar}}\right)^{1/2}\boxed{\left(\frac{\kappa}{10\ {\rm cm}^2/g}\right)}^{1/2}$$

1 day ⇒ 10 days

$$L_{\rm peak} \sim 10^{41}\ {\rm erg/s}\left(\frac{f}{10^{-6}}\right)\left(\frac{v}{0.3c}\right)^{1/2}\left(\frac{M}{0.01M{\rm solar}}\right)^{1/2}\boxed{\left(\frac{\kappa}{10\ {\rm cm}^2/g}\right)}^{-1/2}$$

1/10 dimmer

$$T^{\rm eff}_{\rm peak} \sim 2\times10^3\,{\rm K}\left(\frac{f}{10^{-6}}\right)^{1/4}\left(\frac{v}{0.3c}\right)^{-1/8}\left(\frac{M}{0.01M{\rm solar}}\right)^{-1/8}\boxed{\left(\frac{\kappa}{10\ {\rm cm}^2/g}\right)}^{-3/8}$$

Opt-UV ⇒ NIR

- Although it gets difficult to observe, they are still among the promising EM counterparts ⇒ needs more studies to clarify the ejecta properties

Mass ejection from BNS merger (1): Tidal torque + centrifugal force

Hotokezaka et al. (2013)

- Less massive NS is tidally deformed
- Angular momentum transfer by spiral arm and swing-by
- A part of matter is ejected along the orbital plane
- **reflects low Ye of cold NS** (β-eq. at T~0), no shock heating, rapid expansion (fast T drop), no time to change Ye by weak interactions

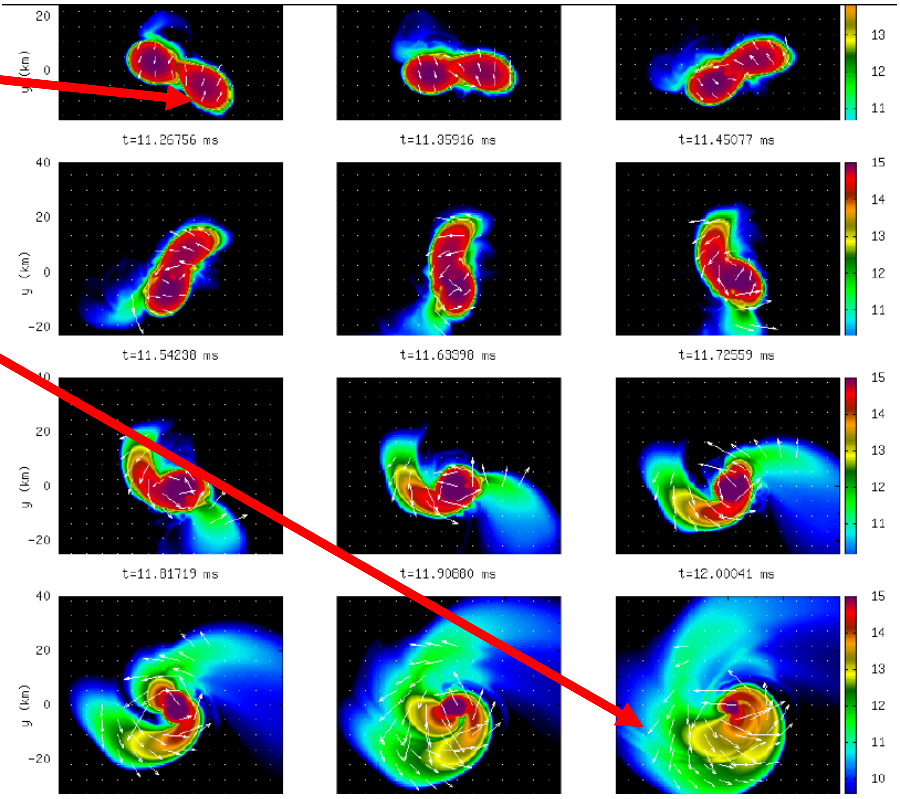

Density contour
[log (g/cm³)]

Mass ejection from BNS merger (2): Shock driven

- Shocks occur due to oscillations of massive NS and collisions of spiral arms
- Isotropic mass ejection, could **change Ye via weak processes (could have large Ye)**

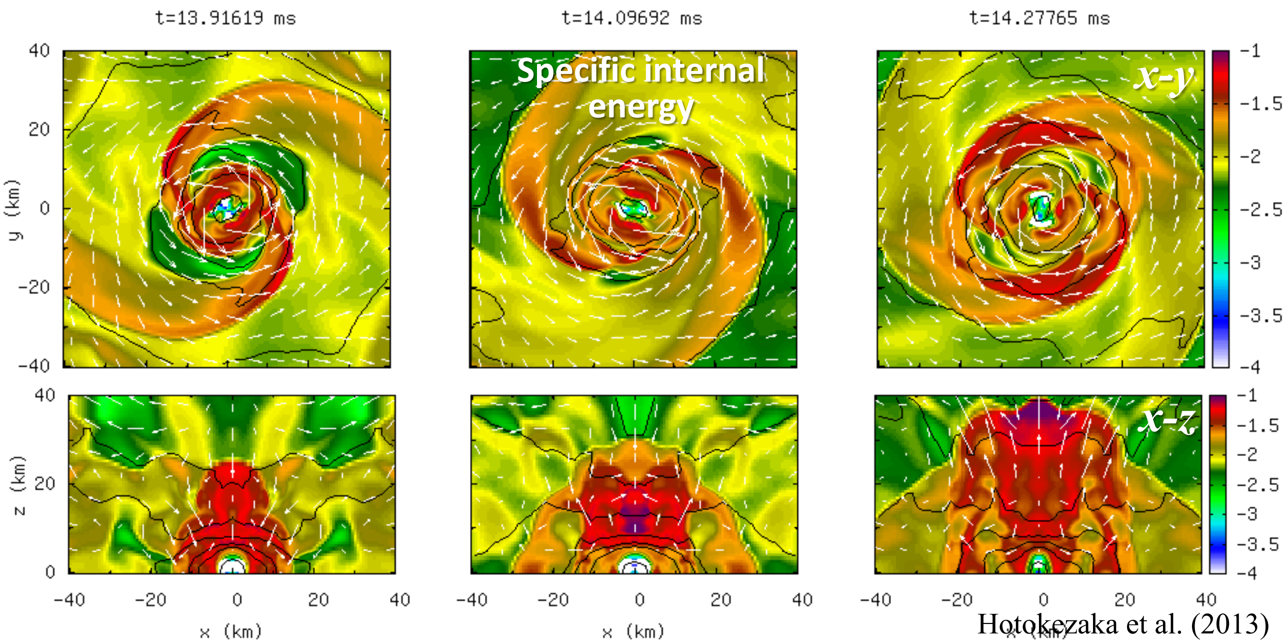

Hotokezaka et al. (2013)

'Robustness' of r-process in NS-NS merger ?

- **Korobkin et al. 2012 :**
  - *Ye of the ejecta is low as < 0.1 and depends weakly on the binary parameters so that r-process in the NS-NS is 'robust'*
    - Main mass ejection mechanism : tidal effects
    - Very low Ye, too effective neutron capture and r-process only 2nd (A~130; N=82) and 3rd (A~195; N=126) peaks are produced : **almost no production of 1st peak**
  - They adopted only one 'stiff' EoS (**Shen EoS**) : dependence on EoS is not explored
  - Newtonian SPH simulation: GR effects are not explored

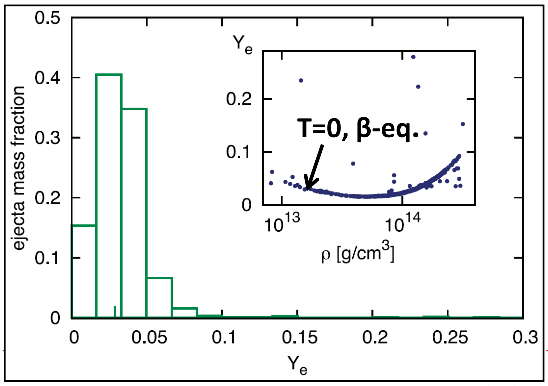

Korobkin et al. (2012) MNRAS 426 1940

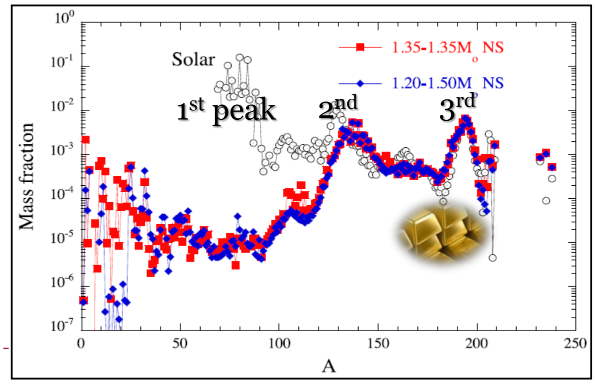

Goriely et al. (2011) ApJL 738 32

'Robustness' of r-process in NS-NS merger ?

- **This work : Full GR study with two EOS: Steiner EoS and Shen EoS**
- Full GR: stronger shock heating, relative importance of tidal/shock mechanisms can be altered
- Shen EOS: 'Stiffer'
  - Larger NS radius: Mass ejection is driven mainly by tidal force
  - Adopted in Korobkin et al.
- Steiner EOS: 'Softer'
  - Smaller NS radius: Tidal effect less important
  - Shock driven components increase

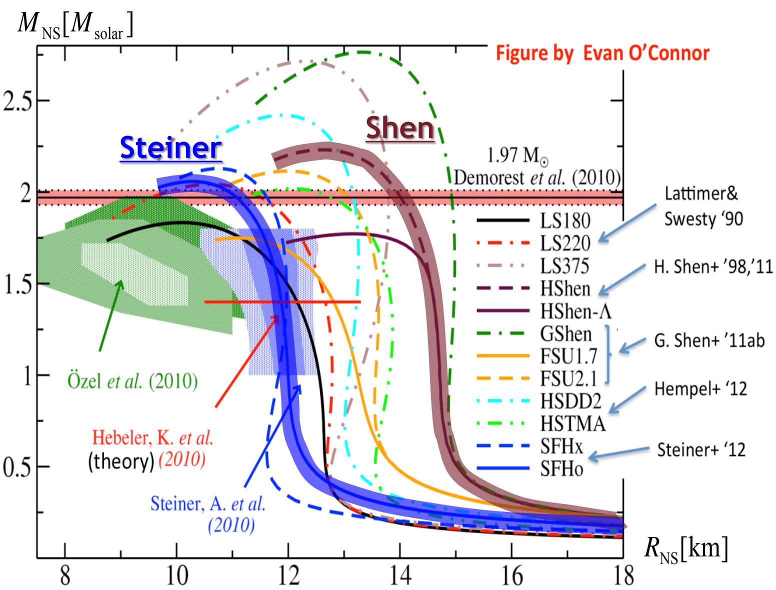

Full GR Radiation-Hydrodynamics

- **Einstein's equations:** Puncture-BSSN/Z4c formalism
- **GR radiation-hydrodynamics** (*Sekiguchi 2010; Sekiguchi + in prep.*)
  - **Advection terms :** Truncated **Moment scheme** (*Shibata et al. 2011*)
    - EOS : any tabulated EOS with 3D smooth connection to Timmes EOS
    - gray or multi-energy but advection in energy is not included
    - Fully covariant and relativistic
    - M-1 closure
  - **Source terms :** two options
    - Implicit treatment : Bruenn's prescription
    - Explicit treatment : trapped/streaming ν's
      - e-captures: thermal unblocking/weak magnetism; NSE rate
      - Iso-energy scattering : recoil, Coulomb, finite size
      - e±annihilation, plasmon decay, bremsstrahlung
      - diffusion rate (Rosswog & Liebendoerfer 2004)
      - two (beta- and non-beta) EOS method
  - **Lepton conservation equations**

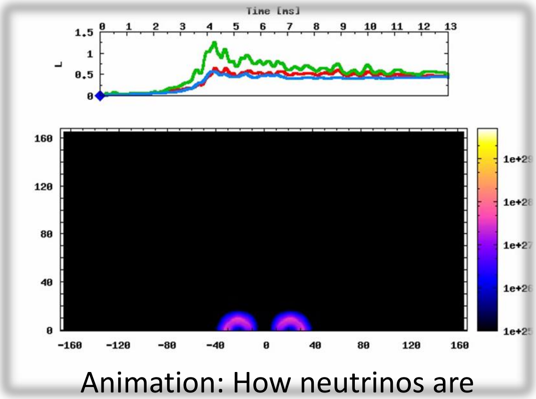

Animation: How neutrinos are emitted from BNS merger

Ejecta properties depend strongly on EOS

- **Steiner EOS: shock driven**
- **Higher temperature, more e+**

- **Shen EOS: tidal driven**
- **lower temperature**

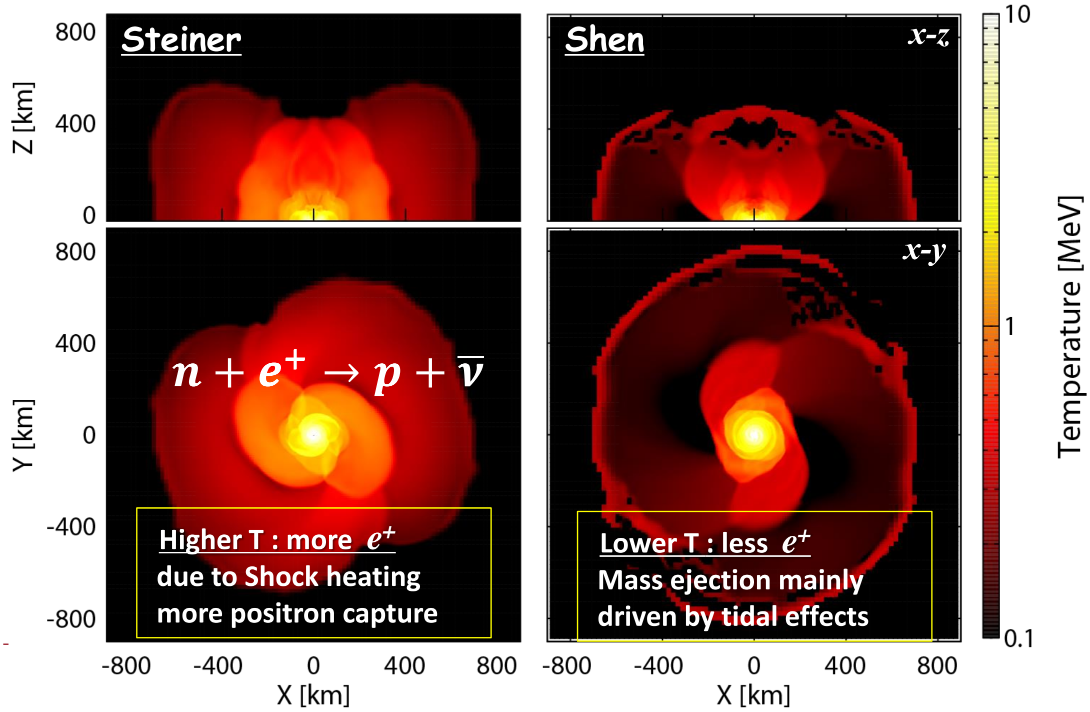

anti-electron neutrino emission

- **Steiner EOS: larger anti-neutrino emissivity due to positron capture**

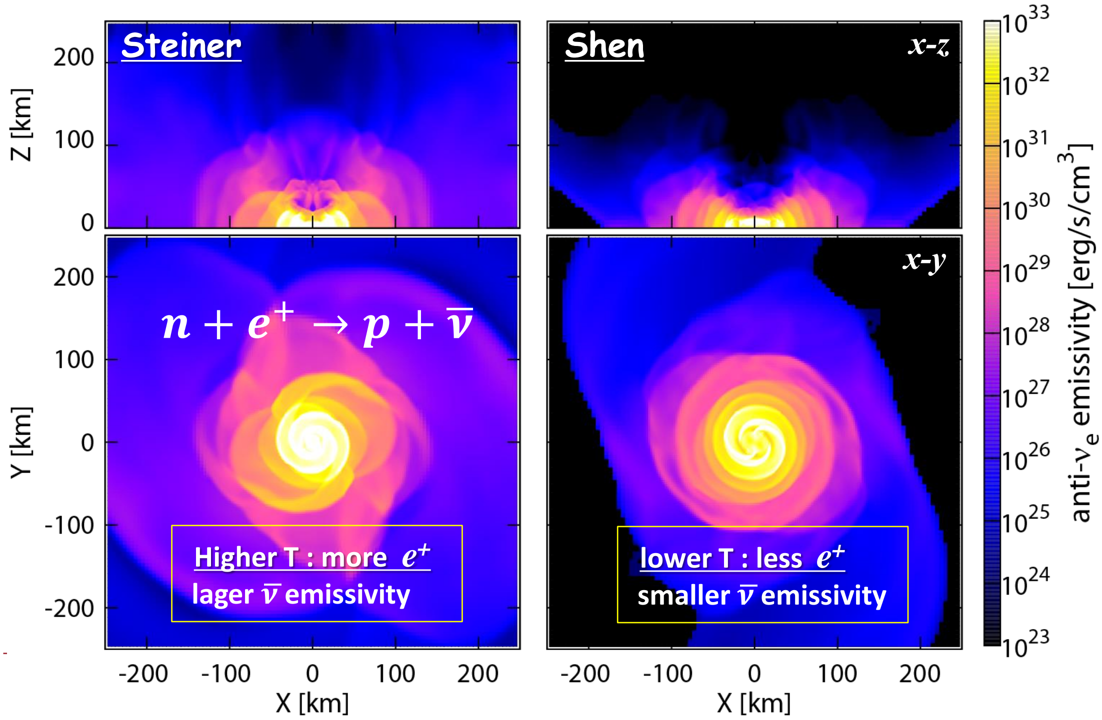

Ye in ejecta depends on EOS

- Positron capture substantially increases ejecta Ye

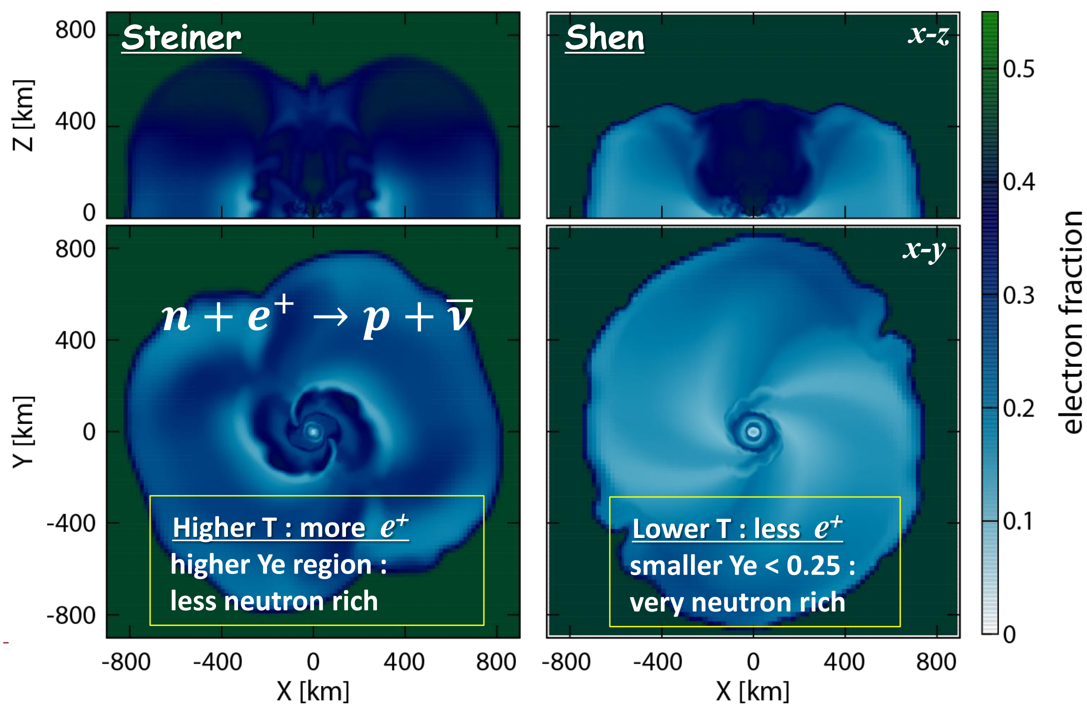

Impact on r-process nucleosynthesis

- r-process nucleosynthesis calculation based on the ejecta thermodynamic properties (*__Wanajo, YS et al. in prep__*.)
  - Gives the yield distribution which agrees with the solar abundance !
  - Highlights importance of neutrinos and EOS
  - BNS mergers as the origin of heavy elements (The alchemist 's pot to make gold) ?

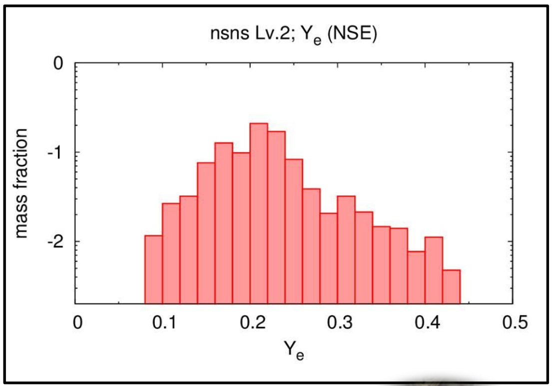

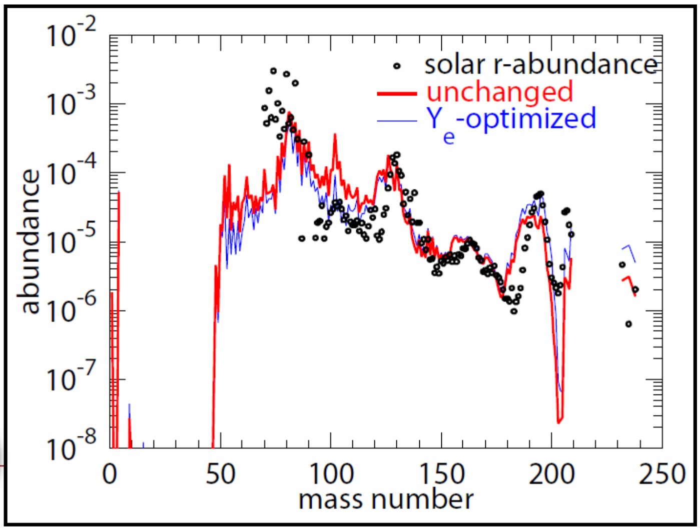

Summary

- Neutrino-Radiation-Hydrodynamics in numerical relativity is now feasible !
  - based on truncated moment formalism with M-1 closure
  - both implicit and explicit schemes can be adopted

- **Importance of neutrinos and EOS for r-process in BNS merger**
  - strong EOS dependence : challenge to the robustness (Korobkin et al. 2012)
  - For a softer EOS **shock heating** is more important and **ejecta *T* increases**
  - As a result, **positron capture** proceeds more and **__ejecta Ye increases__**
  - **__Resulting r-process yield agrees well with the solar abundance__**
  - BNS merger as origin of heavy elements ?

- Future studies
  - Further investigation of EOS dependence
  - EM counterpart study based on r-process nucleosynthesis calculation
  - Collapsars, BH-NS mergers, …

“Nonlinear r-mode instability in rotating stars”

by Motoyuki Saijo

[JGRG23(2013)110611]

Nonlinear R-mode Instability in Rotating Stars: Hydrodynamical Treatment

Motoyuki Saijo (Waseda University)

CONTENTS

1. Introduction

Various Instabilities in Secular Timescale

CFS instability (Chandrasekhar 70, Friedman & Schutz 78)

- Fluid modes (f, p, g-modes) may becomes unstable due to gravitational radiation
- Instability occurs in dissipative timescale

r-mode instability

(Andersson 98, Friedman & Morsink 98)

- Fluid elements oscillate due to Coriolis force
- Instability occurs due to gravitational radiation

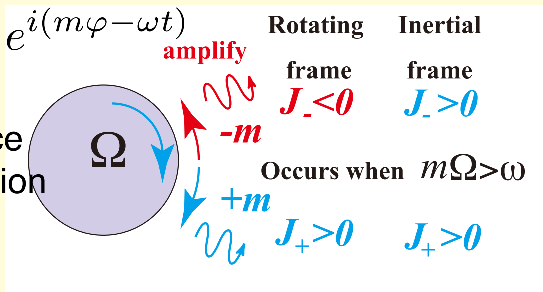

g-mode instability

- Fluid elements oscillate due to restoring force of buoyancy
- Instability occurs in nonadiabatic evolution or in convective unstable case

Kelvin-Helmholtz instability

- Instability occurs when the deviation of the velocity between the different fluid layers exceeds some critical value

Dynamics of r-mode instabilities

Saturation amplitude of r-mode instability

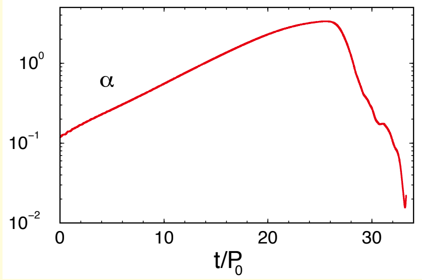

3D simulation

- Saturation amplitude of o(1)
- Imposing large amplitude of radiation reaction potential in the system to control secular timescale with dynamics (Lindblom et al. 00)

1D evolution with partially included 3 wave interaction

- Saturation amplitude of ~ o(0.001), which depends on interaction term (Schenk et al. 2001)

Final fate of r-mode instability

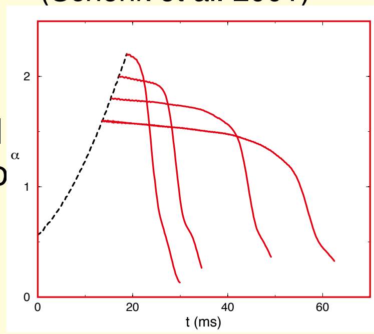

3D simulation

- Evolution starting from the amplitude o(1)
- Imposing large amplitude of radiation reaction potential
- Energy dissipation of r-mode catastrophically decays to differentially rotating configuration in dynamical timescale

1D evolution including mode couplings network

- After reaching the saturation amplitude ~o(0.001), Kolmogorov-type cascade occurs
- Destruction timescale is secular

(Gressman et al. 02, Lin & Suen 06)

Amplitude of r-mode instability (LIGO 10)

- Isolated neutron star in the supernova remnant Cassiopeia A
- Compelling evident that the central compact object is neutron star
- Restriction to the amplitude of the r-mode instability by not detecting gravitational waves

$$\alpha \approx 0.14 - 0.005$$

Possibility of gravitational wave source (Bondarescu et al. 09)

- Possibility of parametric resonance by nonlinear mode-mode interaction
- Amplification to $\alpha \sim 1$

Necessary to obtain a common knowledge for the basic properties of r-mode instability !

2. Newtonian hydrodynamics including radiation reaction

Minimum requirements to go beyond acoustic timescale

- Timescale which cannot be reached by GR hydrodynamics
  ▶ Need to separate the hydrodynamics and the radiation
- Instability driven by gravitational radiation
  ▶ Need to impose gravitational waves

"Newton gravity + gravitational radiation reaction" are at least necessary

Hydrodynamics including radiation reaction force

Including 5th and 6th time derivative in inertial frame in radiation reaction term

$$\frac{\partial \rho}{\partial t} + \nabla_j (\rho \Delta v^j) = 0$$

$$\frac{\partial}{\partial t}[\rho(v^i_{\rm eq} + \Delta v^i)] + \nabla_j[(\rho(v^i_{\rm eq} + \Delta v^i)\Delta v^j + P\delta^{ij}]$$

$$= -\rho\nabla^i\Phi - \rho(v^j_{\rm eq} + \Delta v^j)\nabla_j v^i_{\rm eq} + F^i_{3.5PN}$$

$$\frac{\partial e}{\partial t} + \nabla_j (e\Delta v^j) = 0 \quad e \equiv (\rho\epsilon)^{1/\Gamma}$$ assuming $P = (\Gamma - 1)\rho\epsilon$

Hydrodynamics with radiation reaction

(e.g. Rezzolla et al. 99)

PN expansion

$$\alpha = 1 + \frac{1}{c^2}\phi + \frac{1}{c^4}{}_4\alpha + \frac{1}{c^6}{}_6\alpha + \frac{1}{c^7}{}_7\alpha + \frac{1}{c^8}{}_8\alpha + \frac{1}{c^9}{}_9\alpha + (o^{-10})$$

$$\beta^i = \frac{1}{c^3}\beta + \frac{1}{c^5}{}_4\beta^i + \frac{1}{c^6}{}_6\beta^i + \frac{1}{c^7}{}_7\beta^i + \frac{1}{c^8}{}_8\beta^i + (o^{-9})$$

$$\gamma_{ij} = \delta_{ij}\left(1 - \frac{2}{c^2}\phi\right) + \frac{1}{c^4}{}_4h_{ij} + \frac{1}{c^5}{}_5h_{ij} + \frac{1}{c^6}{}_6h_{ij} + \frac{1}{c^7}{}_7h_{ij} + (o^{-8})$$

3.5PN term : Lowest current quadrupole radiation reaction term

Gauge choice

(Blanchet 97)

$$_9\alpha = 0$$

$$_8\beta^i = \frac{16}{45}\epsilon_{ijk}x_j x_l S^{(5)}_{kl}$$

$$_7h_{ij} = 0$$

$$S_{ij} = \int d^3x\ \epsilon_{kl(i}x_{j)}x_k\rho v_l$$

Reaction Force from current multipole moment

$$F^{3.5\rm PN}_i = \frac{16}{45}\varepsilon G(2v_j\epsilon_{jil}x_m S^{(5)}_{lm} + v_j\epsilon_{jkl}x_k S^{(5)}_{li} - v_j\epsilon_{ikl}x_k S^{(5)}_{lj} - \epsilon_{ikl}x_k x_m S^{(6)}_{lm})$$

amplification factor
for the radiation reaction force

Treatment of Time Derivative in Radiation Reaction Force

Current multipole moment

$$J_{lm} = \int d^3x\ \rho r^l \boldsymbol{v} \cdot \mathbf{Y}^{B*}_{lm}$$

Introduce characteristic frequency

$$\omega_{\rm chr} = -\frac{1}{|J_{22}|}\left|\frac{dJ_{22}}{dt}\right|$$

N.B. time derivative is computed in internal frame

Time derivative of current multipole moment

$$S^{(n)}_{ij} = (i\omega_{\rm chr})^n S^{(0)}_{ij}$$ e.g. $S^{(5)}_{ij} = \omega^4_{\rm chr} S^{(1)}_{ij}$ $S^{(6)}_{ij} = -\omega^6_{\rm chr} S^{(0)}_{ij}$

3. R-mode instability in Linear Regime

Equilibrium configuration of the star

- Slowly rotating neutron star
- Uniformly rotating, n=1 polytropic equation of state

r_p/r_e	T/W
0.975	0.00576

Impose perturbation

Eigenfunction of the velocity

$$\delta \boldsymbol{v} = \alpha \Omega R \left(\frac{r}{R}\right)^l \mathbf{Y}^{(B)}_{ll}$$

Impose eigenfunction type perturbation on the equilibrium velocity to trigger r-mode instability

Characteristic Frequency of R-mode Instability

r-mode frequency
(incompressible star)

$$\omega = \frac{2m}{l(l+1)}\Omega - m\Omega$$

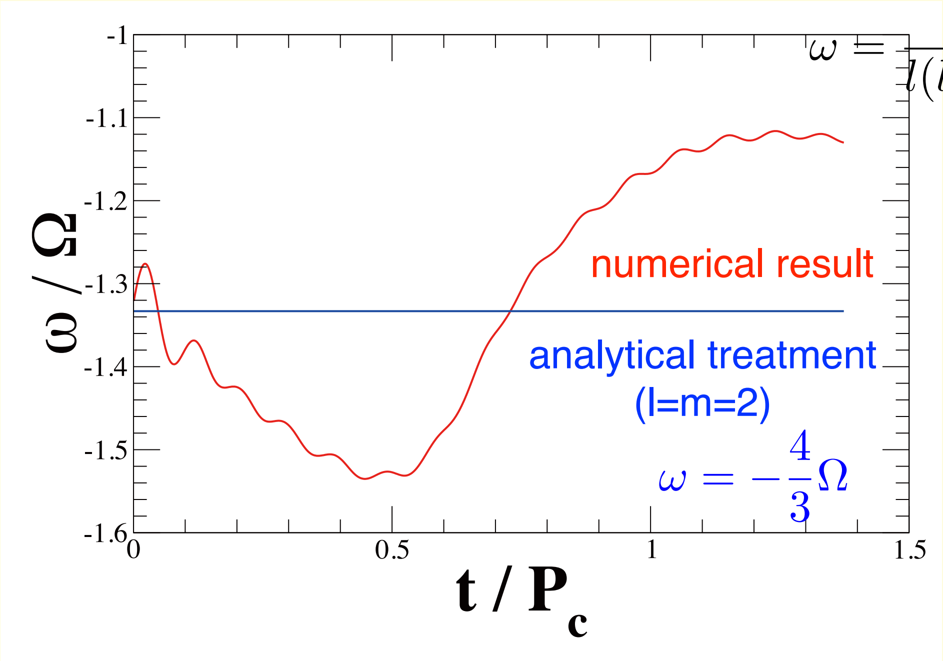

Extracts the dominant part of r-mode instability

Growth Time of R-mode Instability

Amplitude

$$\alpha_2 \equiv \frac{2|J_{22}|}{\tilde{J} M R^3 \Omega_c}$$

Analytic treatment of growth time

$$\frac{1}{\tau_{gw}} = -\frac{dE/dt|_{\rm gw}}{2E} = 2\pi \left(\frac{256}{405}\right)^2 \varepsilon \frac{G}{c^7} \tilde{J} M R^4 \Omega_c^6 \qquad \tilde{J} = \frac{1}{MR^4}\frac{1}{4\pi}\int d^3x\, \rho r^4$$

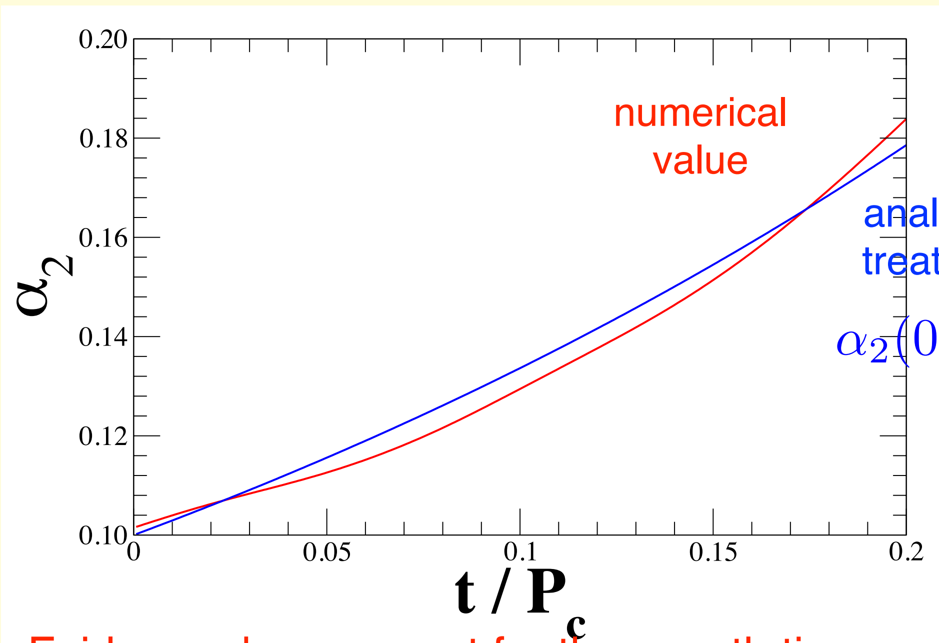

Fairly good agreement for the growth timescale!

4. Saturation Amplitude of R-mode Instability

Initial amplitude dependence

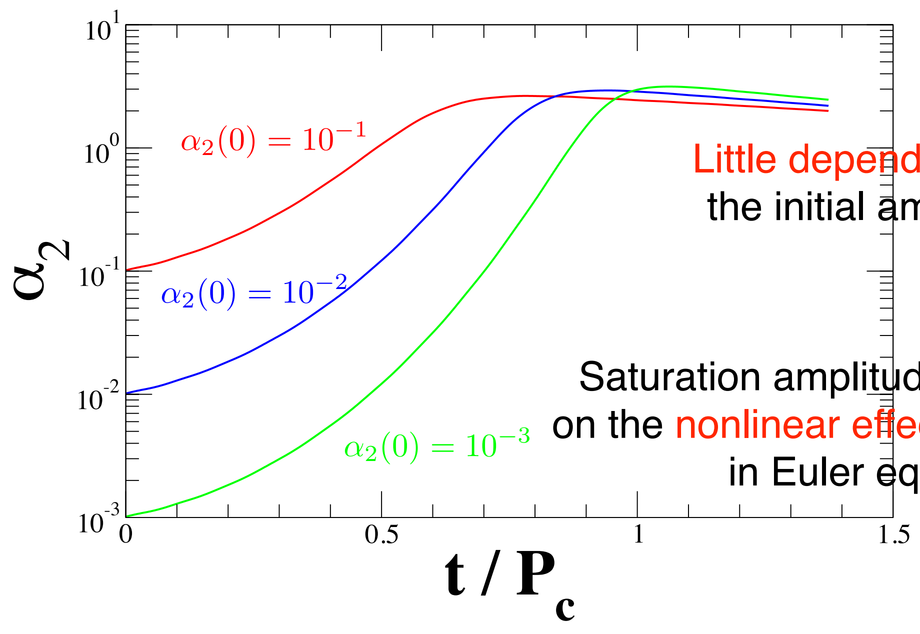

Little dependence on the initial amplitude

Saturation amplitude may depend on the nonlinear effect of the velocity in Euler equation

Amplification factor dependence

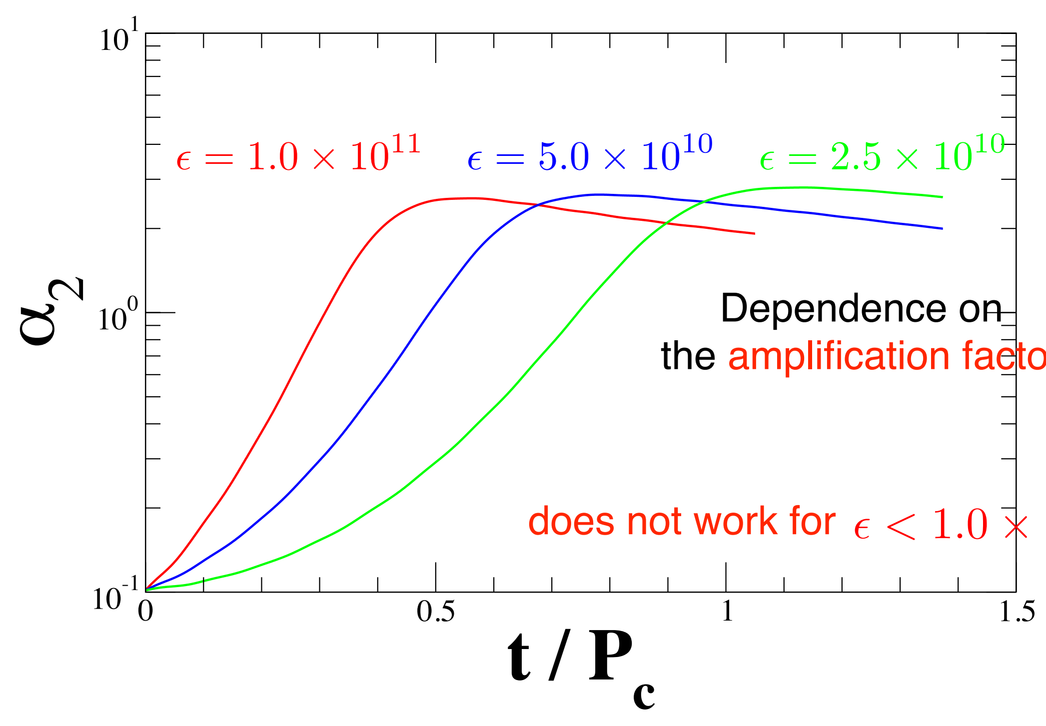

Dependence on the amplification factor

does not work for $\epsilon < 1.0 \times 10^{10}$

Rough Explanation of Saturation Amplitude

Assuming that the Euler equation takes the dominant contribution

$$\frac{\partial}{\partial t}[\rho(v^i_{\rm eq}+\Delta v^i)]+\nabla_j[(\rho(v^i_{\rm eq}+\Delta v^i)\Delta v^j+P\delta^{ij}]$$
$$=-\rho\nabla^i\Phi-\rho(v^j_{\rm eq}+\Delta v^j)\nabla_j v^i_{\rm eq}+F^i_{3.5PN}$$

For simplicity

$$\frac{d}{dt}(\rho\Delta v^i)\approx \text{(RR Force)} - \text{(Coriolis Force)}(\rho\Delta v^i)^1 - \text{(Advection)}(\rho\Delta v^i)^2$$

Neglecting advection term

$$(\rho\Delta v^i)\approx\frac{\text{(RR Force)}}{\text{(Coriolis Force)}}(e^{\gamma t}-1)$$ γ: growth timescale (RR Force)

- No dependence on initial amplitude
- Dependence on the amplitude of RR force
- Wider range survey of the amplitude of RR force may be needed

5. Summary

We investigate the r-mode instability of a uniformly rotating star by means of three dimensional hydrodynamical simulations in Newtonian gravity including radiation reaction

- We have succeeded in reproducing the features of r-mode instability in linear regime
- We have succeeded in extracting the saturation amplitude with help of amplification factor, which does not significantly depend on initial amplitude
- Longer evolution (low amplification factor) with help of anelastic approximation is needed
- Application to rapidly rotating (relativistic) stars

“Cosmological Upper-Bound for f(R) Gravity through Redshift-Space Distortion”

by Akira Oka

[JGRG23(2013)110612]

JGRG 23 @ Hirosaki University

Cosmological Upper-Bound for f(R) Gravity through Redshift-Space Distortion

- Akira OKA (Univ. of Tokyo)
- Atsushi Taruya (YITP, Kyoto Univ.)
- Takashi Hiramatsu (YITP, Kyoto Univ.)
- Kazuya Koyama (Portsmouth Univ.)
- Kazuhiro Yamamoto (Hiroshima Univ.)
- Takahiro Nishimichi (IAP)

Motivation

What is the Origin of ' Cosmic Acceleration ' ... ?

✓ General Relativity (GR) + Dark Energy ?

✓ Modified Gravity (MG) ?

→ Constraining (Hopefully detecting/disproving) MG on the basis of observational data is in demand

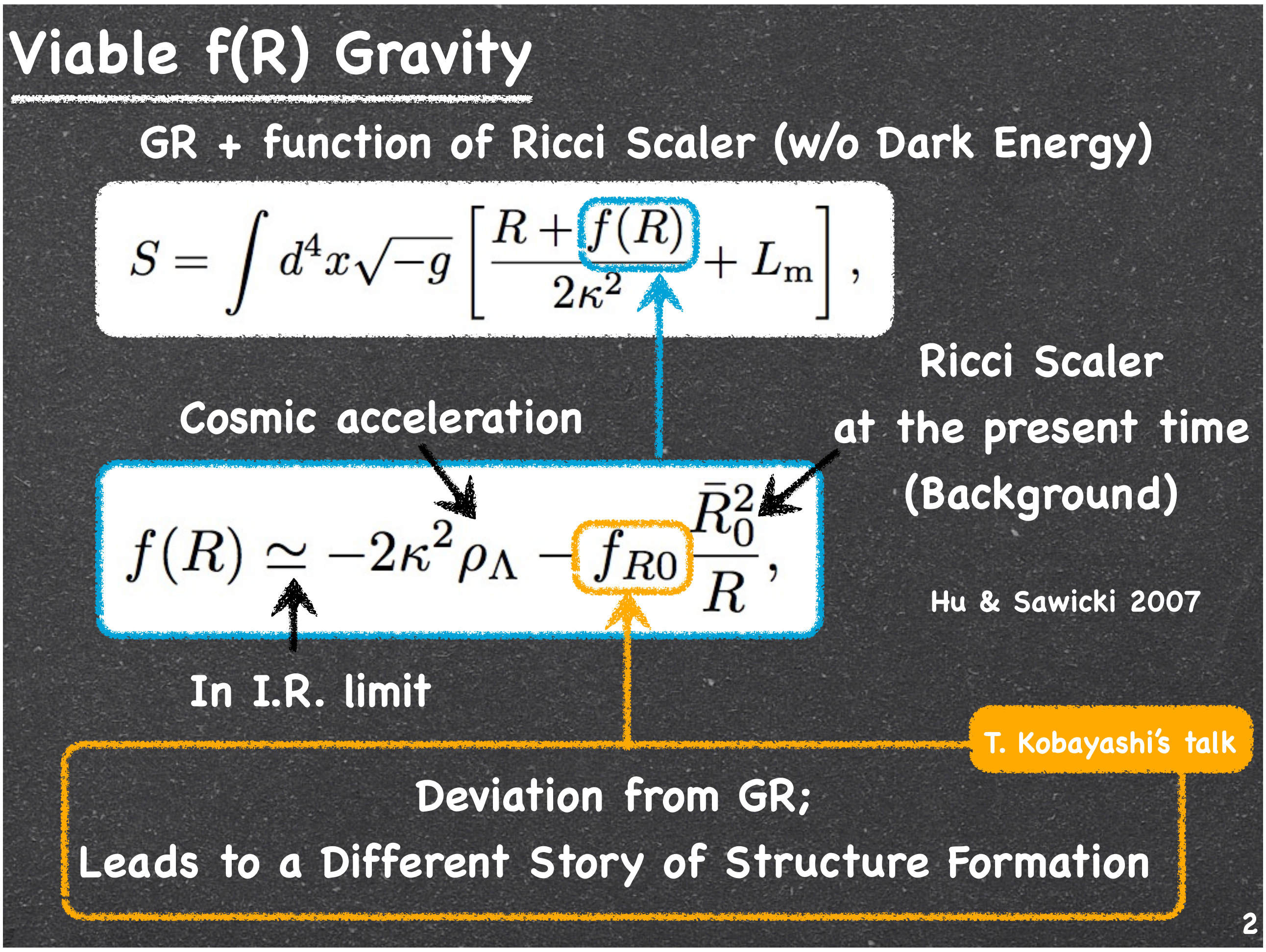
Viable f(R) Gravity
GR + function of Ricci Scaler (w/o Dark Energy)
$$S = \int d^4x\sqrt{-g}\left[\frac{R+\boxed{f(R)}}{2\kappa^2} + L_m\right],$$
Cosmic acceleration
Ricci Scaler
at the present time
(Background)
$$f(R) \simeq -2\kappa^2\rho_\Lambda - \boxed{f_{R0}}\frac{\bar{R}_0^2}{R},$$
Hu & Sawicki 2007
In I.R. limit
T. Kobayashi's talk
Deviation from GR;
Leads to a Different Story of Structure Formation
2

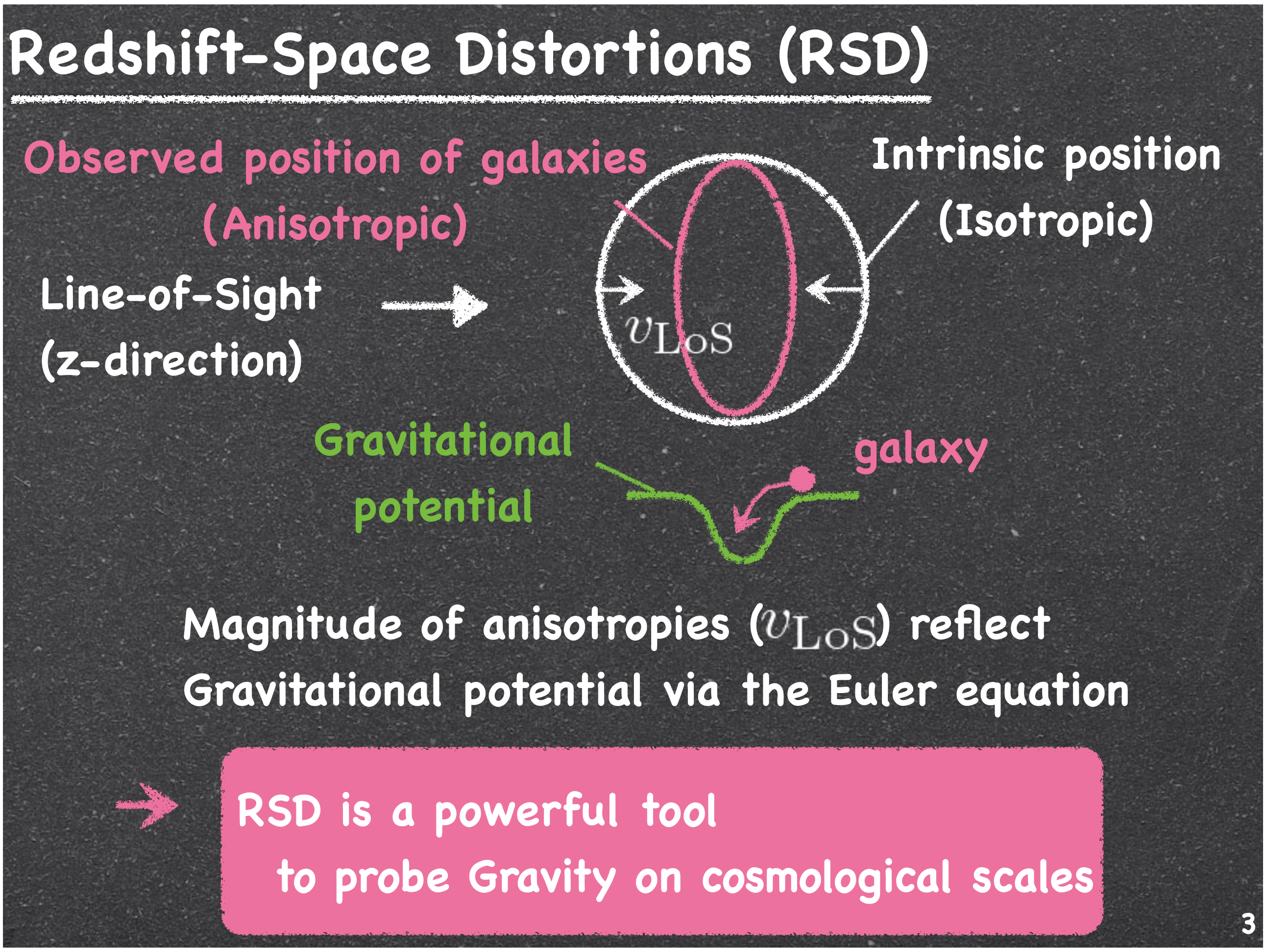
Redshift-Space Distortions (RSD)
Observed position of galaxies
(Anisotropic)
Intrinsic position
(Isotropic)
Line-of-Sight
(z-direction)
$v_{\rm LoS}$
Gravitational
potential
galaxy
Magnitude of anisotropies ($v_{\rm LoS}$) reflect
Gravitational potential via the Euler equation
RSD is a powerful tool
to probe Gravity on cosmological scales
3

Anisotropic Power Spectra; Sensitivity to f_{R0}

Anisotropies are characterized with the coefficient of the Legendre expansion

$$P(k,\mu) = \sum P_0(k)L_0(\mu) + P_2(k)L_2(\mu) + \cdots$$

$\mu = k_z/k$

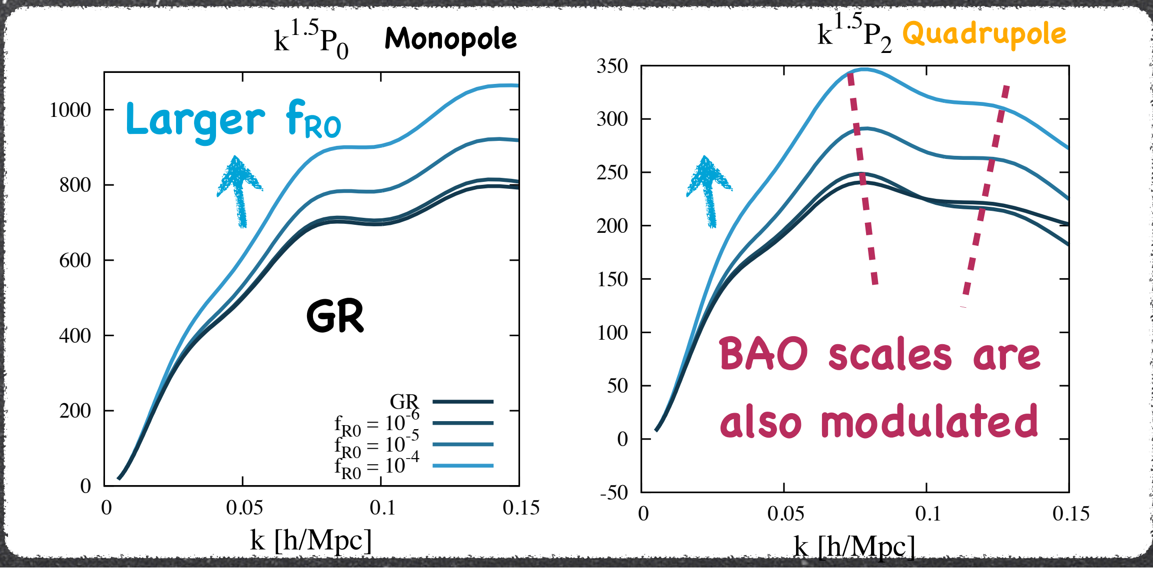

4

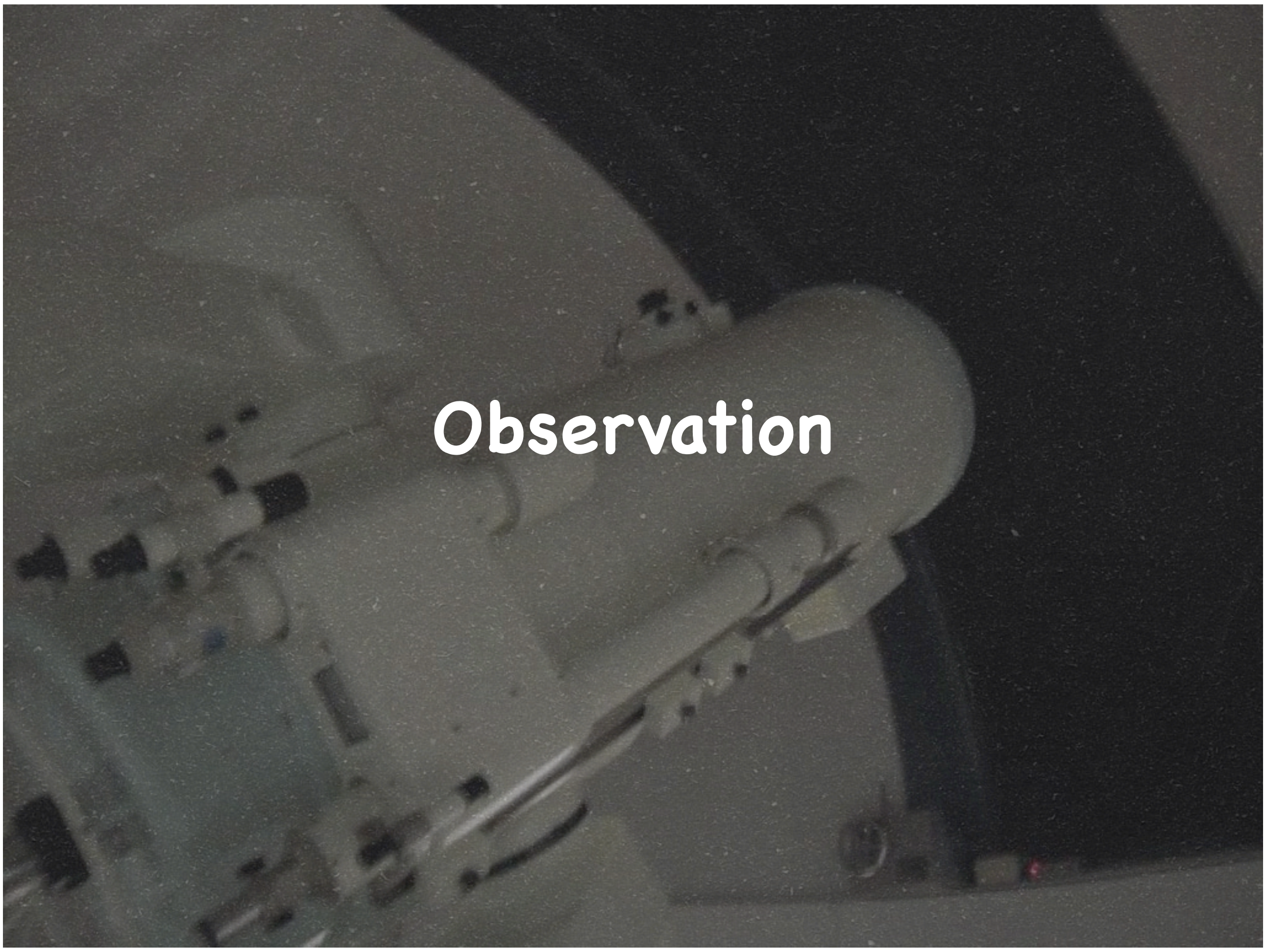

7

SDSS Luminous Red Galaxy Sample

✓ Sloan Digital Sky Survey (SDSS)

- Photometry & Spectroscopy
- Survey Volume ~ 1 [Gpc^3/h^3]

✓ Luminous Red Galaxy (LRG)

- Selected by color (red and bright)
- Observed out to z ~ 0.5
- Number density n ~ 0.0001 [Mpc^{-3}/h^{-3}] (0.16 < z < 0.36)

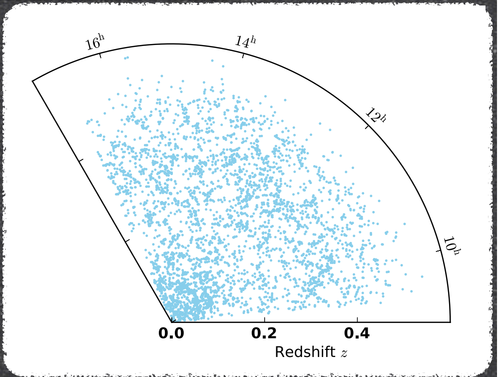

✓ LRGs have been widely used in cosmological context

Eisenstein+ 2005, Wake+ 2006, Percival+ 2007
Reid+ 2010, White+ 2011, AO, S.Saito,TN, AT, KY 2013 ... etc.

In this work,
Multipole of Anisotropic Power Spectra (P_0,P_2) of the SDSS LRGs
↓
Constraints on f_{R0}

5

Anisotropic Power Spectra of SDSS LRGs

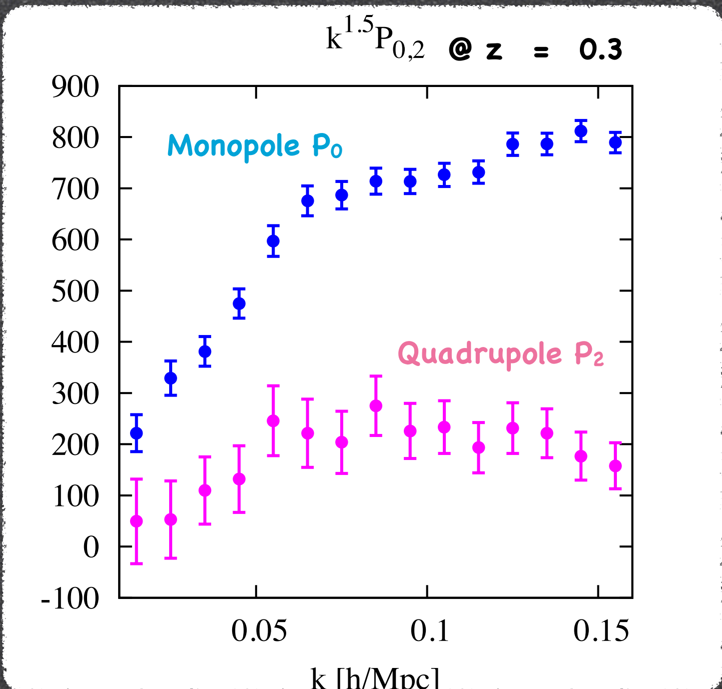

We adopt a flat LCDM model with (Ω_m,h) = (0.32,0.67) when we convert the redshift into distance KY+ 2010

6

Modeling Anisotropic Power Spectra

1. Compute ‘ Matter ’ Power Spectrum in Real Space

2. Map it onto Redshift Space (RSD)

3. Convert ‘ Matter ’ into ‘ Galaxy ’ (galaxy bias)

→ Theoretical template for ‘ Galaxy ’ P_0, P_2

7

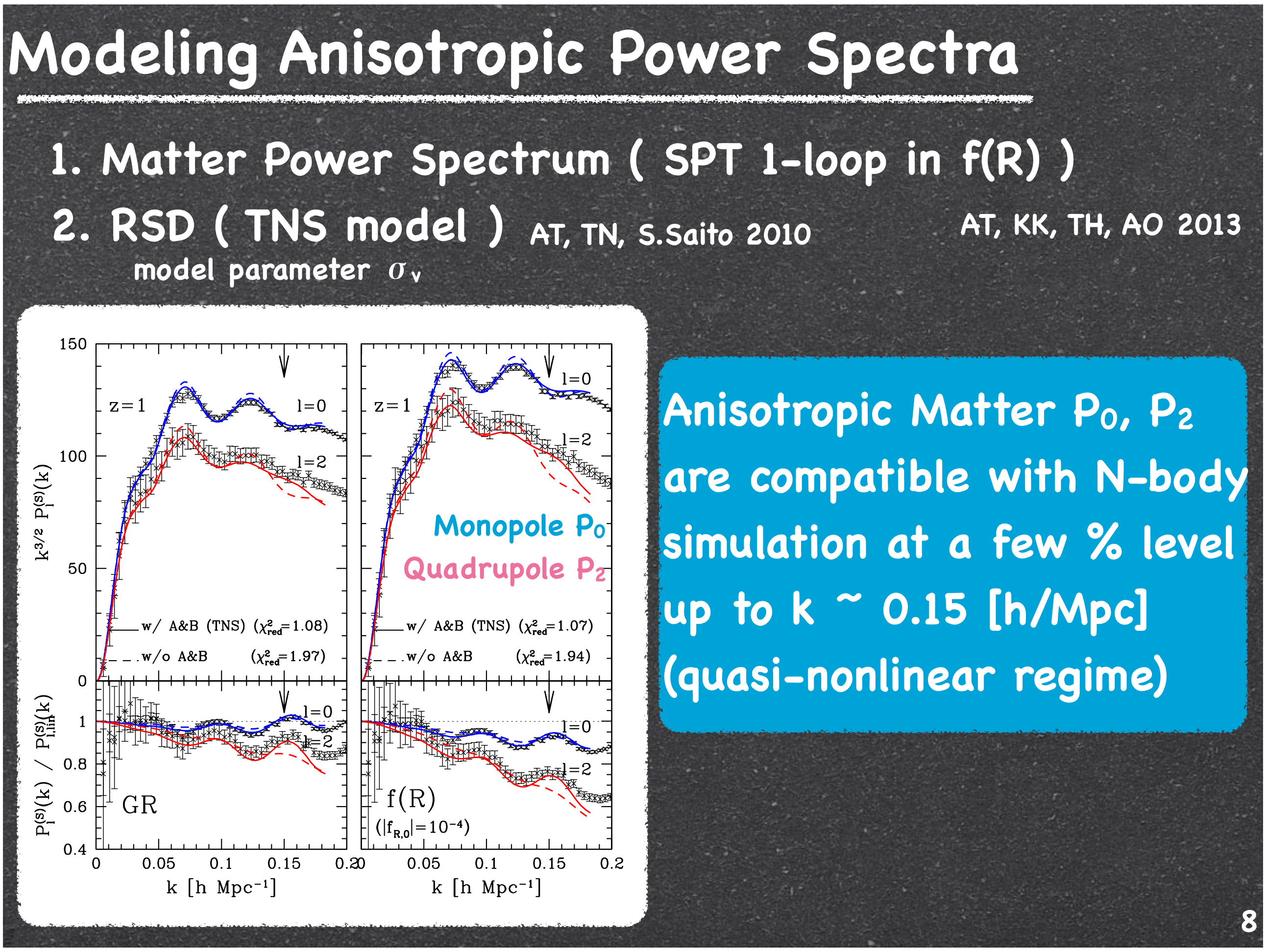
Modeling Anisotropic Power Spectra
1. Matter Power Spectrum (SPT 1-loop in f(R))
2. RSD (TNS model) AT, TN, S.Saito 2010
AT, KK, TH, AO 2013
model parameter σv
z=1
l=0
l=2
Monopole P0
Quadrupole P2
w/ A&B (TNS) (χ²red=1.08)
w/o A&B (χ²red=1.97)
w/ A&B (TNS) (χ²red=1.07)
w/o A&B (χ²red=1.94)
GR
f(R)
(|fR,0|=10⁻⁴)
k [h Mpc⁻¹]
Anisotropic Matter P0, P2 are compatible with N-body simulation at a few % level up to k ~ 0.15 [h/Mpc] (quasi-nonlinear regime)
8

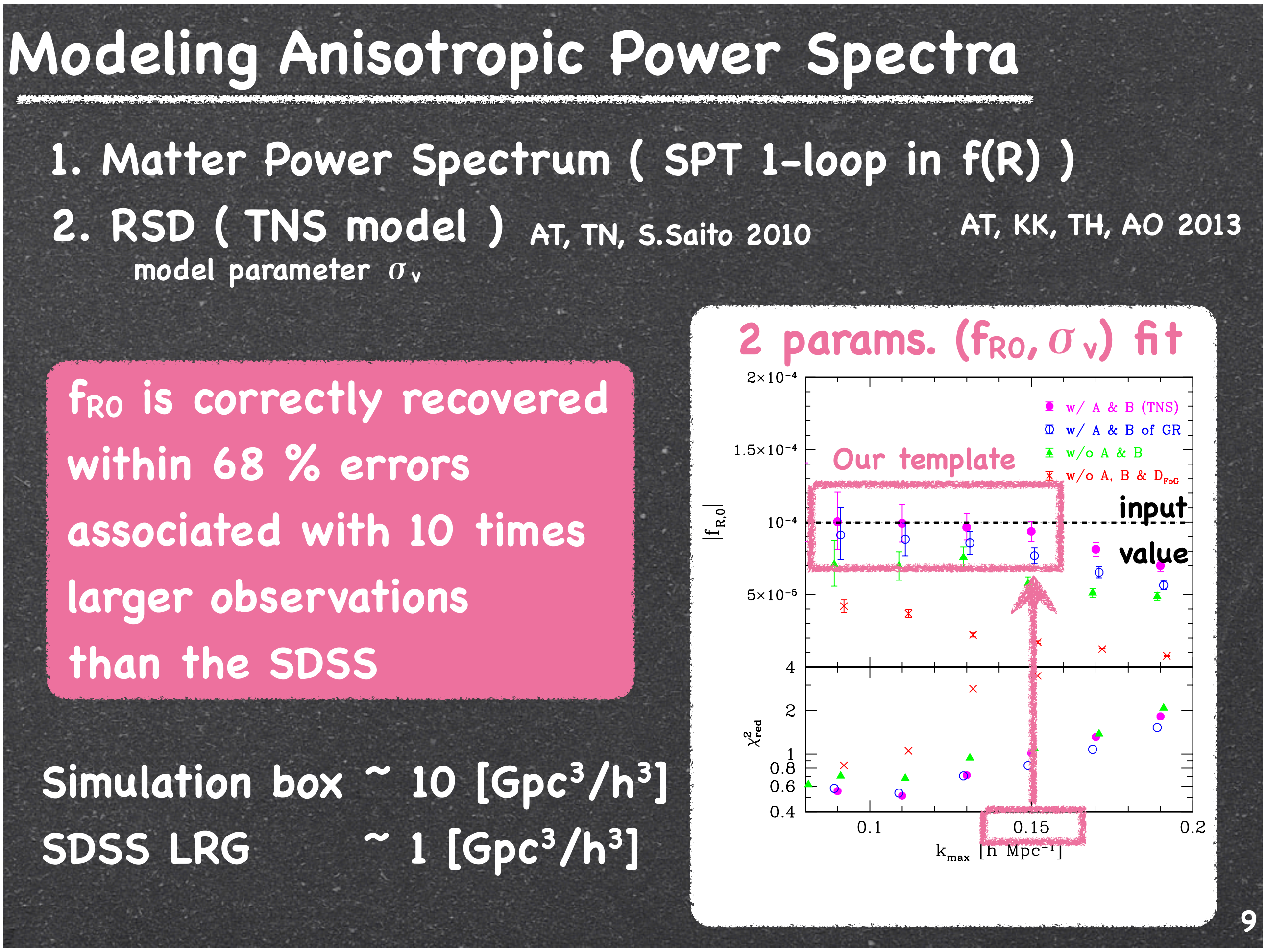
Modeling Anisotropic Power Spectra
1. Matter Power Spectrum (SPT 1-loop in f(R))
2. RSD (TNS model) AT, TN, S.Saito 2010
AT, KK, TH, AO 2013
model parameter σv
fR0 is correctly recovered within 68 % errors associated with 10 times larger observations than the SDSS
Simulation box ~ 10 [Gpc³/h³]
SDSS LRG ~ 1 [Gpc³/h³]
2 params. (fR0, σv) fit
w/ A & B (TNS)
w/ A & B of GR
w/o A & B
w/o A, B & DFoG
Our template
input value
|fR,0|
χ²red
kmax [h Mpc⁻¹]
9

Modeling Anisotropic Power Spectra

1. Matter Power Spectrum (SPT 1-loop in f(R))
2. RSD (TNS model) AT, TN, S.Saito 2010 AT, KK, TH, AO 2013
3. Galaxy bias (Scale-dependent Linear bias)

c.f. AO+ 2013

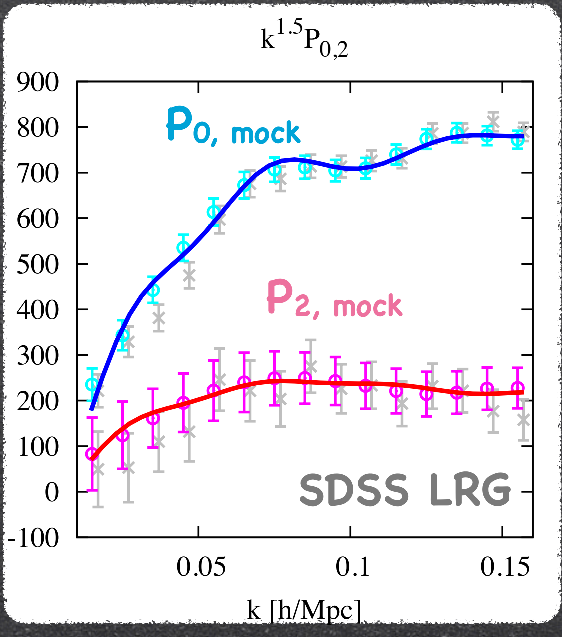

Empirical model

$$\delta_g(k) = \boxed{b(k)}\,\delta_m$$

$$b(k) = b_0 \frac{1 + A_2 k^2}{1 + A_1 k}$$

TN and AO 2013

Modeling Anisotropic Power Spectra

1. Matter Power Spectrum (SPT 1-loop in f(R))
2. RSD (TNS model) AT, TN, S.Saito 2010 AT, KK, TH, AO 2013
3. Galaxy bias (Scale-dependent Linear bias)

c.f. AO+ 2013

5 params. ($f, \sigma_v, b_0, A_1, A_2$) fit

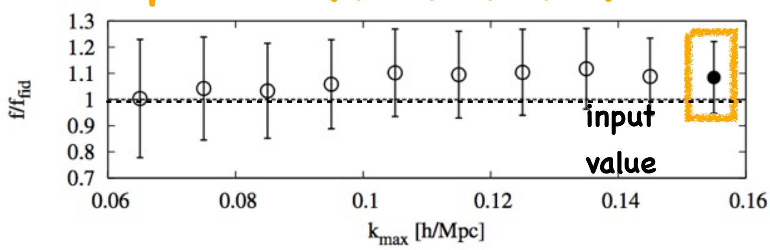

The growth rate f is correctly recovered within 68 % errors associated with the SDSS

Setup for MCMC fitting

- ✓ Matter Power Spectrum (SPT 1-loop in f(R))
  AT, KK, TH, AO 2013
- ✓ RSD (TNS model) AT, TN, S.Saito 2010
  model parameter σ_v
- ✓ Galaxy bias (Scale-dependent Linear bias) c.f. AO+ 2013
  $b(k) = b_0 (1 + A_2 k^2) / (1 + A_1 k)$
- ✓ # of data points : 15*2 (Monopole, Quadrupole)
  corresponding to k_{max} = 0.155 [h/Mpc]
- ✓ 5 parameters : f_{R0}, σ_v, b_0, A_1, A_2

$$\chi^2 \equiv \sum_{\ell=0,2} \sum_{i=1}^{15} \left[\frac{P_\ell(k_i) - P_\ell^{\rm theory}(k_i)}{\Delta P_\ell(k_i)} \right]^2$$

12

fitting Result

13

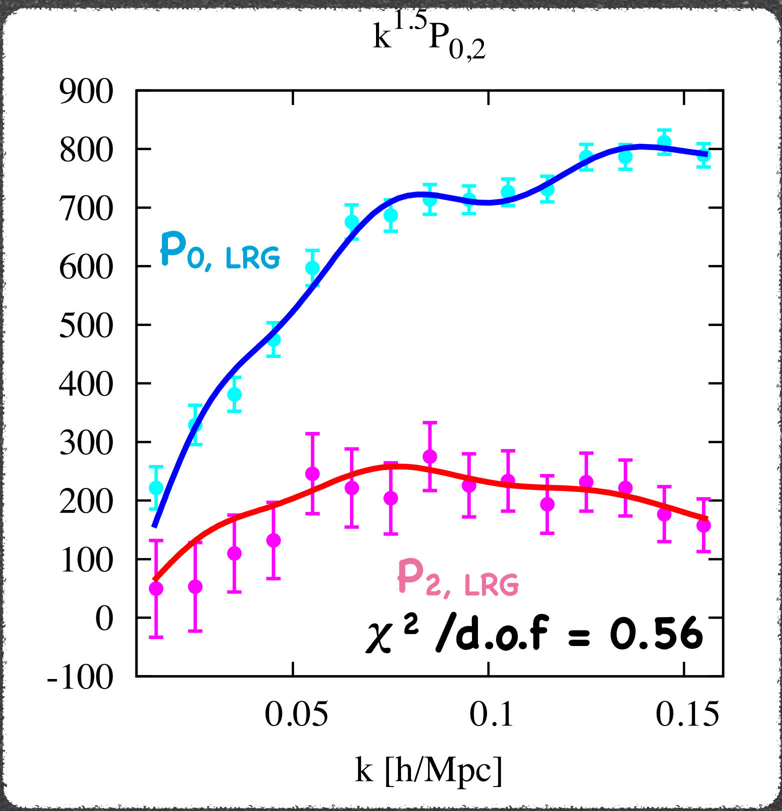

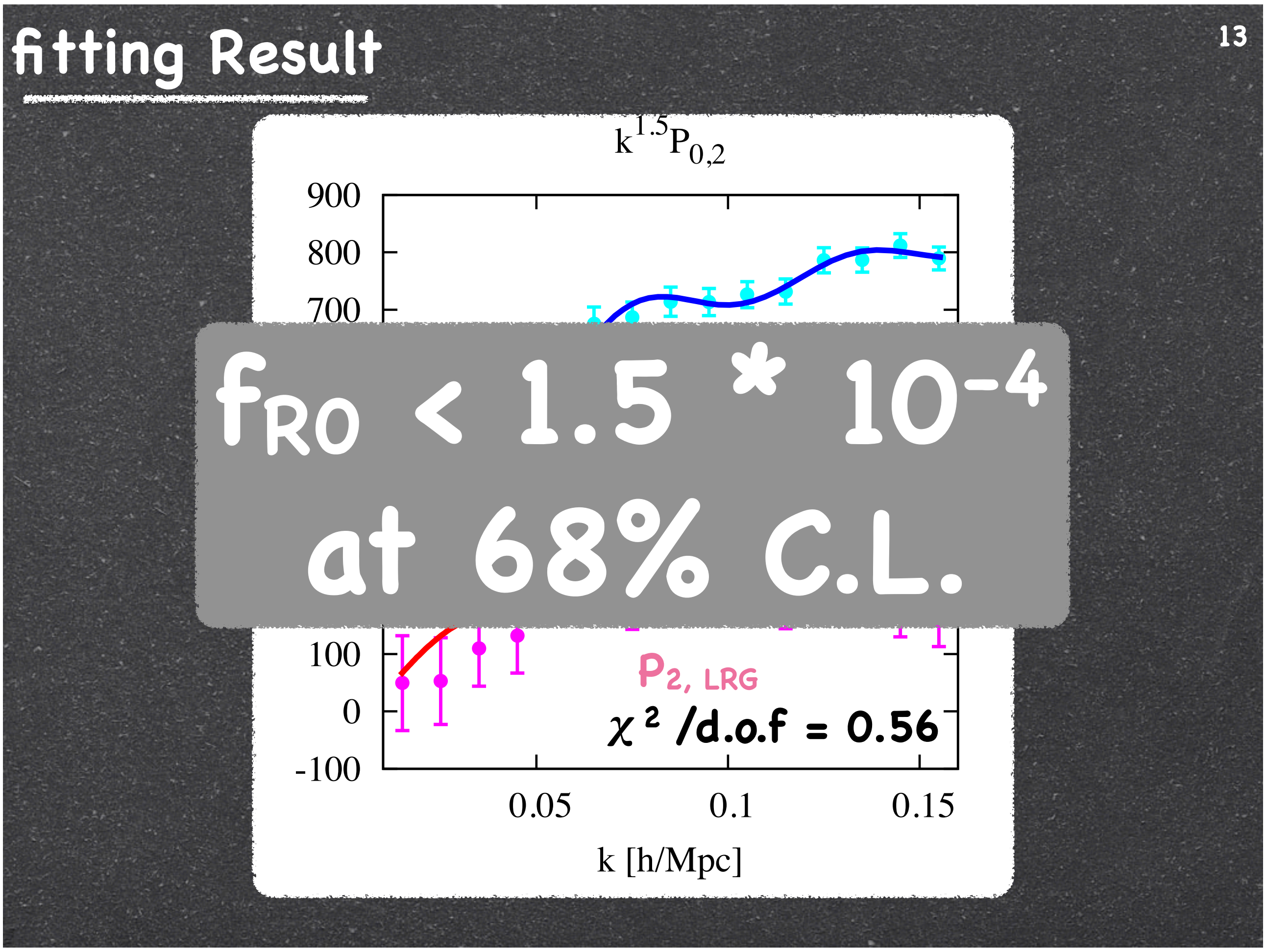

fitting Result
13
k^1.5 P_0,2
900
800
700
100
0
-100
0.05
0.1
0.15
k [h/Mpc]
P2, LRG
χ² /d.o.f = 0.56
fR0 < 1.5 * 10^-4
at 68% C.L.

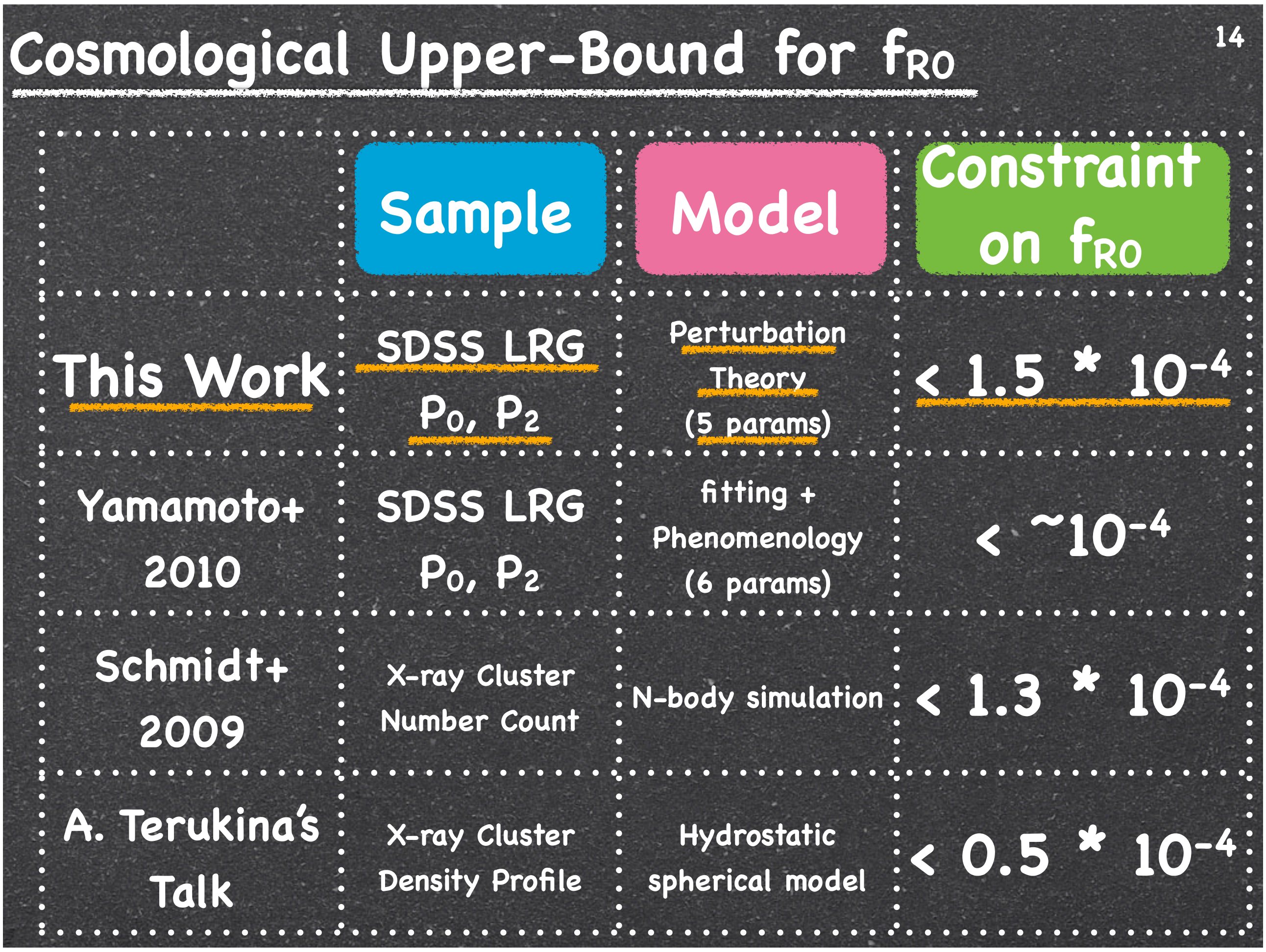

Cosmological Upper-Bound for fR0
14
Sample
Model
Constraint on fR0
This Work
SDSS LRG P0, P2
Perturbation Theory (5 params)
< 1.5 * 10^-4
Yamamoto+ 2010
SDSS LRG P0, P2
fitting + Phenomenology (6 params)
< ~10^-4
Schmidt+ 2009
X-ray Cluster Number Count
N-body simulation
< 1.3 * 10^-4
A. Terukina's Talk
X-ray Cluster Density Profile
Hydrostatic spherical model
< 0.5 * 10^-4

Summary & Prospects

What we did

- ✓ Sample : SDSS LRG (P_0,P_2) @ $z = 0.3$
- ✓ Model : Perturbation Theory

→ $f_{R0} < 1.5*10^{-4}$

What we will do

- ✓ Simultaneous Constraints on Cosmic Expansion & f_{R0}
- ✓ With More General Gravity Model
- ✓ With More Refined Galaxy Samples; SDSS-III BOSS, Subaru PFS (Upcoming) … etc

15

“Testing the cosmic censorship conjecture with observations”

by Lingyao Kong

[JGRG23(2013)110613]

Testing the weak cosmic censorship conjecture with observations

Lingyao Kong

Fudan University

JGRG23, 6 Nov. 2013

This talk is based on a work with Cosimo and Daniele Malafarina.
[1]. arXiv:1310.8376
[2]. arXiv:1310.1320

Motivation

- Naked singularity
  - Quantum gravity phenomena in high curvature region
  - Strong gravity
  - New physics...
- Distinguish Naked Singularity from Black Hole by observations
- Radiation emitted from astrophysical collapsing

Introduction

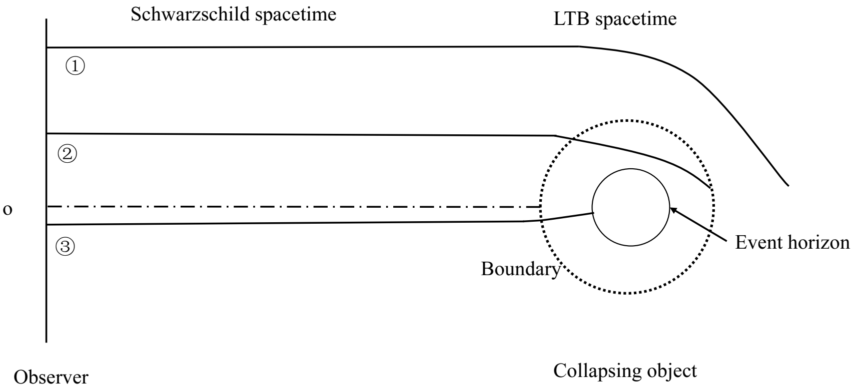

Solution Exterior: Geodesics in Schwarzschild Spacetime

$$ds^2 = -\left(1 - \frac{2M}{R}\right) dT^2 + \left(1 - \frac{2M}{R}\right)^{-1} dR^2 + R^2 d\phi^2$$

$$E = \left(1 - \frac{2M}{R}\right) \dot{T} = 1$$

and

$$L = R^2 \dot{\phi} = b$$

are conserved along geodesics

$$\left(\frac{dR}{dT}\right)^2 = \left(1 - \frac{2M}{R}\right)^2 - \left(1 - \frac{2M}{R}\right)^3 \frac{L^2}{R^2} \frac{1}{E^2} \tag{1}$$

Solution Interior: Dust LTB Model

A sphere Dust LTB model with pressure is 0.

$$ds^2 = -dt^2 + \rho'^2 dr^2 + \rho^2 d\Omega^2$$

$$\frac{d\rho}{dt} = \sqrt{\frac{F}{\rho}}$$

Homogeneous case

$$F(r,t) = r^3 M_0$$

$$\rho(r,t) = r\left(1 - \frac{3}{2}\sqrt{M_0}\,t\right)^{\frac{2}{3}}$$

M2 inhomogeneous case

$$F(r,t) = r^3 M_0 + r^5 M_2$$

$$\rho(r,t) = r\left(1 - \frac{3}{2}\sqrt{M_0 + r^2 M_2}\,t\right)^{\frac{2}{3}}$$

where, $M_0 > 0$, $M_2 < 0$

Solution Interior: Dust LTB Model

singularity: $\rho(r, t_s) = 0$
apparent horizon:
$\rho(r, t_{ah}) = F(r)$

$$t_{ah} = t_s - \frac{2}{3}F(r)$$

event horizon:
$\rho(r_b, t_{eh}) = F(r_b) = 2M$

$$t_{eh} = t_{ah}(r_b)$$

Homogeneous case

$$t_s(r) = \frac{2}{3\sqrt{M_0}}$$

M2 inhomogeneous case

$$t_s(r) = \frac{2}{3\sqrt{M_0 + r^2 M_2}}$$

Solution Interior: Dust LTB Model

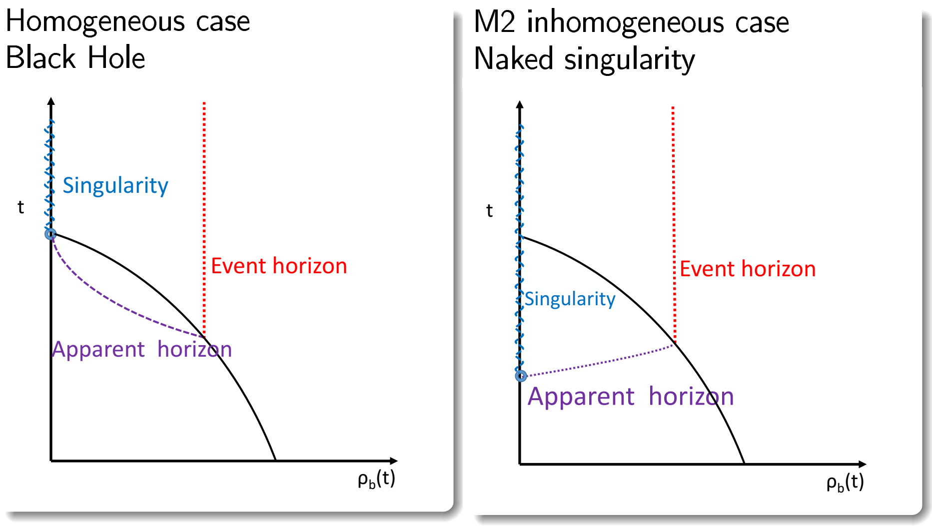

Matching the Metric on the boundary

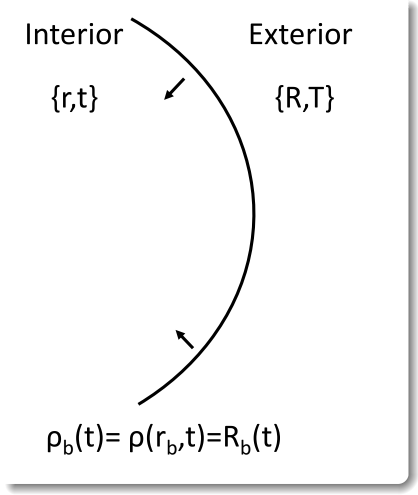

$$\frac{dt}{dT} = 1 - \frac{2M}{R_b} \tag{2}$$

$$\frac{dR_b}{dT} = -\sqrt{\frac{2M}{R_b}}\left(1 - \frac{2M}{R_b}\right) \tag{3}$$

$$\frac{dt}{d\tau} = \frac{dT}{d\tau} + \frac{1}{C\,(R)}\sqrt{\frac{2M}{R}}\frac{dR}{d\tau} \tag{4}$$

$$\frac{dr}{d\tau} = \frac{1}{\rho'}\sqrt{\left(\frac{dt}{d\tau}\right)^2 - \frac{L^2}{R_b^2}} \tag{5}$$

Luminosity

$$I\,(T,\nu_{\rm obs}) = \int 2\pi b^2 db \int_\gamma g^3 j dl \qquad (6)$$

$$g = \frac{\nu_{\rm obs}}{\nu_e} = \frac{k_\mu v^\mu_{\rm obs}}{k_\nu v^\nu_e} = \frac{E}{\frac{dt}{d\lambda}}$$

$$dl = \sqrt{{}^3g_{ij}\frac{dx^i}{d\tau}\frac{dx^j}{d\tau}}d\tau = dt$$

delta function emissivity

$$j = \varepsilon^2\delta\,(\nu_e - \nu_\star)$$

exp function emissivity

$$j = \varepsilon^2\nu_e^2 \exp\left(-\frac{\nu_e}{\varepsilon^{1/4}}\right)$$

Result: Luminosity

delta function emissivity

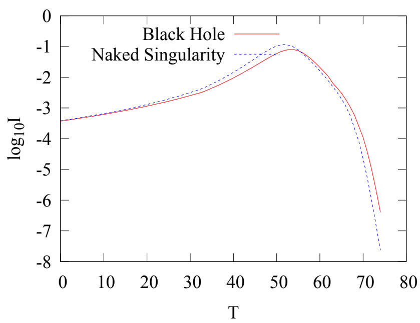

exp function emissivity

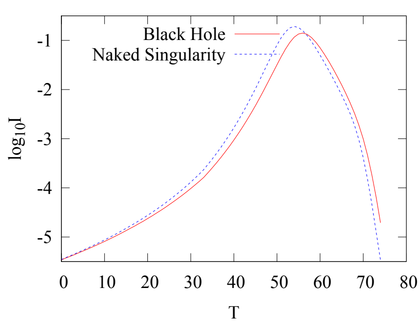

Gravitational blueshift: Spectrum for delta emissivity

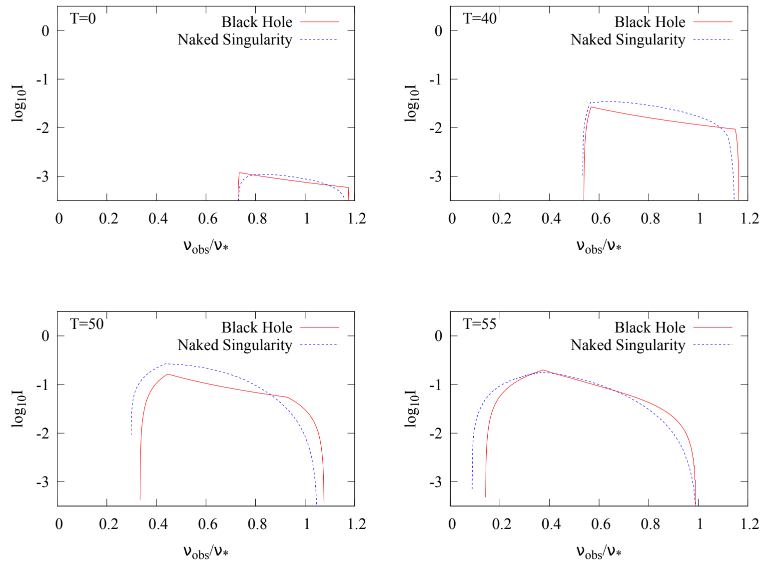

Summary

We use a toy model to calculate the observation of the gravitational collapsing which can birth a black hole or a naked singularity.

- We can not distinguish them.
  - When Naked Singularity forms, the region is too small and the time before event horizon forms is too short.
- Observational tests of the cosmic censorship conjecture may be very difficult.

More realistic model ...

Thanks!

“Microlensed image centroid motions by an exotic lens object with negative convergence or negative mass”

by Takao Kitamura

[JGRG23(2013)110614]

Microlensed image centroid motions by an exotic lens object

Takao Kitamura(Hirosaki Univ.)

with Koji Izumi, Koki Nakajima, Chisaki Hagiwara, and Hideki Asada

TK et al.

arXiv:1307.6637 [gr-qc]

Contents

- Motivation
- Gravitational lensing
  - Amplification
  - Image centroid
- Summary & Future work

- Motivation
- Gravitational lensing
  - Amplification
  - Image centroid
- Summary & Future work

Accelerating universe → Dark energy

※S. Perlmutter, Brian P. Schmidt, et al.
Norbel prize in physics 2011

Galaxy formation and evolution → Dark matter

Exotic energy and matter may exist somewhere whole our universe.

Theoretical interest

H. Bondi, Rev. Mod. Phys. (1957)

Exotic energy and exotic matter

These have not been found yet

We consider gravity by the exotic object
to probe those

References

[F. Abe, Astrophys. J. 725, 787 (2010).]

[Y. Toki, TK, H. Asada, and F. Abe, Astrophys. J. 740, 121 (2011).]

[N. Tsukamoto, and T. Harada, Phys. Rev. D 87, 024024 (2013).]

[N. Tsukamoto, T. Harada, K. Yajima, Phys. Rev. D 86, 104062 (2012).]

[K. Nakajima, and H. Asada, Phys. Rev. D 85, 107501 (2012).]

[K. Izumi, C. Hagiwara, K. Nakajima, TK, and H. Asada, to be published in Phys.Rev. D(2013)]

[TK, K. Nakajima, and H. Asada, Phys. Rev. D 87, 027501 (2013).]

[R. Takahashi, and H. Asada, Astrophys. J. 768, L16 (2013).]

- Motivation
- Gravitational lensing
  - Amplification
  - Image centroid
- Summary & Future work

Configuration 1

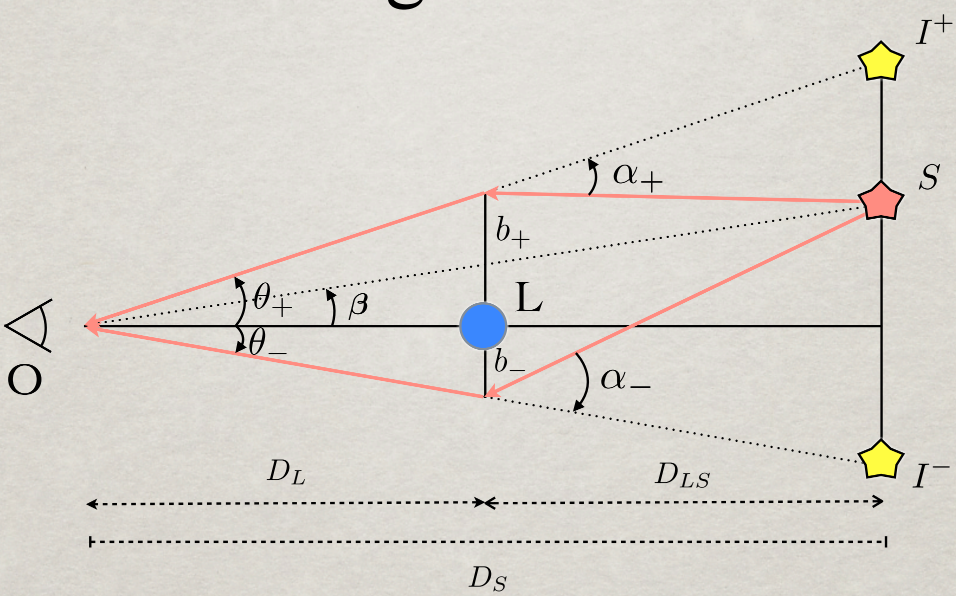

Lens equation

$$\beta = \theta_\pm - \frac{D_{LS}}{D_S}\alpha_\pm$$

Configuration 2

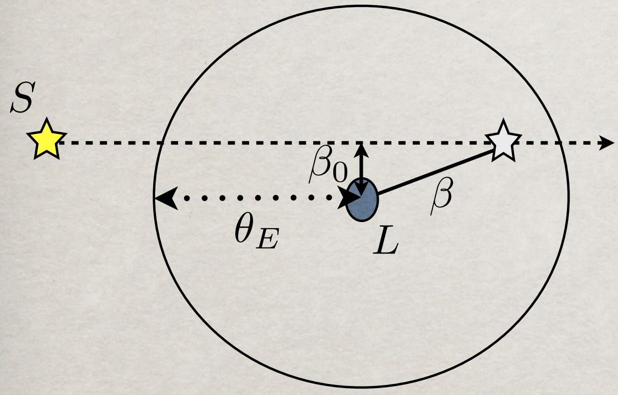

β_0 : distance of the closest approach

β : distance between the lens object and the source object

θ_E : Einstein ring radius

$$\frac{\theta_E}{v} = 1$$

v : the velocity of the source

- Motivation
- Gravitational lensing
  - **Amplification**
  - Image centroid
- Summary & Future work

Gravitational microlensing

$$\text{Amplification} = \frac{\text{Brightness of images}}{\text{Brightness of the source}}$$

$$A_{\pm} = \left| \frac{\theta_{\pm} d\theta_{\pm}}{\beta d\beta} \right| \Rightarrow$$

Total amplification

$$\boxed{A_{tot} = A_{+} + A_{-}}$$

We observe time variation of amplification ⇒ Light curve

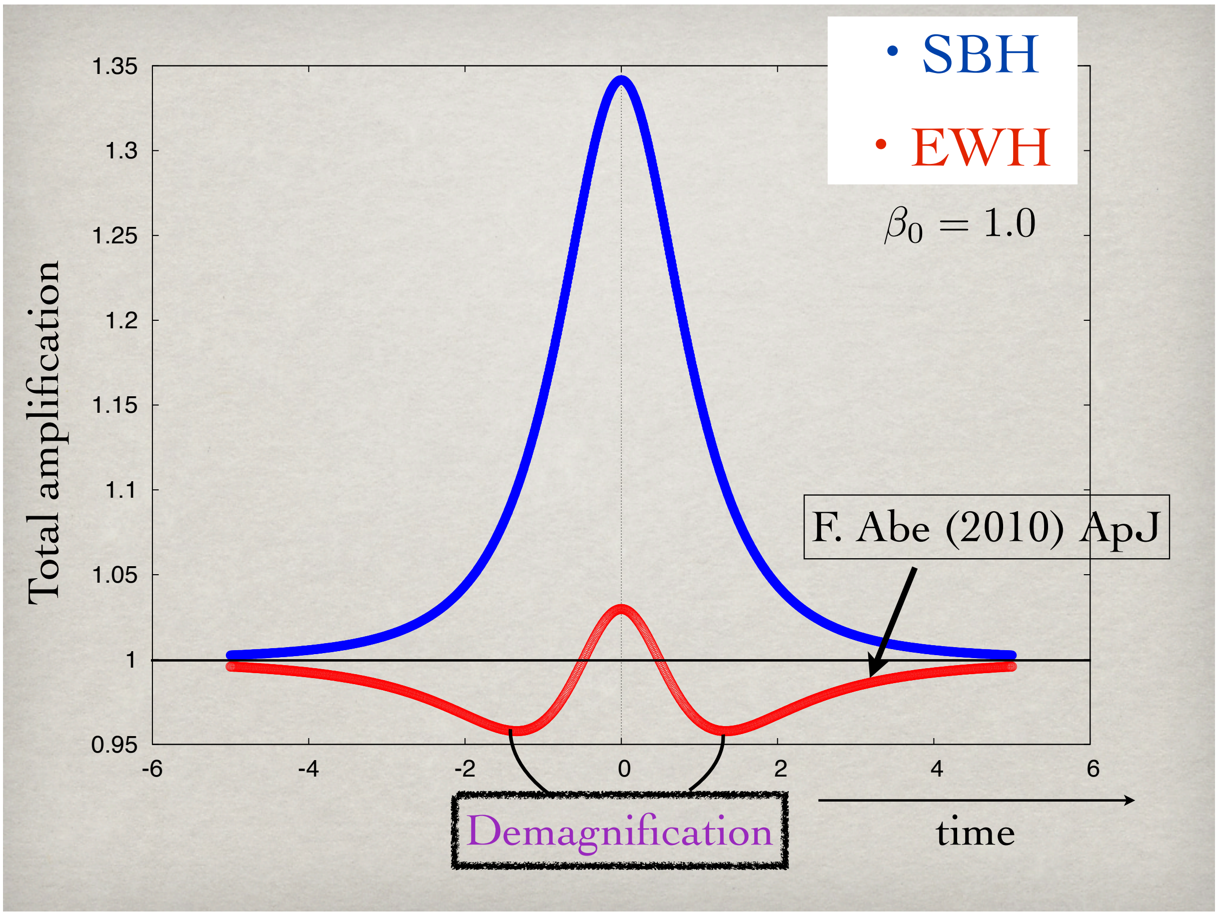

Convergence "κ"

(Surface mass density projected onto the lens plane)

In the Schwarzschild case...

$$\kappa = 0 \quad \text{(Vacuum solution)}$$

In the Ellis wormhole case...

$$\kappa = \frac{-a^2}{2b^2} \quad \text{(negative convergence)}$$

Ellis wormhole is one of exotic objects.

Modified space-time

$$ds^2 = -(1 - \frac{\varepsilon_1}{r^n})dt^2 + (1 + \frac{\varepsilon_2}{r^n})dr^2 + r^2(d\theta^2 + \sin^2\theta d\phi)$$

spherical symmetric

$$(\left|\frac{\varepsilon_1}{r^n}\right| \& \left|\frac{\varepsilon_2}{r^n}\right| \ll 1,)$$

asymptotically flat

TK et al. (2013) PRD

static

$$\alpha = \frac{\bar{\varepsilon}}{b^n}$$

$\bar{\varepsilon} = \text{(positive constant)} \cdot (n\varepsilon_1 + \varepsilon_2)$

N.Tsukamoto, T. Harada. (2013) PRD

TK et al. (2013) PRD

Convergence

$$\kappa(b) = \frac{\bar{\varepsilon}(1-n)}{2}\frac{1}{b^{n+1}}$$

$\kappa > 0$	$\varepsilon > 0 \,\&\, n < 1$
	$\varepsilon < 0 \,\&\, n > 1$
$\kappa = 0$	$n = 1$
$\kappa < 0$	$\varepsilon > 0 \,\&\, n > 1$
	$\varepsilon < 0 \,\&\, n < 1$

The modified space-time includes many models in the weak field.

Modified Lens Equation

$$\beta = \theta - \frac{1}{\theta^n} \qquad (\theta > 0)$$

$$\beta = \theta + \frac{1}{(-\theta)^n} \qquad (\theta < 0)$$

Einstein ring radius： $|\theta_E| = \left(\bar{\varepsilon}\frac{D_{LS}}{D_L^n D_S}\right)^{n+1}$

Numerical calculation

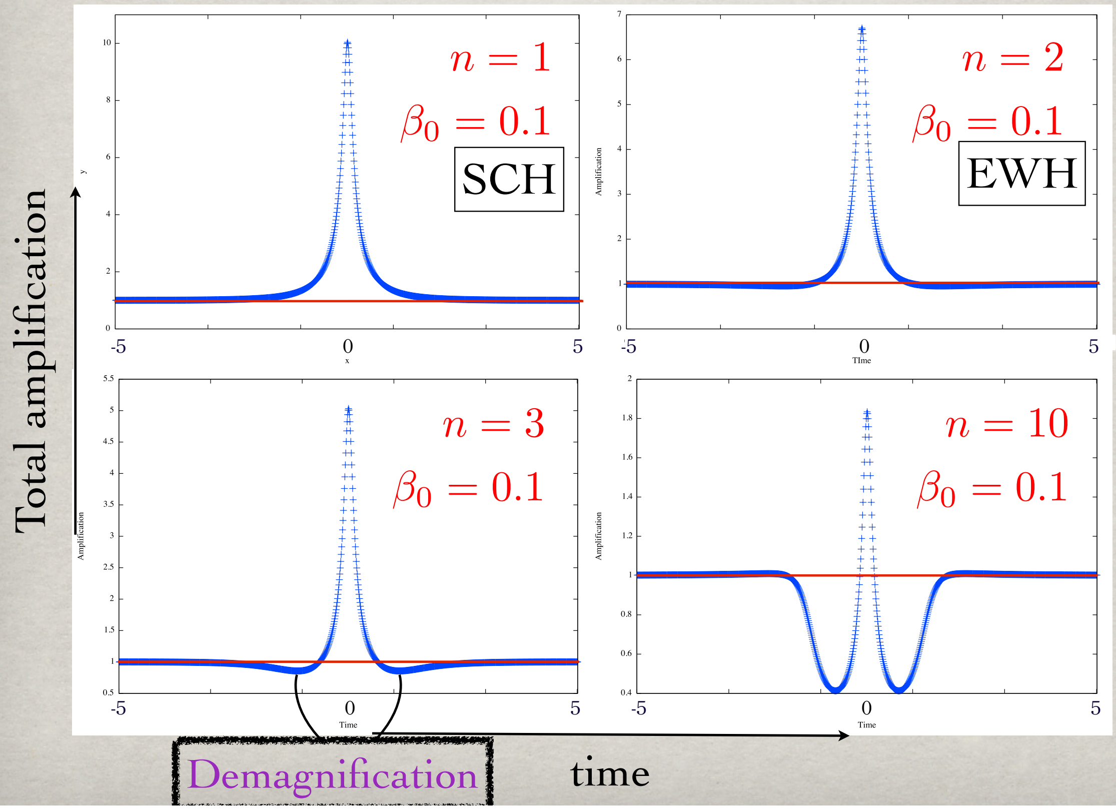

- Motivation
- Gravitational lensing
  - Amplification
  - Image centroid
- Summary & Future work

Image centroid

$\boxed{\text{Observables of astrometry}}$

Center of gravity $$X_G = \frac{x_1 m_1 + x_2 m_2}{M_{tot}}$$

Image centroid $$\theta_{PC} = \frac{\theta_+ A_+ + \theta_- A_-}{A_{tot}}$$

$\boxed{\text{Astrometry satellite “Gaia” \& “JASMINE”}}$

Centroid shift

- Remainder between the motion of the image centroid and the source motion(on the same time).

$$\Delta\theta_{pc} = \theta_{pc} - \beta$$

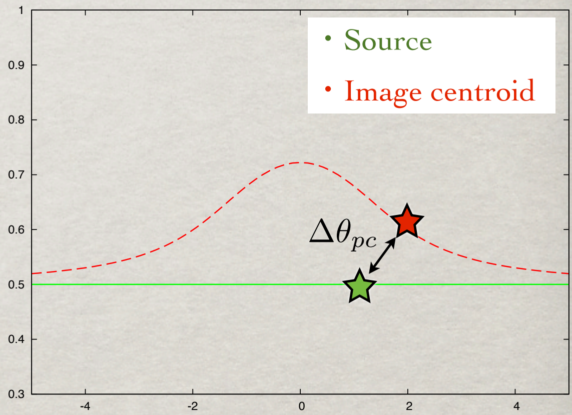

$\boxed{\text{One of observables of astronomy}}$

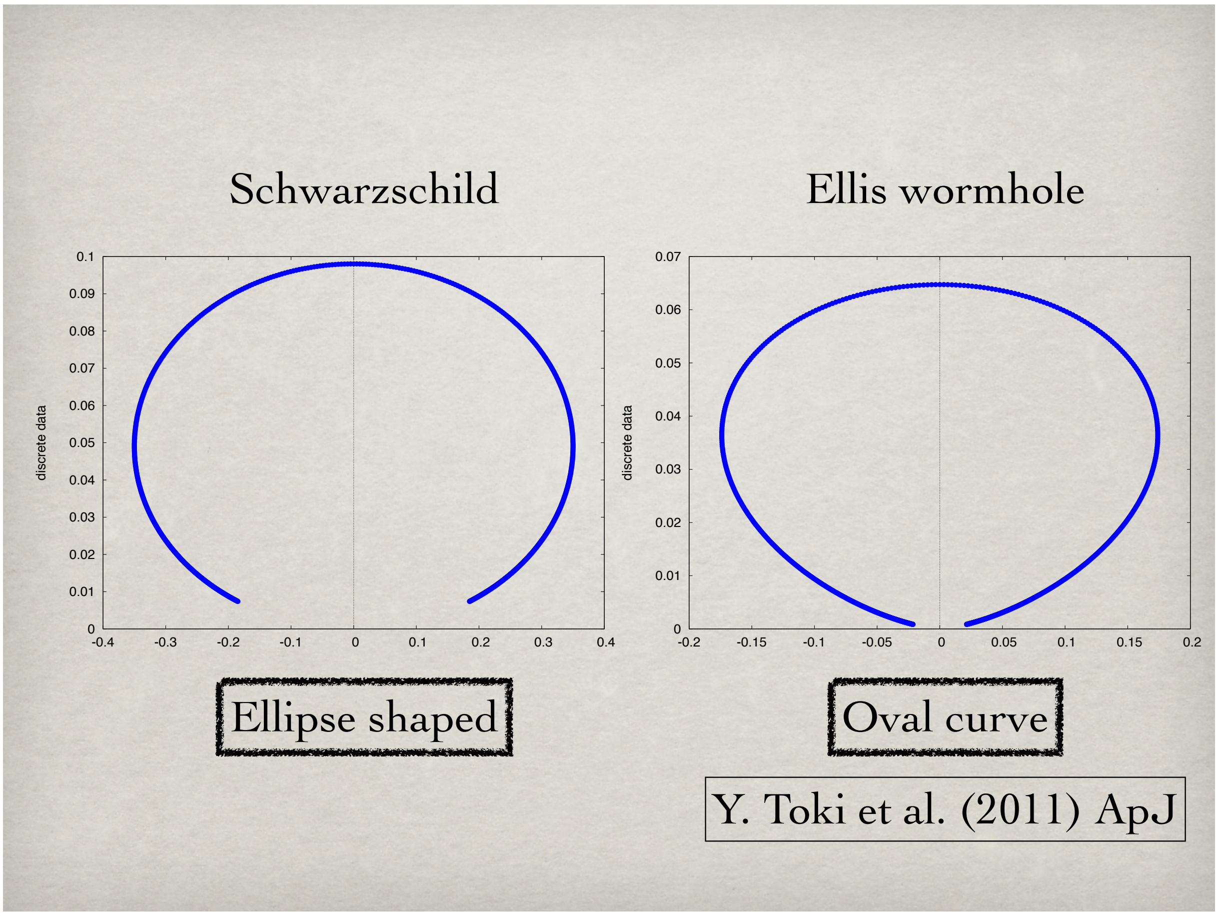
Schwarzschild
Ellis wormhole
discrete data
discrete data
Ellipse shaped
Oval curve
Y. Toki et al. (2011) ApJ

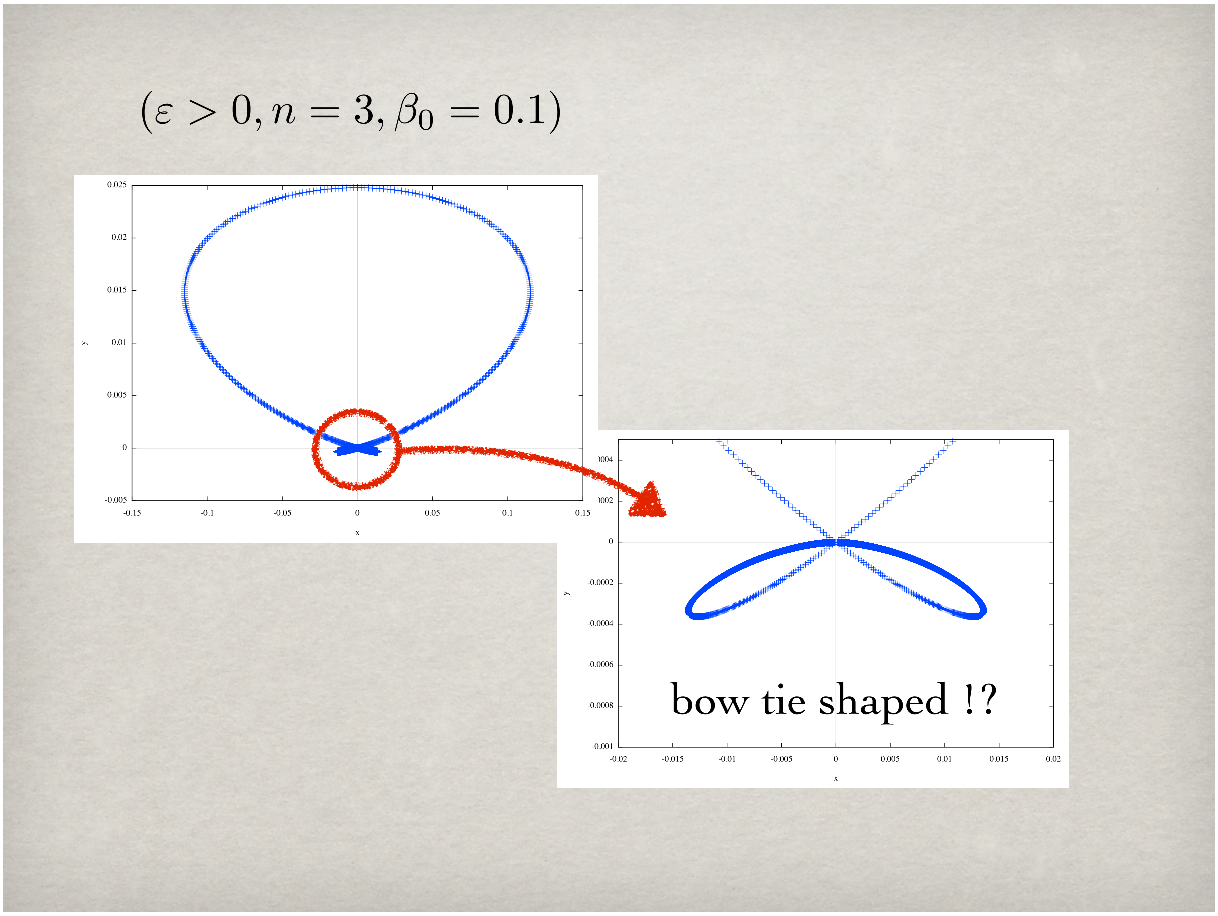
$(\varepsilon > 0, n = 3, \beta_0 = 0.1)$
x
y
bow tie shaped !?

$$(\varepsilon > 0, n = 10, \beta_0 = 0.1)$$

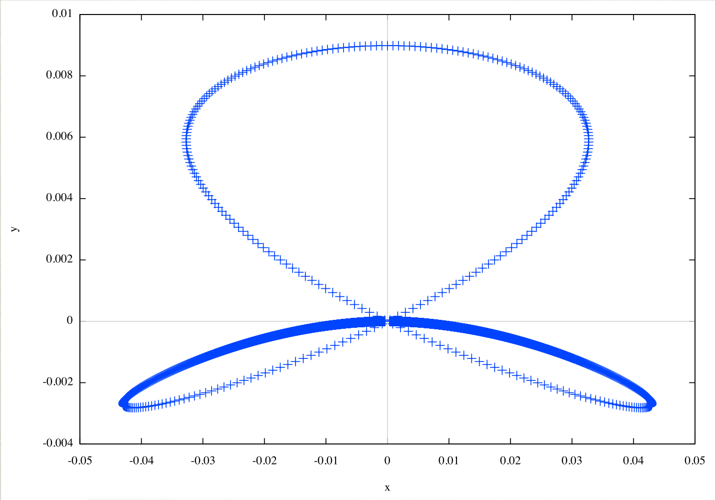

Same topology

- Motivation
- Gravitational lensing
  - Amplification
  - Image centroid
- Summary & Future work

Summary

- Possibility to demagnify in the case of general n
- The light curve in the modified space-times
- The centroid motion and the centroid shift in the modified space-times.

expect future observation

Future works

- Other gravitational lensing effect
- Non spherical symmetric space-time

P04 K. Izumi “Weak lensing by exotic object”

P05 K. Nakajima “Shapiro delay by exotic object”

P07 C. Hagiwara “Micro lensing by negative mass object”

[110803] R. Takahashi "Observational Upper Bound on the Cosmic Abundances of Negative-mass Compact Objects and Ellis Wormholes from the SDSS Quasar Lens Search"

THANK YOU FOR YOUR ATTENTION

Gravitational lensing effect

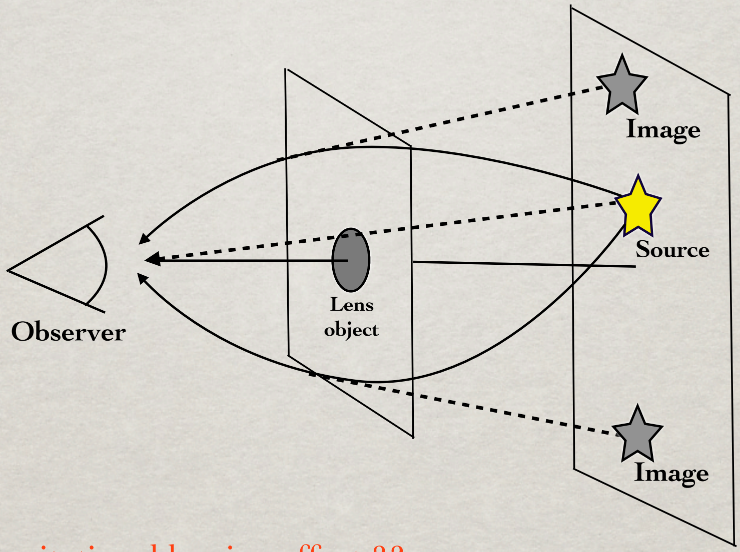

What is Gravitational lensing effect ??

- Separate the source
- Magnify the brightness of the source as with convex lens.

Einstein's equation

$$G_{\mu\nu} = T_{\mu\nu}$$

Gravity term

Mass or energy term

Celestial event by a Gravity

- Gravitational lensing observation $\longrightarrow$ ○ We can observe by the optical observations

We consider gravitational lensing effect by the exotic lens objects for searching those.

Sch & EWH

Metric of Spacetime

Sch

$$ds^2 = -(1 - \frac{2GM}{r})dt^2 + (1 - \frac{2GM}{r})^{-1}dr^2 + r^2(d\theta^2 + \sin^2\theta d\phi^2)$$

EWH

$$ds^2 = -dt^2 + (1 - \frac{a^2}{R^2})^{-1}dR^2 + R^2(d\theta^2 + \sin^2\theta d\phi^2) \quad (R^2 = r^2 + a^2)$$

Deflection angle & Lens equation

Sch

$$\alpha_{sc} = \frac{4GM}{c^2 b}$$

$$\hat{\beta} = \hat{\theta} - \frac{1}{\hat{\theta}}$$

$$\left(\hat{\ } \quad = \frac{1}{\theta_E} \right)$$

EWH

$$\alpha_{wm} = \frac{\pi a^2}{4c^4 b^2}$$

$$\hat{\beta} = \hat{\theta}_+ - \frac{1}{\hat{\theta}_+^2} \qquad (\hat{\theta} > 0)$$

$$\hat{\beta} = \hat{\theta}_- + \frac{1}{(-\hat{\theta}_-)^2} \qquad (\hat{\theta} < 0)$$

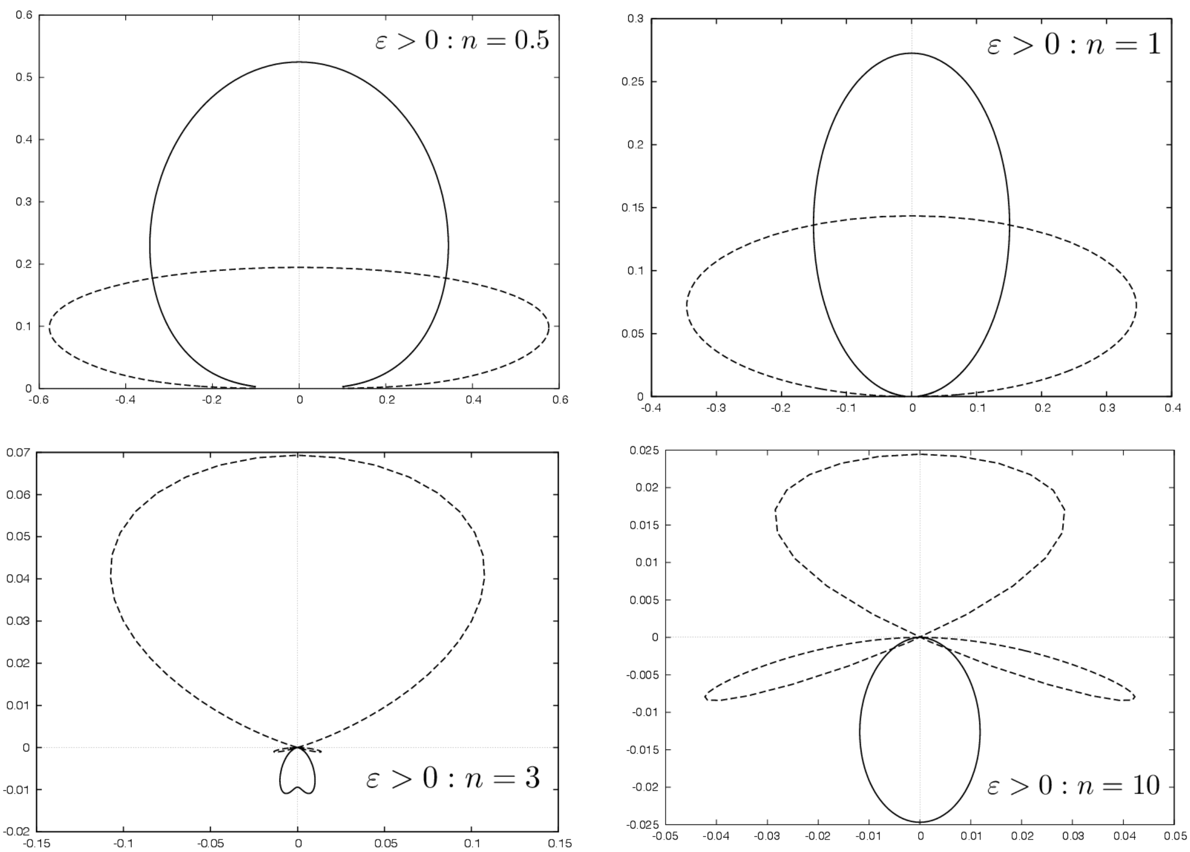

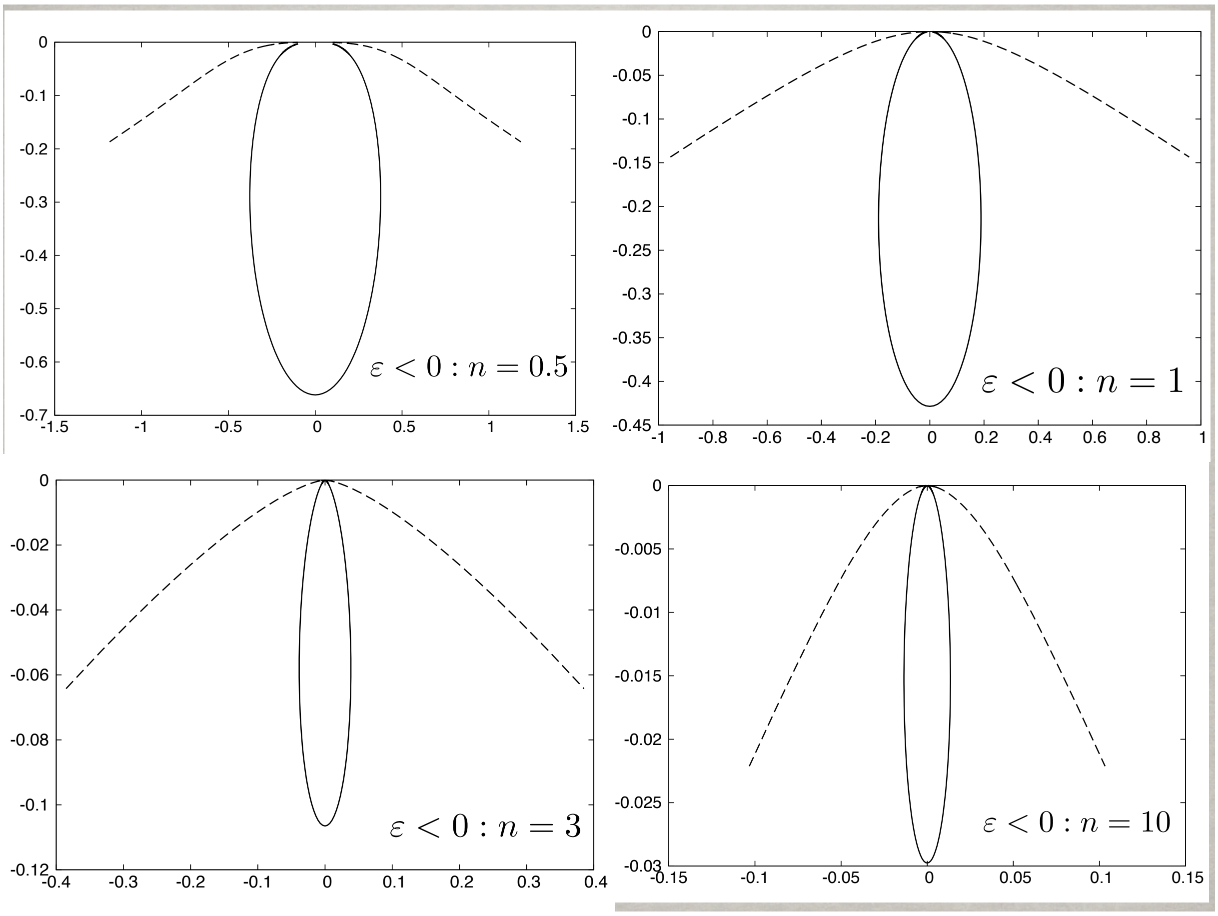
$\varepsilon < 0 : n = 0.5$
$\varepsilon < 0 : n = 1$
$\varepsilon < 0 : n = 3$
$\varepsilon < 0 : n = 10$

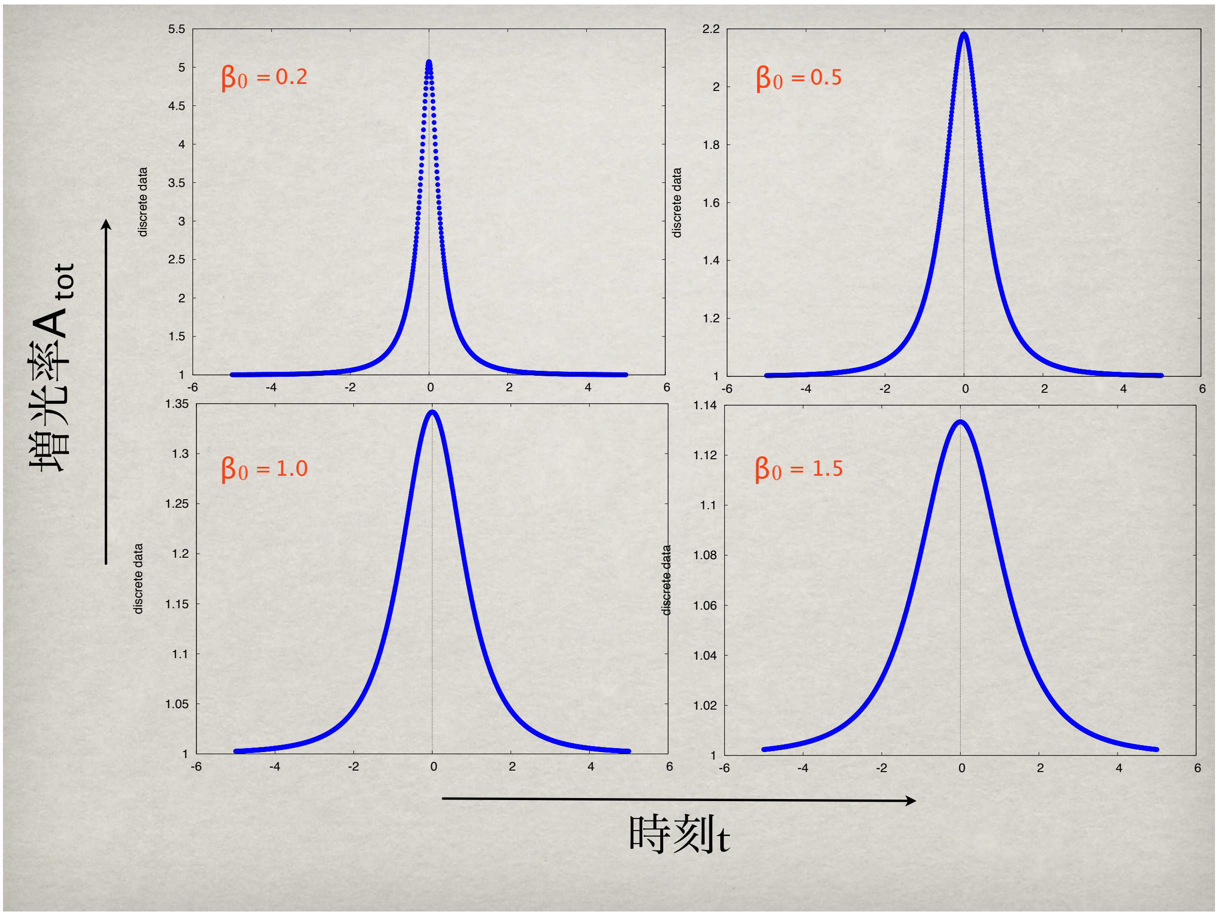
$\beta_0 = 0.2$
$\beta_0 = 0.5$
$\beta_0 = 1.0$
$\beta_0 = 1.5$
discrete data
増光率A_{tot}
時刻t

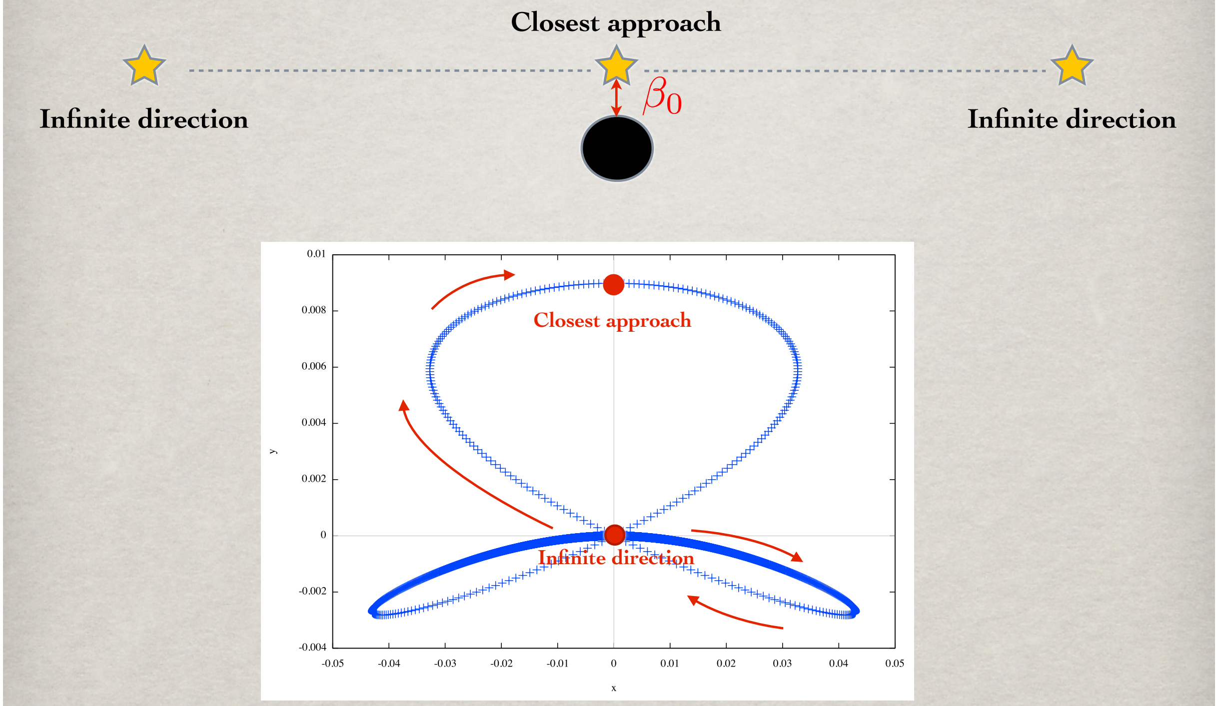

	Bulge		LMC	
$\theta_E(mas)$	$R_E(km)$	$\frac{\bar{\varepsilon}}{R_E^n}$	$R_E(km)$	$\frac{\bar{\varepsilon}}{R_E^n}$
10^{-3}	6.0×10^5	1.0×10^{-11}	3.7×10^6	1.0×10^{-11}
10^{-2}	6.0×10^6	1.0×10^{-10}	3.7×10^7	1.0×10^{-10}
10^{-1}	6.0×10^7	1.0×10^{-9}	3.7×10^8	1.0×10^{-9}
1	6.0×10^8	1.0×10^{-8}	3.7×10^9	1.0×10^{-8}
10	6.0×10^9	1.0×10^{-7}	3.7×10^{10}	1.0×10^{-7}
10^2	6.0×10^{10}	1.0×10^{-6}	3.7×10^{11}	1.0×10^{-6}
10^3	6.0×10^{11}	1.0×10^{-5}	3.7×10^{12}	1.0×10^{-5}

$t_E(day)$	$R_E(km)$	$\frac{\bar{\varepsilon}}{R_E^n}$ [Bulge]	$\frac{\bar{\varepsilon}}{R_E^n}$ [LMC]
10^{-3}	1.9×10^4	3.1×10^{-13}	5.0×10^{-14}
10^{-2}	1.9×10^5	3.1×10^{-12}	5.0×10^{-13}
10^{-1}	1.9×10^6	3.1×10^{-11}	5.0×10^{-12}
1	1.9×10^7	3.1×10^{-10}	5.0×10^{-11}
10	1.9×10^8	3.1×10^{-9}	5.0×10^{-10}
10^2	1.9×10^9	3.1×10^{-8}	5.0×10^{-9}
10^3	1.9×10^{10}	3.1×10^{-7}	5.0×10^{-8}

Bulge	LMC
$D_L = 4kpc$	$D_L = 25kpc$
$D_S = 8kpc$	$D_S = 50kpc$